

SSC-269

(SL-7-11)

STRUCTURAL TESTS OF SL-7 SHIP MODEL

**This document has been approved
for public release and sale; its
distribution is unlimited.**

SHIP STRUCTURE COMMITTEE

1977

SHIP STRUCTURE COMMITTEE

AN INTERAGENCY ADVISORY
COMMITTEE DEDICATED TO IMPROVING
THE STRUCTURE OF SHIPS

MEMBER AGENCIES:

United States Coast Guard
Naval Sea Systems Command
Military Sealift Command
Maritime Administration
American Bureau of Shipping

ADDRESS CORRESPONDENCE TO:

Secretary
Ship Structure Committee
U.S. Coast Guard Headquarters
Washington, D.C. 20590
SSC-269

6 September 1977

This report is one of a group of Ship Structure Committee Reports which describes the SL-7 Instrumentation Program. This program, a jointly funded undertaking of Sea-Land Service, Inc., the American Bureau of Shipping and the Ship Structure Committee, represents an excellent example of cooperation between private industry, classification society and government. The goal of the program is to advance understanding of the performance of ships' hull structures and the effectiveness of the analytical and experimental methods used in their design. While the experiments and analyses of the program are keyed to the SL-7 Containership and a considerable body of the data will be developed relating specifically to that ship, the conclusions of the program will be completely general, and thus applicable to any surface ship structure.

The program includes measurement of hull stresses, accelerations and environmental and operating data on the S. S. Sea-Land McLean, development and installation of a microwave radar wavemeter for measuring the seaway encountered by the vessel, a wave tank model study and a theoretical hydrodynamic analysis which relate to the wave induced loads, a structural model study and a finite element structural analysis which relate to the structural response, and installation of long term stress recorders on each of the eight vessels of the class. In addition, work is underway to develop the initial correlations of the results of the several program elements.

Results of each of the program elements will be published as Ship Structure Committee Reports and each of the reports relating to this program will be identified by an SL- designation along with the usual SSC- number. A list of all of the SL reports published to date is included on the back cover of this report.

This report contains the structural model data and analyses of the vessel. This report was funded by the American Bureau of Shipping in its entirety but is included in the SL-series for the sake of continuity.



W. M. BENKERT
Rear Admiral, U.S. Coast Guard
Chairman, Ship Structure Committee

SSC-269
(SL-7-11)

STRUCTURAL TESTS OF SL-7 SHIP MODEL

by

W. C. Webster¹ and H. G. Payer²

1. University of California,
Berkeley
2. Germanischer Lloyd

*This document has been approved for public release
and sale: its distribution is unlimited.*

U. S. Coast Guard Headquarters
Washington, D.C.
1977

ABSTRACT

A steel structural 1:50 model test program has been conducted for the 942-ft., 33-knots, SL-7 Containership. This report describes development of the model, through the test program and then to the test results. The principal stresses measured were longitudinal normal stresses and shear stresses. The model was loaded by means of calibrated steel weights and precision pulleys. The vertical and lateral bending responses corresponded closely to elementary beam theory; the vertical shear amidships pattern appeared to have the correct shape for the known boundary conditions at the keel and deck edges; and the torsional responses indicated that the bow and stern sections and machinery box offered considerable warping restraint. A finite element analysis of the model and ship midship sections indicated that nearly the same torsional response was observed for each.

CONTENTS

	<u>PAGE</u>
INTRODUCTION	1
DEVELOPMENT OF THE MODEL	2
Introduction	2
Scaling Laws	3
Summary of Scaling	9
Selection of Material	10
Structural Details of the Model	14
Construction of the Model	31
TEST SETUP AND PROCEDURE	44
Introduction	44
Strain Gages	44
Measurement Instruments	50
Data Reduction	52
The Displacement Measurements	53
The Loading Arm and Model Attachments	53
The Loading Method	55
Model Support	58
The Test Procedure	59
TEST PROGRAM	61
Introduction	61
The Test Program	62
THE TEST RESULTS	64
Introduction	64
Vertical Bending	64
Lateral Bending	66
Large Midship Shear	67
Torsion	68
Lateral Bending and Torsion	70
SUMMARY AND CONCLUSIONS	71
The Model	71
The Measuring Instrumentation	72
The Loading	72
The Results	72
ACKNOWLEDGEMENTS	74
APPENDIX A - EVALUATION OF MODEL DESIGN BY FINITE ELEMENT METHODS (FEM)	A-1
APPENDIX B - TEST DATA	B-1

SHIP STRUCTURE COMMITTEE

The SHIP STRUCTURE COMMITTEE is constituted to prosecute a research program to improve the hull structures of ships by an extension of knowledge pertaining to design, materials and methods of fabrication.

RADM W. M. Benkert, USCG (Chairman)
Chief, Office of Merchant Marine Safety
U.S. Coast Guard Headquarters

Mr. P. M. Palermo
Asst. for Structures
Naval Ship Engineering Center
Naval Ship Systems Command

Mr. M. Pitkin
Asst. Administrator for
Commercial Development
Maritime Administration

Mr. John L. Foley
Vice President
American Bureau of Shipping

Mr. C. J. Whitestone
Engineer Officer
Military Sealift Command

SHIP STRUCTURE SUBCOMMITTEE

The SHIP STRUCTURE SUBCOMMITTEE acts for the Ship Structure Committee on technical matters by providing technical coordination for the determination of goals and objectives of the program, and by evaluating and interpreting the results in terms of ship structural design, construction and operation.

NAVAL SEA SYSTEMS COMMAND

Mr. R. Johnson - Member
Mr. J. B. O'Brien - Contract Administrator
Mr. C. Pohler - Member
Mr. G. Sorkin - Member

U.S. COAST GUARD

LCDR E. A. Chazal - Secretary
LCDR S. H. Davis - Member
CAPT C. B. Glass - Member
LCDR J. N. Naegle - Member

MARITIME ADMINISTRATION

Mr. F. Dashnaw - Member
Mr. N. Hammer - Member
Mr. R. K. Kiss - Member
Mr. F. Seibold - Member

MILITARY SEALIFT COMMAND

Mr. T. W. Chapman - Member
CDR J. L. Simmons - Member
Mr. A. B. Stavovy - Member
Mr. D. Stein - Member

AMERICAN BUREAU OF SHIPPING

Mr. S. G. Stiansen - Chairman
Dr. H. Y. Jan - Member
Mr. I. L. Stern - Member

NATIONAL ACADEMY OF SCIENCES SHIP RESEARCH COMMITTEE

Prof. J. E. Goldberg - Liaison
Mr. R. W. Rumke - Liaison

SOCIETY OF NAVAL ARCHITECTS & MARINE ENGINEERS

Mr. A. B. Stavovy - Liaison

WELDING RESEARCH COUNCIL

Mr. K. H. Koopman - Liaison

INTERNATIONAL SHIP STRUCTURES CONGRESS

Prof. J. H. Evans - Liaison

U.S. COAST GUARD ACADEMY

CAPT W. C. Nolan - Liaison

STATE UNIV. OF N.Y. MARITIME COLLEGE

Dr. W. R. Porter - Liaison

AMERICAN IRON & STEEL INSTITUTE

Mr. R. H. Sterne - Liaison

U.S. NAVAL ACADEMY

Dr. R. Bhattacharyya - Liaison

Section I. INTRODUCTION

Modern containerships are constructed with extremely large hatch openings in the main deck so that the containers can be loaded into the ship directly with an overhead crane. The tendency recently has also been to increase the speed of these ships, thereby resulting in very fine hull forms. The combination of these two features leads to a hull which is much more flexible in torsion than ordinary break-bulk cargo ships and tankers, since the ability of the open main deck to carry shear loadings is virtually nil. Probably one of the most significant examples of the state-of-the-art in containership design is the Sea-Land containership SL-7. The principal features of this design are

Length between perpendiculars	880'-8"
Length overall	942'-0"
Beam	105'-6"
Depth	64'-0"
Design Draft	30'-0"
Service Speed	33 knots

This report details a structural model test program on this ship. The purposes of this study were many. First, since it would not be possible to provide a large amount of instrumentation on board the full scale ship and since the seaway loadings of the ship are not known in any real detail, a structural model could provide a more comprehensive view of the structural deflections and stresses for various component loadings than the real ship data. Second, even though the structure of the ship is amenable to analysis by finite element techniques, no comparisons are available of torsional response calculations with those of a typical ship structure. It is hoped that the structural model data will provide sufficient information with which to check and validate the finite element calculations, or to determine which effects need to be included in order to model accurately the structural mechanics. Third, the effect of warping restraint afforded by closed sections of the hull on torsional response is not clearly known for hull forms with a significant amount of shape, such as this ship. The test program has been designed to investigate this specific point.

The following sections outline the development of the model, the instrumentation, the test program and procedures, and, finally, the test results arrived at in this study.

II. Development of the Model

Introduction

In the development of the actual model, the model scale was of primary concern. From the point of view of ease of construction and amount of structural detail, the larger the model the better. However, large models are expensive and require very large loadings in order to produce significant stress levels. A study was conducted to consider all of these factors and a model scale of 1:50 was decided upon. This corresponds to a model length of 18'-10" (overall).

In order to construct a scale model so that it will have exactly the same structural response as the full scale ship, it is necessary to:

- a. construct the model from the same material as the ship, using the exact ship geometry.
- b. scale the thickness of the material by the scale ratio. For instance, this would mean that the model plating thickness would be one-fiftieth of the prototype plating thickness.
- c. include all of the structural components (including all brackets, plates, rolled section, etc.)
- d. duplicate in scale all of the welds.

Clearly it is not feasible to achieve this perfect scaling. Constructing the model from the same material is feasible; reducing the plating thickness by a ratio as small as 1:50 is also feasible, but it is not feasible to scale the welding. Further, plating cannot be obtained commercially to an accuracy better than +0.001". Considering that there are literally thousands of pieces in the structure of this ship, it is also clearly impossible to construct a model including all of these pieces except at an extraordinary expense. Further, since many of the smaller pieces are only a few inches in full size, they would have to be tiny indeed in the model scale.

As a result of these practical considerations, one is forced to retreat from the concept of perfect modeling. This retreat must also be made along several fronts. First it is necessary to increase the thickness of the structural components to reasonable commercial sizes; second, to greatly reduce the number of parts; and third, to simplify the complicated three-dimensional form of the ship hull. The following sections detail the rational steps used to perform these simplifications.

Scaling Laws

An examination of available steel plates and feasible welding techniques led to the selection of a plating thickness three times that required by exact scaling. Thus if

$$n_L = \frac{\text{length of the model}}{\text{length of the prototype}} = \frac{L_m}{L_p},$$

and

$$n_t = \frac{\text{thickness of plate in the model}}{\text{thickness of plate in the ship}} = \frac{t_m}{t_p}$$

the values of $n_L = \frac{1}{50}$ and $n_t = \frac{3}{50}$ were selected.

In order for the shape of deformation of the model to be the same as that of the prototype under loading, i.e., true scale displacements, the loads had to be scaled such that the strains in the model equaled those in the prototype.

$$n_\epsilon = \frac{\text{strain in the model}}{\text{strain in the prototype}} = 1$$

The strains of the model (or prototype) can arise from several different loading situations. These are discussed below.

- a. Axial load. The strain arising from a given axial force F acting on an area A is given by

$$\epsilon = \frac{F}{EA}$$

Consequently,

$$n_{\epsilon} = \frac{(\epsilon)_{model}}{(\epsilon)_{prototype}} = \frac{n_F}{n_E n_A}$$

where

$$n_F = \frac{Fm}{Fp}$$

$$n_E = \frac{Em}{Ep}$$

$$n_A = \frac{Am}{Ap}$$

In order for n_{ϵ} to be unity, the force must be scaled by the factor

$$n_F = n_E n_A$$

For a distorted scale model discussed above $n_A = n_L n_t$

and finally

$$n_F = n_E n_L n_t$$

- b. Bending. The bending strain is related to the applied moment M by using elementary beam theory.

$$\epsilon = \frac{Mr}{EI}$$

where r is the distance from the neutral axis
 I is the section moment of inertia

Consequently

$$n_{\epsilon} = \frac{n_M n_r}{n_E n_I}$$

where

$$n_r = \frac{r_m}{r_p}$$

$$n_I = \frac{I_m}{I_p}$$

In order for n_{ϵ} to be unity, the moment must be scaled by the factor

$$n_M = \frac{n_E n_I}{n_r}$$

For the distorted scale model $n_I \cong n_L^3 n_t$ and $n_r = H_L$

The approximation requires that the ship have thin plating with respect to overall dimensions such as beam or depth, a situation certainly met here. Thus

$$n_M = n_E n_L^2 n_t$$

c. Shear. The shear strain is related to the local value of shear, Q , by (elementary beam theory).

$$\gamma = \frac{1}{Gt} \cdot \frac{Qm(s)}{I}$$

where

$m(s) = \int^s z t ds$ the moment of the section about the neutral axis from a point of zero shear stress up to the point on the section periphery at s . G is the shear modulus.

Thus

$$n_{\gamma} = \frac{n_Q n_m}{n_t n_G n_I}$$

For the strains to be the same, $n_{\gamma} = 1$. For the distorted scale model $n_m = n_L^2 n_t$ and, as before $n_I \cong n_L^3 n_t$ and thus

$$n_Q = \frac{n_t n_G n_I}{n_m} = n_G n_L n_t$$

d. Torsion. For similarity of deflected shape, the total angle of twist, ϕ , must be the same at corresponding points for model and prototype. Thus, if L_m is a distance to a particular section (say, aft of the bow) on the model and L_p is the distance for the corresponding section for the prototype, then

$$\phi_m(L_m) = \phi_p(L_p)$$

Consider the total twist angle at an adjacent section located at $L_m + \Delta L_m$ in the model and the corresponding adjacent section on the prototype $L_p + \Delta L_p$. Then if the angles of these sections are also equal, ϕ

$$\frac{\phi_m(L_m + \Delta L_m) - \phi(L_m)}{\Delta L_m} = \frac{\phi_p(L_p + \Delta L_p) - \phi(L_p)}{\Delta L_p} \cdot \frac{\Delta L_p}{\Delta L_m}$$

If $\Delta L_m \rightarrow 0$, and since we are dealing with corresponding sections $\Delta L_p \rightarrow 0$ also, then $\theta_m = \theta_p \left(\frac{dL_p}{dL_m} \right)$

where

$\theta = \frac{d\phi}{dL}$, the angle of twist per unit length and finally, for the distorted scale model

$$n_\theta = \frac{\theta_m}{\theta_p} = \frac{1}{n_L}$$

Torsional deflections arise from both free torsion and from warping effects. These will be considered separately.

1. Free Torsion

Almost all of the free torsional rigidity arises from the tube-like parts of the ship's section since the contribution from the single walled regions (St. Venant torsion) is negligible. The relation between θ and torque, TF, can be expressed as

$$\theta = \frac{TF \oint \frac{ds}{t}}{4G \Sigma A_i^2}$$

where

t is the local plating thickness. \oint means that a line integral is to be performed about all tubes, presumed in this case to be separate cells. The analysis of adjacent cells is more complicated, but since the result is the same, the analysis is not presented here.

A_i is the enclosed area of each of the separate cells.

Whence
$$n_{TF} = \frac{T_{Fm}}{T_{Fp}} = \frac{n_{\theta} n_G n_A^2}{n_i}$$

where
$$n_{\theta} = \frac{\theta m}{\theta p}$$

$$n_G = \frac{Gm}{Gp}$$

$$n_A^2 = \frac{(\Sigma A_i^2) m}{(\Sigma A_i) p}$$

$$n_i = \frac{(\oint ds/t) m}{(\oint ds/t) p}$$

For the distorted scale model $n_A^2 = n_L^4$ and $n_i = n_L/n_t$.

Using these results and the previous result $n_{\theta} = 1/n_L$, then

$$n_{TF} = n_G \cdot n_L^2 n_t$$

2. Warping Torsion

The relation between θ and the torque, TW , carried by a structure due to restraint against warping can be written as

$$TW = C_1 \frac{d^2 \theta}{dx^2}$$

where C_1 is called the warping rigidity and is defined as

$$C_1 = E \int_0^m (\int_0^s r ds)^2 t ds,$$

where r is the distance from the neutral axis, as before. It follows from the previous argument that for equal total angles of twist

$$\frac{\left(\frac{d^2\theta}{dx^2}\right)_m}{\left(\frac{d^2\theta}{dx^2}\right)_p} = n_{d^2\theta} = 1/n_L^3$$

also

$$n_{C_1} = \frac{(C_1)_m}{(C_1)_p} = n_E \cdot n_q$$

$$n_q = \frac{(\int_0^m (\int_0^s r ds)^2 t ds)_m}{(\int_0^m (\int_0^s r ds)^2 t ds)_p}$$

For the distorted scale model, $n_q = n_L^5 n_t$ and, thus,

$$n_{TW} = \frac{(T_w)_m}{(T_w)_p} = n_{C_1} n_{d^2\theta} = n_E n_t / n_L$$

e. Buckling. The compressive, in-plane force at which buckling occurs in a flat plate buckling is given by:

$$F_c = \frac{-\pi^2 DK}{b}$$

where

b is the plate width

K is a constant depending on the plate aspect ratio and edge boundary conditions. (the same for model and prototype)

$$D = \frac{Et^3}{12(1-\mu^2)}, \text{ the flexural rigidity,}$$

thus

$$n_c = \frac{(Fc)_m}{(Fc)_p} = \frac{n_{\tilde{E}} n_t^3}{n_b}$$

where

$$n_{\tilde{E}} = \frac{(E/(1-\mu^2))_m}{(E/(1-\mu^2))_p}$$

$$n_b = \frac{b_M}{b_p}$$

For a scale model $n_b = n_L$ and thus

$$n_c = n_{\tilde{E}} \frac{n_t^3}{n_L}$$

Summary of Scaling

In summary, for the distorted scale model,

Forces	(criterion)
$n_F = n_E n_L n_t$	(axial strain)
$n_Q = n_G n_L n_t$	(shear strain)
$n_c = \tilde{n}_E n_t^3 / n_L$	(critical buckling force)
Moments	
$n_M = n_E n_L^2 n_t$	(bending strain)
$n_{TF} = n_G n_L^2 n_t$	(free torsion strain)
$n_{TW} = n_E n_t / n_L$	(warping strain)

If the model is loaded with forces which are equal to $(n_E n_L n_t)$ times those forces which act on the prototype,

then the model moments which arise from these forces are $(n_E n_L n_t)$ times those acting on the prototype. The above summary shows that if $n_E = n_G$ then the model will develop the same strains from these primary loadings as would exist on the prototype. For simple elastic materials

$$G = \frac{E}{2(1+\mu)}$$

where μ is Poisson's ratio. Therefore $n_E = n_G$ as long as μ is the same for both model and prototype. Poisson's ratio for most structural materials (steel, aluminum, etc.) is little different from 0.3. Some plastics have different Poisson's ratios.

When the critical buckling force criterion is examined, the loadings which yield the same strains for both prototype and model do not yield the same scaled buckling force unless $n_t = n_p$. In other words, only for an undistorted scale model will the buckling be properly modeled. In particular, if $n_t > n_p$, then the scaled force for buckling on the model will be relatively larger than for the prototype. Therefore if a loading exists for which the prototype exhibits buckling effects, the corresponding buckling may not occur in the distorted scale model. Care must be taken, therefore, to limit the loadings of a distorted model to those which would not lead to buckling in the prototype.

Selection of Material

A wide range of materials was available for use in the structural model. Foremost amongst these were steel, aluminum, plexiglass, brass, PVC (polyvinyl chloride). All of these materials were given careful consideration for the SL-7 model.

In addition various castable plastics of the resin and epoxy types were also investigated. The final selection of a material depended on many factors, as discussed below.

Plastic Materials: All of the plastic materials considered had one very attractive property, that of a very low modulus of elasticity. Typically the plastic materials had a value of $E \approx 5 \times 10^5$ which is 1/60 that of steel. This implies that the model loadings required to obtain comparable strains in model and prototype can be quite moderate. Unfortunately, all of the plastics considered exhibited qualities which were undesirable. These were creep (non-elastic stretching under load), extreme sensitivity to environment (temperature and humidity) and questionable joining techniques. For these reasons, all of the plastics were not considered further.

Metals: The selection from amongst the various metals available was made primarily on two bases: fabrication and commercially available thicknesses. Brass was considered briefly but was considered too expensive. Also, brass can best be joined by brazing. The problem of brazing a model with over 500 pieces seemed insurmountable. Aluminum appeared to be a prime candidate since it was readily available. Further, aluminum has a modulus of elasticity one-third that of steel, an advantage in the loading of the model. In order to uncover any problem areas, a 1:50 scale midship section (between adjacent bulkheads) was constructed. Unfortunately, this model showed large welding-induced distortion of the plates (that is, large relative to the plate thickness). Further, exploration of this welding problem indicated that it was virtually impossible to avoid this distortion when thin plating is used. It was also determined that the non-linear stress-strain characteristics of aluminum could lead to difficulties in interpreting the data. In conclusion, steel was selected since it was easily welded, and supplied in a large variety of gages. Hot-rolled steel was chosen since cold-rolled steel is not as isotropic and also not available in as wide a selection of gauges. The disadvantage of steel is that its modulus of elasticity is high and the resulting loads required became quite large.

After some experimentation with shipyard welding techniques, it was determined that it was possible to join plates thicker than 16 gage (0.0598").

Scantlings The model was designed with a geometric scale ratio of 1:50. The plate thicknesses were increased most in the scale ratio of 3:1. The tables below give the distortions of the major components.

Bottom plating: Model: .0598"(1.519 mm) Ship: 35 mm

$$\text{Ratio: } \frac{.0598 \cdot 25.4}{35} = \frac{1}{23}$$

$$\text{Distorted scale: } \frac{50}{23} = \frac{2.17}{1}$$

Inner bottom plating: Model: .0598"(1.519 mm) Ship: 32 mm

$$\text{Ratio: } \frac{.0598 \cdot 25.4}{32} = \frac{1}{21.1}$$

$$\text{Distorted scale: } \frac{50}{21.1} = \frac{2.37}{1}$$

Side plating: Model: .0598"(1.519 mm) Ship: 20.5 mm

$$\text{Ratio: } \frac{.0598 \cdot 25.4}{20.5} = \frac{1}{13.5}$$

$$\text{Distorted scale: } \frac{50}{13.5} = \frac{3.7}{1}$$

Torsion box between decks:

Main deck: Model: .120"(3.05 mm) Ship: 50 mm

$$\text{Ratio: } \frac{.120 \cdot 25.4}{50} = \frac{1}{16.4}$$

$$\text{Distorted scale: } \frac{50}{16.4} = \frac{3.05}{1}$$

Second deck & sides: Model: .120"(3.05 mm) Ship: 42 mm

$$\text{Ratio: } \frac{1.20 \cdot 25.4}{42} = \frac{1}{13.8}$$

$$\text{Distorted scale: } \frac{50}{13.8} = \frac{3.62}{1}$$

Transverse torsion box between decks;

Main deck: Model: .0598"(1.519 mm) Ship: 15 mm

$$\text{Ratio: } \frac{.0598 \cdot 25.4}{15} = \frac{1}{9.88}$$

$$\text{Distorted scale: } \frac{50}{9.88} = \frac{5.06}{1}$$

Second deck, bulkheads: Model: .0598"(1.519 mm) Ship: 12.5mm

$$\text{Ratio: } \frac{.0598 \cdot 25.4}{12.5} = \frac{1}{8.23}$$

$$\text{Distorted scale: } \frac{50}{8.23} = \frac{6.08}{1}$$

The following conclusions were made when looking at the scale distortions of the plate thicknesses.

1. The torsional stiffness of the torsion box between decks was relatively stiffer on the model than on the ship.
2. The torsional stiffness at the transverse torsion box was relatively stiffer on the model than on the ship.
3. The torsional stiffness of the double bottom was relatively stiffer on the ship than on the model.
4. Since the distortion was not constant over the cross section, the ship and the model did not necessarily have the same relative position of the center of shear.

Structural Details of the Model

It was of course impossible to include all of the structural details of the ship in a 1:50 scale model. In fact the number of component pieces was reduced by several orders of magnitude. This meant that all of the brackets and small details, and many of the stiffeners, longitudinals, etc. were eliminated. Since these latter elements were part of the primary structure of the model and as such could not be eliminated altogether, they were lumped together in some reasonable fashion.

Another important consideration in building the small-scale model was the shape of the hull itself. Ship hulls are of a complex shape with a wealth of double-curved plates. On the model scale these shapes are particularly difficult to reproduce, since it was not possible to break the hull surface into as many pieces as used in the full-scale ship. Thus a simplification of the hull form was also required for the model.

Reduced scale drawings of the ship model are shown in Figures 1 through 11. The simplification of both the hull form and the number of pieces were made in accord with the type of measurements that were to be made. Where the response of a localized section of the ship was required, that portion was modeled in great detail. The simplifications appropriate for investigation of buckling characteristics would be different from those used for primary bending response. For these particular model tests, the point of view was adopted that primary torsional responses was of the major interest. Late in the development of the model, a desire was expressed for modelling transverse and vertical primary bending responses, insofar as they would not affect the torsional response of the model.

The torsional response of a ship or model is a very complicated process involving several phenomena. These include: free torsion of the individual elements (such as the twisting of longitudinal stiffeners); torsion of closed, tube-like elements; and the effects of warping restraint offered by the shell of the hull and deep transverse bulkheads. Current analytical techniques were not sufficiently

well developed to determine the combined effect of these responses, and thus the finite-element method (FEM) was used. Finite element calculations described in Appendix A were performed on various critical subsections of the hull to determine the proper lumping of parameters.

It was also decided to omit the raised forecastle deck, since the closed forward section of the ship already provided nearly perfect warping restraint.

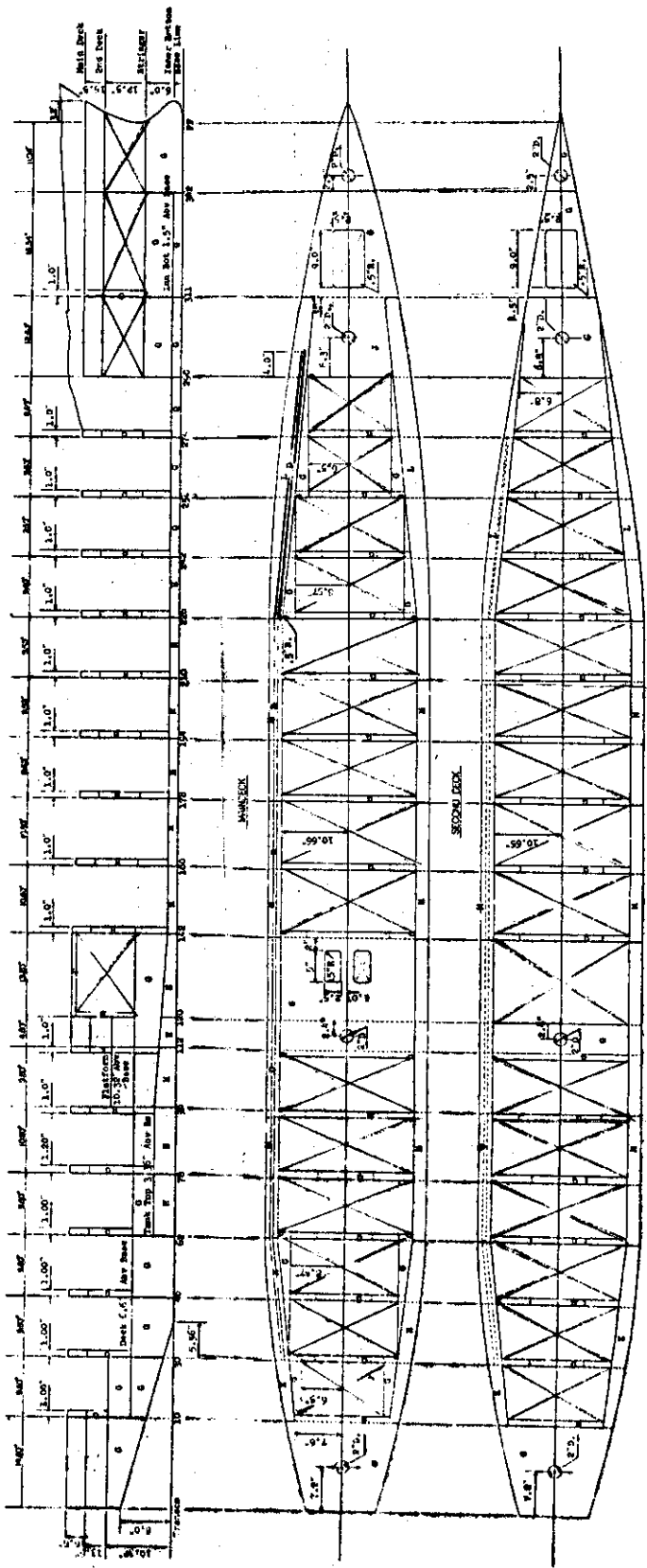
a. Midship Section

Figure 12 shows the midship section of the SL-7. The inner bottom has a center vertical keel, several side girders and a multitude of longitudinals. The sides of the ship are transversely framed with a series of heavy longitudinal girders and deep web frames. Just below the deck, at the sides there is a heavy tube-like structure (presumably to enhance the torsional rigidity). This tube contains many closely spaced longitudinal deep girders. The purpose of these members appears to be for providing sufficient section modulus for vertical bending.

Reduction of the elements used included consideration of the following:

1. Innerbottom structure. Clearly, on the 1:50 model it would be impossible to duplicate the myriad of small longitudinal stiffeners. These stiffeners are primarily for local strength of the inner bottom and have a very small contribution to the torsional stiffness of the ship. A calculation of the total area of the longitudinals available for axial stresses compared to that of the inner bottom or bottom shell was only about 7-8%. Another consideration is that of the floors. For the most part floors provide local strength to the bottom plating and interact very little with the overall structural response of the ship. As a result these stiffeners were neglected. A more difficult consideration is that of the longitudinal side girders. These girders break up the inner bottom into a number of joined torque tubes. However, practical considerations of model construction obviated the possibility of including all of these girders. It was felt that a lumping of the side girders into one girder, port and starboard, and the retention of the center vertical keel represented the

CENTERLINE PROFILE



Code	Material
A	1/2" x 1/8"
B	7/8" x 3/16"
C	5/8" x 1/8"
D	1/2" x 1/4"
E	1" x 3/16"
F	1/4" x 1/4"
G	0.06"
H	0.13"
I	0.109"
J	0.075"
K	0.09"
L	0.12"
M	5" x 2" x 0.12"
N	3/4" x 30.09"
P	3/4" x 0.06"
Q	.125"

CENTERLINE PROFILE,
MAINDECK, & SECOND
DECK

FIGURE 1

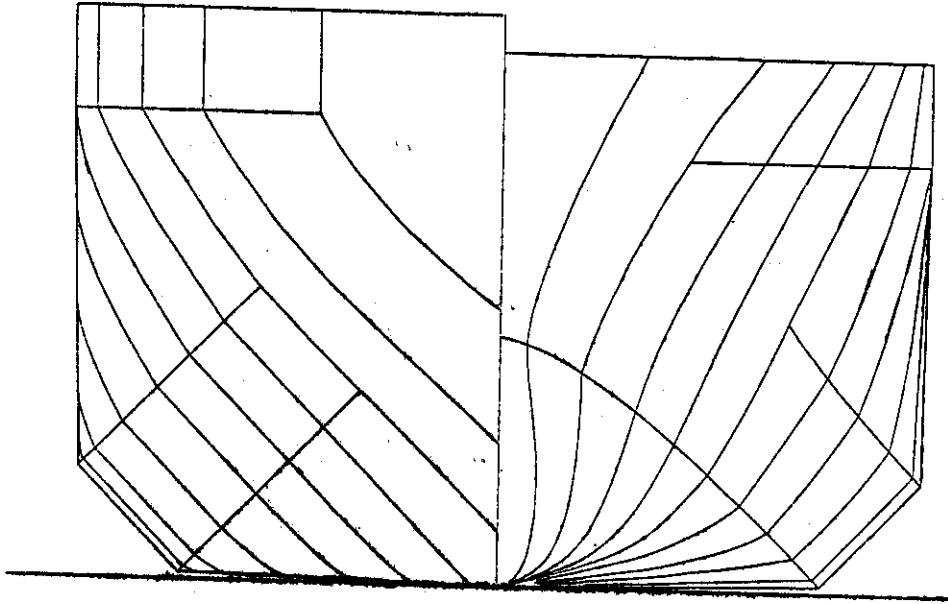


FIGURE 3

BODY PLAN

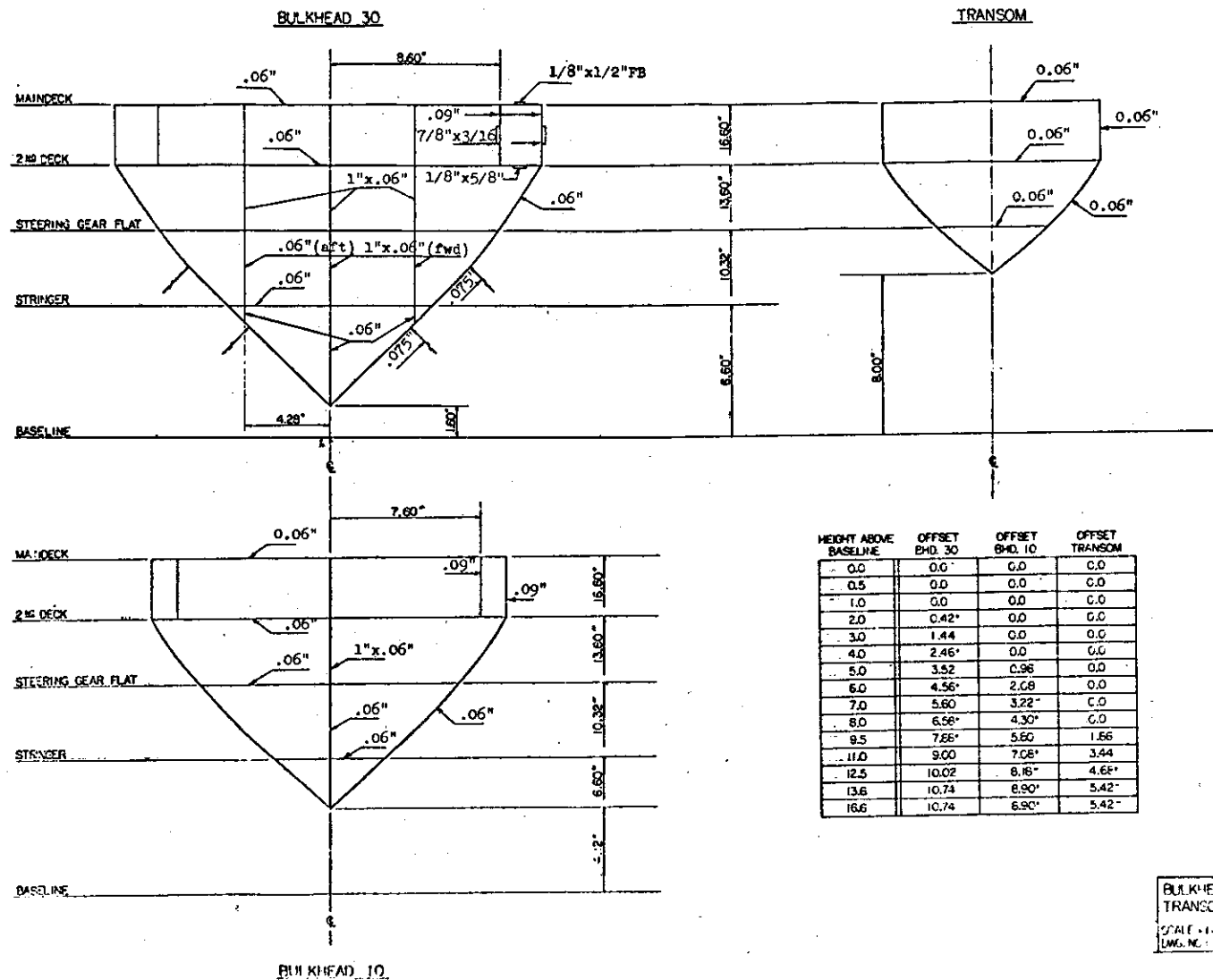
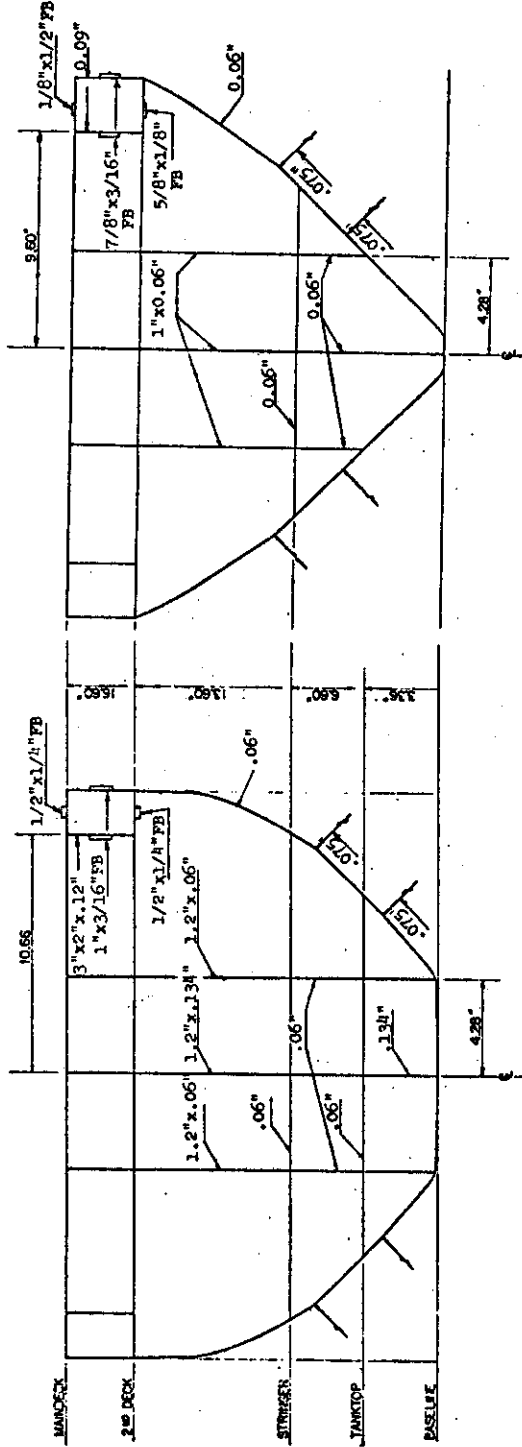
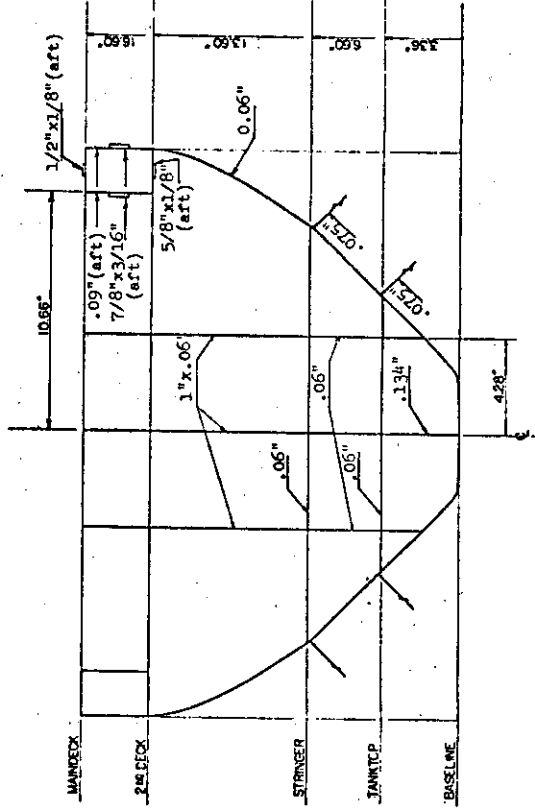
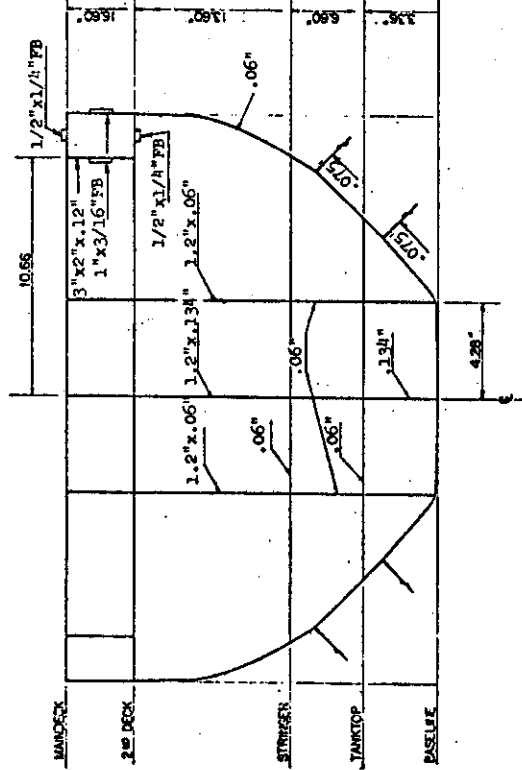


FIGURE 4

BULKHEAD 46



BULKHEAD 78

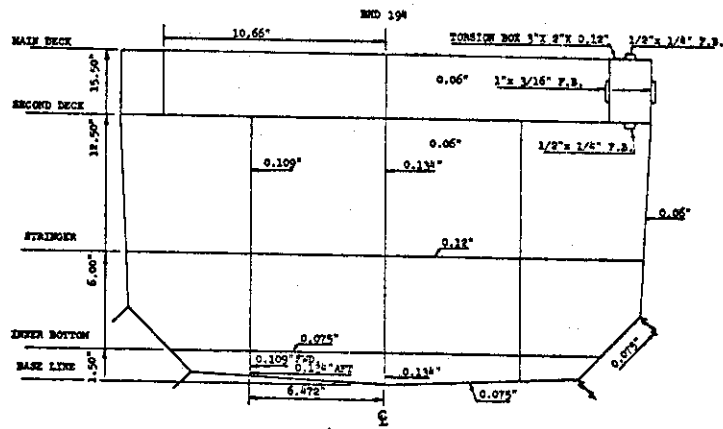


BULKHEAD 62

HEIGHT ABOVE BASELINE	OFFSET BHD. 78	OFFSET BHD. 62	OFFSET BHD. 46
0.0	0.0	0.0	0.0
0.5	4.52"	3.12	1.24"
1.0	5.94"	3.68	1.76
2.0	6.53"	4.72	2.76
3.0	7.65"	5.74	3.73
4.0	8.65"	6.74	4.72
5.0	9.65"	7.74	5.71
6.0	10.46"	8.74	6.70
7.0	11.08	9.56	7.70
8.0	11.63	10.22	8.55
9.5	12.26	11.15	9.61
11.0	12.61	11.94	10.62
12.5	12.64	12.47	11.50
13.6	12.66	12.66	12.04
16.6	12.65	12.66	12.04

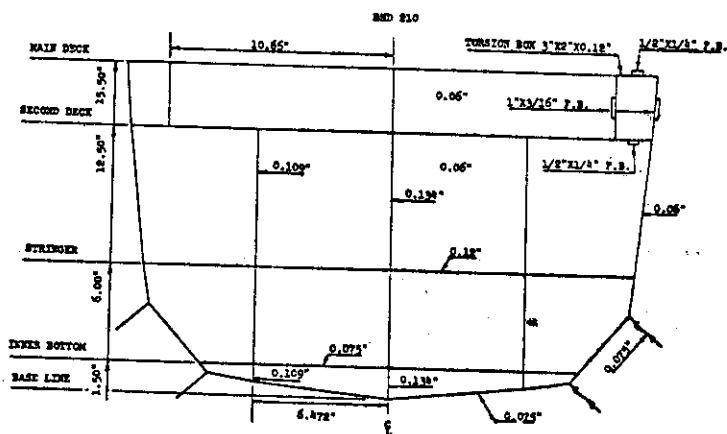
BULKHEADS:
78, 62, & 46
SCALE: 1:12
DWG. NO.: BL-7-011

FIGURE 5



OFFSETS

HEIGHT ABV. BASE:	DISTANCE FROM:	
	BHD 194	BHD 210
0.0" (base)	0.0"	0.0"
0.5"	9.35"	5.74"
1.0"	9.95"	6.66"
2.0"	10.53"	9.66"
3.0"	11.26"	10.56"
4.0"	12.26"	11.34"
5.0"	12.32"	12.60"
6.0"	12.35"	11.76"
7.0"	12.40"	11.66"
8.0"	12.42"	12.00"
9.5"	12.52"	12.16"
11.0"	12.60"	12.37"
12.5"	12.65"	12.46"
14.0"	12.66"	12.56"
15.5"	12.68"	12.66"



BULKHEADS 194 & 210

FIGURE 8

OFFSETS

HEIGHT ABV BASE	DISTANCE FROM: ϕ	
	BHD 274	BHD 290
0.0"	0.0"	0.0"
0.5"	1.73"	1.45"
1.0"	2.76"	2.15"
2.0"	3.77"	2.85"
3.0"	4.47"	3.29"
4.0"	5.02"	3.63"
5.0"	5.51"	3.94"
6.0"	5.96"	4.27"
7.0"	6.40"	4.56"
8.0"	6.86"	5.12"
9.5"	7.62"	5.92"
11.0"	8.40"	6.78"
12.5"	9.24"	7.70"
14.0"	10.05"	8.68"
15.5"	10.92"	9.70"

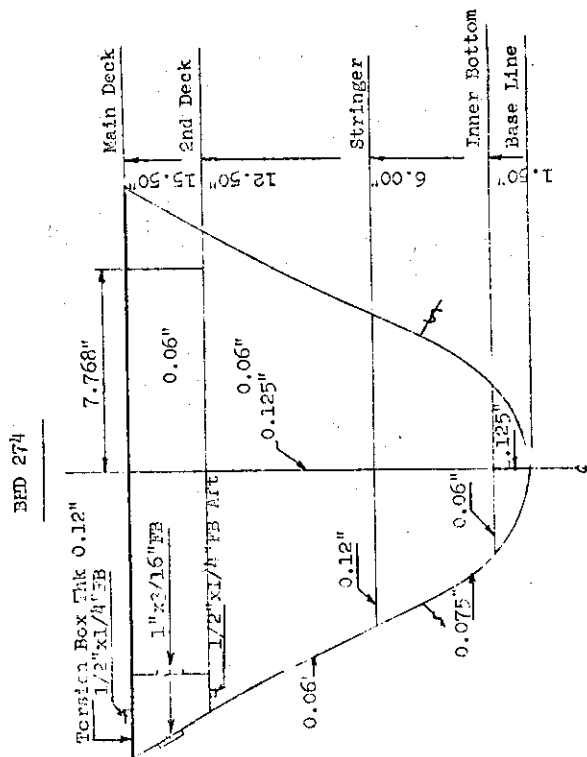
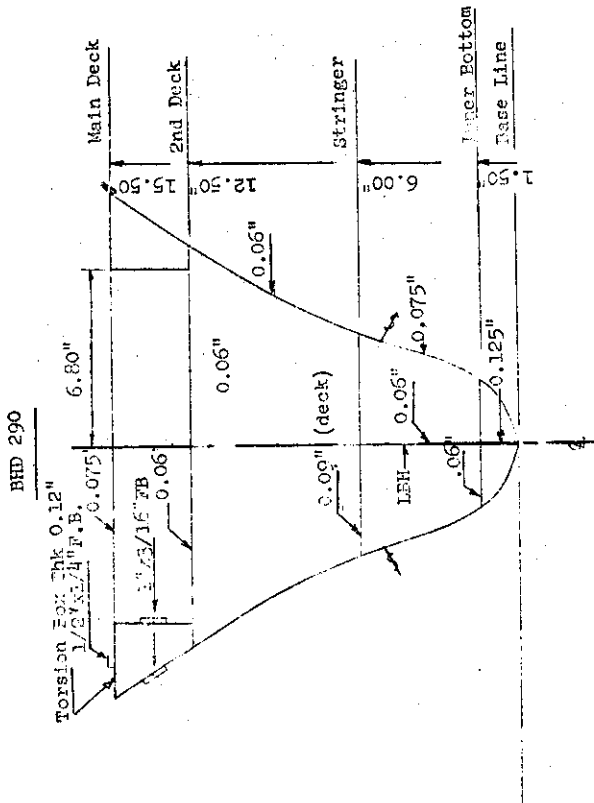
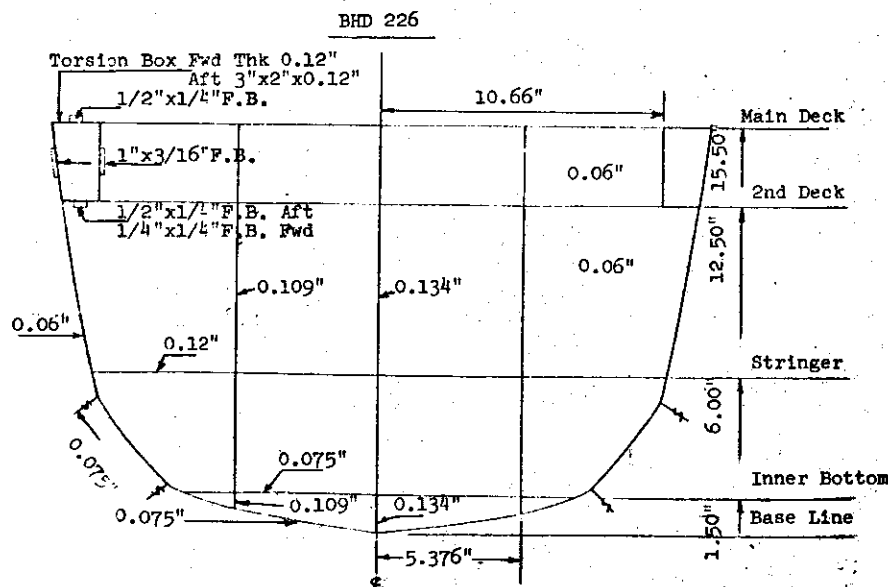
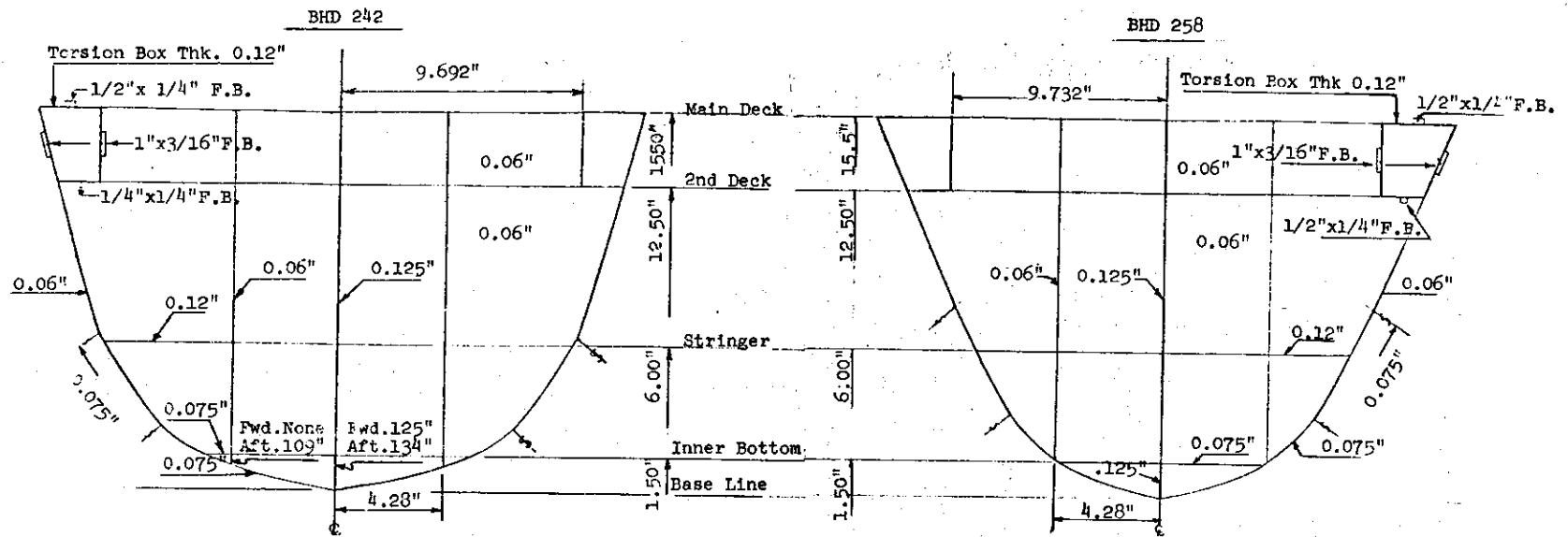


FIGURE 9



OFFSETS

HEIGHT ABV BASE	DISTANCE FROM ϕ		
	BHD 226	BHD 242	BHD 258
0.0" (base)	0.00"	0.00"	0.00"
0.5"	3.64"	2.44"	1.98"
1.0"	6.04"	4.30"	3.38"
2.0"	8.13"	6.39"	4.86"
3.0"	8.97"	7.44"	5.85"
4.0"	9.73"	8.16"	6.53"
5.0"	10.45"	8.85"	7.10"
6.0"	10.88"	9.48"	7.62"
7.0"	11.22"	10.00"	8.11"
8.0"	11.53"	10.41"	8.56"
9.5"	11.94"	10.97"	9.30"
11.0"	12.32"	11.50"	10.02"
12.5"	12.66"	12.00"	10.75"
14.0"	12.66"	12.18"	11.26"
15.5"	12.66"	12.36"	11.80"

BULKHEADS 226, 242 & 258

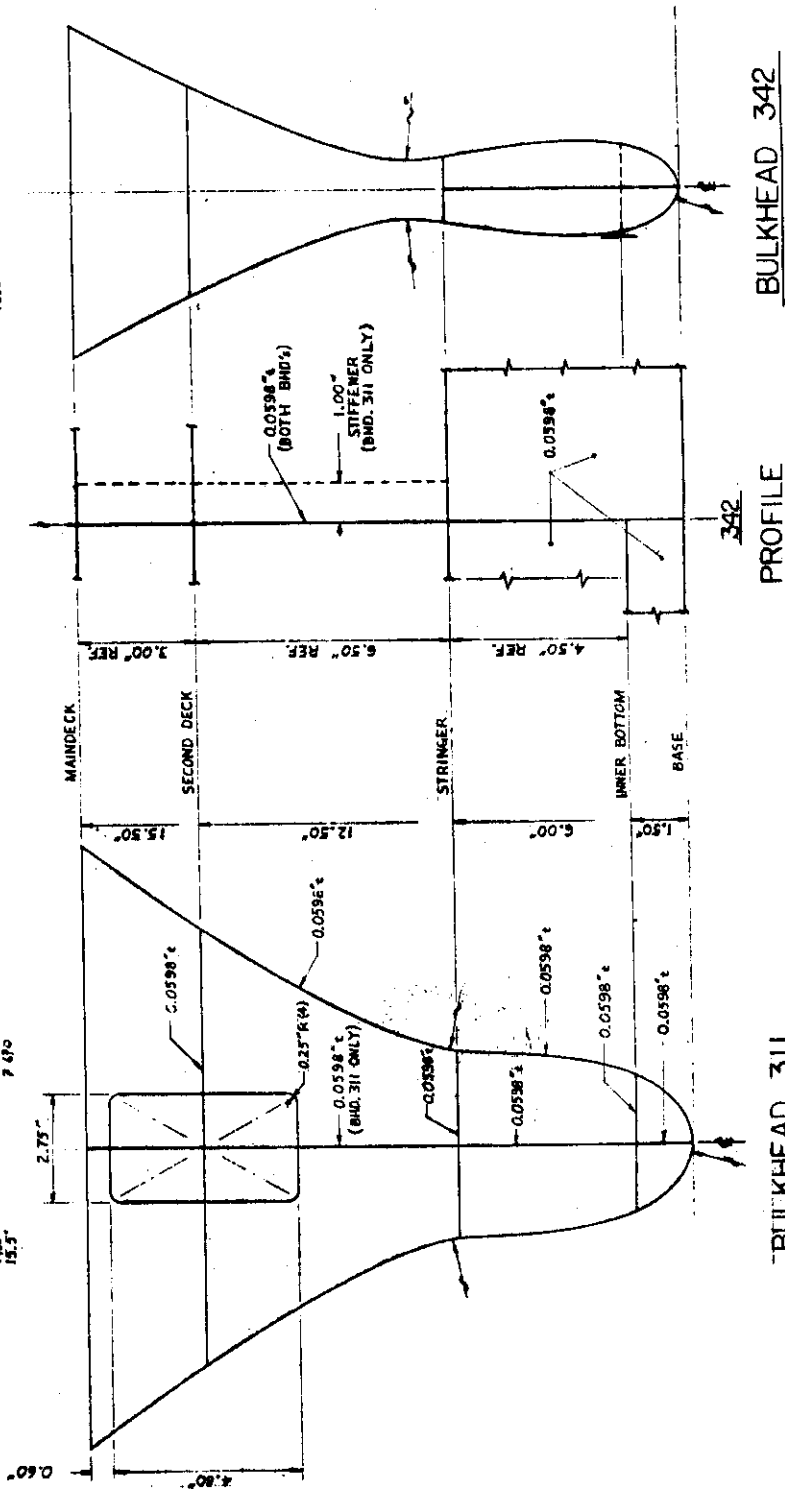
FIGURE 10

OFFSETS
HEIGHT ABOVE BASE — DISTANCE FROM §

0.0'	0.0
0.5'	0.490
1.0'	0.888
1.5'	1.250
2.0'	1.575
2.5'	1.850
3.0'	2.075
3.5'	2.250
4.0'	2.375
4.5'	2.450
5.0'	2.475
5.5'	2.450
6.0'	2.375
6.5'	2.250
7.0'	2.075
7.5'	1.850
8.0'	1.575
8.5'	1.250
9.0'	0.888
9.5'	0.490
10.0'	0.0

OFFSETS
HEIGHT ABOVE BASE — DISTANCE FROM §

0.0'	0.0
0.5'	1.87
1.0'	4.98
1.5'	8.99
2.0'	12.79
2.5'	16.25
3.0'	19.38
3.5'	22.10
4.0'	24.45
4.5'	26.38
5.0'	27.85
5.5'	28.90
6.0'	29.50
6.5'	29.65
7.0'	29.35
7.5'	28.60
8.0'	27.40
8.5'	25.75
9.0'	23.68
9.5'	21.20
10.0'	18.35



BULKHEADS 311 & 342

FIGURE 11

maximum acceptable complexity for construction. In order to test the effect of this lumping, two different models were tested in torsion using FEM: one model with all side girders, and one with only 2 side girders. Sketches of the structure are shown below.

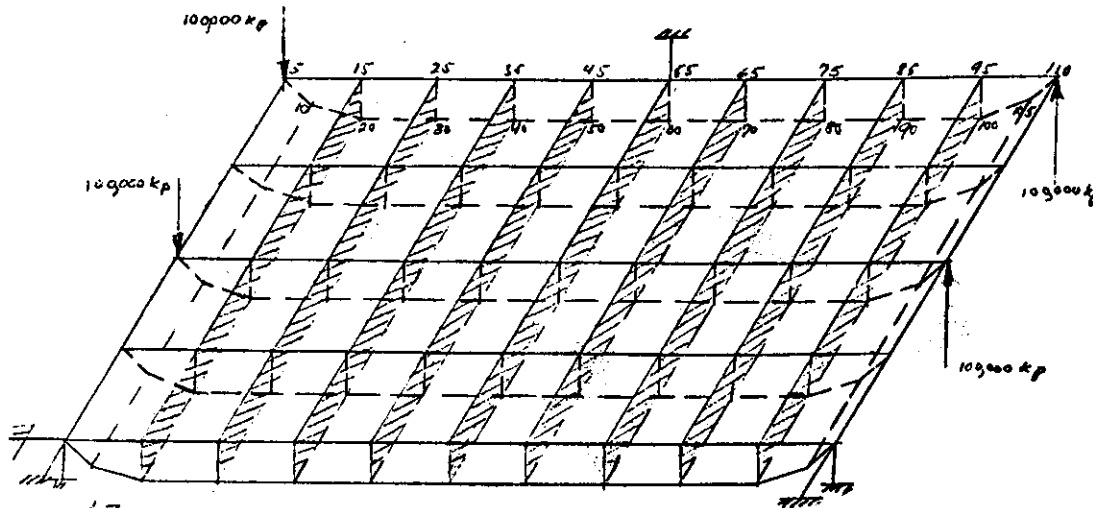


Figure 13. All Side Girders

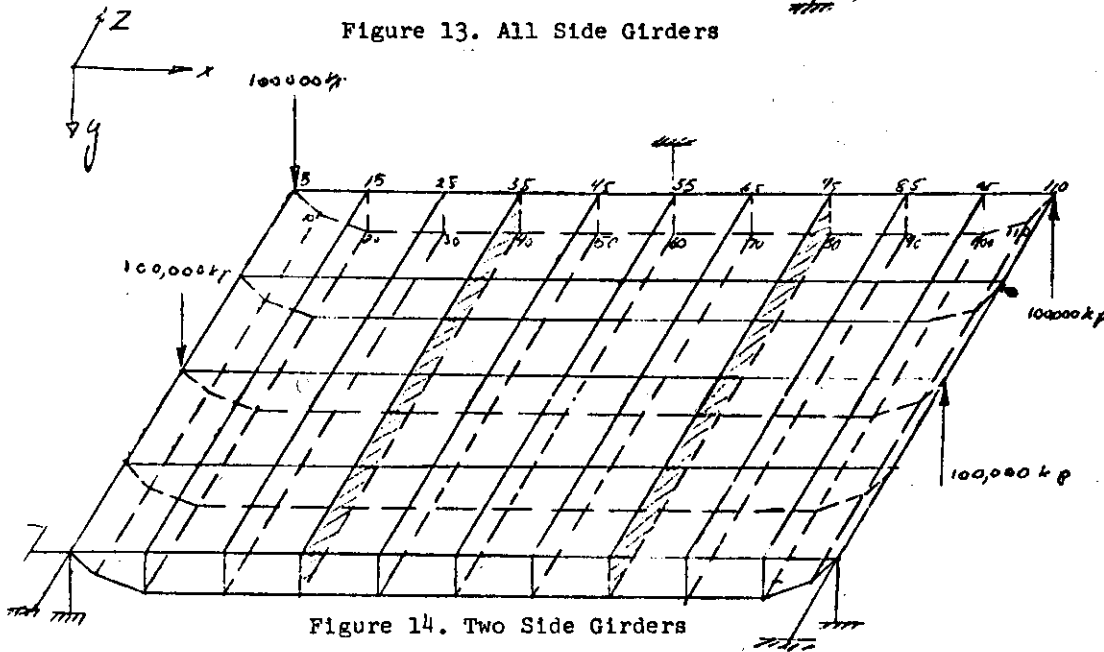


Figure 14. Two Side Girders

Figures 13 and 14 show the mesh, the boundary conditions and the applied loads. The same loading and the same boundary conditions were applied on both structures, yielding the following deflections along the free end, Figure 15.

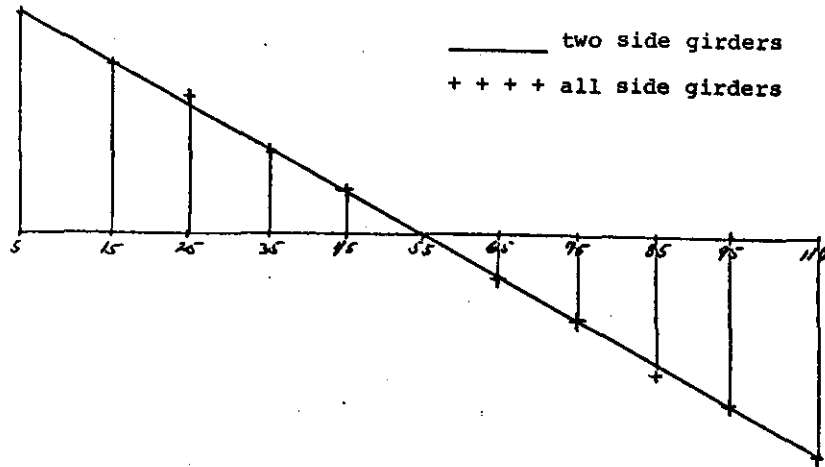


Figure 15. Response Of Bottom Structure

It is interesting to note that the numerical difference in the results are very small. The two points outside the straight line of nodal points 25 and 85 seemed to be caused by the use of spar-elements because no forces in the vertical direction can be transmitted between elements at this point. However, the shear flow due to torsion of the structure is transmitted as it should be, and no noticeable error will occur if this disturbance is neglected.

Both structures were not restrained from warping. However, the importance of warping is relatively small because the section is a closed tube.

From these calculations it can be concluded that the effect of lumping side girders together is very little. Therefore it is justified to make these simplifications on the model.

2. Side Structure. The side structure consists of the hull side stiffened by a grid of frames (regular and deep web) in the vertical direction and a set of three horizontal flats. These flats are, in fact, deep longitudinal stringers. As far as both kinds of frames are concerned their major function is to provide local stiffness of the shell plating. They are not important as far as the primary structural response of the hull is concerned and were therefore not included in the model. The situation with the longitudinal stringers is different. They are primary structural elements and must be accounted for. These stringers were too closely spaced for ease in model construction and it was decided to replace them with only one stringer. One of these stringers is continuous with a deck within the machinery box and it was felt that it was important to preserve this continuity. Straps were placed on four sides of the longitudinal box beams. Their purpose was to reflect the deep stringers inside of the box, so that the section modulus of the ship for both vertical and horizontal bending is correct to the same scale as torsion. As a prefabricated tube of rectangular cross-section was used to model the longitudinal torsion boxes, it was not possible to fit them with interior stiffening. The stringers do, of course, carry warping stresses in torsion too.

The finite element calculations of a midship section described in Appendix A indicate that the structural responses of the ship and model are almost identical.

b. Bulkhead Structure.

In addition to the midship section studies, a separate FEM study of a typical transverse bulkhead was made, since it was impossible to model the myriad of stiffeners which exist in the real bulkhead. A crucial comparison appeared to be the warping restraint offered by a modified bulkhead model. The computations are described in Appendix A, p. A-31.

Deflection and Shear stress distribution results show that it is justified to assume lumping the stiffeners on the bulkhead together, and that that assumption will not change the response significantly.

Construction of the Model

The model was constructed from hot-rolled steel plates of the dimensions given in a previous section. Although cold-rolled steel would have been preferable, particularly with regard to the surface finish (thus easing the application of the strain gages) it was not possible to obtain this steel in the range of sizes required. Even though the model was designed to have a plate thickness three times that required for absolute structural scaling, the plates were rather thin and required special care in construction. Of particular importance was the weld metal deposited. With one exception, all longitudinal welds were made intermittent so that the effect of this weld metal is minimized, particularly with regard to primary bending stresses. The exception is the longitudinal welds joining the hull plating which were made continuous, since it was felt that it would be difficult to get satisfactory intermittent butt welds and that these curved plates might tend to separate under loading. Special care was taken to minimize the added weld metal along these seams.

Figures 16 through 22 show the model in various stages of the construction.

The Test Frame A test frame which straddles the model and provides the loading to the model was designed and constructed. The frame was constructed out of heavy H-beam sections and welded together. A reduced scale drawing of it is shown in Figure 23. Mounted on this frame were a series of "Unistrut" channel sections which were used to attach the pulleys for the loading system and anchors for the ends of the ropes used in loading.

The test frame rested firmly on the concrete floor of the test facility and was carefully leveled.

The Deflection Reference It was desired to measure the deflections of the model as well as the strains at various locations on the ship. This requirement led to special problems since the technique of loading (described in a subsequent section) would not necessarily lead to the same vertical or horizontal position of the model before and after loading. It was decided therefore to mount the measuring reference to the ship itself. A very stiff rectangular aluminum torque tube was designed and constructed which was supported at the bow and stern of the model. The support at the bow was a single ball joint mounted at the ship's centerline (see Figure 24). The vertical support at the stern was provided by two casters riding on flat horizontal plates mounted on the model. The transverse

support was provided by an automotive-type Hotchkiss link arm, provided with two ball joints. One end of this long link was mounted to the model, the other to the torque tube (see Figure 25).

As a result, the references for the displacement measurement were the transverse line connecting the two flat plates at the stern (that is, the deck at the stern) and a straight line connecting the ship centerline at the deck at the stern and that at the deck at the bow. A series of displacement gages were placed at the deck edge at several longitudinal locations along the model and attached to the torque tube. These gages measured the horizontal and vertical displacements of the deck edges.



Fig. 16 - Transverse Bulkhead with Stiffening and Transverse Box

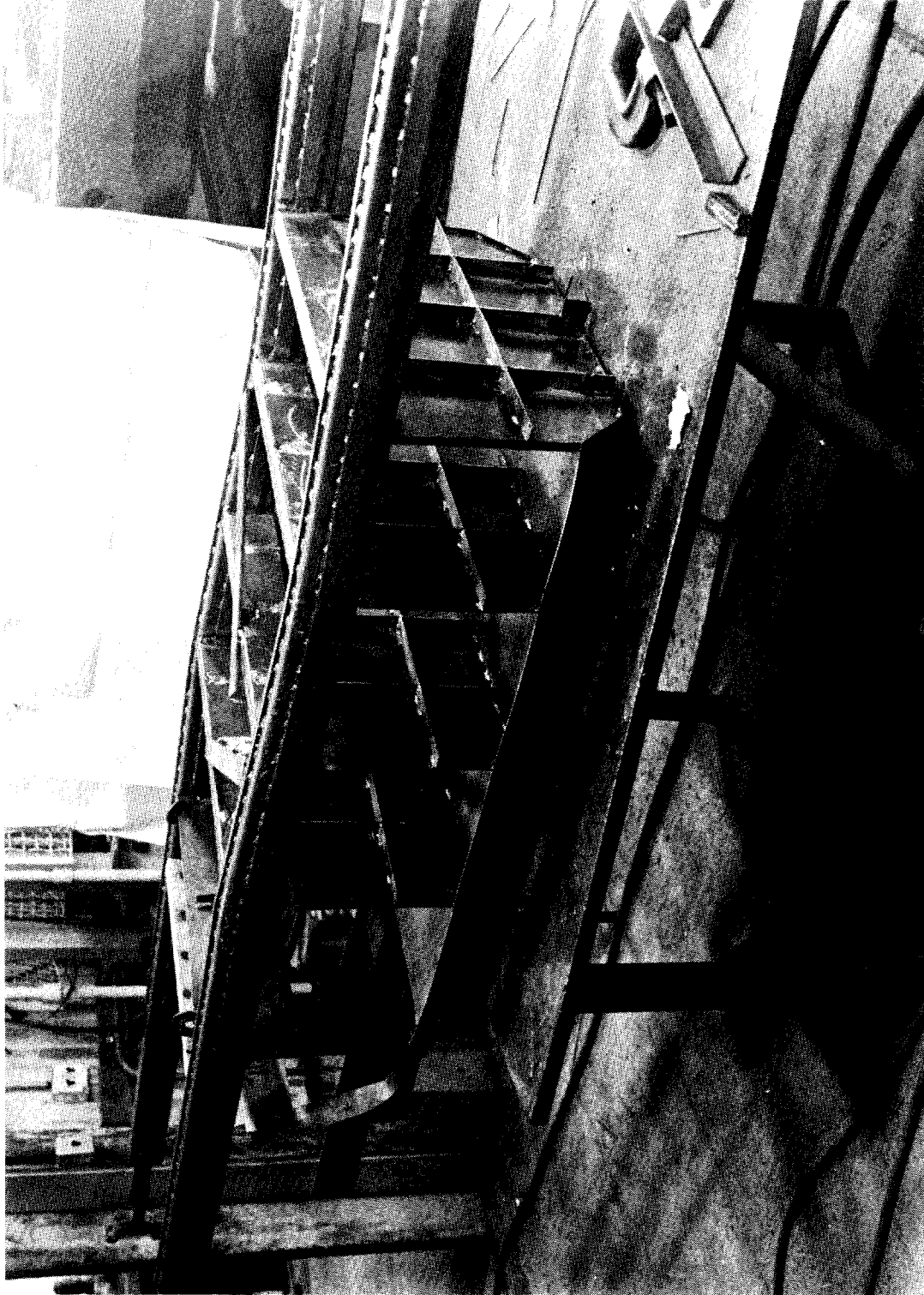


Fig. 17 - Partly Assembled Midship Section of the SL-7 Model



Fig. 18 - Stern Plating Details

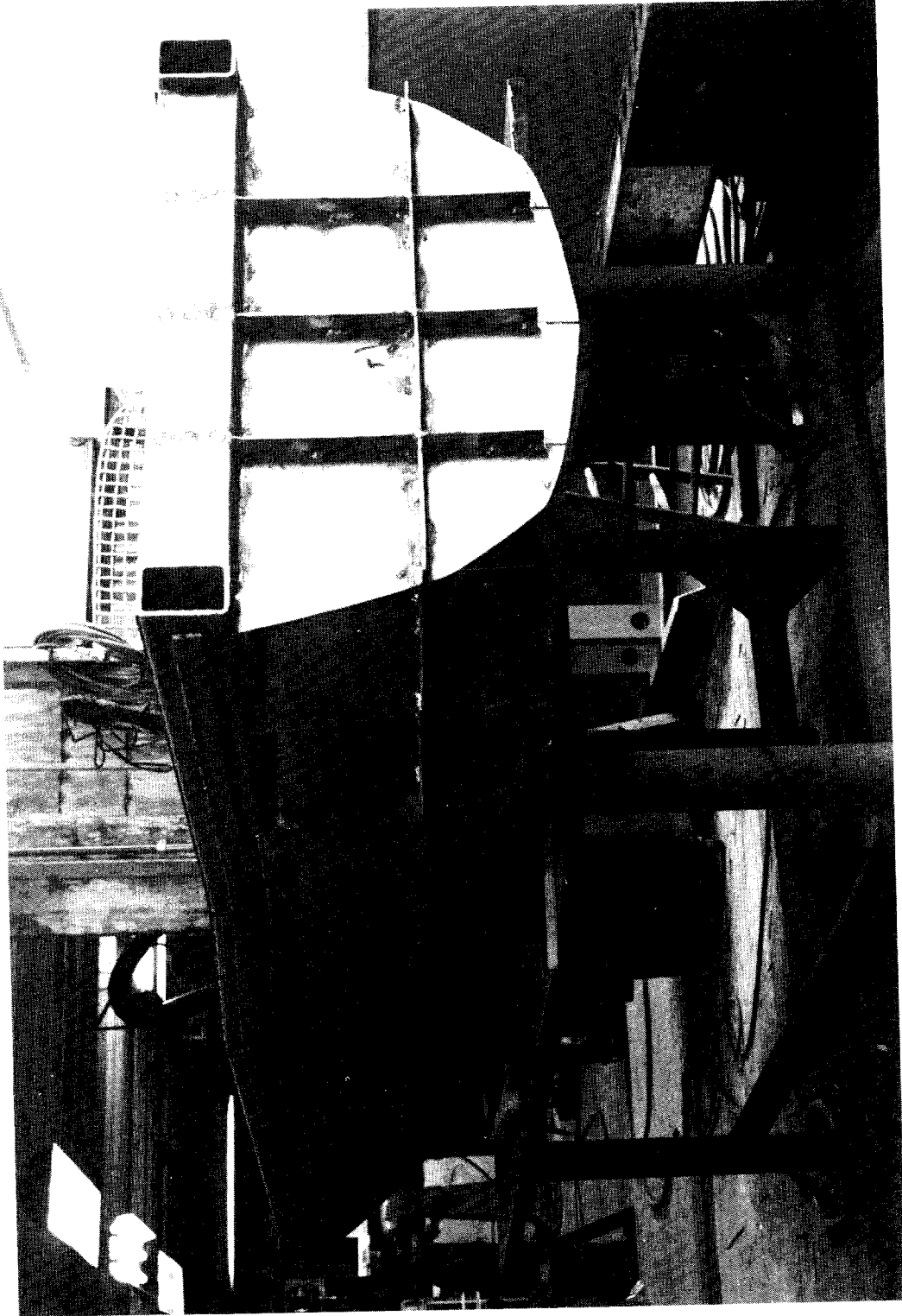


Fig. 19 - Forward Bulkheads

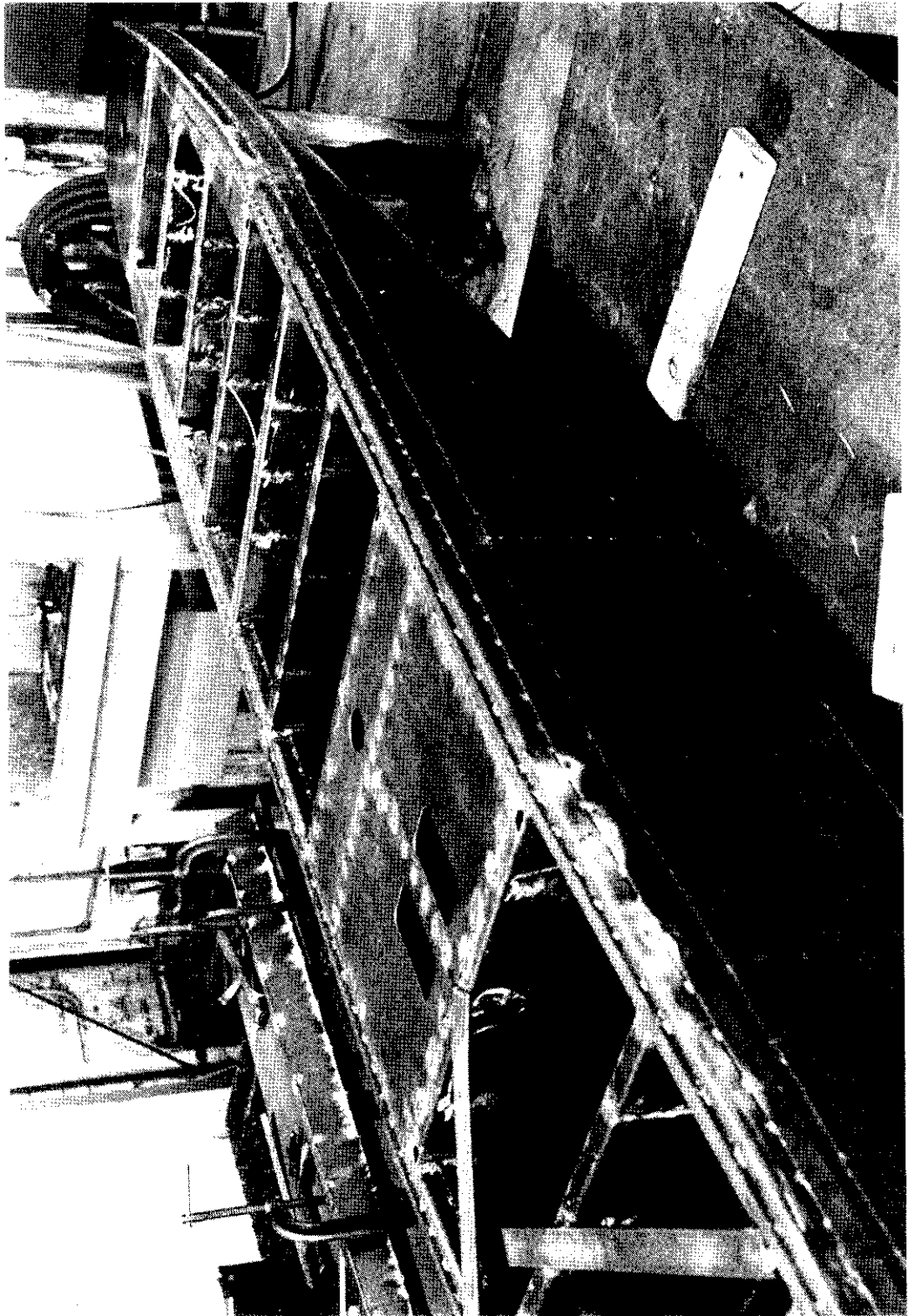


Fig. 20 - Completed Stern Section

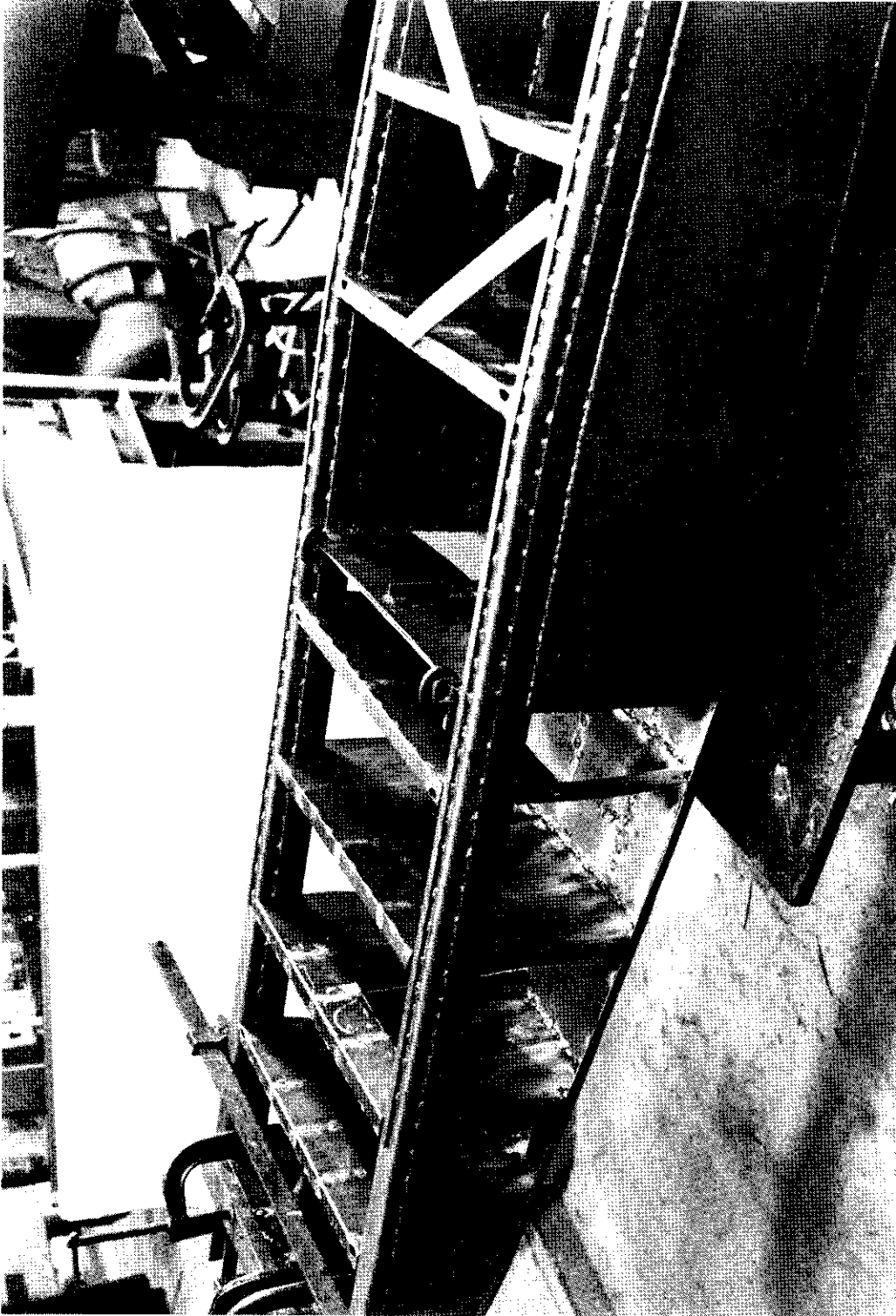


Fig. 21 - Midship Area and Engine Room Bulkheads

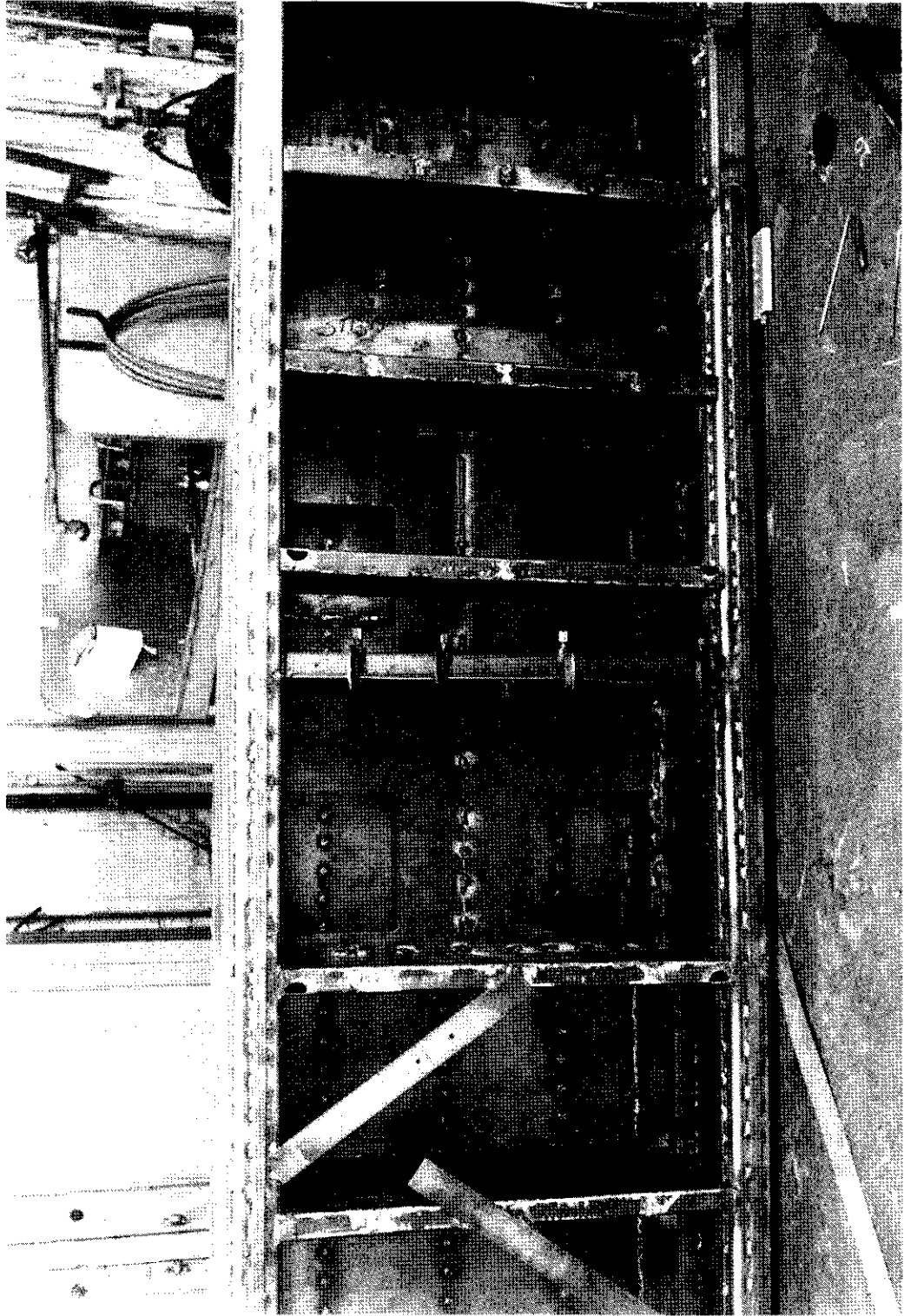


Fig. 22 - Engine Room Flats

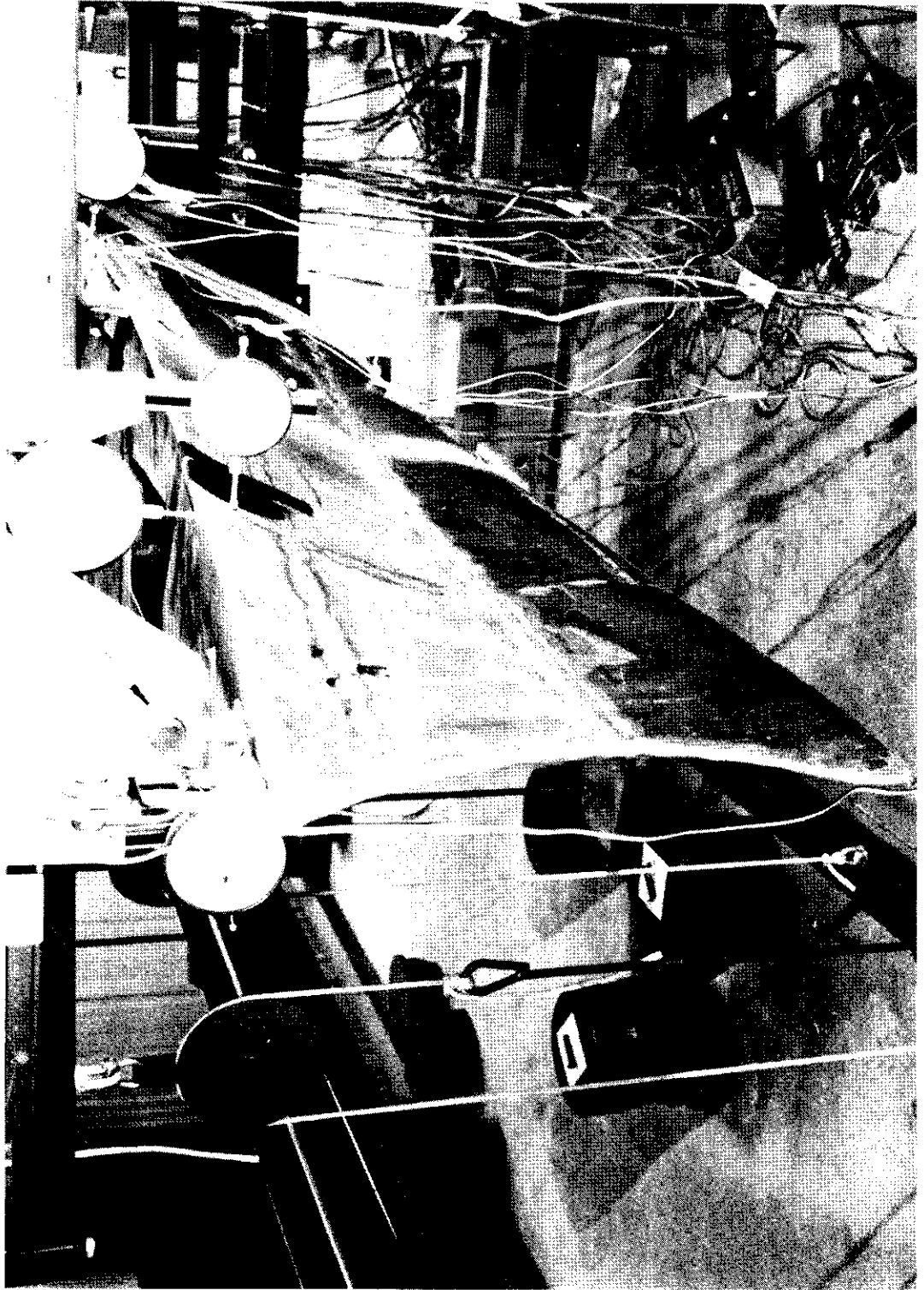


Fig. 24 - Details of Bow Section and Deflection Reference Tube Support

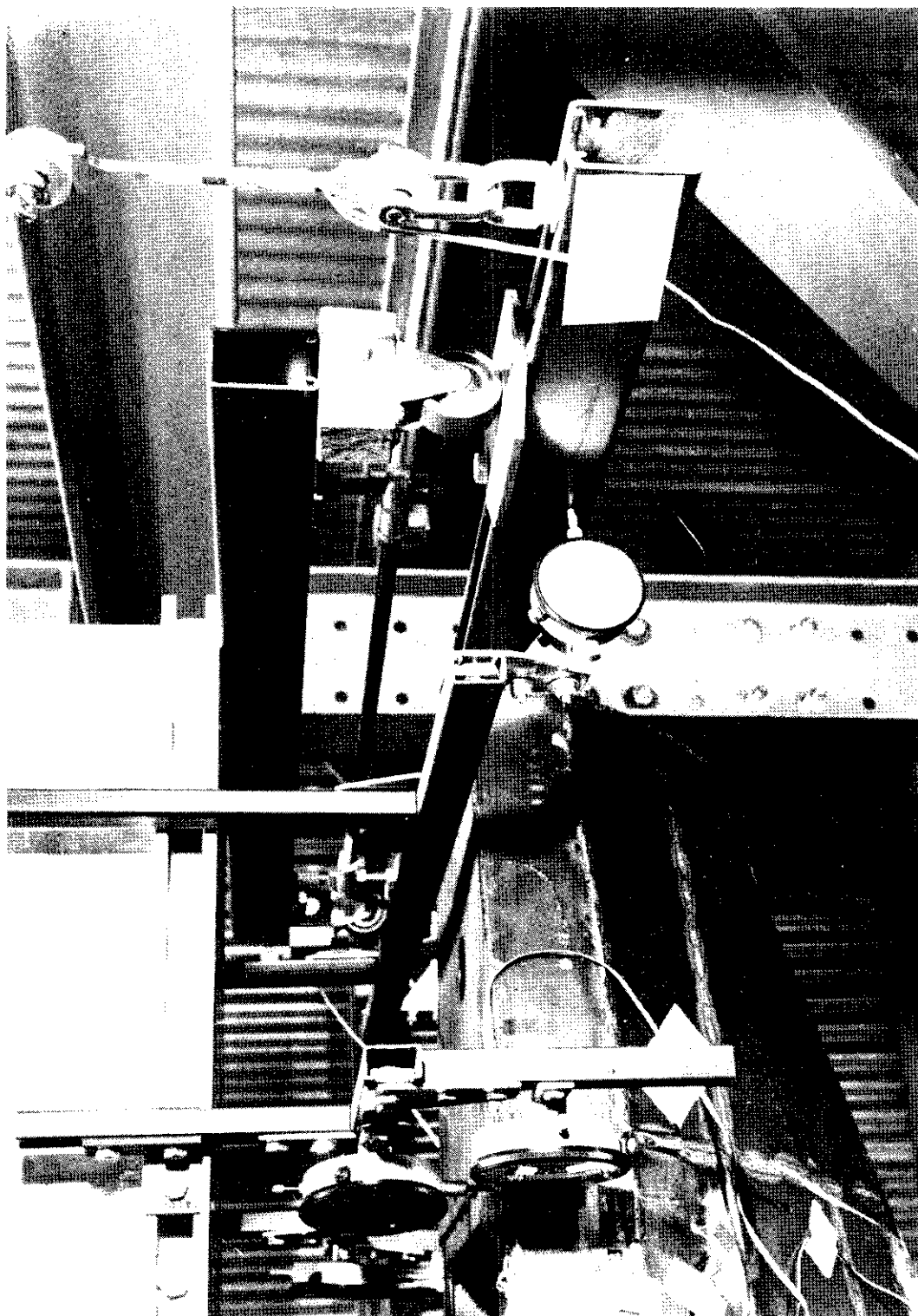


Fig. 25 - Details of Stern Attachments

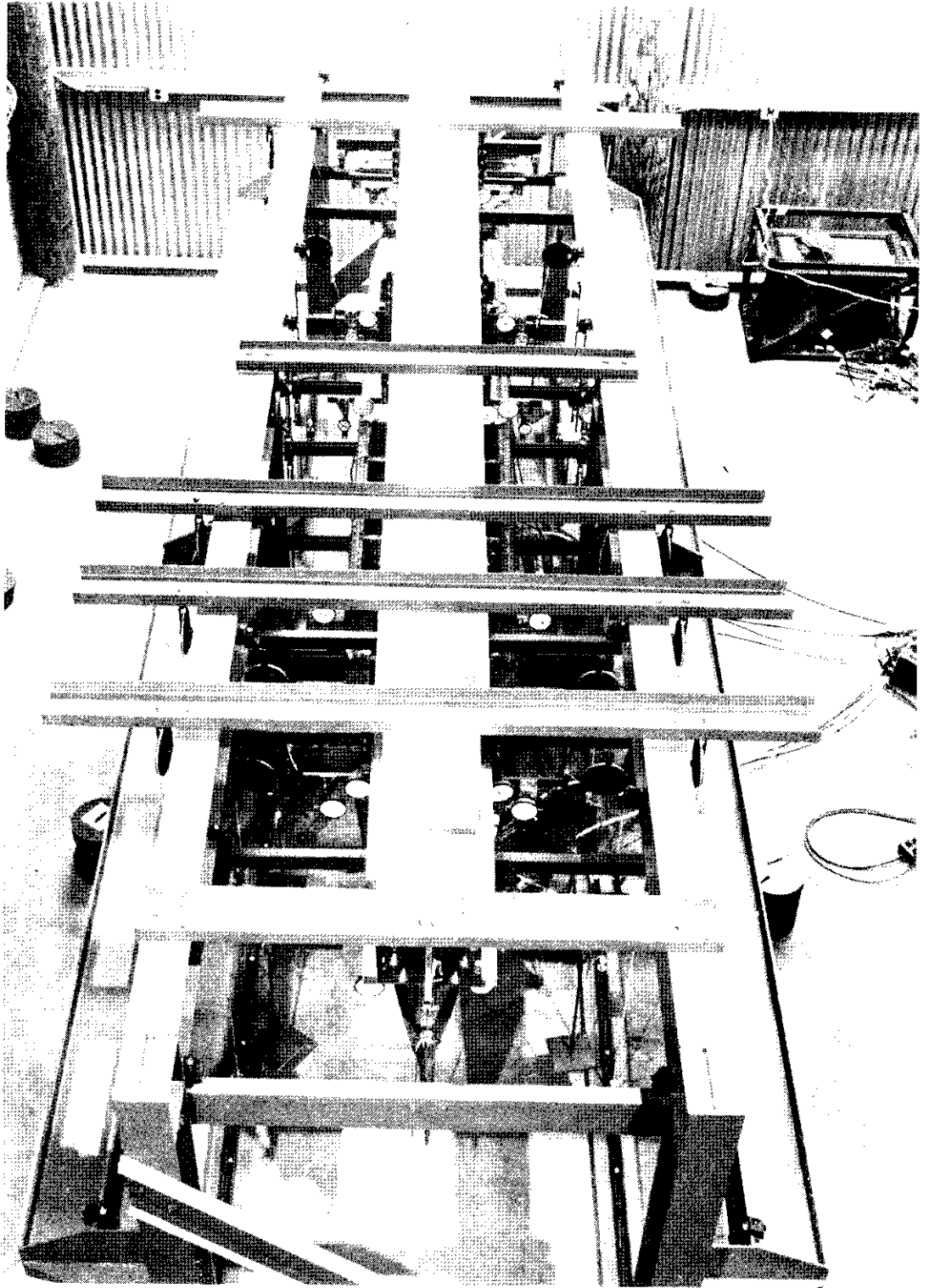


Fig. 26 - Overview of Model in Test Frame

Section III: TEST SETUP AND PROCEDURES

Introduction

In order to subject the structural model to a reasonable set of loads and accurately determine its response, it was necessary to control all aspects of this process extremely carefully if meaningful results were to be obtained at all. The following sections describe in detail the measurement techniques and the loading procedure, including the precautions which were taken to eliminate extraneous loads and strain signals.

Strain Gages

A series of strain gages were placed on various sections of the ship so that several different types of responses could be measured and categorized. Figure 27 shows a profile of the ship and the locations of the gages. These locations were:

a. Frame 10. A series of strain gages were applied on the port side of the ship just forward of the aft-most hatch opening, and two additional gages were applied on the deck just aft of the hatch opening. The gages forward of the hatch were located so that the effect of the warping restraint of the stern could be measured. Four gages were applied to the torsion box at the main deck and additional gages were placed on the side shell and near the keel. One of the gages on the torsion box and two on the side shell were rosettes. The gages on the deck aft of the hatch opening were placed so that the gross effects of any stress concentration due to the hatch could be determined.

b. Hatch corner at Frame 62. In this location the hatch size changes (smaller width aft than forward). The corner of the hatch was instrumented to determine the effects of stress concentration and also the warping stresses developed in the transverse box-longitudinal box intersection.

c. Section Between frames 78 and 96 (5.4" fwd. of frame 78 on the model). This section is at the center of the three full width hatches aft of the machinery box and was chosen because it is a typical aft section. A series of gages were placed around the main deck torsion box, as well as on the side shell, near the bilge, and near the keel. The gages were placed only on the port side. Rosettes were used for most of the gages.

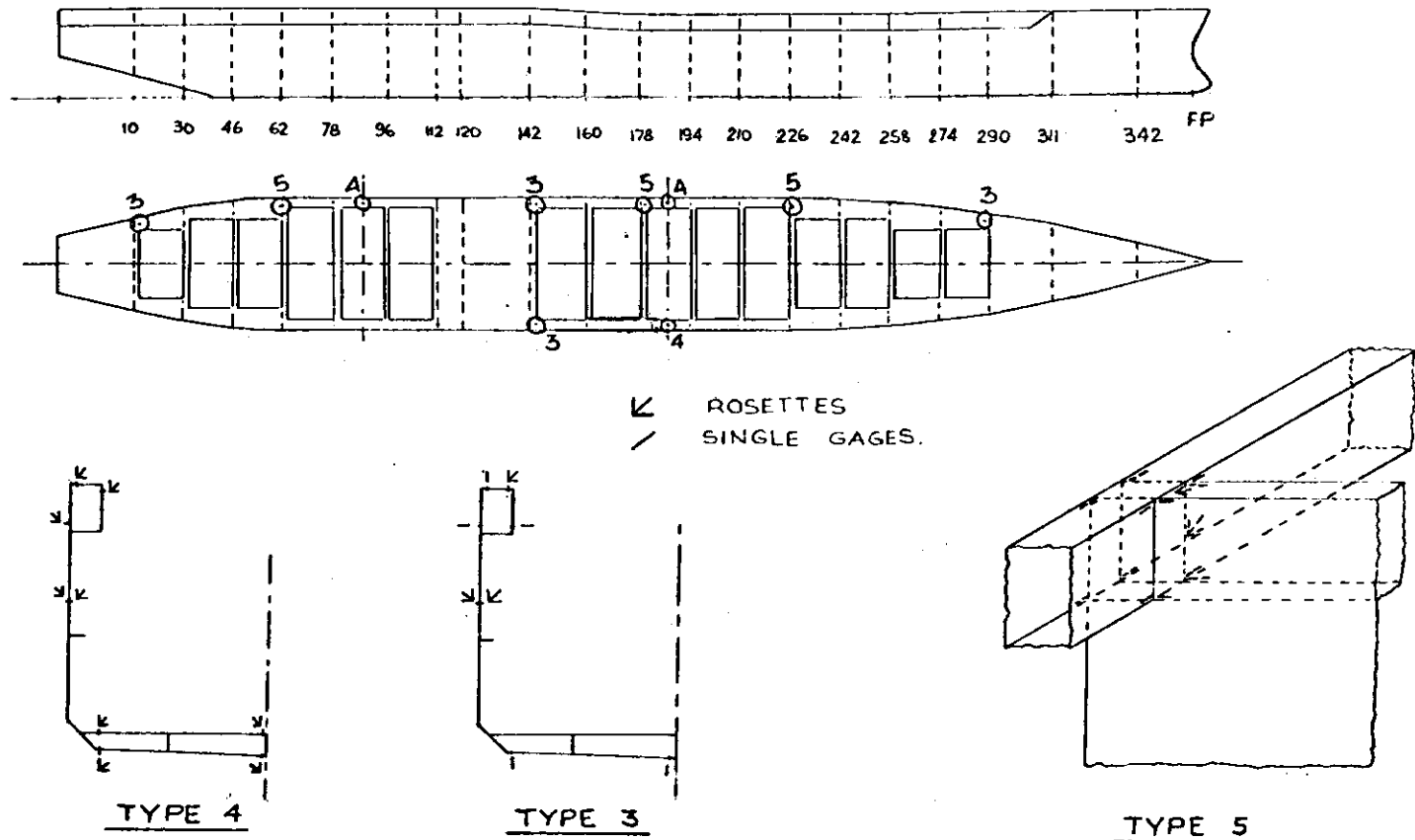
d. Frame 142. The section just forward of frame 142 (2" forward on the model) was completely gaged, port and starboard. The major purpose of this instrumentation was to determine the effects of the warping restraint offered by the machinery box on the open sections forward of the box and to determine any gross stress concentrations due to the dramatic change in geometry at this location. Both port and starboard sides were fully instrumented with several of the gages being rosettes.

e. Hatch corner at Frame 178. This hatch corner is typical of the forward hatches and was instrumented primarily to determine the stress distributions at the intersection of the longitudinal and transverse boxes. Of fundamental interest was the warping restraint offered by the transverse box.

f. Section Between frame 178 and 194. This section is almost exactly amid ships and was, by far, the most instrumented section of the ship. Strain gages were placed port and starboard, internally and externally. Many of these gages were rosettes so that the complete state of strain could be determined. Gages were placed around the torsion boxes and in the inner bottom in order to determine the free torsion response of these closed tubes.

g. Hatch corner at Frame 226. At this section the hatch size changes and the corner was instrumented in the same way as the hatch at frame 62 (see b. above.)

h. Frame 290. This section was instrumented to determine the warping restraint of the bow section in a fashion similar to the section at frame 10 (see a. above).



PROPOSED ARRANGEMENT FOR MEASURING STRAIN AND DEFORMATION.

- ① Vertical displacements of deckedge over the total length → angle of twist → measured by dial gages.
- ② Horizontal displacements at deckedge → measured by dial gages.
- ③ Warping stresses at hatch corner.
- ④ Strain gage rosettes for bending and shear stresses.
- ⑤ Stresses at hatch corner.

FIGURE 27. STRAIN GAGE ARRANGEMENT FOR SL-7 STRUCTURAL MODEL

The strain gages used in these experiments were of the foil type (Micro-Measurements #250 BG single component gages, and #250 RA and #125 RS rosette gages). These gages were selected to have a coefficient of thermal expansion the same as the steel plating used on the model. The gages were bonded to the model using Eastman 910 adhesive, after the steel surface was carefully cleaned and etched. The overall size of each of the active elements of the 250 RA and 250 BG gages was $\frac{1}{2}$ " x $\frac{1}{4}$ " and that of the 125 RA was $\frac{1}{4}$ " x $\frac{1}{8}$ ". This means that the larger gages covered an area approximately 2' x 1', full scale, and the smaller gages 1' x $\frac{1}{2}$ ', full scale. It is clear, therefore, that these gages are too large to detect the fine scale variations in stress one might be likely to encounter around a stress concentration.

Figure 28 shows a schematic of the electrical hook-up of each of the strain gages. The gages were set in a bridge configuration and a constant value of 6 volts was applied to the bridge. Measurement of the voltage across the bridge is indicative of the value of resistance (and thus strain) of the gage. The three completing resistors for the strain gage bridge were specially selected, precision, wire-wound resistors. The resistors directly connected to each of the strain gages were chosen to have the same temperature coefficient of resistivity as the strain gages. These resistors were placed next to one another in an insulated box.

As a result of the selection of strain gage type and resistor characteristics, the measurement system was nominally temperature compensated. However, temperature problems did arise for a variety of reasons. First, the completing resistors for the strain gages (see Figure 28) were located in junction boxes below the model. In other words at a different physical location than the strain gage on the model. Whenever significant temperature variations occurred in the room in which the model was kept, it was reasonable to assume that the gages and completing resistors were also at a different temperature. Thus, in this situation false strain readings can occur.

A second and equally important result of temperature variations within the room is the development of thermal stresses in the whole ship structure itself. The matching

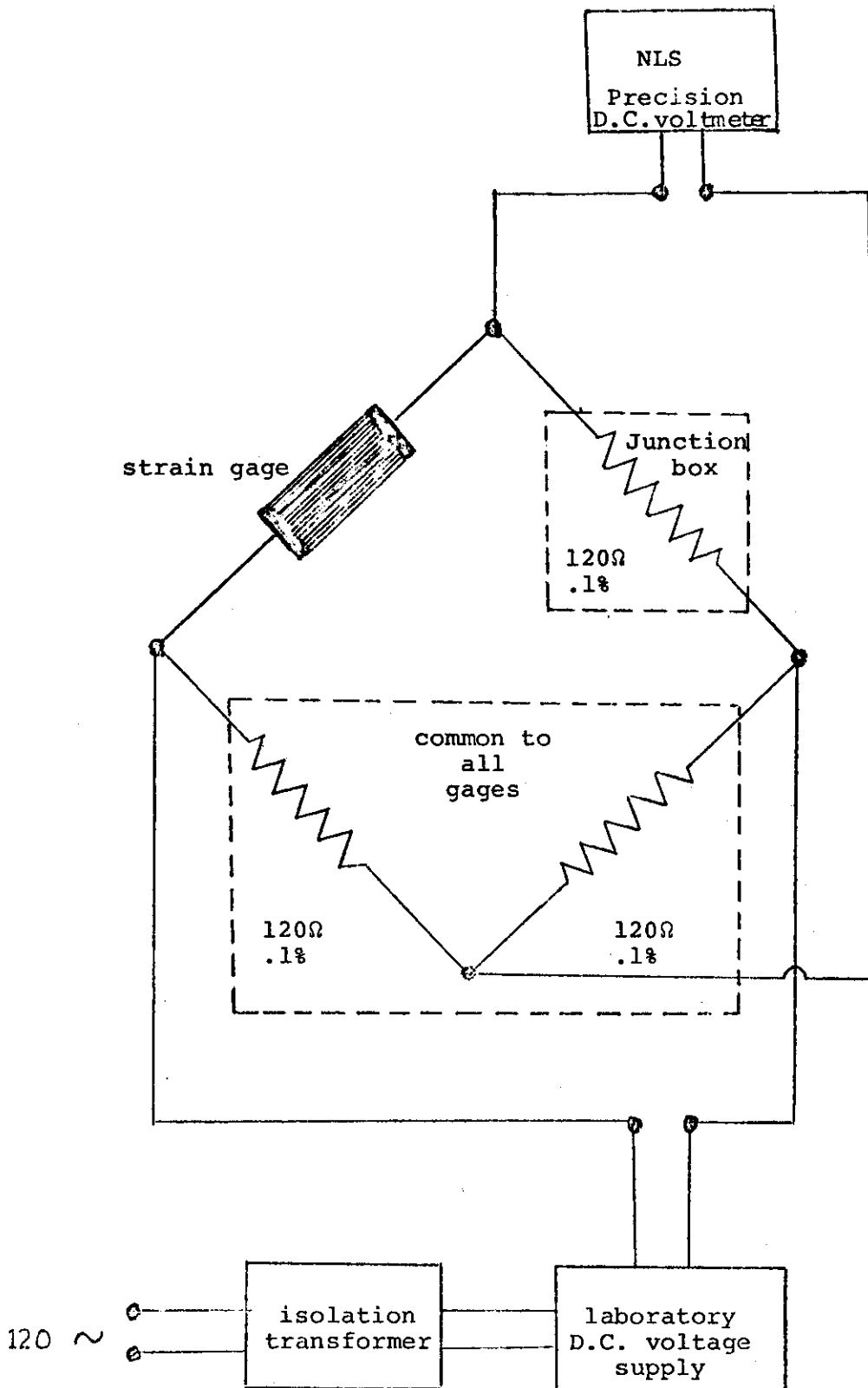


Figure 28. Schematic of Strain Gage Bridge

of the gage and the steel coefficients of linear expansion only assures that no false strains will be read if the whole model undergoes a change in temperature. However, thermal gradients along the model will, in general, lead to significant internal thermal stresses (and therefore strains). This pattern will be superimposed on the strain pattern induced by the loads. There is no known way of sorting out the resulting strain readings short of measuring the actual gradients on the model and computing the thermal strains resulting. This process would indeed be as complicated as computing the structural response of the model and would, in fact, obviate the need for a model in the first place.

Two details of the model arrangement made these two uncompensated thermal effects of paramount importance. The model itself was placed in a room which was not uniformly heated. This was the result of the geometry of the room and the placement of the forced hot-air heaters. Of equal importance was that owing to the model's being constructed of rather heavy gage steel, feasible loadings of the model resulted in very small strains. During a typical test the maximum strains observed were in the order of 100 micro-strain. This is an order of magnitude below the value one might like to achieve during structural model tests. Temperature induced errors of the order of 10 to 20 micro-strain were unacceptable in these tests, whereas they would have been entirely acceptable for more normal structural model tests.

After several attempts were made to alleviate this serious problem of measurement accuracy, only one solution seemed forthcoming. This solution was to test only on cloudy or foggy days which were warm enough so that little, if any, heat was required in the building. On these days, the air temperature varied by only a few degrees during the day and no significant radiate heat loading of the model existed. The latter condition was a problem on cloudless days, since the southwest wall of the steel building in which the model was housed could get quite warm in the afternoon sun. Waiting for "good" days to test caused a very significant delay in the test schedule.

Measurement Instruments

The voltage supplied to the strain gage bridge was typically 6V D.C. Higher voltages were attempted (in order to improve the size of the bridge unbalance) but had to be discarded since they led to problems of heating of the gages. The voltage was supplied by a very heavily stabilized laboratory power supply. This supply was zener diode controlled and produced an output which varied less than 1 millivolt throughout any experiment (an error of less than 0.02%). The leads from the center of each gage-completing resistor pair was led to a Honeywell crossbar scanner. This device permitted automatic, successive scanning of all of the gages. The relays used in the scanner had extremely low resistivity, gold-plating contacts. Throughout the experiments there was no indication of any difficulty resulting from the scanner operation.

The voltage difference across the center of the bridge was measured by a NLS digital voltmeter, capable of resolving one microvolt. In order to obtain this accuracy, it was necessary to use the built-in high-frequency filter (with a one-second time constant). Scanning therefore took place at the rate of about one gage every 6 to 8 seconds. The digital voltmeter was also attached to a teletype terminal through a special serializer. Thus, all of the measurements were printed out and punched out on paper tape for permanent reference.

Figure 29 shows the instrumentation in adding the scanner (lower instrument in rack), digital voltmeter (upper instrument), serializer (middle instrument) and teletype terminal.

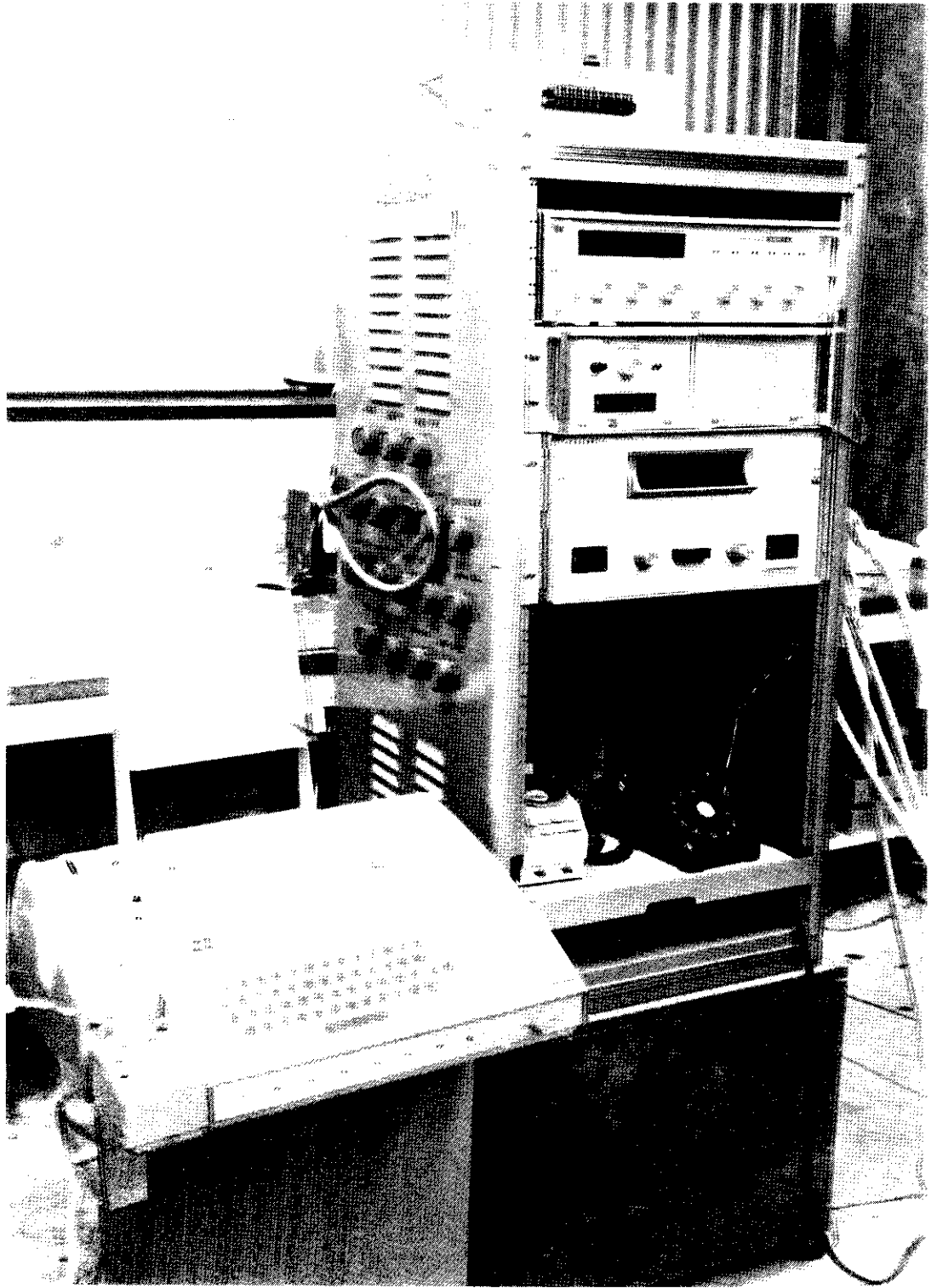


Fig. 29 - Data Acquisition System

Data Reduction

The strain gauge measurements were reduced by a standard digital computer program written explicitly for the purpose by the Civil Engineering Department of the University of California. The microvolt readings inserted into this program were always obtained by subtracting the values read for the strain gauges when no load was applied from those read after the load was applied.

The assumption involved here is one of linearity. Before the loads are applied, the model is not in a state of zero stress. Manufacturing of the model by welding (the model was not annealed) certainly introduced some stresses. The support of the model at both ends leads to a bending moment amidships due to the model's weight, and this implies an additional stress distribution of the model. What is assumed is that the changes in the stress pattern due to the loading is the same as what would occur if the model were originally at zero stress. For an ordinary structure this is true, as long as non-linear problems such as buckling or large initial deformations did not exist. The scaling of the model (the plating thickness three times the geometric scaled thickness) all but precludes any of these non-linear effects. However, the response of the real ship under similar loadings (scaled up to full size) may perform differently, since it is relatively more prone to buckling.

In conclusion, the assumption of linearity is probably correct for the model, but difficulty may be encountered in interpreting these results for the full scale ship, particularly for the very high load cases. In any event, the measured data will demonstrate that linearity is a good assumption for the model.

The Displacement Measurements

Measurements of both the horizontal and vertical motions of the deck edge were made by an array of precision dial gauges located at intervals along the length of the model. These gauges were attached to the aluminum reference frame previously described. Since this frame remained aligned between the centerline of the model at the bow and at the stern the gauges read the deflections relative to this line.

The Loading Arms and Model Attachments

It was necessary to load the model at a finite number of locations rather than to apply distributed loads, as would occur in the real ship. As a result, it was decided to provide these loading locations at bulkheads, since this would best provide for a good distribution of the load around the girth of the model.

Further, the addition of brackets at the bulkheads would least interfere with the structural response of the model, since the model (and ship) have great transverse stiffness at these points anyway. The purpose of the loading bars was to introduce discrete vertical, longitudinal, and twisting loads into the model. In order to introduce a torsional moment into the model two attachment points were required. It was attempted to provide these attachments as far apart as possible so that the local forces would not be excessive.

The locations at which the loading arms were attached were:

- Bulkhead at frame 30 (mounted on deck)
- Bulkhead at frame 78 (mounted on bottom)
- Bulkhead at frame 112 (mounted on bottom)
- Bulkhead at frame 160 (mounted on bottom)
- Bulkhead at frame 210 (mounted on bottom)
- Bulkhead at frame 242 (mounted on deck)
- Bulkhead at frame 274 (mounted on deck)
- Bulkhead at frame 311 (mounted on deck)

From the configuration of the test frame and from the test plan, mounting the loading bars on the ship bottom was preferable. This location provided the opportunity for a 2:1 purchase in the pulley system for both up and down forces, whereas mounting on the deck permitted a 2:1 purchase only for the down forces. Further, it was desired to load the model in transverse bending as well as vertical bending. In order to avoid introducing unwanted torsional moments in the model due to these transverse forces, it was desired to provide all of transverse loads in one plane, at the baseline of the ship. Loading bars along the bottom could then be used for both horizontal and vertical forces. However, near the bow and stern, the bottom was so narrow that it was not possible to locate the bars there. In these locations the bars had to be mounted on the deck. Also, at these locations, additional brackets were welded to the hull at the bottom for supplying transverse loads when these were desired, through the use of additional loading structure.

Great care was taken to assure that the distance between the model centerline and that of the load attachment was the same port and starboard. In this way, when torsional moments were applied to the loading bar (by means of an up force on one side of the bar and an equal down force on the other side), no net vertical forces were simultaneously introduced into the structure.

The bars themselves were manufactured from "unistruts", commercial deep channel sections. A detailed view of the loading bars can be seen in Figure 30.

The attachment of the bars to the model was by means of simple bolts. The holes in both the loading bar brackets and model-mounted brackets were purposely drilled somewhat oversized and the bolts were not tightened very securely. This procedure assured that the loads were introduced in a statically deterministic fashion, with no locked in loads.

In the case of the largest bending moments applied to the ship, the loads on the two center loading bars were so large that an appreciable twist of these bars occurred. In the special situation, a structure between these two loading bars was added which prevented their individual twisting. Since the attachments to the model were somewhat loose, this intervening structure caused no redistribution of the loads.

The Loading Method

A series of weights for loading of the model were manufactured from ordinary hot-rolled steel. These weights were disks approximately 13 inches in diameter with a slot cut in them for the support. Disks of three thicknesses were manufactured: 0.25", 0.50", and 1.00". These disks were to have the nominal weights of 5, 10, and 20 pounds, respectively. However, since the disks were cut (using an acetylene torch) from the raw steel plate, variations did occur. Each weight was carefully weighed to within 0.01 lb. and the exact weight was stamped onto the disk edge. In this way a combination of disks could be carefully selected to obtain any given weight. A total of 6000 pounds of disks were manufactured and certified in this way.

The loads were applied to the model through a nylon rope which ran over a series of pulleys, some attached to the test frame itself, others to the loading arms. One end of the nylon rope was attached to a weight pan, in which the steel disks were stacked. The pulley system was arranged so that no more than a 2:1 mechanical advantage was achieved. It was feared that any larger purchase would lead to intolerable friction losses within the pulley system. All of the pulleys were precision type with either ball or aircraft-type needle bearings. Figure 30 shows the pulley arrangement, weight pans, and loading bars near the bow of the model. The two loading bars on the left have a 1:1 purchase; that on the right has the loading bar below the model with a purchase of 2:1. A separate pulley arrangement was made for up forces than for down forces at each loading arm.

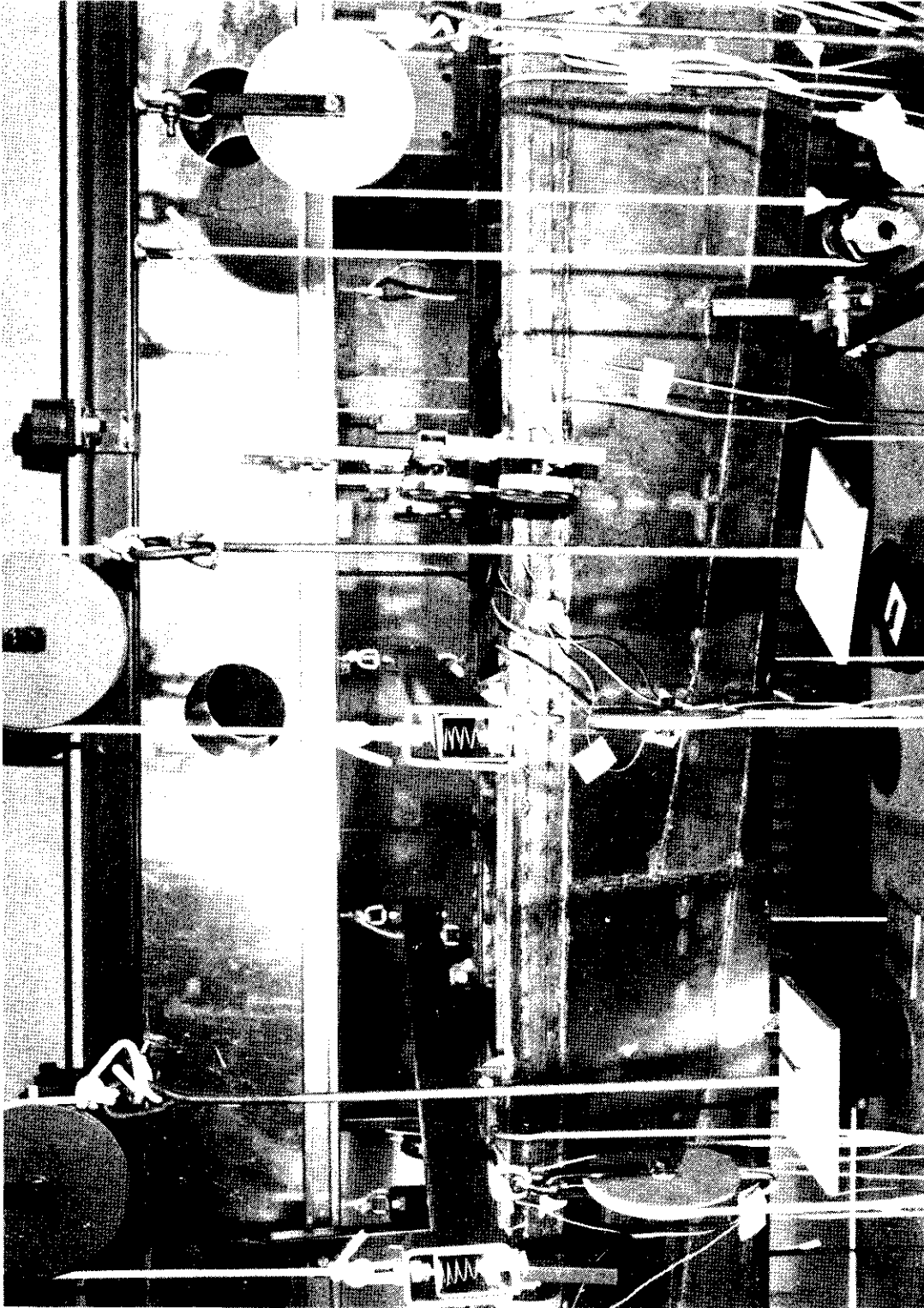


Fig. 30 - Details of Weight Pans and Pulleys

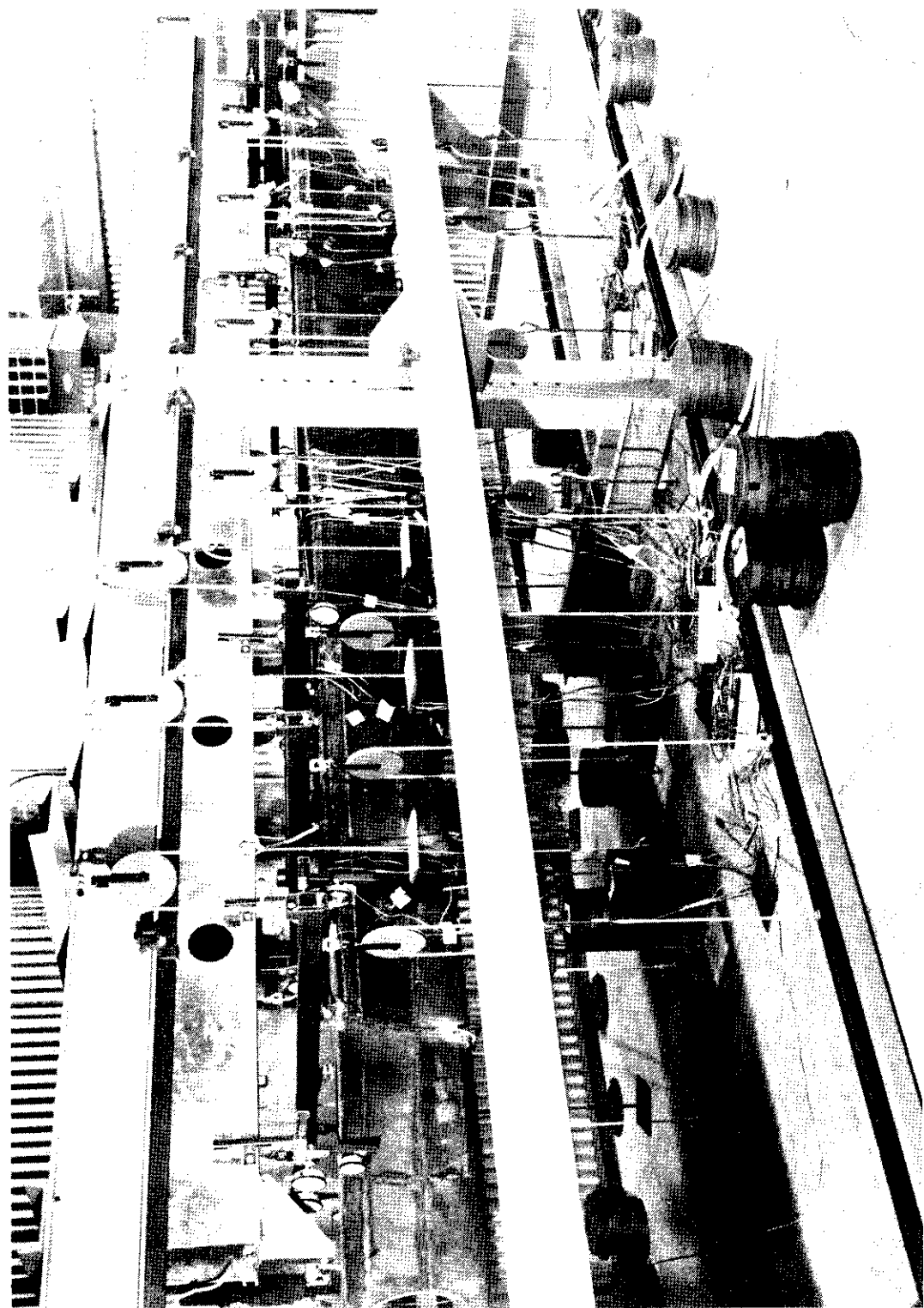


Fig. 31 -- Model Prior to Test

For any given loading the weights were selected and stacked in front of the appropriate pan. The loading of the model was performed as quickly and as evenly as possible to avoid any local overstressing. That is, a few weights were added to each pan all around the model and this procedure was continued until all the loads were applied. As an extra precaution, the model was vibrated to eliminate any residual pulley friction. Figure 31 shows the model just prior to a test with all of the weights set out.

Model Support

When a ship floats in the water, it is in stable equilibrium with regard to vertical motions. That is, the weight of the ship is exactly counterbalanced by the vertical hydrostatic force distribution, and no external forces are required to maintain this position. It is difficult, or even impossible, to duplicate this arrangement in the model scale. First, since the plating thicknesses are not scaled in the same proportion as the overall dimensions of the ship, the ship is too heavy for immersion into water. The use of other liquids, such as mercury, bromine, etc. would be too dangerous. Second, it is difficult to work with electronic equipment such as strain gauges in any kind of wet environment.

It was decided, therefore, to simulate the model floating without requiring support from a liquid. The model was attached to the test frame by three load cells, manufactured in the same way as one manufacturer's tensile test specimen. One of the two stern cells can be seen clearly in Figure 25 and the bottom of the bow cell can be seen in Figure 24. The applied loadings to the model were calculated so that they would reflect the floating condition. That is, so that they would require no net vertical force or moment for equilibrium. Before the model was loaded, the stresses in the load cells reflected the three forces necessary to support the model. After loading,

if these three forces remained the same, then this implied that the loading did correspond to a realistic seaway loading system: that is, one which does not require external loads for equilibrium. Further, since the initial loadings were specifically chosen to reflect the floating situation, confirmation of this by means of these load cells demonstrates that the weights used were correctly selected and that the pulley friction had been effectively eliminated.

In about twenty of the early tests (before meaningful data were obtained) this check was performed and the loadings confirmed. During the later tests, efforts were made to develop the maximum structural response of the model and, in order to do this, it was necessary to provide a simple support of the ship bow and stern. The load cells were not of sufficient capacity for this purpose and were thus not attached. These end reactions were calculated from statics instead. Clearly, our earlier experiments demonstrated that no difficulties were encountered with the pulleys. Accordingly, the only checks performed for these tests were double-checking of the weights.

The Test Procedure

Before any particular test was performed, the type of loading was analyzed and the exact weights to be used at each loading station determined. The appropriate weights were assembled near each weight pan. The electronic power supplies and meter were left running for at least 24 hours before each test so that no problems with a lack of steady state heating of the strain gauges occurred.

The first step in the actual test process involved the reading of all of the dial gauges and strain gauges in their initial state. This took about 30 minutes. The weights were applied to the model in a distributed fashion (as described above). When all of the weights were on the weight pans, the model was vigorously vibrated to eliminate, as much as possible, any effects of static friction in the pulleys. After about 10 minutes was allowed for the model to relax, the next step was performed. The second step involved a reading of all of the dial and strain gauges for the loaded model. Following this (usually performed twice to guard against any reading error), the weights were removed and the first step, above, was repeated. Rereading the dial and strain gauges provided an indication of significant drifts of the instrumentation or, more likely, significant thermal effects occurring during the test.

The data reduction of the strain gauges was done by taking the difference between the average loaded readings and the average unloaded readings. This process eliminates linear time drifts of the readings. Further, whenever the difference between the two loaded readings of any one gauge (taken before and after the application of the load) was larger than 20 percent of the average measured difference due to loading, the point was thrown out. That is, it was required that the non-repeatability of the gauge zero be no more than one-fifth of the net gauge reading.

No similar problems occurred for the dial gauges and thus no such procedure was required for them.

Section IV. TEST PROGRAM

Introduction

The purposes of the test program were many. Of course, it was desired to characterize the structural response of the ship under a variety of different loading conditions. However, before such test results can be relied upon, sufficient tests must be performed to demonstrate that the model is constructed properly, that the strain gauges are working, and that the data reduction program is working. At one point or another during the early testing of the model each of these possible pitfalls was uncovered and corrected. The overwhelming difficulty was the thermal stress problem mentioned in the previous section. This, too, was overcome.

The model test program was then divided into two major parts: a demonstration phase and a combined loading phase. During the demonstration phase, the model was subjected to a series of simple loadings, such as vertical bending, wherein the structural response could be quite well characterized in advance. In the case of vertical bending it is reasonable to assume that Navier theory will apply. The combined loading phase concentrated on typical combinations of expected loadings wherein no simple known solution would be adequate; for example, a combination of horizontal bending and torsion.

The demonstration phase also concentrated on another feature of the basic assumptions, that of linearity. It was necessary to assume linear structural responses to develop the model and to reduce the strain gauge readings. As a result, a series of tests incorporating similar loading distributions but with differing magnitudes and signs were conducted to demonstrate the linearity of the response. Any non-linearity would indicate buckling, or more likely in this case, large initial deformations of the structure due to welding.

A major part of the emphasis of the combined loading phase was to develop a picture of the response of the structure to antisymmetric loadings, i.e., torsion and horizontal bending. In the full-scale ship, if stresses are measured at the same locations port and starboard, it is possible to separate the effects of vertical bending from those due to the combined action of horizontal bending and torsion by a symmetry argument. There is no practical way of taking full-scale measured raw data and separating the individual contributions of the last two effects. Of particular importance for this container ship is the torsional response and the effect of warping restraints afforded by the bow, stern, machinery box, and the many transverse deck box beams. At sea one obtains only combined horizontal bending and torsion and, as a result, it is impossible to answer the question of torsional response directly from the at-sea measurements. The tests here involved separate loadings of the model under torsion alone and horizontal bending alone, as well as tests combining these loadings. An additional test series including all three loadings, lateral and horizontal bending as well as torsion, was performed.

Finally, an additional set of tests was conducted in which the ship was subjected to a torsional loading comparable to the dockside trials.

The Test Program

The test program was the following:

- i. Demonstration Phase
 - a. Vertical Bending
 - b. Lateral Bending
 - c. Large Midship Shear
 - d. Torsion
- ii. Combined Loadings
 - a. Lateral Bending and Torsion
 - b. Longitudinal Bending, Lateral Bending, and Torsi
- iii. Dockside Torsion Trial

At least two tests of each of these combinations were performed by reversing the sign of the loads. In addition, several tests were performed using half of the required loads (both signs) so that linearity could be tested. The individual results of each of these tests were submitted to ABS as they were performed and the data reduced. Accordingly, these individual run data will not be presented here. The data of similar runs have been combined into comparable data and these are presented in Appendix B. The subsequent section will discuss these results in detail.

Section V. THE TEST RESULTS

Introduction

The test results in Appendix B are combined into five different groups:

1. Vertical Bending
2. Lateral Bending
3. Large Midship Shear
4. Torsion
5. Combined Lateral Bending and Torsion

For each of these groups that data is presented in a similar fashion. First, the model scale loading actually used in each individual test is presented. This includes the weights used, the mechanical advantage of the pulley system employed, and the net force on the model. The loading is integrated to show the shear and bending moment distribution, or for the case of torsion, the torsion moment distribution. Following this is a series of sectional views of the model at each of the measuring stations on which the various stresses are plotted. The principal stresses measured were longitudinal normal stresses and shear stresses. The plots are arranged so that if the model responses were absolutely linear and if no reading errors were encountered, all the points would fall on top of one another. Finally, the measured vertical and horizontal deck edge deflections are presented both in tabular and graphical form.

Vertical Bending

A series of tests of the vertical bending response of the model were performed. In these tests the model was simply supported at the ends so that very large midships bending moments could be developed. It was discovered after the tests were performed that the vertical bending moment distributions for the model were almost, but not exactly, similar. As a result, the data presented here has been normalized in a special way. The measured stresses were divided by the local bending moment at each station. If Navier bending applies, then this ratio would be constant

and equal to the inverse of the section modulus at each location. That is, the resulting values should be equal to y/I where y is the distance from the neutral axis of the station to the point in question and I is the moment of inertia of that station. The three tests that were performed are:

<u>Label</u>	<u>Max. Bending Moment(B.M.)</u>	<u>Sense</u>
(-) Large B. M.	325,725 in/lb.	hogging
(-) $\frac{1}{2}$ Large B.M.	170,480 in/lb.	hogging
(+) $\frac{1}{2}$ Large B.M.	170,480 in/lb.	sagging

In examining the bulk of data one sees that most of the points lie on top of one another or nearly so, indicating good linearity and repeatable measurements. The following are worthy of special note.

1. Section 2 inches forward of Frame 10. The results for this section show an almost linear variation of longitudinal stress with depth, indicating a nearly perfect elementary beam theory distribution. Of particular interest is that the two gauges located about one inch aft of Frame 10, that is, aft of the hatch opening, indicate a stress level almost twice that in the box beam just forward of the hatch. Further, the inboard gauge indicated yet a further increase over the outboard gauge, presumably indicative of a stress concentration around the hatch opening itself.

2. Section 2 inches forward of Frame 142. This section was instrumented both port and starboard so that the effects of symmetry could be noted. In both port and starboard sides there is a slight bending of the line connecting the longitudinal stress point in the neighborhood of the main deck. There is also an increase in stress across the deck edge box beam. It is felt that both of these effects are a reflection of shear lag effects caused by the drastic change in section occurring here, that is, because of the change from the closed machinery box to the open hatch. The stresses on the bottom are relatively constant, but with an apparent dip in the center, again presumably due to shear lag effects.

3. Section between Frames 178 and 194. This section is the midships section and was the most highly instrumented section. The longitudinal stress distribution is almost linear along both sides, but the distribution is not as symmetric as that of 2. above. In particular, the rosette on the starboard bottom bilge (gauges 87, 88, 89) appeared to lead to a much lower longitudinal stress reading. This gauge was replaced no less than five times in an attempt to improve readings in this area, but to no avail. It must be concluded that some manufacturing defect exists in this neighborhood, although none was apparent. The stress distribution on the bottom of the model on the starboard side shows the lower stress pattern behavior. The port side does appear to behave as one would expect for Navier bending. The measured stresses on the tank top also appear reasonable on the average. It is not known why the stress near the centerline is about 20 percent less than that near the edge.

4. Section 1 inch aft of Frame 290. This section clearly demonstrates Navier bending.

In conclusion, one can see that the data are very repeatable and consistent. With the exception of a small area on the starboard amidships bottom, the stress pattern is very nearly that predicted by elementary beam theory.

Lateral Bending

A series of tests were run in which the lateral bending response of the model was tested. In these tests the ends of the model were free, so that no end restraints were necessary. Two tests were performed, in one of which the bending moment deformed the midship section to port (relative to a line between the bow and the stern) and in the other the midship section was bent to starboard. The model is much larger in beam than it is in depth, and as a result the stresses measured were quite small. Further, since the loads were applied at the base line, (the loading holes were all located within 1/32" of the base line) some torsion was introduced because the shear centers of the oper

sections were below this line and those of the machinery were above this line. In order to put the stresses on a comparable basis, the stresses for the lateral bending moment were changed in sign. If the readings were exactly repeatable, then the points would fall on top of one another. The following sections are of special interest.

1. Section 2 inches forward of Frame 142. The longitudinal stresses show fairly good symmetry and repeatability considering the very low magnitude of strains. Again elementary beam bending theory seems to be a reasonable approximation of the situation with nearly constant stresses in the sides and a linear variation of stress in the bottom.
2. Section between Frames 178 and 194. Elementary beam bending theory appears to be exhibited here, but the discrepancy on the starboard bottom still persists. The shear stress distribution also is close to that predicted by beam theory, but these stresses were so low that it is not possible to draw many conclusions from them.
3. The deck edge deflections. The horizontal displacements of the deck edge appeared to be reasonable, if somewhat small. The vertical deflections were vanishingly small.

Large Midship Shear

Both the vertical and horizontal bending loadings discussed above did not lead to large shear stresses within the structure. In order to validate the shear response of the model, a loading was developed which yielded a very large vertical shear amidships. The loading was performed twice, once with the opposite sign of shear to the other. The resulting stresses were plotted by reversing the sign of one run so that the stresses would be comparable.

In this case, the end of the model was simply supported so that a larger midship shear could be obtained. The end reactions due to these supports were calculated by statics. Except at midships, a very substantial bending moment also occurred, so that at other stations a substantial Navier bending pattern could be observed.

At the midship station (between Frames 178 and 194) the longitudinal stresses are very small all around the periphery. This is an indication of the small bending moment in this region. Since this is a symmetrical loading, the shear stress distribution should likewise be symmetrical. Further, the shear stress should become zero at the top of each side and also at the centerline at the bottom, again, from symmetry. For the most part all of these conditions are met. An exception is the starboard bottom which has positive shear stresses when, from symmetry, it should have negative stresses. This is the same region which produced incorrect results in the other simple loadings.

As expected, the model deflected very little in the horizontal direction, but did deform with an "S" shape curve in the vertical direction as expected.

Torsion

A series of four experiments were performed in which the model was loaded in pure torsion. The loading was performed so that the ends of the model were free of load and it was unnecessary to provide any end supports. Two of the tests used a distribution which yielded a maximum torque of 93,000 in/lbs. amidships (one test of this was a clockwise moment, the other test was a counterclockwise moment). The remaining two tests used distributions similar to the previous distributions, but with a maximum torque exactly half that of the previous two cases. The results of these four cases should correspond exactly if one accounts for the signs and factors of two. This arithmetic has been performed in a way such that the data points presented in Appendix B should fall on top of one another, if the tests and electronics were perfectly repeatable.

The following aspects of the presented data are worthy of note:

1. Section 2 inches forward of Frame 10. Although the distribution of loads leaves this section free of load, there are small but not negligible longitudinal stresses here. These stresses in the side shell and in the torsion box indicate that the stern section (itself a closed box) is offering a considerable amount of warping restraint to the twisting of the forward part of the ship, which is under load.

2. Section 5.4 inches forward of Frame 78. This section is roughly in the center of the three full width hatches aft of the machinery section. The gauges indicate a significant shear stress around the section, which one would expect in this situation.
3. Section 2 inches forward of Frame 142. At this section, the longitudinal stresses in the side shell are linearly distributed with depth, indicating significant bending of the shell. This means that the machinery box is affording a considerable amount of warping restraint. Also, the longitudinal stresses in the torsion box at the deck edge are very large. The stress pattern in this box indicates a significant amount of transverse bending of the box, further indication of the warping restraint offered by the machinery box. The overall response of this section is nearly antisymmetric, as it should be.
4. Section between Frames 178 and 194. Here the longitudinal stress pattern is rather less linear in the side shell, indicating a somewhat reduced effect of warping restraint. The antisymmetry is nearly preserved again, however, the outboard bottom gauge again yields stresses not in keeping with the rest of the stress pattern. The shear stress pattern indicates that both the side shell and the closed tubes are participating nearly equally in response to the loading.
5. Section 1 inch aft of Frame 290. The response of this section is similar to that of Station 10 near the stern. There is no torsional load in this area, but the linear distribution of longitudinal stress indicates that the closed box section is offering a large warping restraint. Notice also that the stresses in the deck edge torsion box are large and vary in sign between the deck at side and the hatch. This indicates a very strong transverse bending of the box in this area and evidence that the warping restraint of the bow includes not only the side shell but the torsion box as well.

The deck edge deflections under this loading give a good picture of the overall hull response. The vertical deflections show that most of the twist of the hull occurs in the forward section of the ship, that is, between the machinery box and the bow. This is not surprising since the applied torques are highest here and there is a long run of open hatch sections. The horizontal deflections also

show this, but one must remember that the reference line lies between the centerline of the stern and the bow. Relative to this line, the horizontal deflections appear to be an "S" curve. The fact that both the vertical and horizontal deflections do not appear to go to zero at the stern is merely an indication that the reference line is at an angle to the local direction of the ship centerline at the stern. Clearly, the deflections show that the section of full width hatches forward of the machinery box have the least torsional stiffness.

Lateral Bending and Torsion

In order to develop a composite picture of this type of combined loading, five separate tests were performed. In all of the tests, the distribution of lateral bending and torsion loads remained the same in shape and magnitude. Two of the tests were conducted under the same conditions of lateral bending and torsion. One test was conducted in which the signs of both the lateral bending and torsion were reversed.

The remaining two tests included a vertical bending distribution superimposed on the lateral bending and torsion distribution. The first of these tests used one sign for lateral bending and torsion; the other used the opposite sign for these distributions. Thus, the difference between these runs eliminates (if the response is linear) the effect of the vertical bending distribution. The results of all of these tests are presented in Appendix B in a compatible form, as before.

The results for the stress distribution appears nearly the same as for the case of torsion alone, since the magnitude of stresses introduced by the lateral bending are, in general, much smaller than those introduced by the torsional loading.

Section VI. SUMMARY AND CONCLUSIONS

This study included several facets: a model development, model construction, and an extensive test program. A summary of the important highlights and conclusions follows.

The Model

1. It is possible to develop a satisfactory, relatively small scale structural model, but it is necessary to have the plating thickness larger than scale. The model developed here had a plating thickness approximately three times thicker than scale. Due to the availability of standard sizes of steel plate, some elements were thicker than desired, others were thinner.
2. It was not possible to include all of the structural complexity in the model. All of the secondary structure (brackets, stanchions, etc.) was omitted and much of the primary structure was greatly simplified.
3. A finite element analysis of the model and ship midship sections indicated that nearly the same torsional response was observed for both. No analysis was performed for either vertical or horizontal bending.
4. Peculiar stress measurements consistently occurred on the starboard side of the midship section (halfway between Frames 178 and 194). No irregularities in the model could be observed in this location. In spite of repeated changes in strain gauges, the peculiar results persisted. One must conclude that some internal irregularity must exist in the unexposed portion of the double bottom structure in this region.

The Measuring Instrumentation

1. The strain gauges used provided nominal temperature compensation. However, due to the combined effects of small measured strains and large thermal gradients in the test facility, unacceptable large thermal stresses were observed during either hot or cold days. As a result, the tests were performed only on those cloudy or rainy days in which the heaters were not on and the outside temperature varied only slightly.

2. Individual gauge readings were rejected if the drift (presumably due to thermal effects) was greater than 20 percent of the gauge reading due to load. The repeatability and linearity of the retained readings was exceptionally good.

3. The deflection measurements were made by precision, mechanical dial gauges. No difficulty was encountered with this system.

The Loading

1. The model was loaded by means of calibrated steel weights and precision pulleys. The purchase of the pulleys was limited to 2:1.

2. The loading was performed through loading bars which were attached by brackets to the model at several bulkheads. The selected bulkheads were at least one hatch length away from any strain measuring station.

The Results

1. Tests of vertical bending yielded results which show that the model responds closely to elementary beam theory. There is some evidence of stress concentration on those sections in which the hull structure changes dramatically, for instance, just forward of the machinery box.

2. Tests of horizontal bending show that Navier bending occurs for this loading as well. However, because the ship is very stiff transversely, the resultant stresses were quite small and not as well defined as for vertical bending.
3. Tests involving a very large vertical shear amidships developed a shear stress pattern in this area large enough to measure accurately. This pattern appeared to have the correct shape and meet the known boundary conditions at the keel and at the deck edges.
4. The response of the ship to pure torsion demonstrated several things:
 - a. Both the bow and stern sections offer a considerable warping restraint.
 - b. The machinery box is a particularly effective warping restraint.
 - c. Transverse bending of the deck edge torsion box yields very large stresses on the hatch side of this box just forward of the machinery box. This is a further evidence of the warping restraint offered by the machinery box. Similar large bending stresses were observed in the deck edge torsion box just aft of the forecastle.

ACKNOWLEDGEMENTS

This project was sponsored by the American Bureau of Shipping under the supervision of the Ship Structure Committee. The authors would like to thank the Research and Development Division of the American Bureau of Shipping for their cooperation and the fruitful discussions throughout this project.

APPENDIX A

EVALUATION OF MODEL DESIGN BY FINITE ELEMENT METHODS (FEM)

A finite element calculation was performed on a parallel section of the ship and a similar section of the ship model. Additionally, FEM calculations were also performed for a typical transverse bulkhead - both model and full scale.

A. Midship Section

For the midship study, both sections included one long container hold and one short container hold (a total section length of 91.868 ft. full scale). The finite element mesh for the ship is shown in Figures A-1a through A-1c, and that for the ship model in Figure A-2. The following assumptions were made in this analysis:

- i. Symmetry. Because of symmetry, torsional loading could be applied as a pure antisymmetric load and only half of the structure needed to be analyzed.
- ii. Boundary conditions. Along the symmetry line: No deflections occurred in the longitudinal and vertical directions. In the case of full warping restraint at the section $x=0$, this section was completely fixed in all directions. For the case of no warping restraint at the end $x=0$, all nodes were free to move in the x -direction at this section (except nodal points at ϕ).
- iii. Structural Simplifications.
 - a. Several sidegirders and floors in the inner bottom were lumped together.
 - b. Stiffeners were lumped together and included in the structure as bar-elements.
 - c. Plating thicknesses for bottom, sides, deck and bulkheads were not changed. However, the thickness of the bulkhead at the end of the section was reduced with a factor $\frac{1}{2}$.

The finite element model did not include a box beam on the forward most bulkhead as shown in Figure A-2. As will be shown later, these boxes have little effect on the total torsional response and their omission (or inclusion) does not appear crucial.

The loads were applied uniformly as vertical forces along the free end bulkhead. The torque applied to the model was 5×10^3 lbs. in. and the torque applied to the prototype ship was 8.68×10^8 lbs. in. The loading applied on the ship is 4.3 times the corresponding load applied on the model after scaling. Thus, for comparison, the results of the ship were divided by 4.3, and the stress sign is reversed since loading signs were also reversed. In the finite element analysis only one-half of the structure, and the loading were used.

Figures A-3a through A-3j show the resulting stress distribution from the finite element analysis of the model.

Figures A-4a through A-4j show the corresponding stress results of the ship portion.

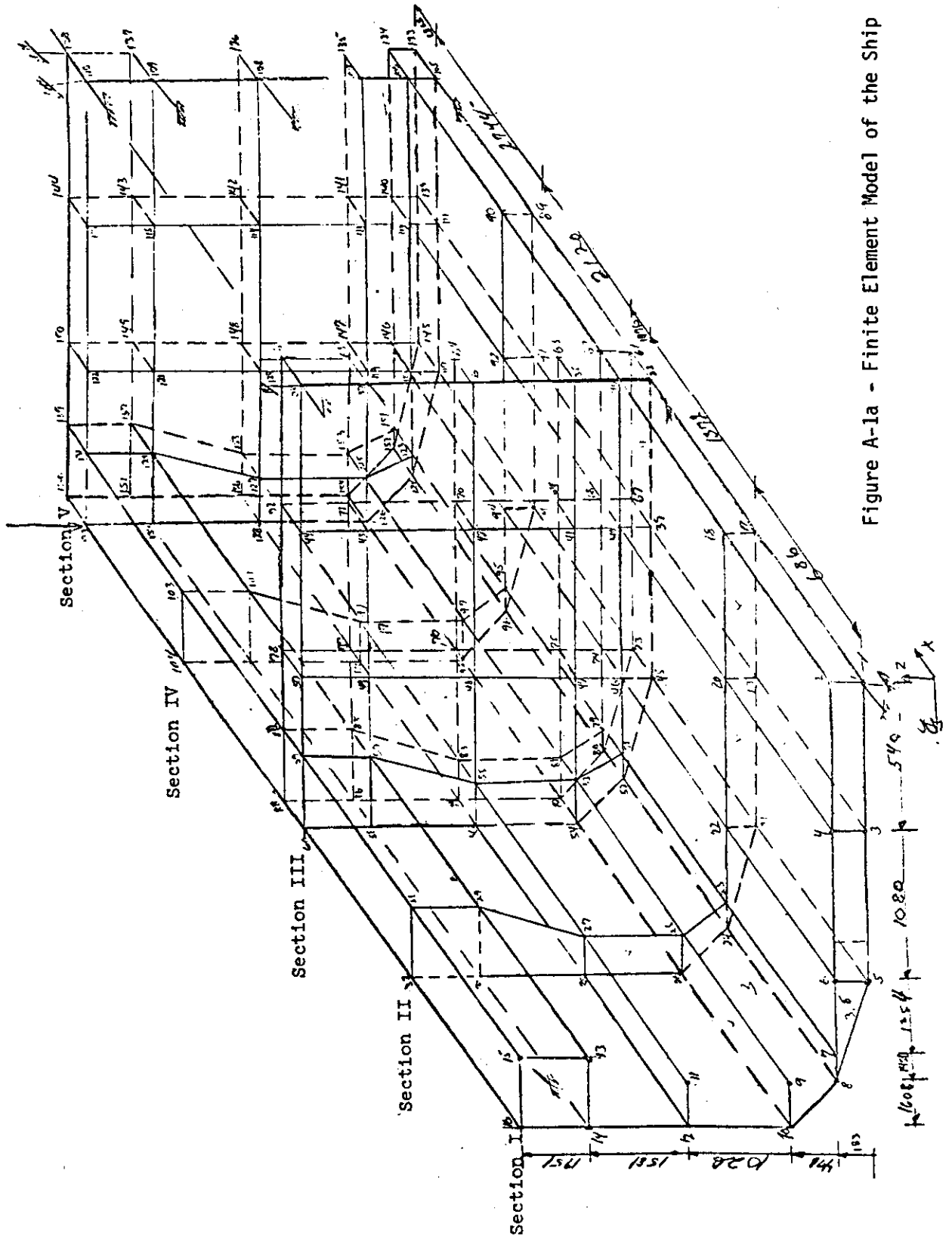


Figure A-1a - Finite Element Model of the Ship

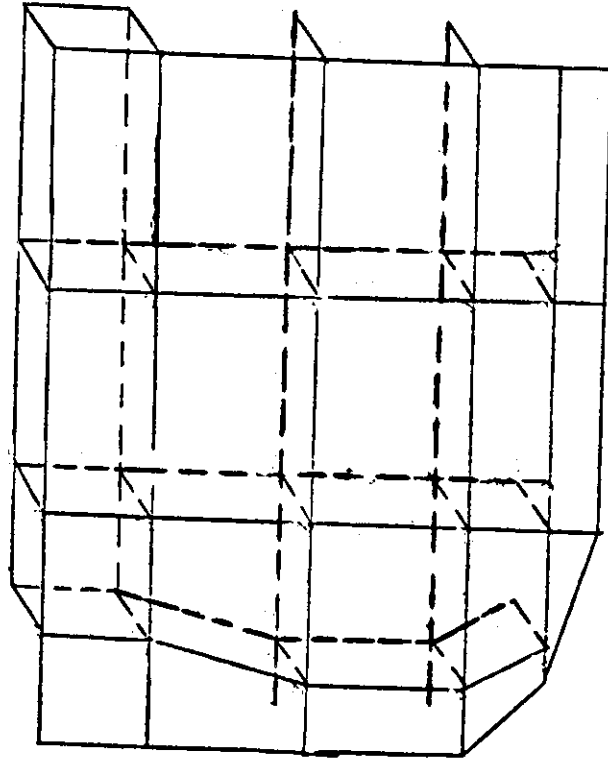
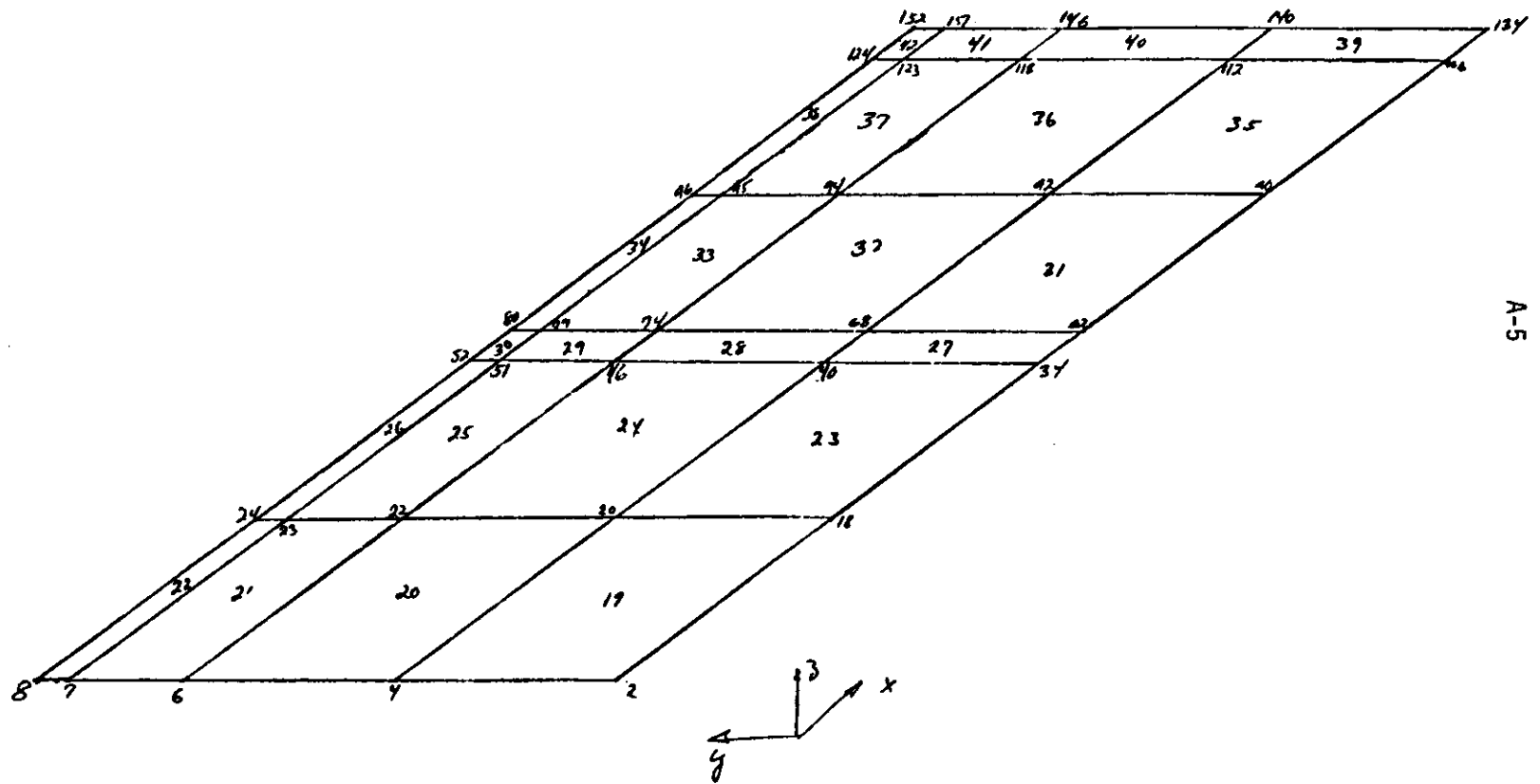


Figure A-1b. Typical Bulkhead Modeling.



A-5

Figure A-10 Inner Bottom Model.

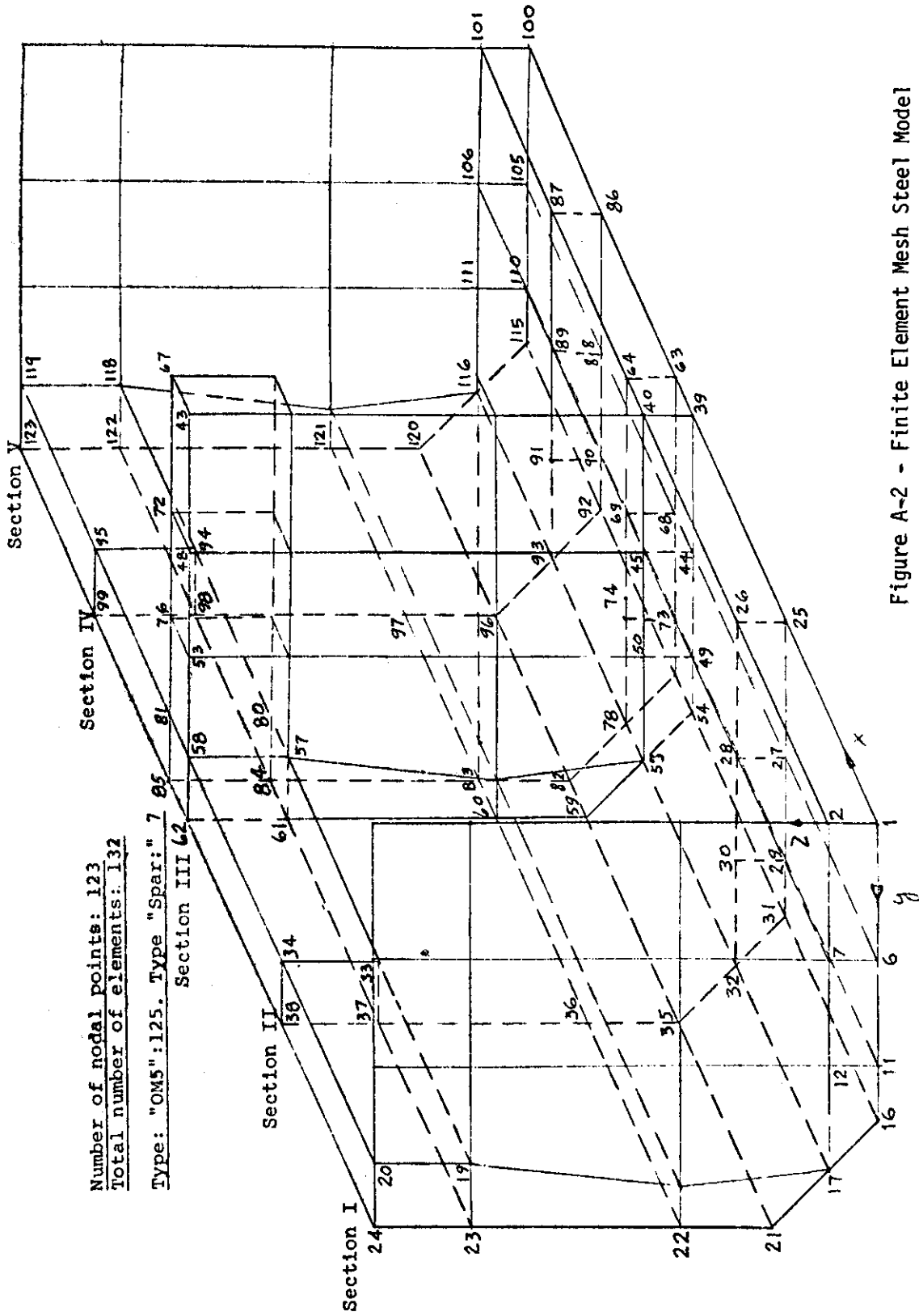


Figure A-2 - Finite Element Mesh Steel Model

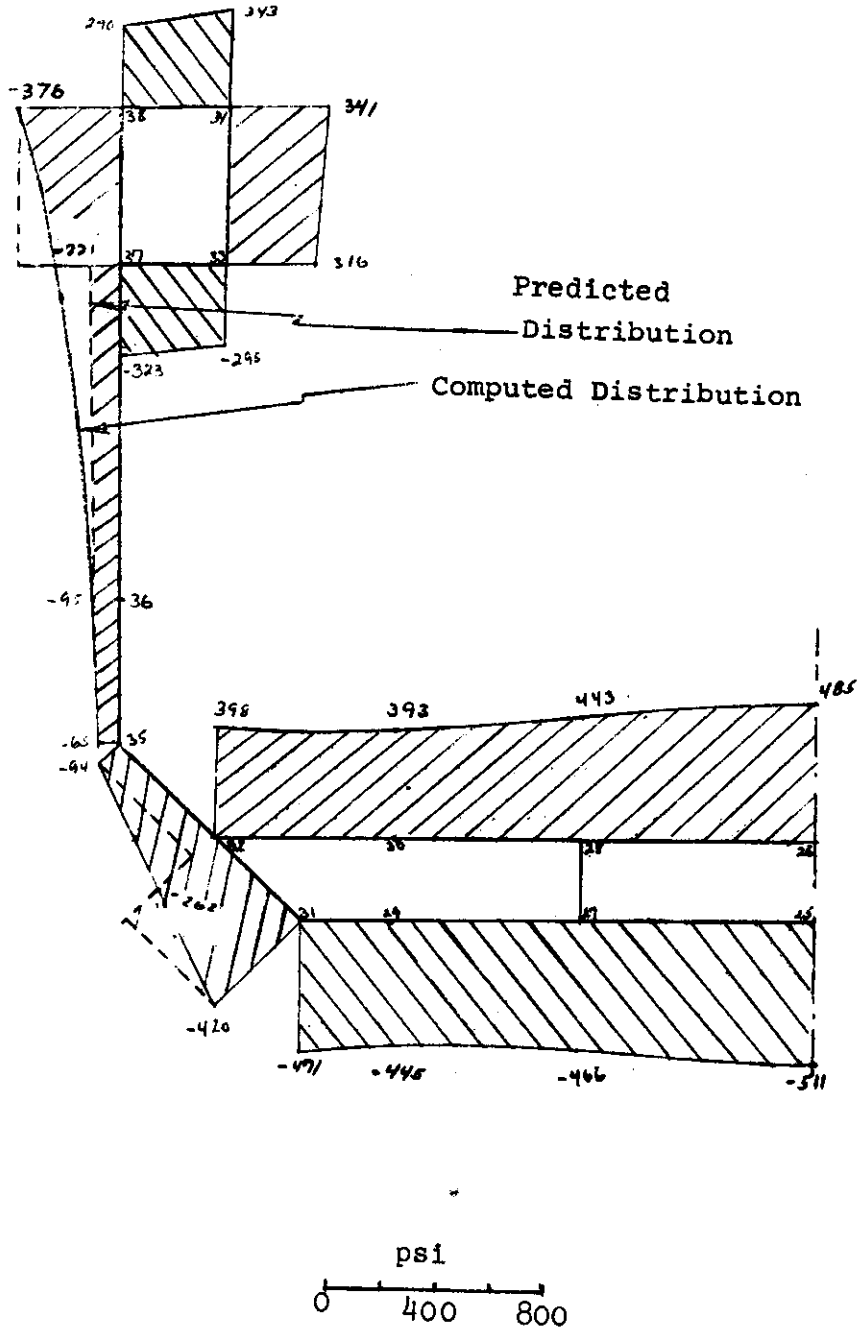


Figure A-3a. Shear Stresses At Section II (Model Results)

Shear stresses over longitudinal cross section at transverse Bhd.

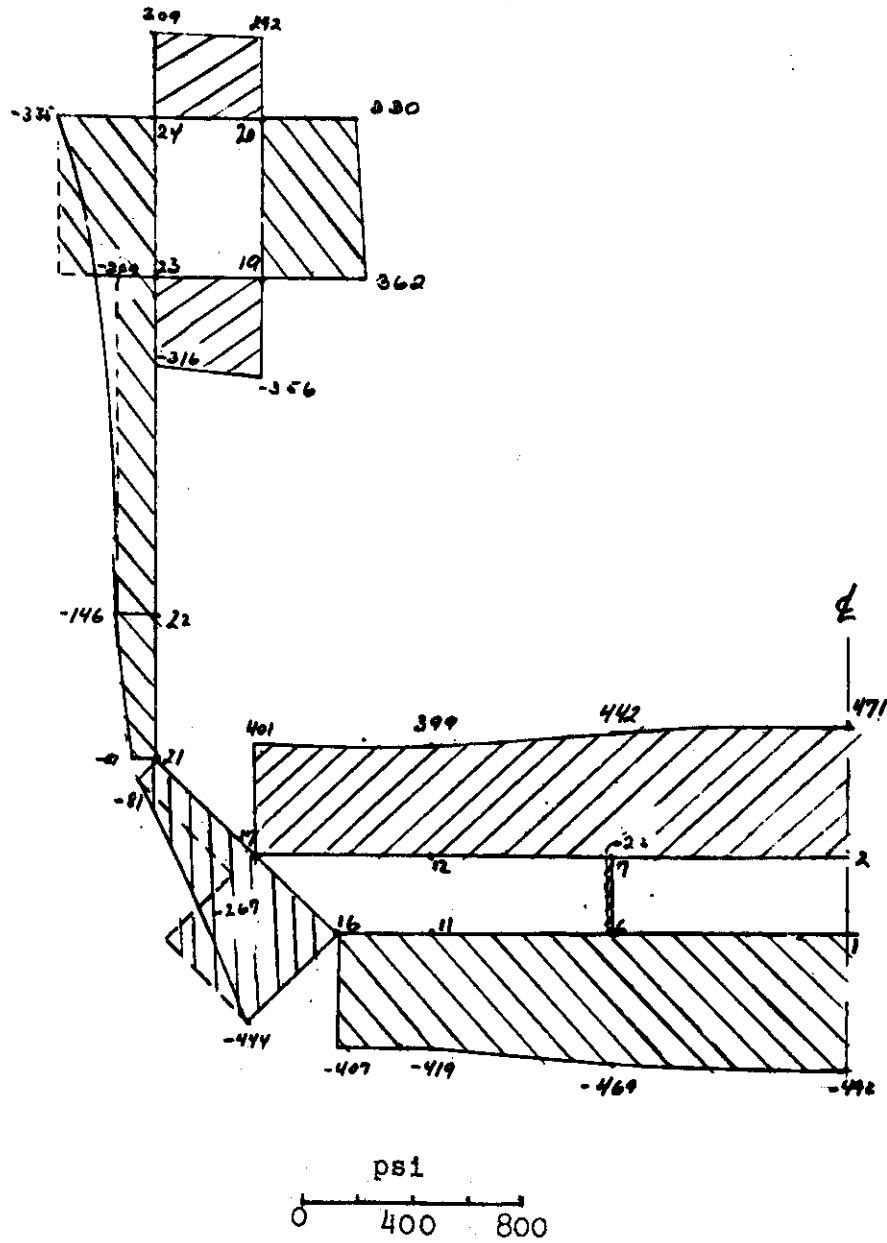


Figure A-3c. Shear Stresses At Bulkhead Section I (Model Results)

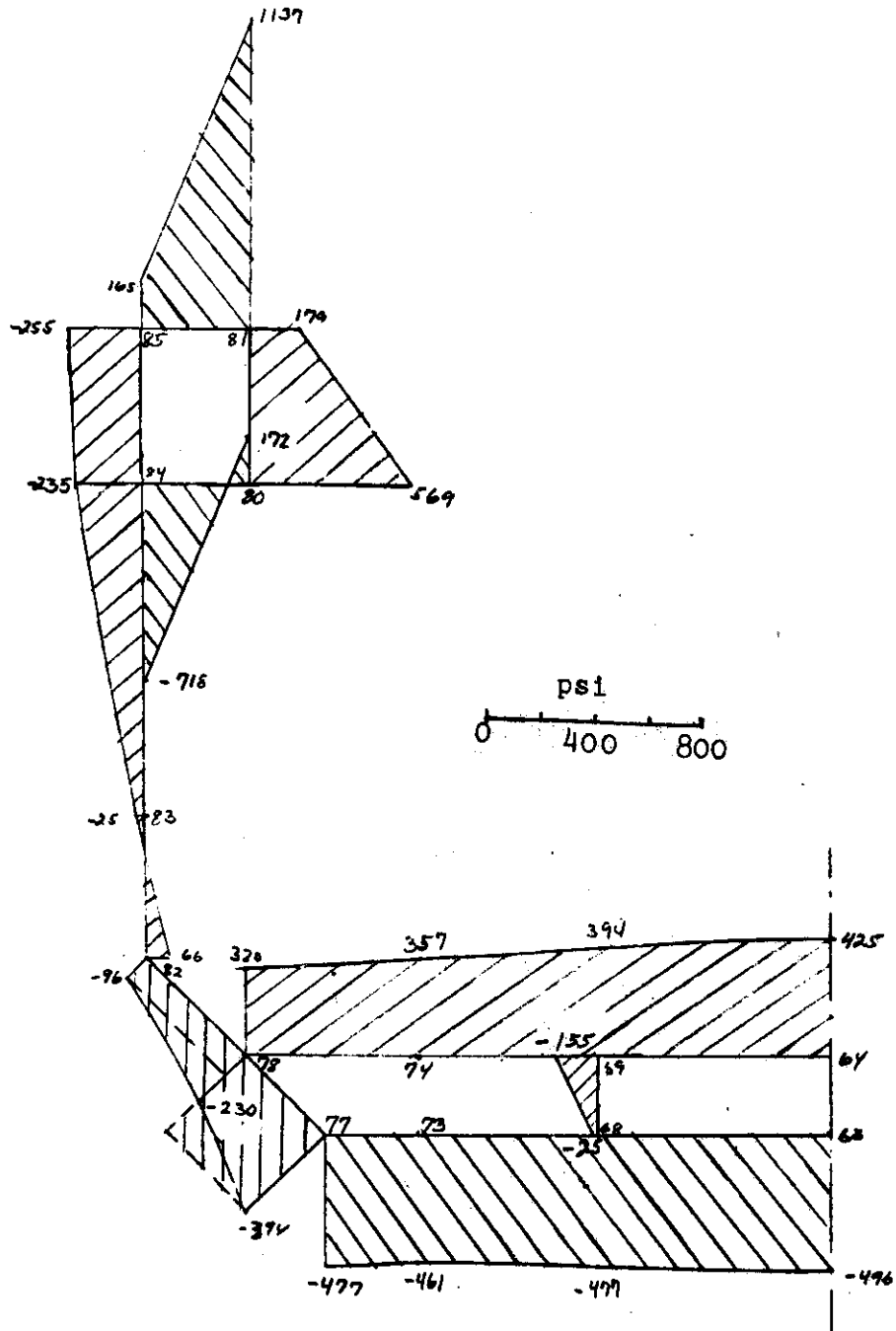


Figure A-3e. Shear Stresses 1 inch Forward Of Bulkhead At Section III (Model Results)

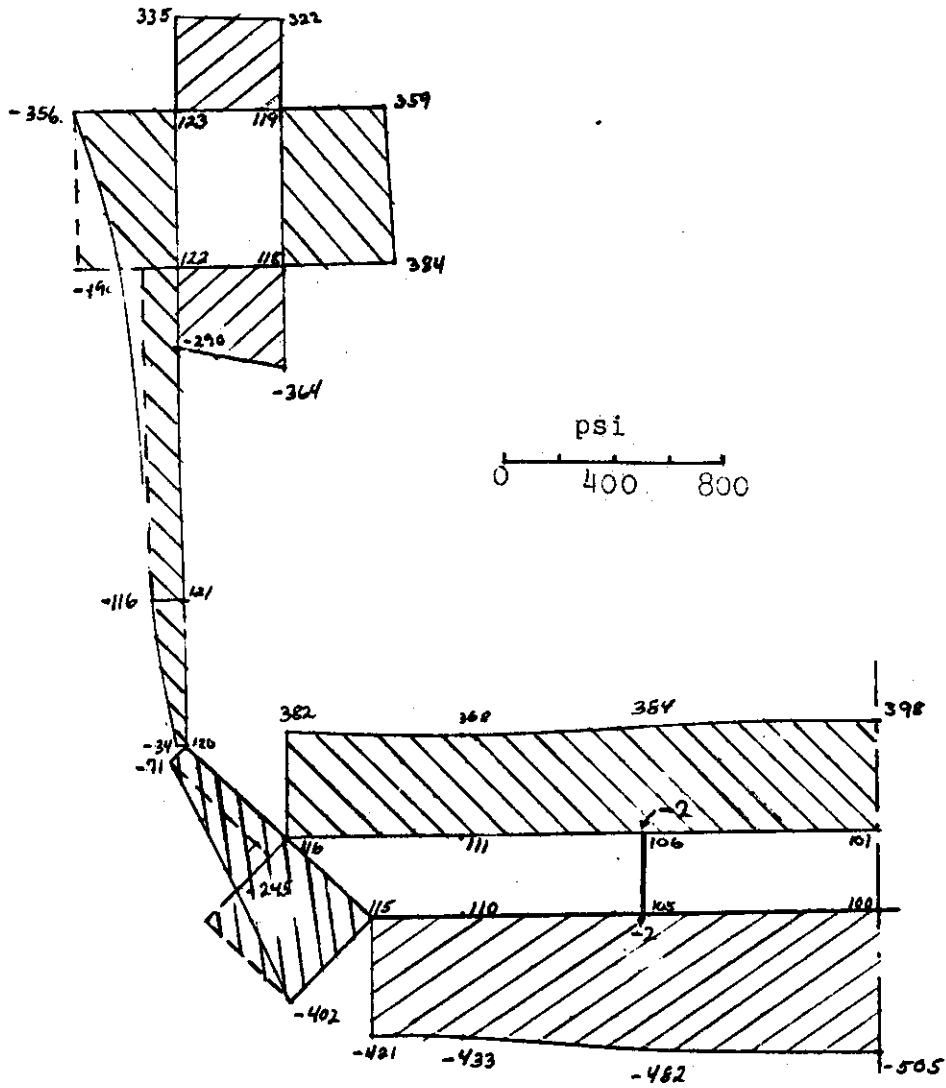


Figure A-3f. Shear Stresses At Section V
 (Model Results)

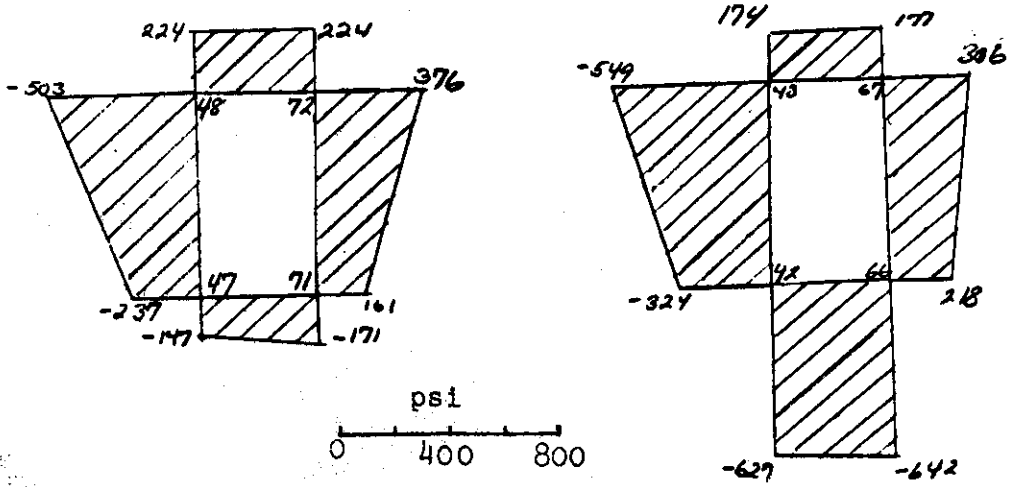


Figure A-31. Shear Stresses At Sections Of The Transverse Box Girder Section III (Model Results)

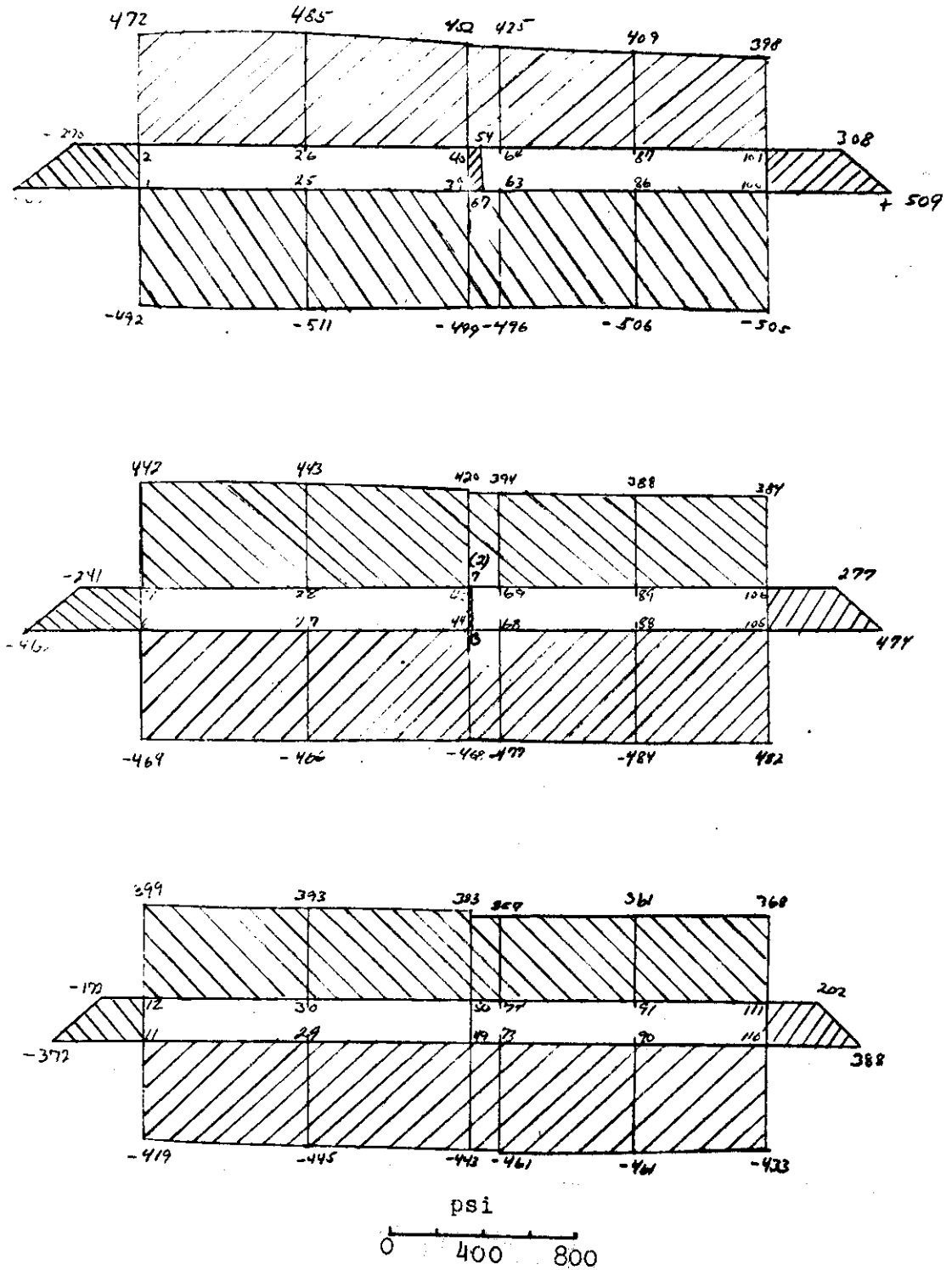


Figure A-3j. Shear Stresses In The Longitudinal Members Of The Double Bottom. (Model Results)

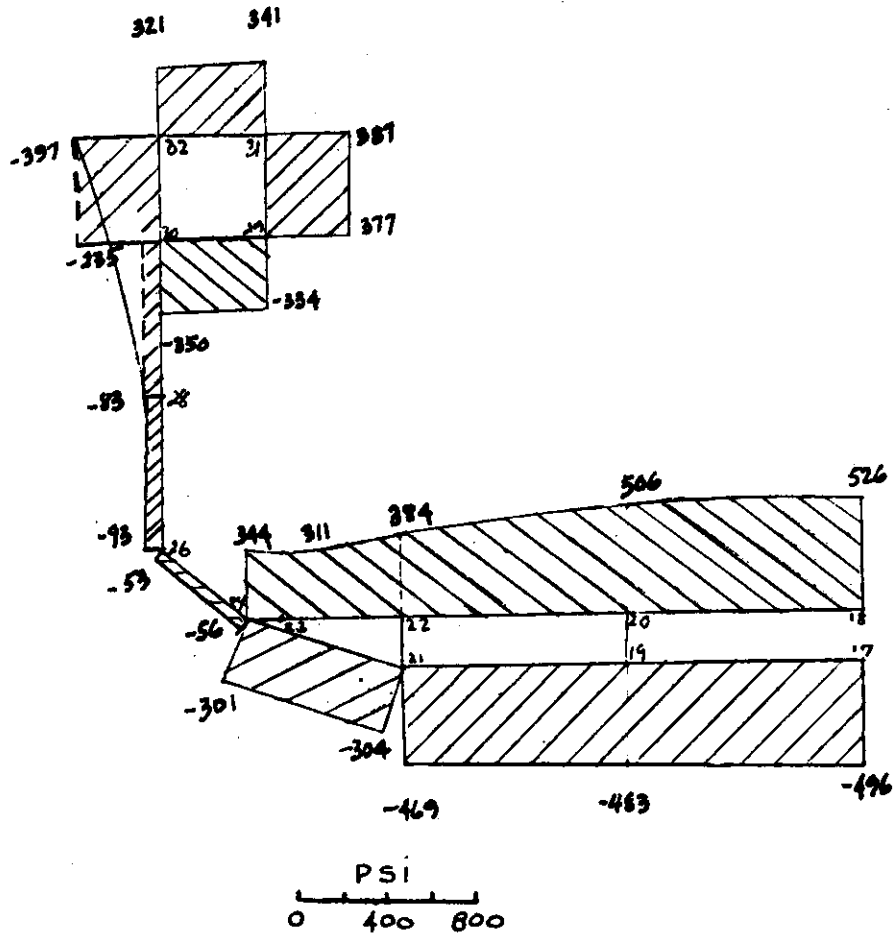


Figure A-4a. Shear Stress At Section II
(Ship Results)

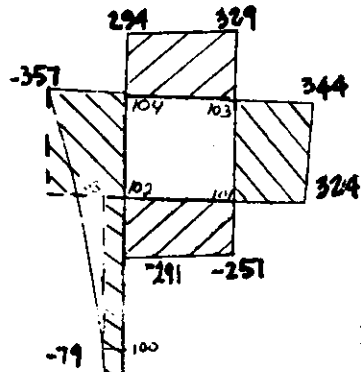


Figure A-4b. Shear Stresses At Section IV (Ship Results)

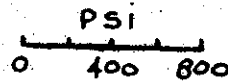
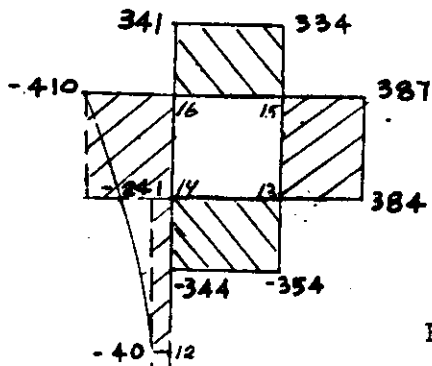
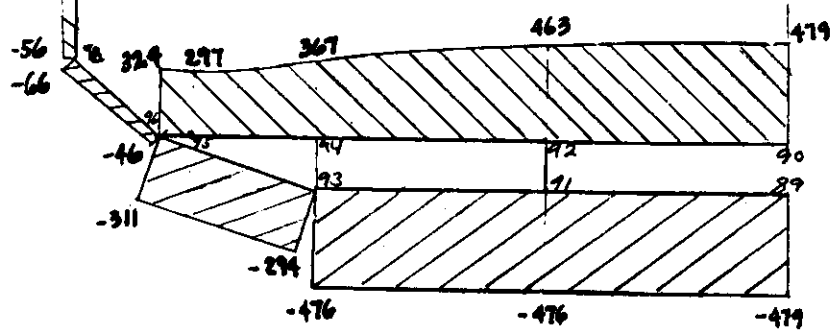
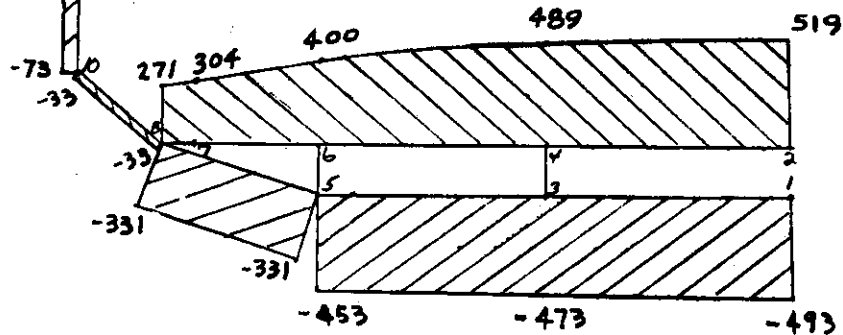


Figure A-4c. Shear Stresses At Section I (Ship Results)



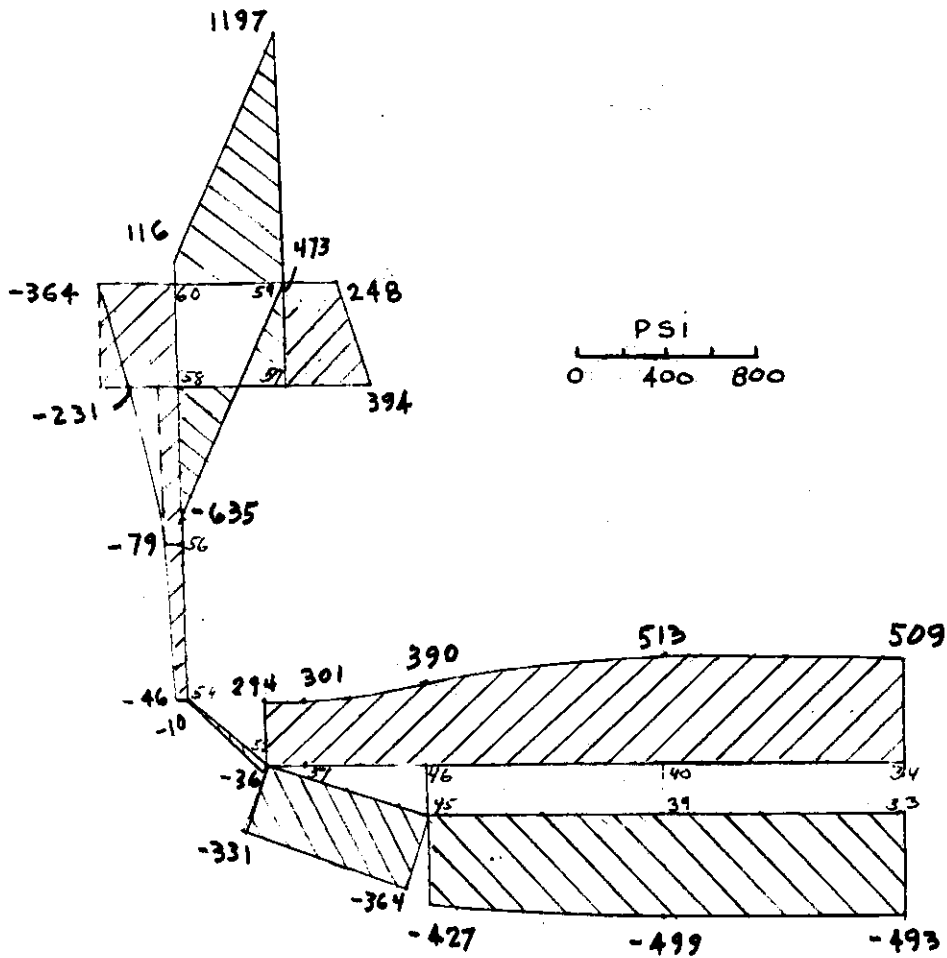


Figure A-4d. Shear Stresses At Bulkhead Section III
(Ship Results)

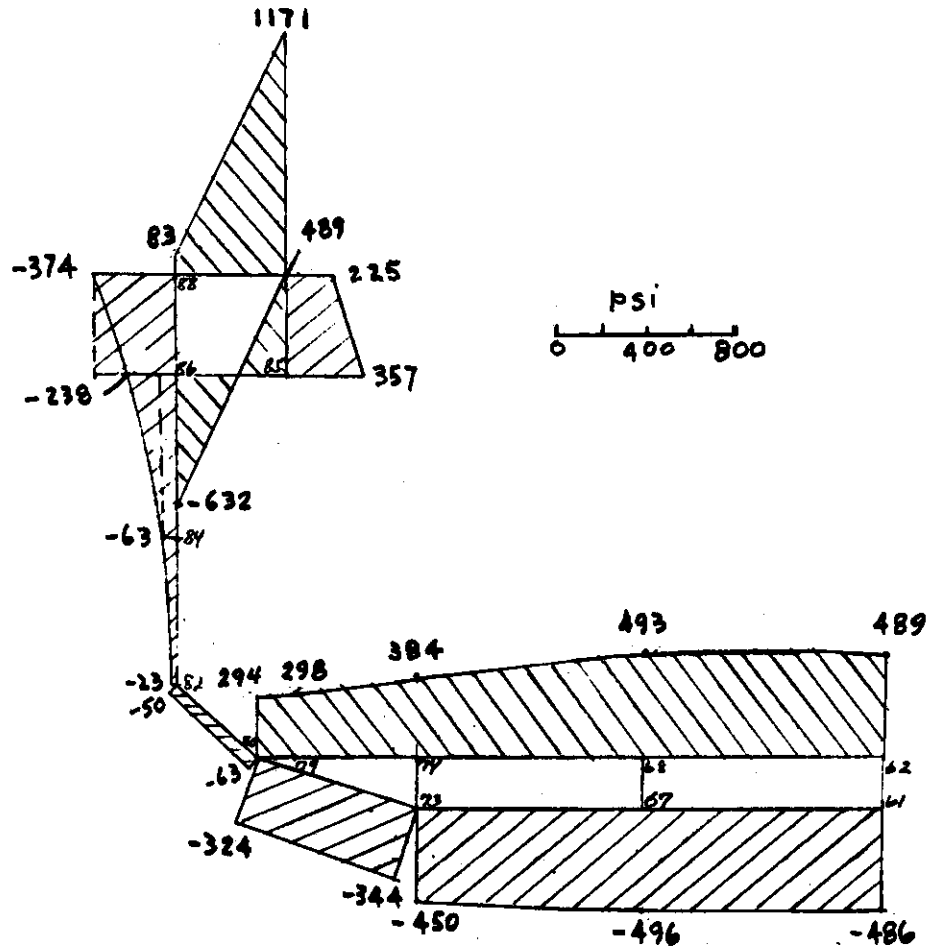


Figure A-4e. Shear Stresses 4' Forward Of Bulkhead Section I (Ship Results)

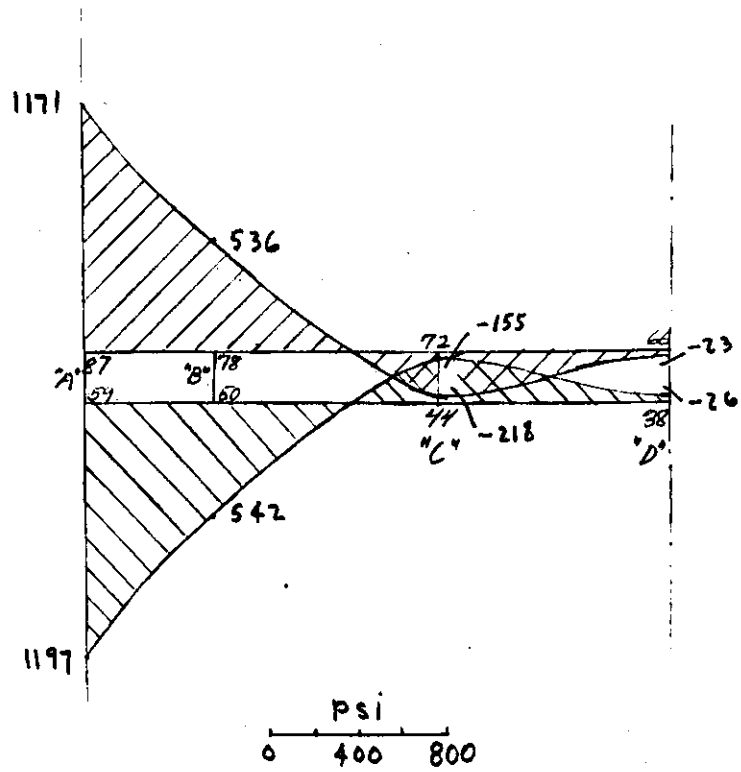
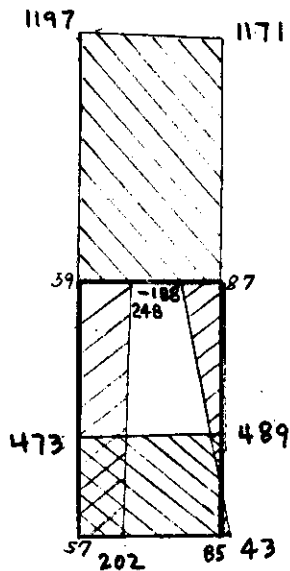
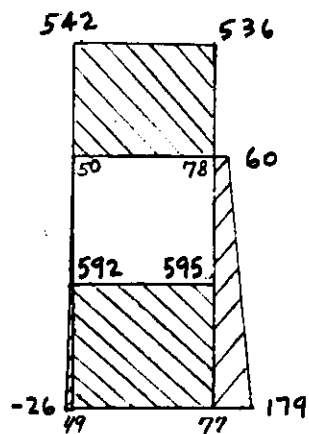


Figure A-4g. Shear Stresses of The Transverse Box Main Deck Plating At Section III (Ship Results)



Section A



Section B

Figure A-4h. Shear Stresses At Sections Of The Transverse Box Girder, Section III (Ship Results)

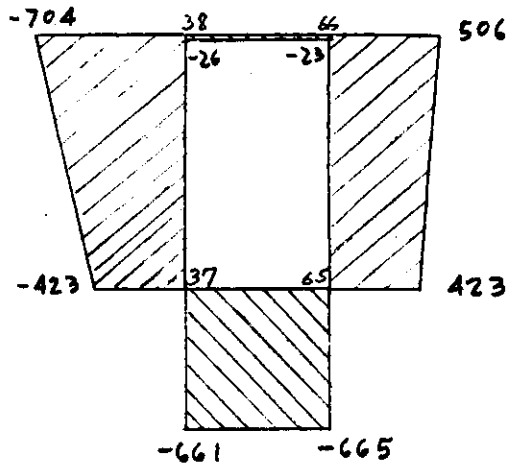
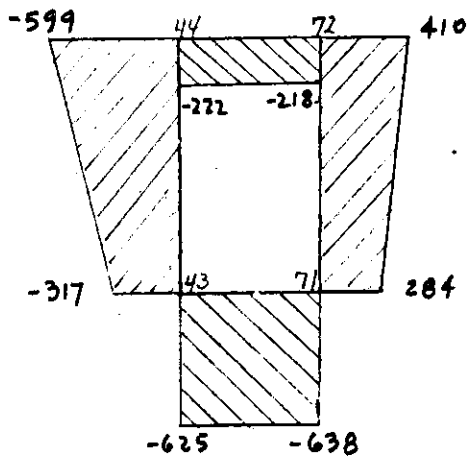
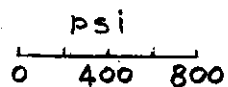


Figure A-4i. Shear Stresses At Sections Of The Transverse Box Girder, Section III (Ship Results)



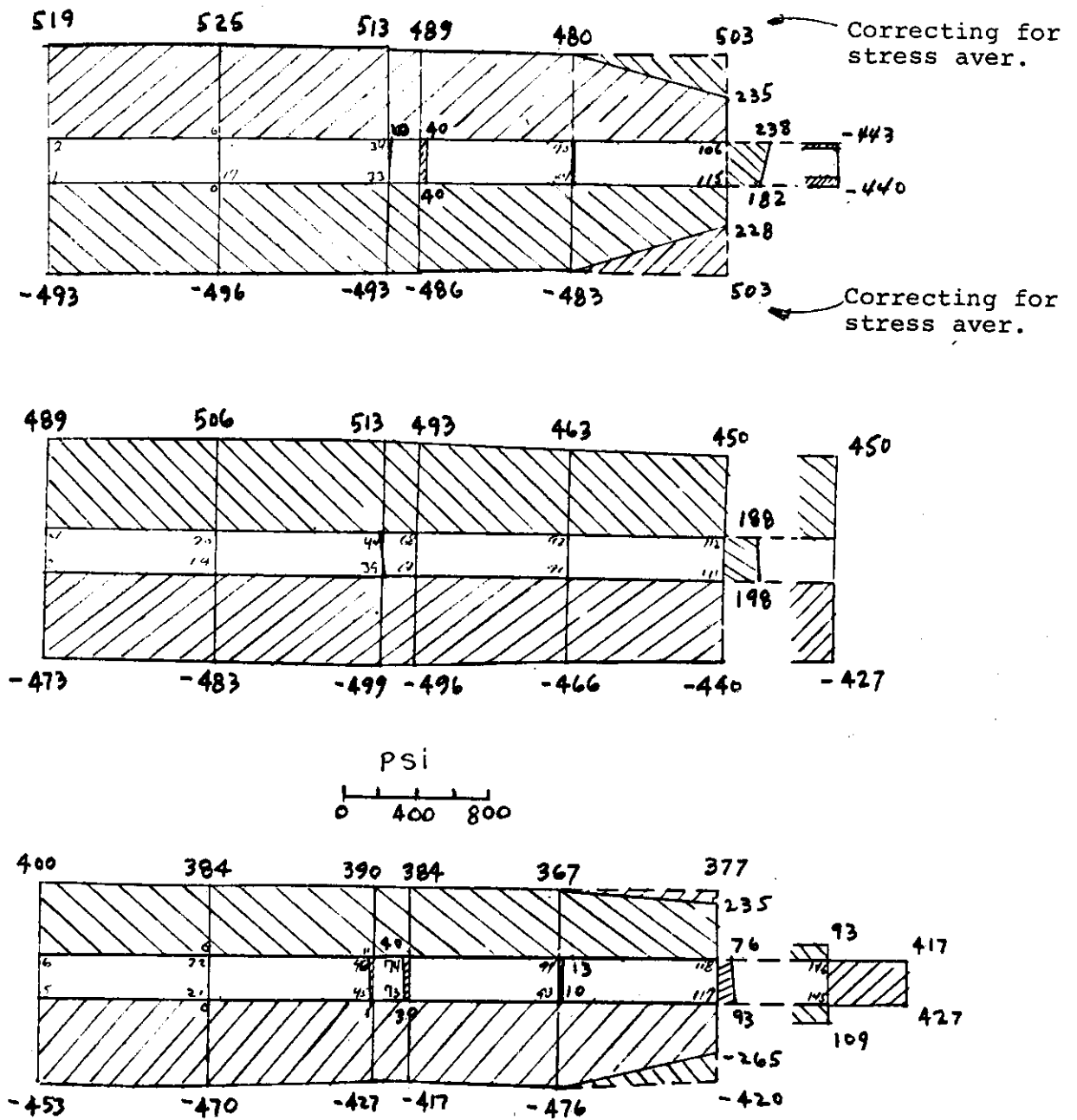


Figure A-4j. Shear Stresses In Longitudinal Members Of the Bottom (Ship Results)

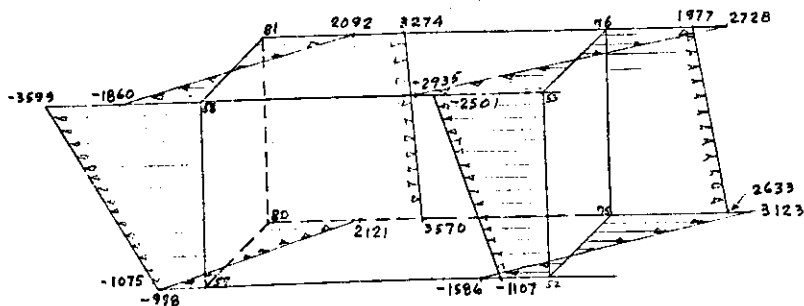
Of particular interest in this study was the warping of the transverse box girder (Figures A-5a & A-5b). With regard to these figures which show the normal stress distribution,

1. The curves show a remarkable similarity with highest stresses near the longitudinal box girder at the ship side. This is expected because the box girder is restrained from warping at the ship side, but free to move at the centerline. Hence, there should be no stresses at the centerline. The calculated stresses are also relatively small. The error, (difference from 0) is caused because the nodal point stresses are averaged stresses.
2. The high difference in stresses at nodal points at the longitudinal box girder at the ship side is caused by the averaging of stresses. Especially, the averaging of stresses in transverse direction along the longitudinal box girder tends to reduce the transverse stresses in the bottom and top plating of the transverse girder.
3. An interesting investigation is to check the horizontal deck displacement of the model and the ship, also taking into account warping and displacement of the transverse deck girder. Previously, the displacement and warping have been discussed separately. The deflected shapes of the main deck both for the model and the ship are drawn in Fig. A-6. It is interesting to see the similarity of the two decks. (Note that the direction of the deflection is changed for the ship and adjustments were made for the model in order to make the results comparable).

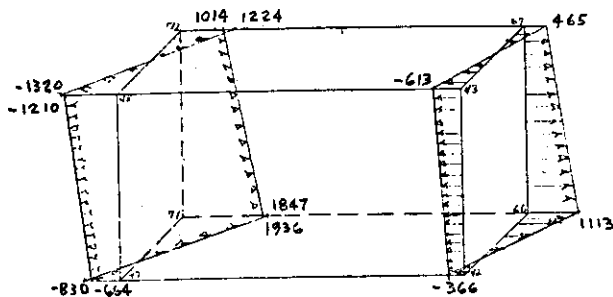
The transverse boxes have very little influence on the torsional rigidity. This should indicate that the effect of warping rigidity caused by the transverse deck-strip is very little, and it is most correct to scale the model according to free torsion. Previously it has been shown by Roren that the influence of a thin deck strip is very little. However, at the deck corners high warping stresses in the transverse box girder were obtained. But because of the large elements used in the calculation, a more detailed study is necessary if the actual stress concentrated effects are to be obtained.

Figures A-6b and A-6c show the computed measurements, both vertical and horizontal, of the deck edge.

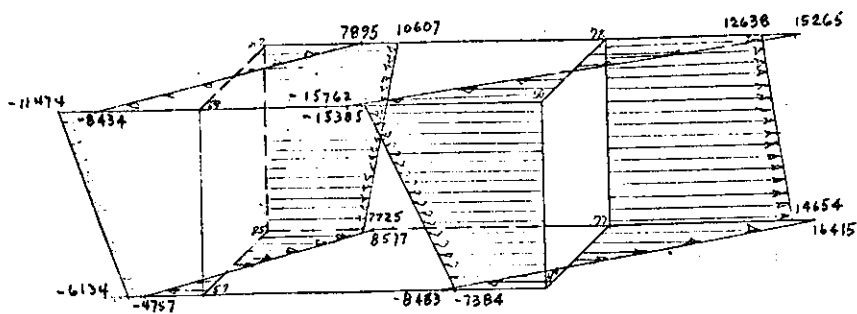
A-25



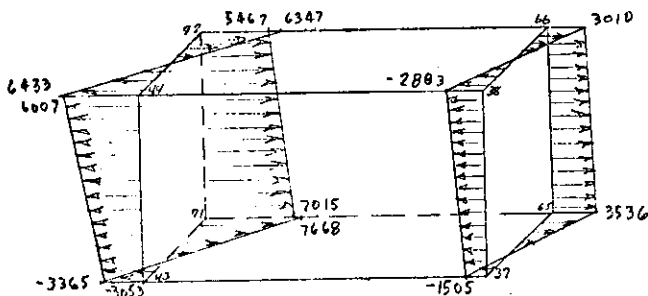
Outboard portion (Model Results)



Inboard portion (Model Results)

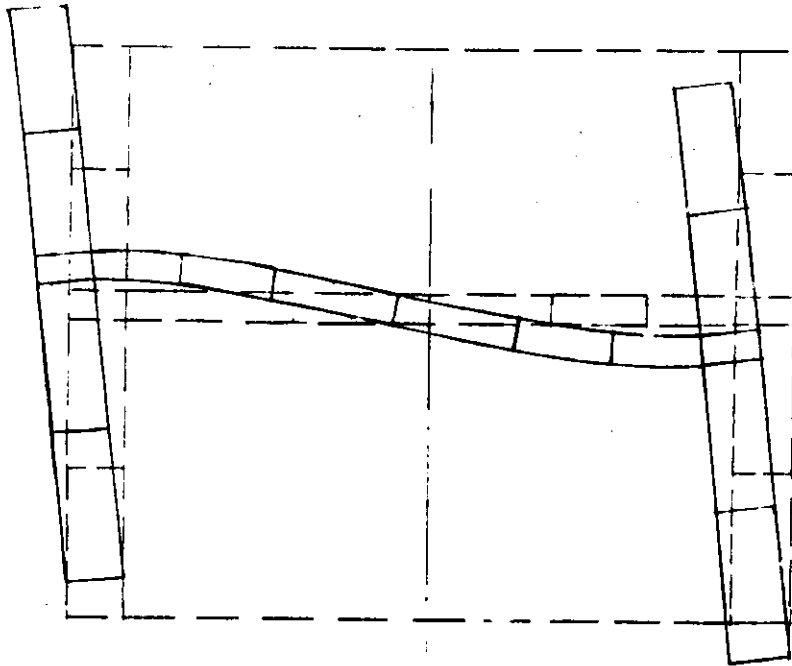


Outboard portion (Ships Results)

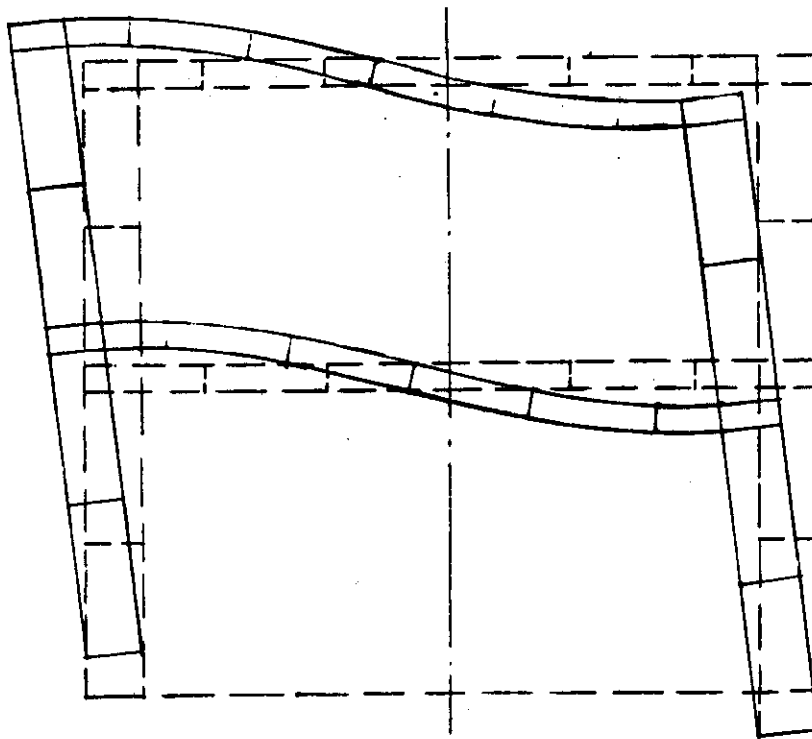


Inboard portion (Ships Results)

Figure A-5. Warping Stresses (PSI) In The Transverse Box Girder-Section III

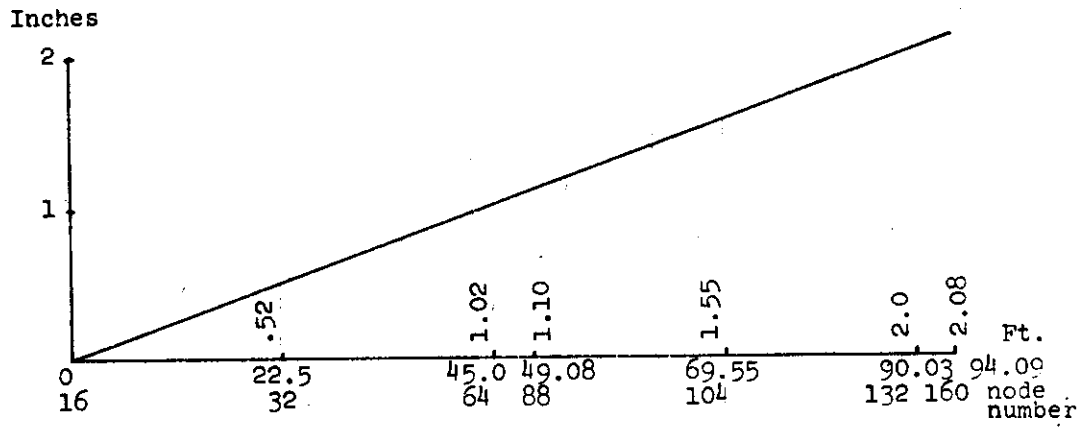
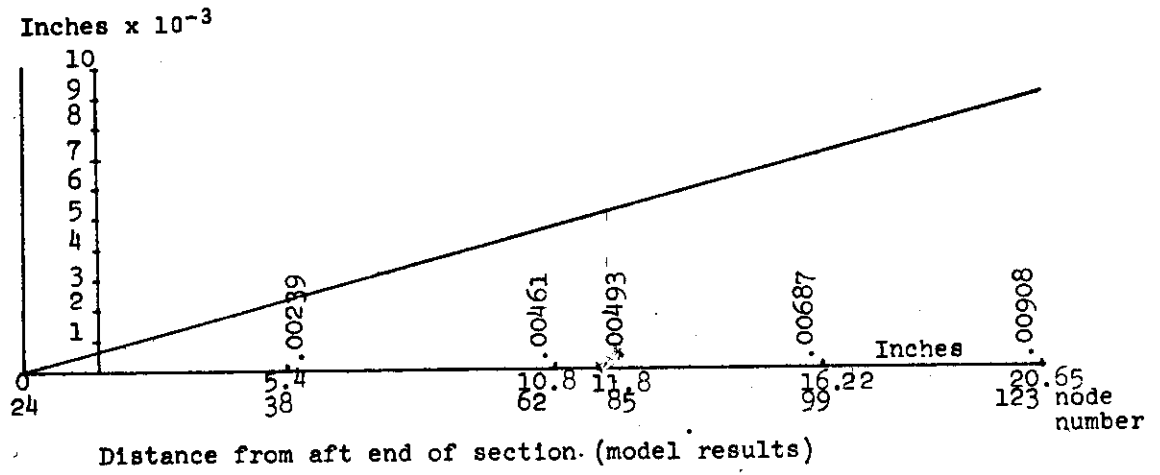


Model results



Ship results

Figure A-6a. Deflected Shape Of Main Deck



Distance from aft end of section (Ship results)
 (Note for comparative purposes the deflection of the aft end
 is 0 in transverse and vertical direction.)

Figure A-6b. Lateral deflection along main deck at ship side.

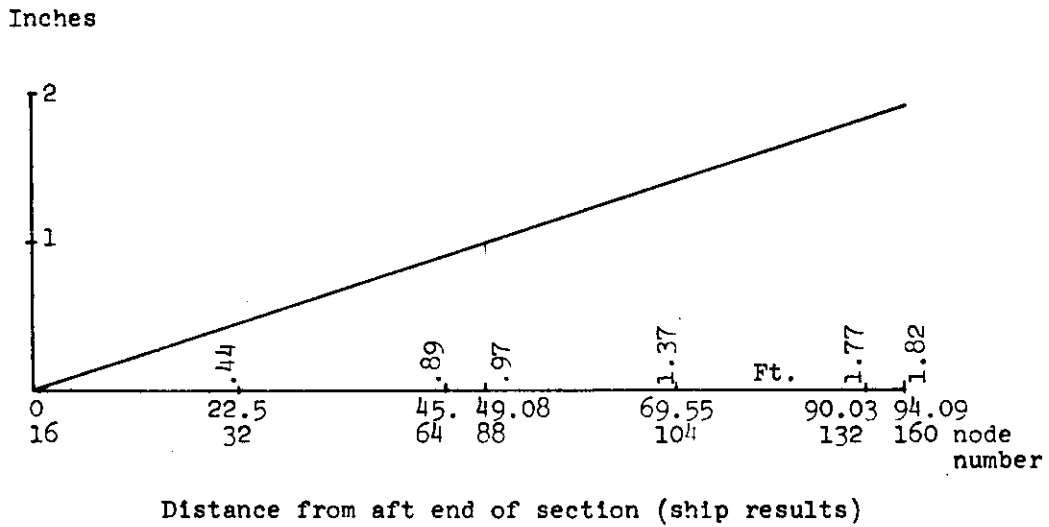
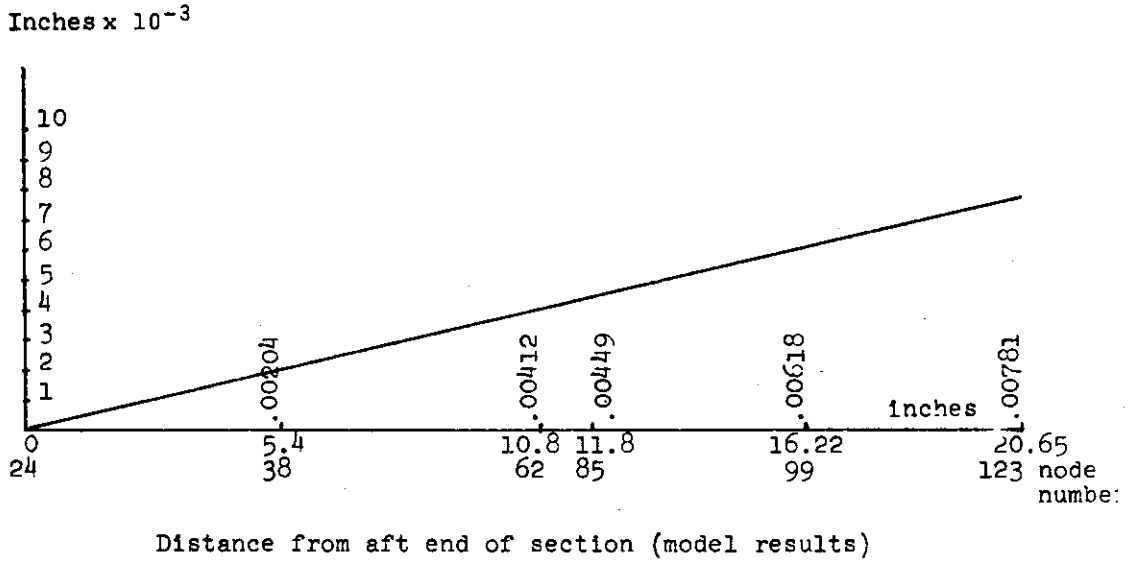


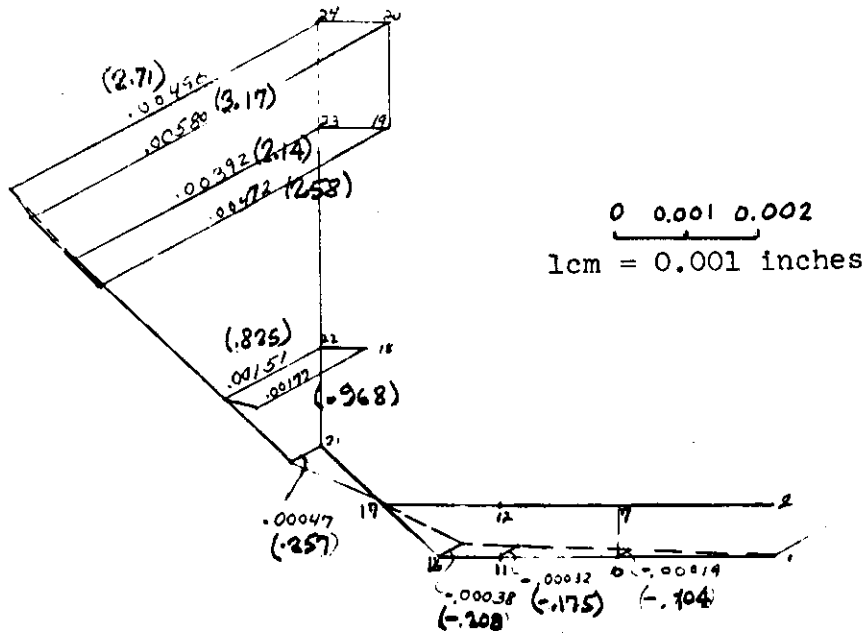
Figure A-6c. Vertical deflection along main deck at ship side.

The warping deformations at the free end of the midship section were also compared. If the same angle of twist exists over a comparable length of the ship and the model, the warping at the end section should be to the linear scale.

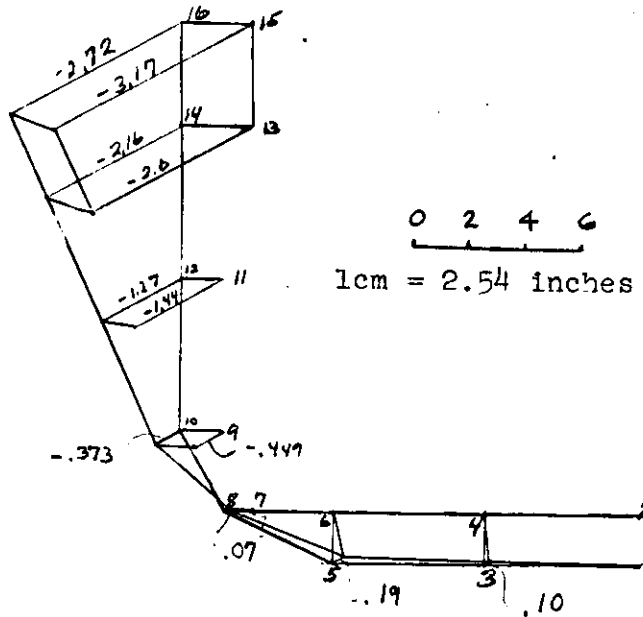
Hence it is necessary to multiply the obtained ordinates with the factor.

$$4.3 \times 50 \times 2.54 = 547$$

To obtain comparable values on the model, when the displacements are multiplied by this factor (the numbers in parenthesis), the warping corresponds very well, and the model pretty well represents the behavior of the ship in free torsion, see Figure A-7.



Model Results



Ship Results

Figure A-7. Warping deflections at free end section I
In Inches

Comparisons were made of the angle of twist over the section by measuring the deflections at the deck edge at the forward most bulkhead. The deflections of this point were:

deflection in cm (inches)	vertical	horizontal	total distance
model	0.0198 (0.0078)	0.02306 (0.0908)	0.0304 (0.01197)
ship	4.307 (1.698)	4.862 (1.9142)	6.50 (2.559)

The distance from the centerline at the keel to the deck edge is 20.0" for the model and 994 in. for the ship. Using these results, the total angles of twist become:

$$\phi_m = \frac{0.01197}{20} = 5.99 \times 10^{-4} \text{ rad.}$$

$$\phi_p = \frac{6.50}{2525} = 2.57 \times 10^{-3} \text{ rad.}$$

The loading of the model was 4.3 times too small (as discussed previously) and thus the corrected angle of twist for the model for a comparable load is

$$\phi_m = 2.57 \times 10^{-3} \text{ rad.}$$

The values of ϕ_p and ϕ_m therefore coincide to 3 decimal places for this case of free torsion. Thus, the simplifications introduced in the model do not lead to differences in twist deflections.

B. Bulkhead Structure.

In the bulkhead structure study a ship-like bulkhead was used (see Figure A-8a) and another representing those used in the model (Figure A-8b).

Boundary conditions used in the calculations were as follows. Along bulkhead at centerline the nodal points were completely fixed in all directions. The rest of the nodal points at the centerline were fixed in the vertical and longitudinal direction, but were free to move in the transverse direction. These boundary conditions were required to take advantage of symmetry in the calculations. To prevent the structure from rigid body rotation about a vertical axis, one nodal point at the shipside was fixed (the upper one on the bulkhead).

Calculations were made for two bulkheads, one similar to the real one, and one where the stiffeners were lumped together. No material was "thrown away," in the simplified case, except for the stiffening plates inside the transverse box girder. This would have no influence on the result, since the box girder was very stiff in itself besides being stiffened by these bulkheads.

A warping moment of 0.868×10^8 lbs. in. on the full scale ship was applied by means of longitudinal forces applied to the outer hull of the ship. The loading was introduced by forces at the nodal points along the ship side. Referring to Figure A-8a forces of -46737.9 lb. were applied at nodes 78 and 64 and of +46737.9 lb. were applied at nodes 36 and 50. Although these loads did not correspond to any known real situation, they were qualitatively correct and represented a reasonable loading for comparison purposes. Figure A-9 shows that longitudinal deflections of the ship side caused by this loading.

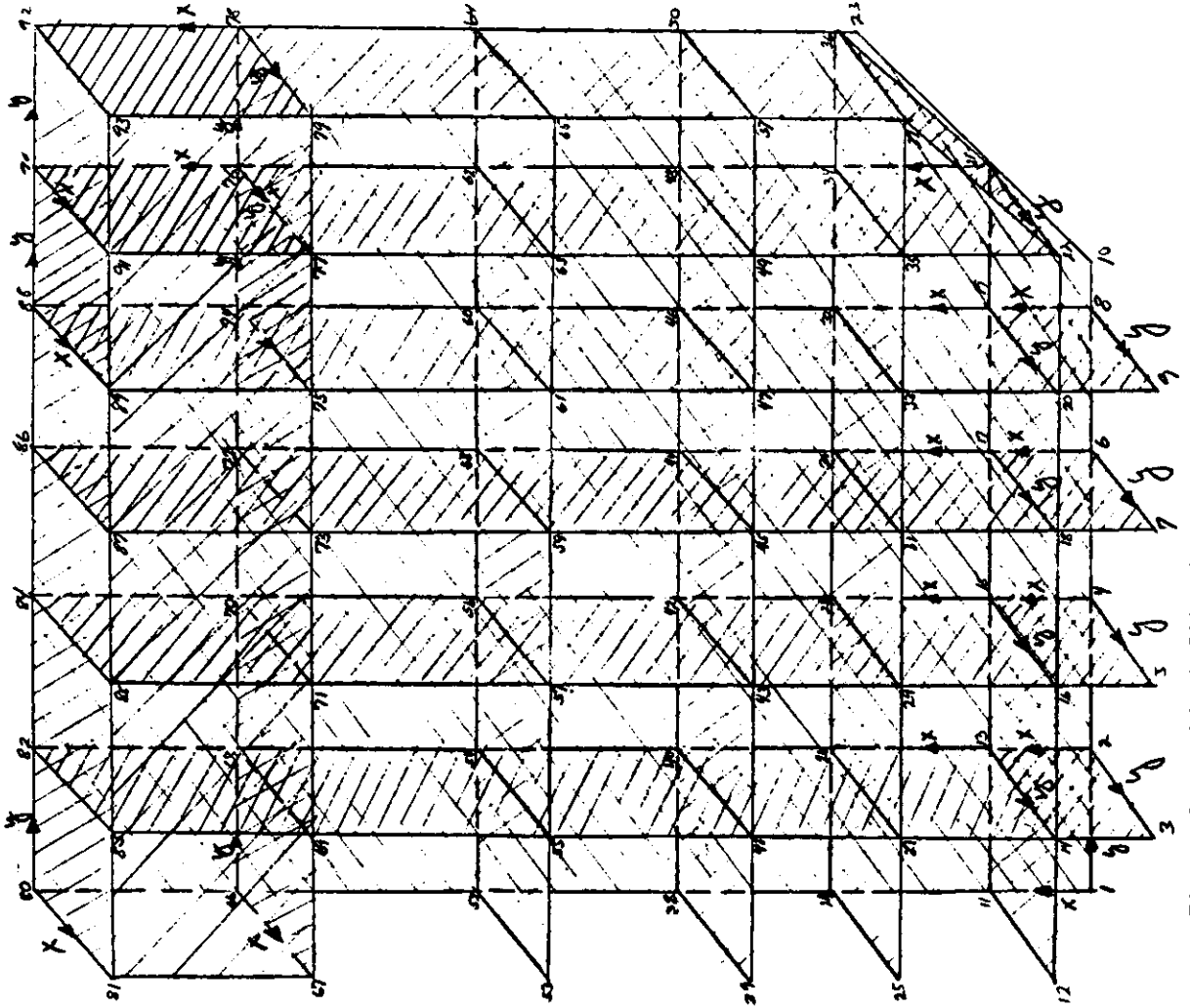
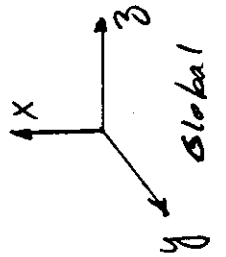


Figure 8a. Ship Bulkhead



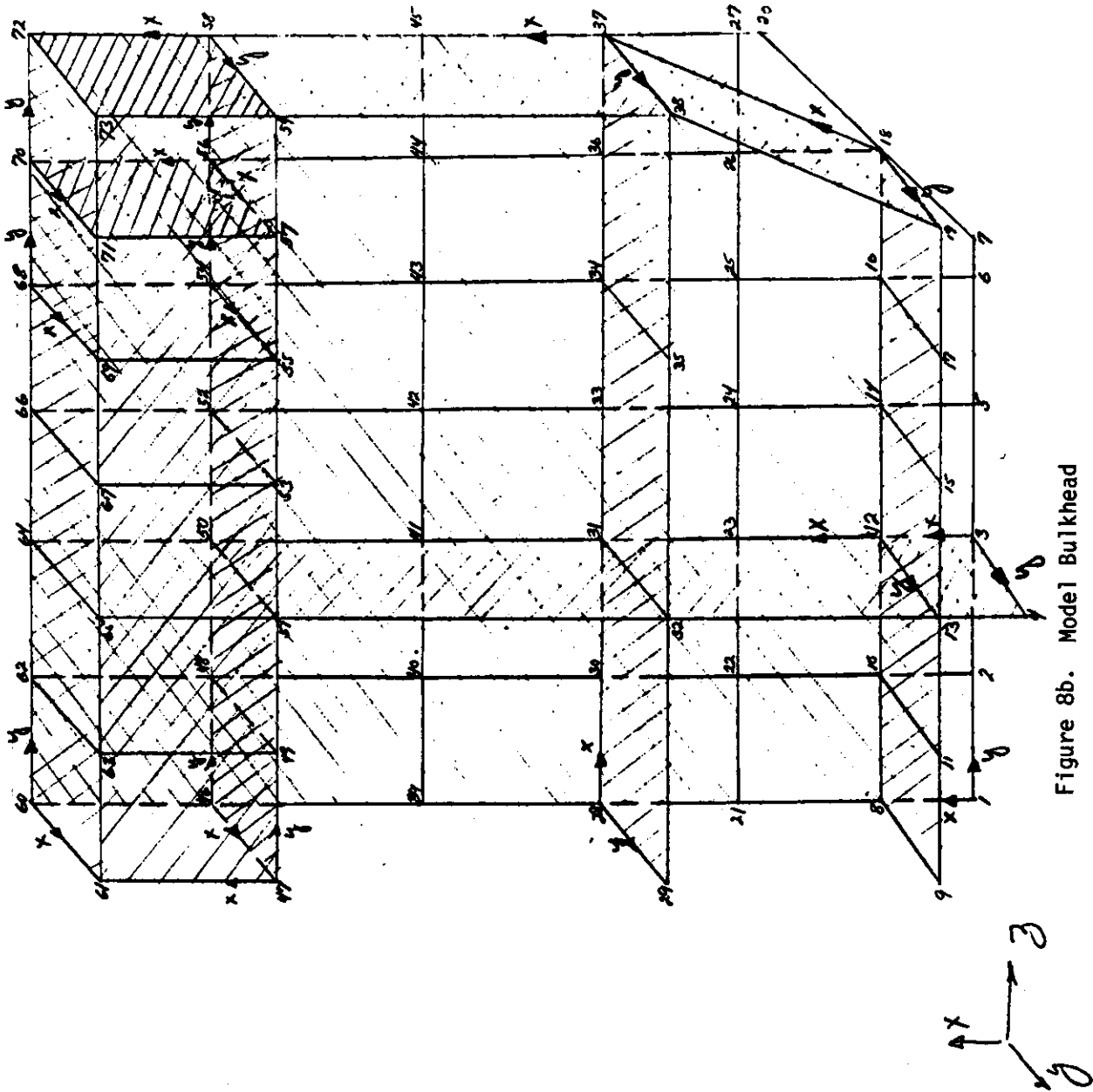


Figure 8b. Model Bulkhead

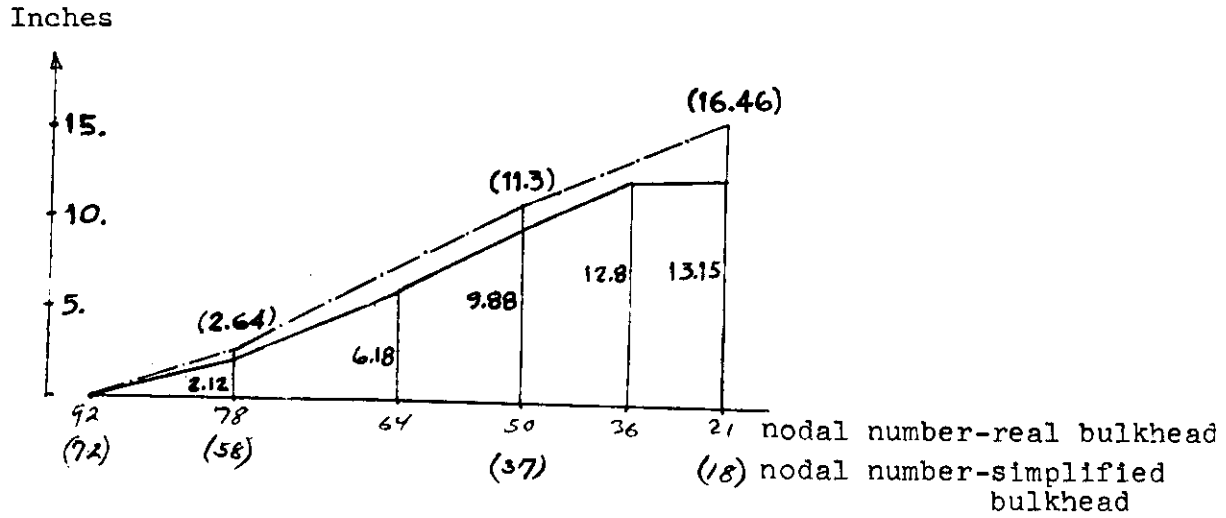


Figure A-9. Longitudinal Deflections

—— Real Bulkhead
 - - - Simplified Bulkhead

A further study of deflections compared the longitudinal deflection at the inner bottom (Fig. A-10a), transverse girder on the bulkhead (Fig. A-10b), the lower (Fig. A-10c) and upper (Fig. A-10d) plating on the transverse box girder, and at the vertical girder (Fig. A-10e).

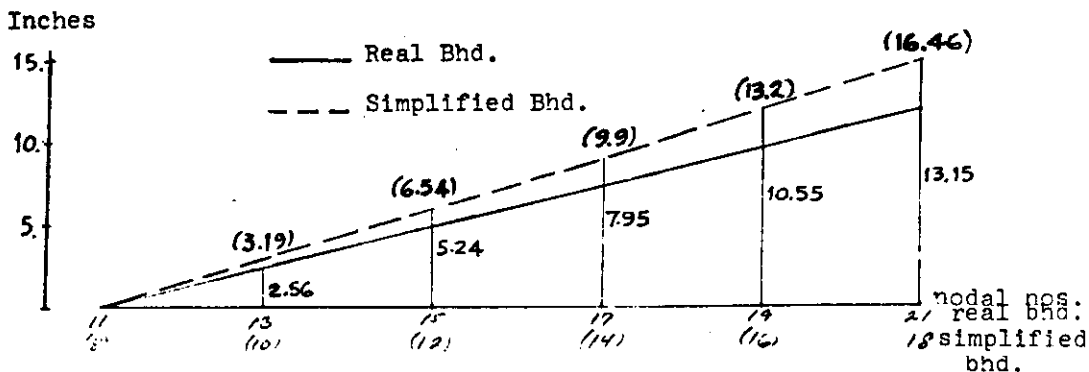


Figure A-10a. Longitudinal deflection of the Inner Bottom Plating

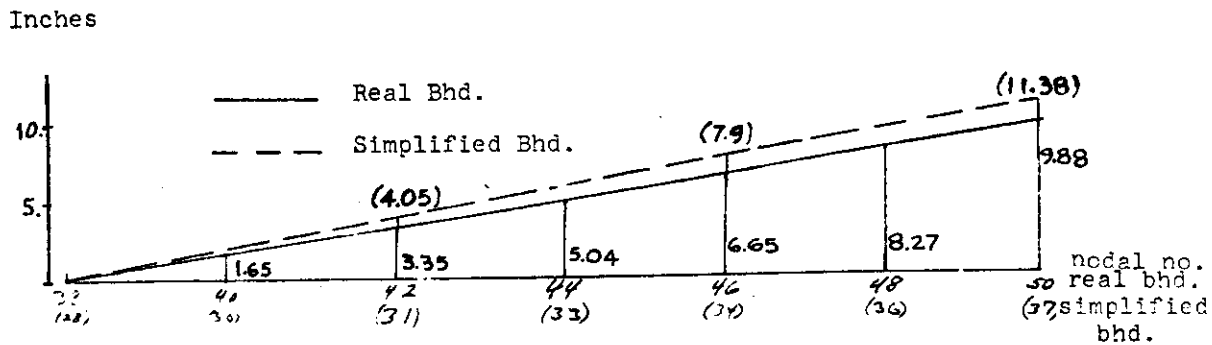


Figure A-10b. Longitudinal deflection of the transverse girder on bulkhead.

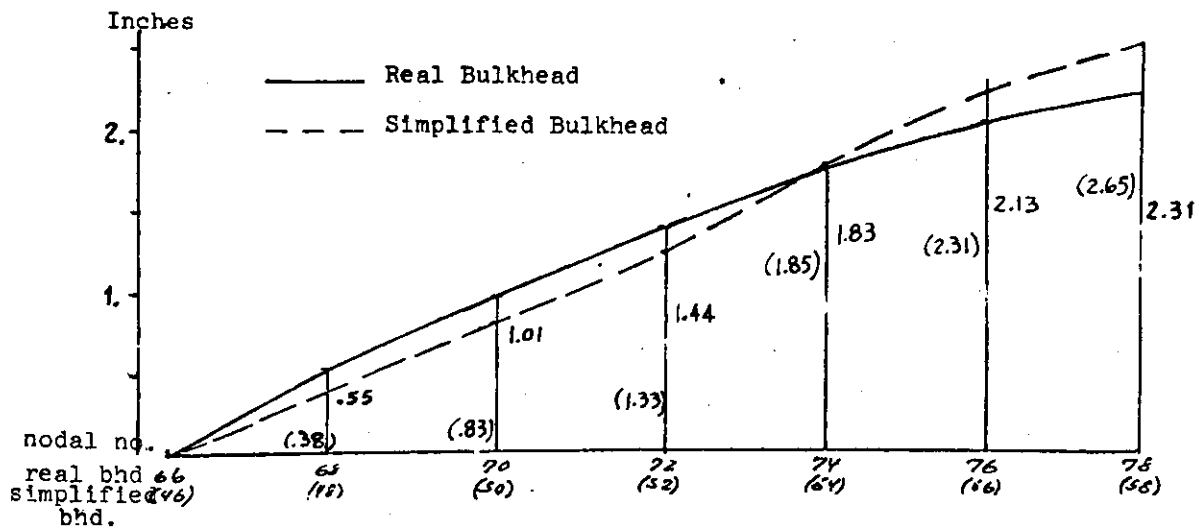


Figure A-10c. Longitudinal deflection in the lower plating (second deck) of transverse box girder.

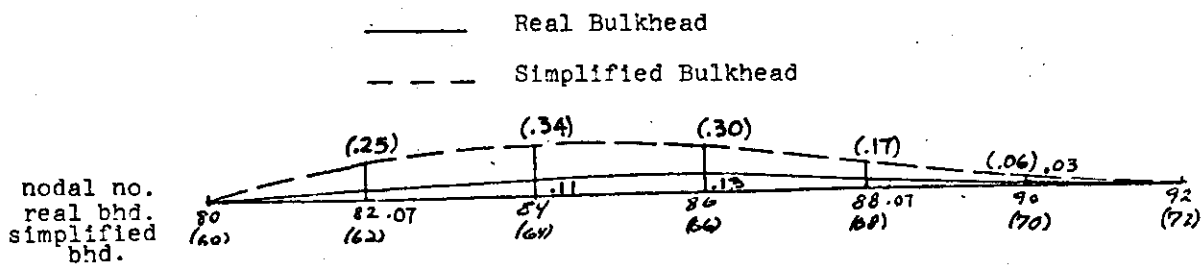


Figure A-10d. Longitudinal deflection in the upper plating (main deck) of transverse box girder.

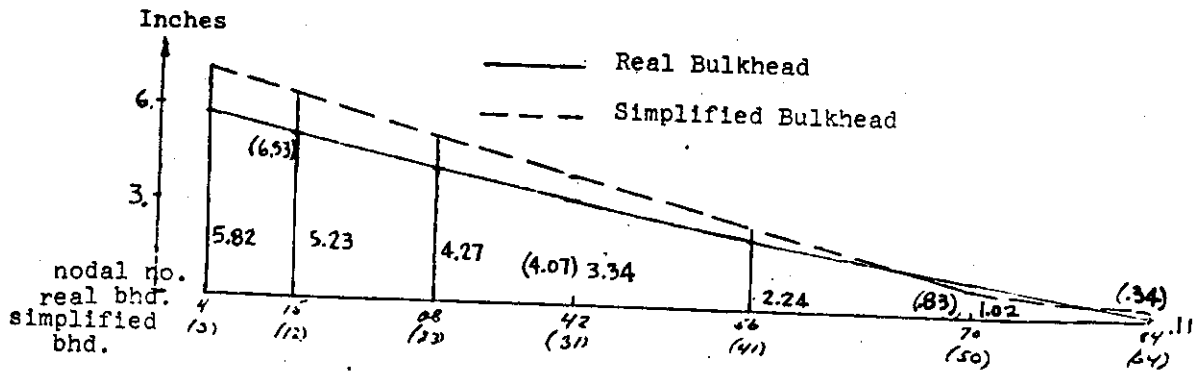


Figure A-10e. Longitudinal deflection at vertical girder 214.2 inches from centerline.

It is interesting to see that the deflection of the real and simplified bulkhead do not differ significantly, even if the lumping of the stiffeners in the simplified case is pretty rough. In general the displacement follows the same pattern with the simplified bulkhead values a little larger than those of the real bulkhead.

Results for the shear stresses in the bulkheads were also analyzed (Fig. A-11a through A-11d). All numbers in () refer to the simplified case. The curve is dotted in this case. Nodal points are underlined. The model simplifications lead to no significant differences.

As a result of these rather comprehensive finite element calculations it can be concluded that the 1:50 scale model exhibits the same structural behavior as the full scale ship. Differences do occur, of course, but these appear to be relatively minor.

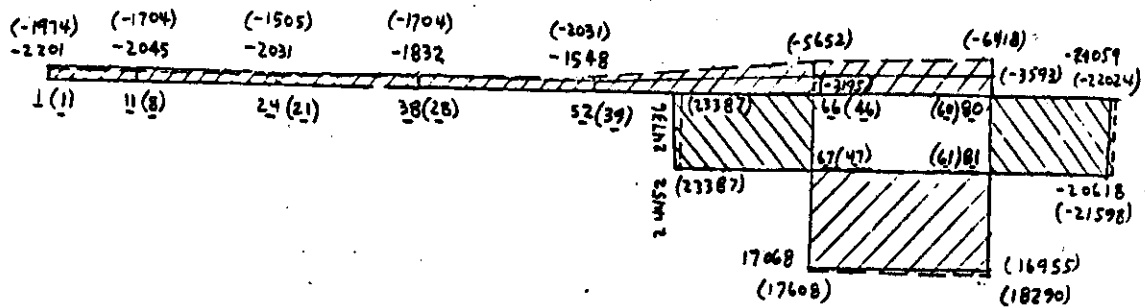


Figure A-11a. Shear stress distribution (psi) vertical section at centerline. Model vs. Ship (Model data and results are in parenthesis)

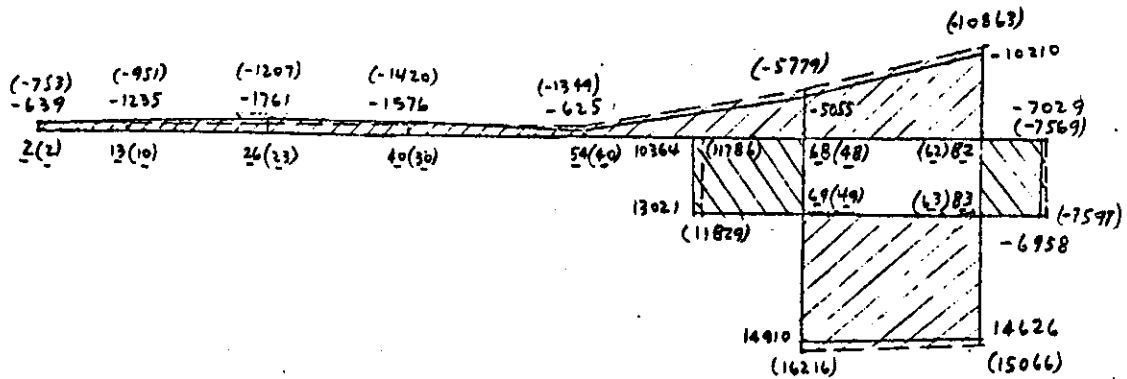


Figure A-11b. Shear stress distribution (psi) vertical section (104.7 in.) from centerline (Note scale change from Fig. A-11a) Model vs. Ship

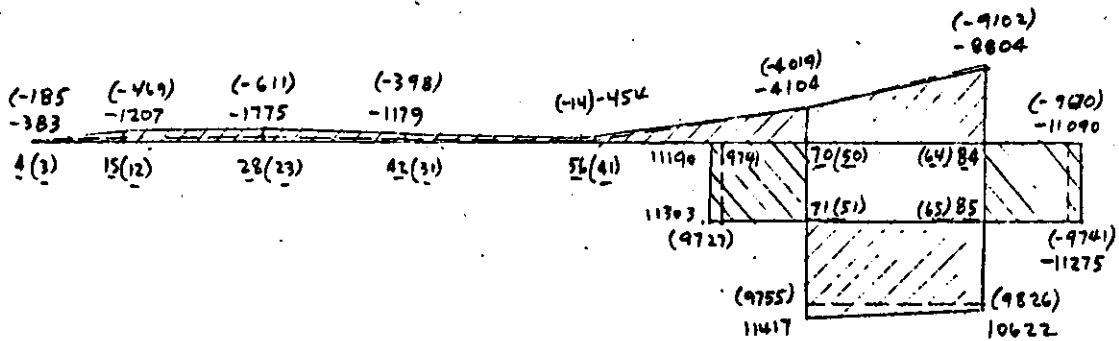


Figure A-11c. Shear stress distribution (psi) vertical section (214.17 in.) from centerline Model vs. Ship

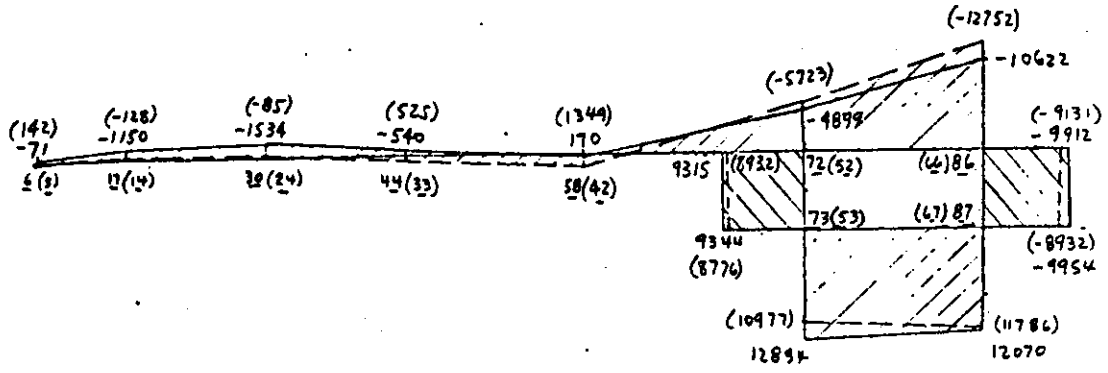


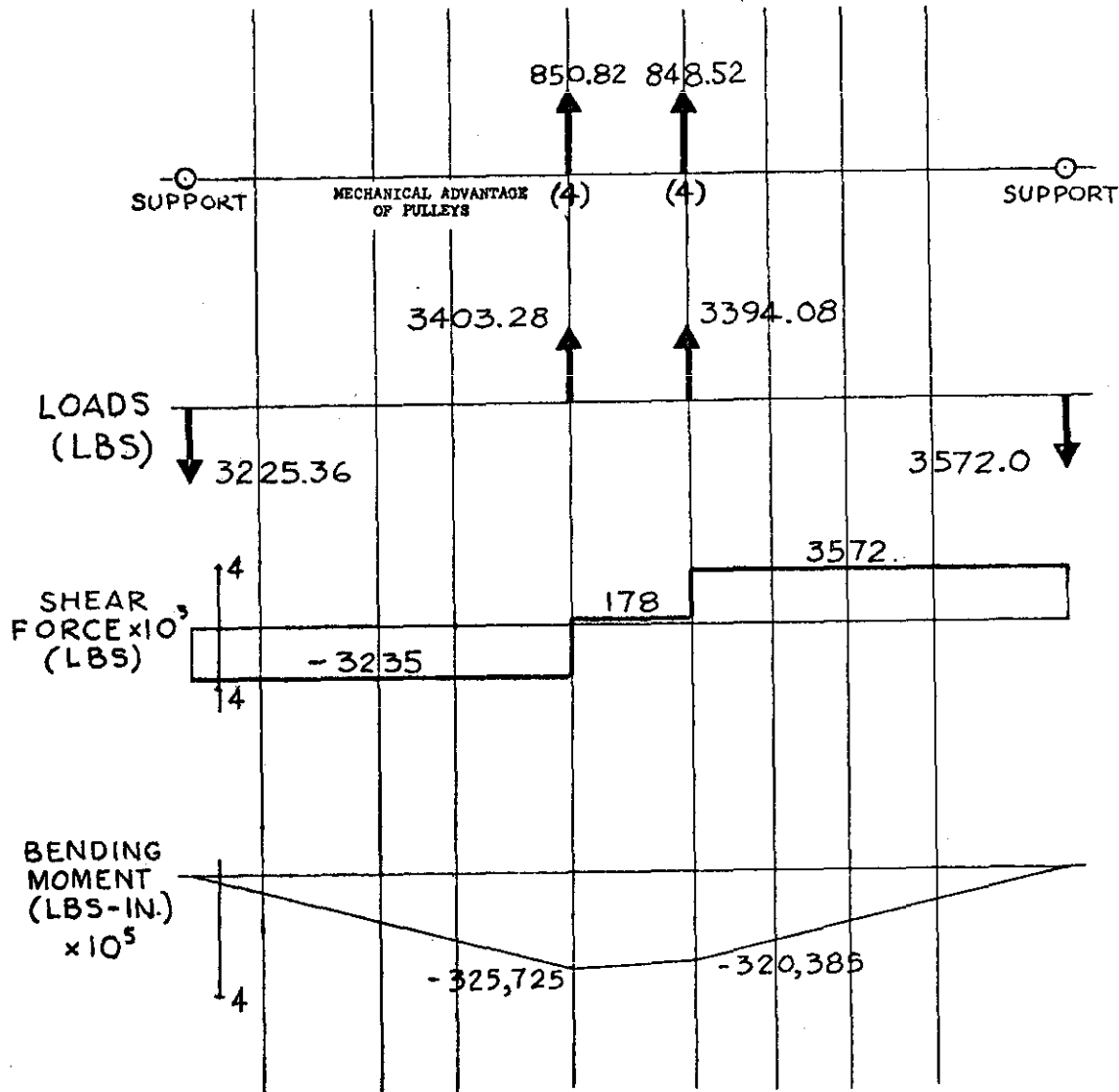
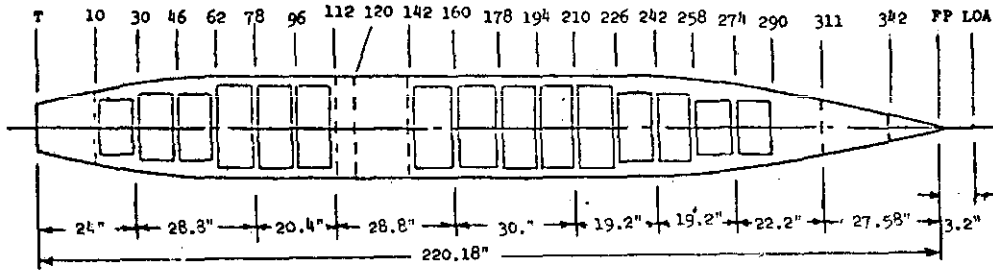
Figure A-11d. Shear stress distribution (psi) vertical section (323.62 in.) from centerline Model vs. Ship

STRUCTURAL TESTS OF SL-7 SHIP MODEL

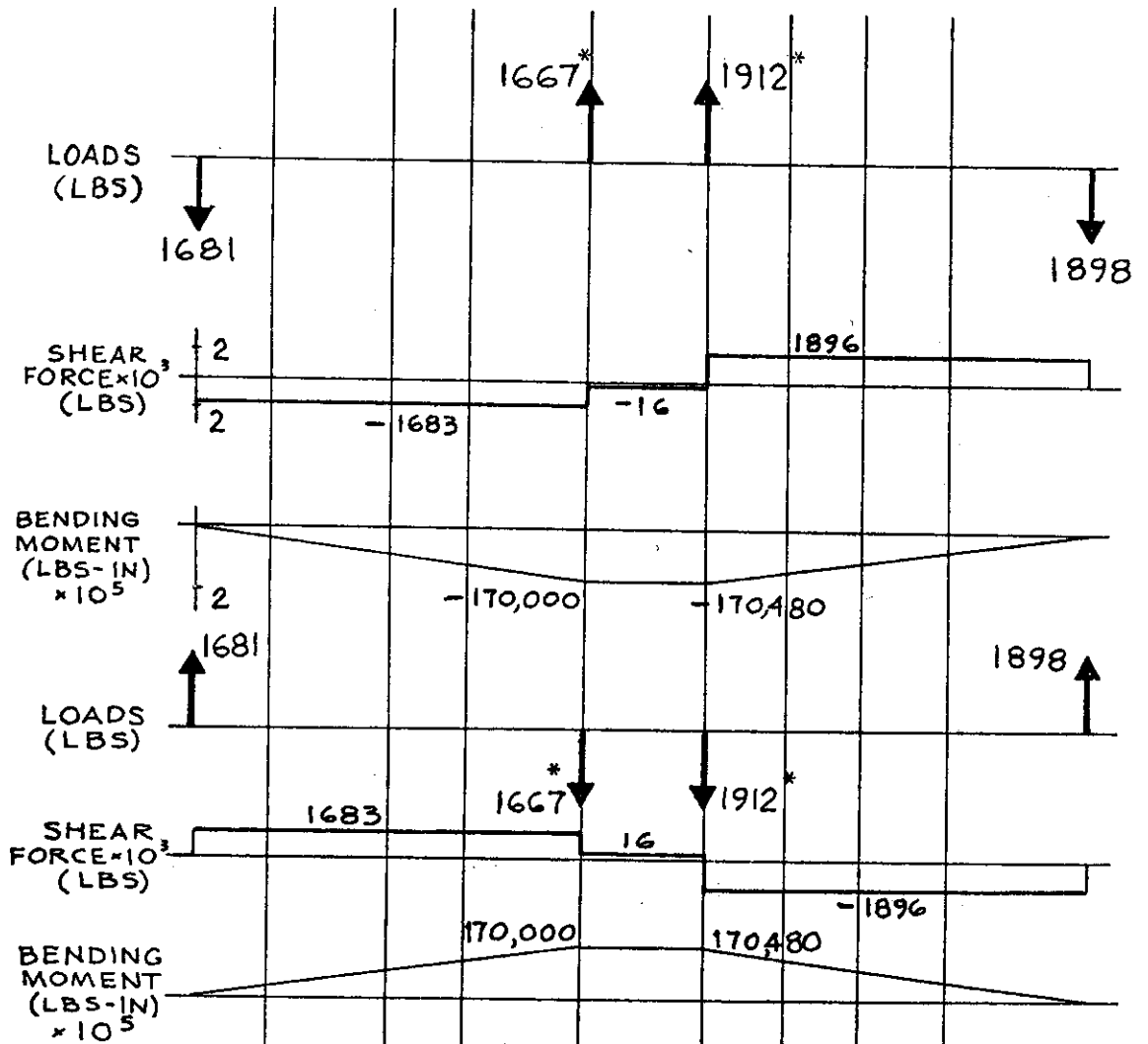
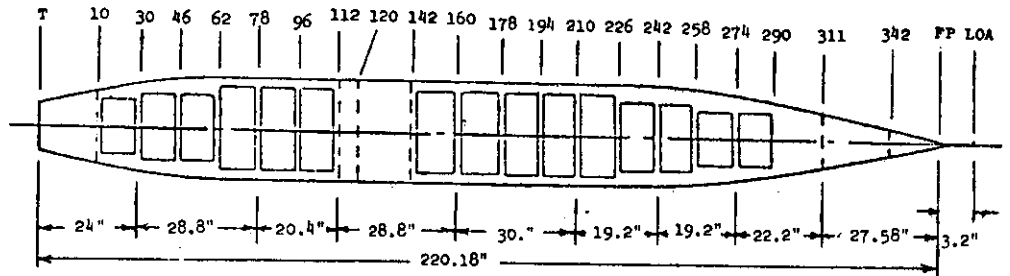
APPENDIX B: TEST DATA

NORMALIZED STRESSES DUE TO
VERTICAL BENDING

(-) LARGE B.M.	MAY 26 & JUNE 27, 1972
(-) $\frac{1}{2}$ LARGE B.M.	JUNE 22, 1972
(+) $\frac{1}{2}$ LARGE B.M.	JUNE 19, 1972



Date of Experiment 29 March, 26 & 27 June 1972



* Includes a mechanical advantage of 4, by the pulleys.

Date of Experiment 22 June 1972

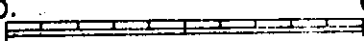
SECTION 2" FORWARD OF FRAME 10

LONGITUDINAL STRESSES DUE TO LONGITUDINAL BENDING

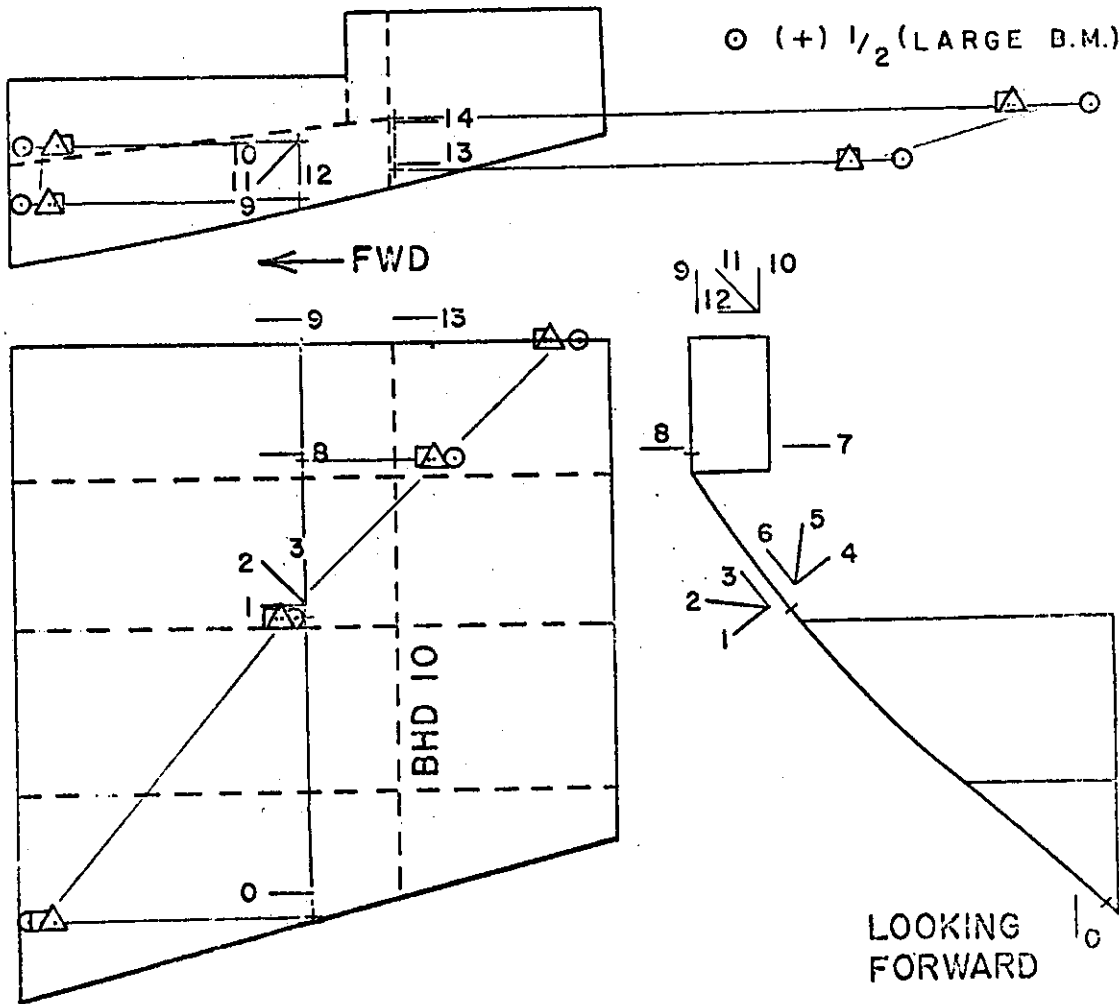
NO. OF ROSETTES - 3 (125 RA)

SINGLE GAGES - 6 (250 BG)

DATE OF EXPERIMENT 1972

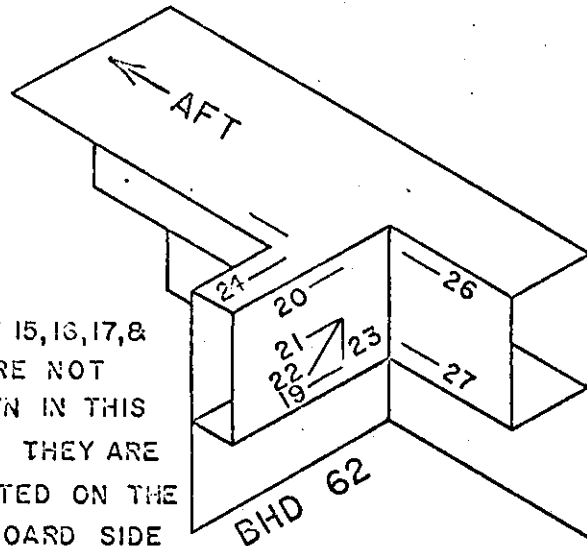
SCALE OF STRESS 0.  0.1 (IN.)⁻³

- △ (-) LARGE B.M.
- (-) 1/2 (LARGE B.M.)
- (+) 1/2 (LARGE B.M.)



SECTION AT HATCH CORNER PORT SIDE FRAME 62

LONGITUDINAL STRESSES DUE TO

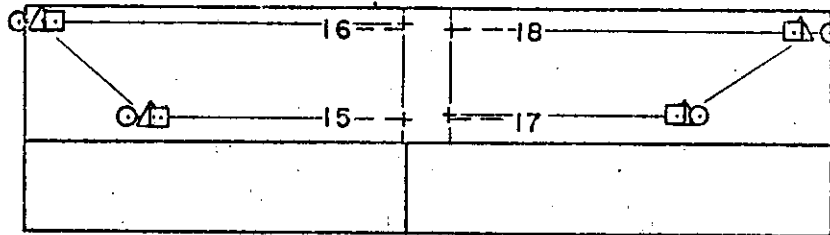


GAGE 15, 16, 17, & 18 ARE NOT SHOWN IN THIS VIEW. THEY ARE LOCATED ON THE OUTBOARD SIDE OF THE SHELL PLATE.

NO. OF ROSETTES
-1(250 RA)
SINGLE GAGES
-10(250 BG)
DATE OF EXPERIMENT
1972

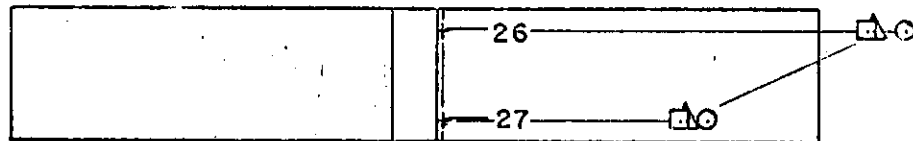
SCALE OF STRESS
0 0.025 (IN.)⁻³

- △ (-) LARGE B.M.
- (-) 1/2 (LARGE B.M.)
- (+) 1/2 (LARGE B.M.)



LOOKING OUTBOARD
SHELL PLATE

FWD →



BHD 62
LOOKING OUTBOARD
TORSION BOX

SECTION 2" FORWARD OF FRAME 142

LONGITUDINAL STRESSES DUE TO

NO. OF ROSETTES - 4 (125 RA)
 - 2 (250 RA)

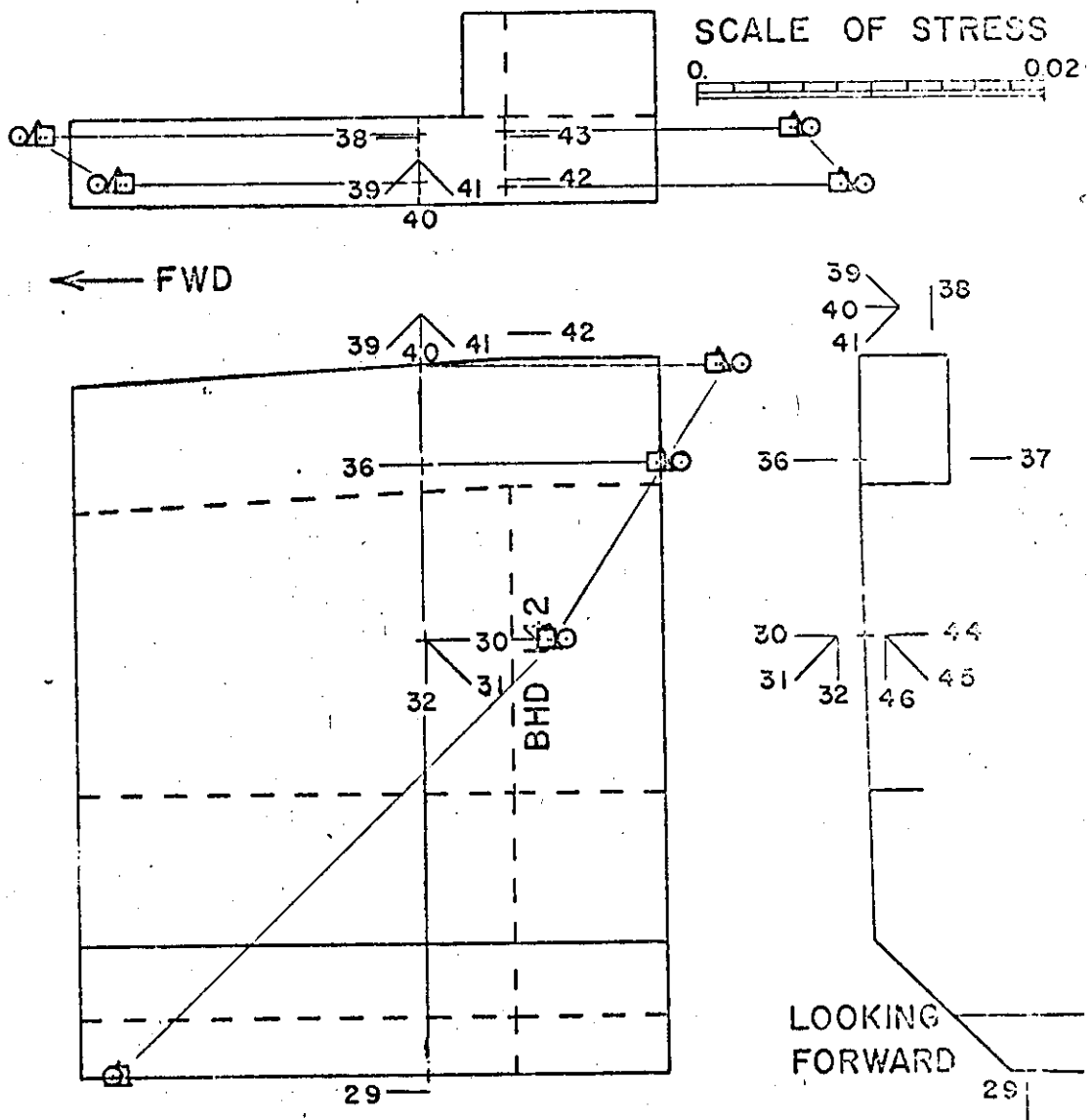
SINGLE GAGES - 9 (250 BG)

DATE OF EXPERIMENT 1972

△ (-) LARGE B.M.

□ (-) 1/2 (LARGE B.M.)

○ (+) 1/2 (LARGE B.M.)



SECTION 2" FORWARD OF FRAME 142

LONGITUDINAL STRESSES DUE TO

NO. OF ROSETTES - 4 (125 RA)
 - 2 (250 RA)

SINGLE GAGES - 9 (250 BG)

DATE OF EXPERIMENT

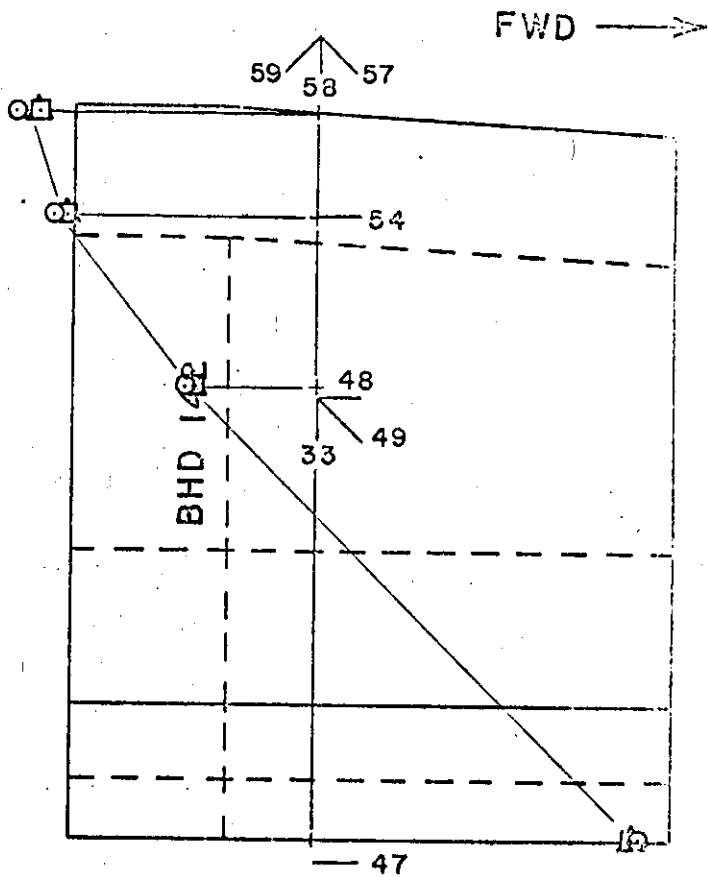
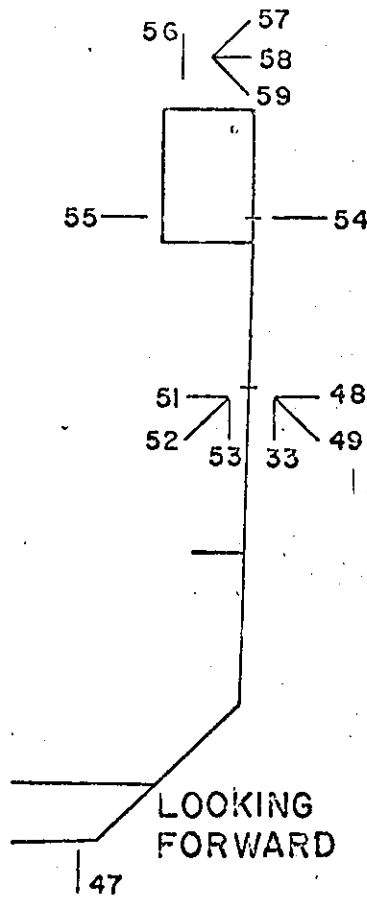
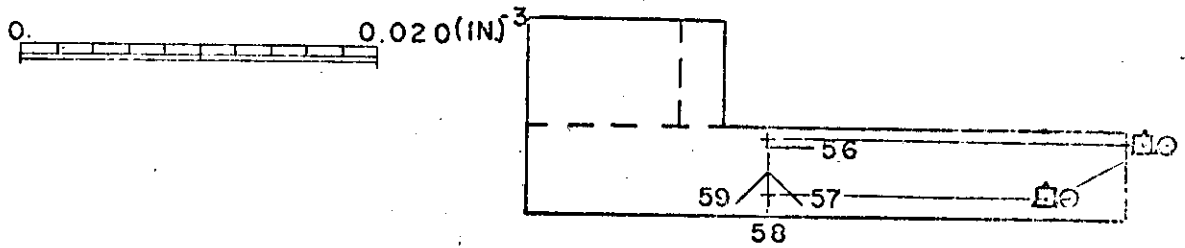
1972

SCALE OF STRESS

△ (-) LARGE B.M.

◻ (-) 1/2 (LARGE B.M.)

○ (+) 1/2 (LARGE B.M.)



SECTION 2" FORWARD OF FRAME 142

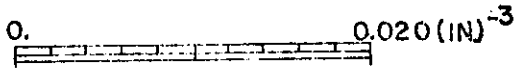
LONGITUDINAL STRESSES DUE TO

NO. OF ROSETTES - 4 (125 RA)
 - 2 (250 RA)

SINGLE GAGES - 9 (250 BG)

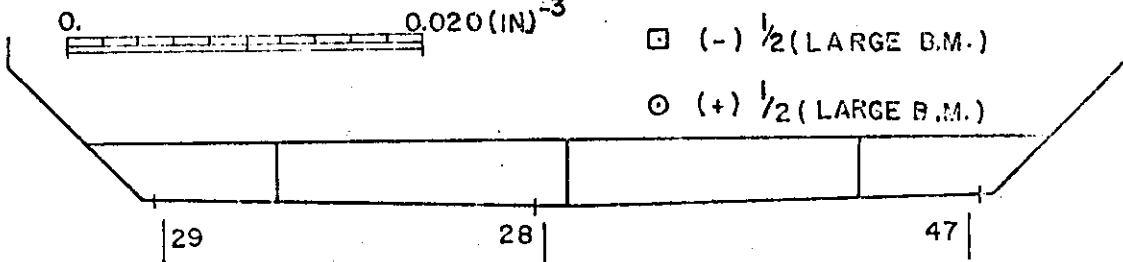
DATE OF EXPERIMENT 1972

SCALE OF STRESS △ (-) LARGE B.M.

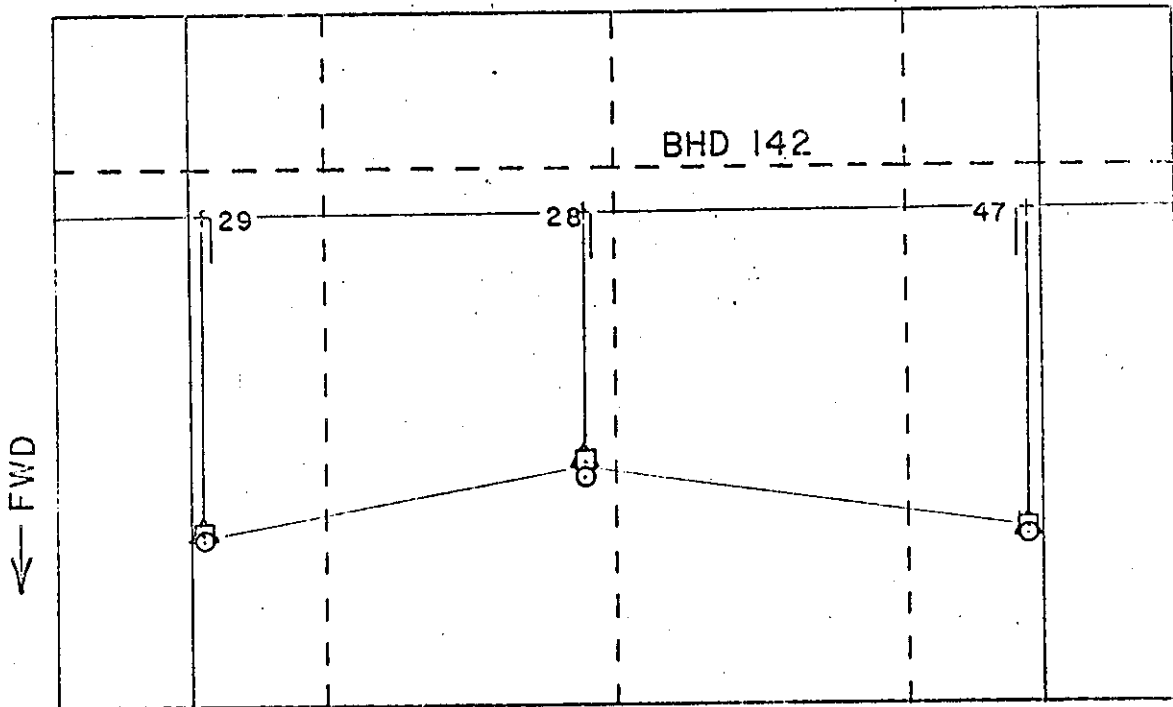


□ (-) 1/2 (LARGE B.M.)

○ (+) 1/2 (LARGE B.M.)



LOOKING FORWARD



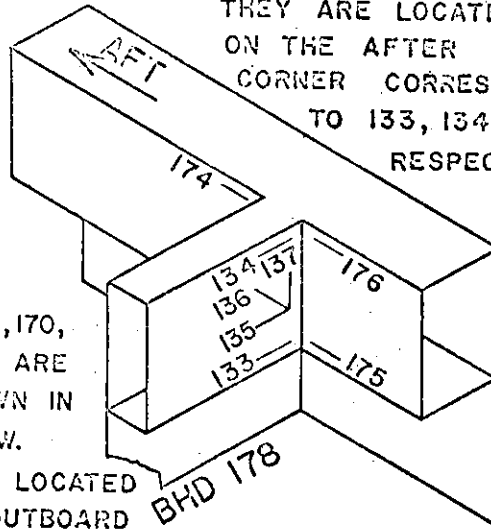
BOTTOM PLATE

SECTION AT HATCH CORNER PORT SIDE FRAME 178

LONGITUDINAL STRESSES DUE TO
GAGES 131, 132, & 173
ARE NOT SHOWN.

THEY ARE LOCATED
ON THE AFTER
CORNER CORRESPONDING
TO 133, 134, & 175
RESPECTIVELY.

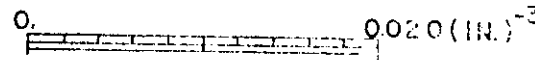
NO. OF ROSETTES
-1(250 RA)
SINGLE GAGES
-12(250 BC)



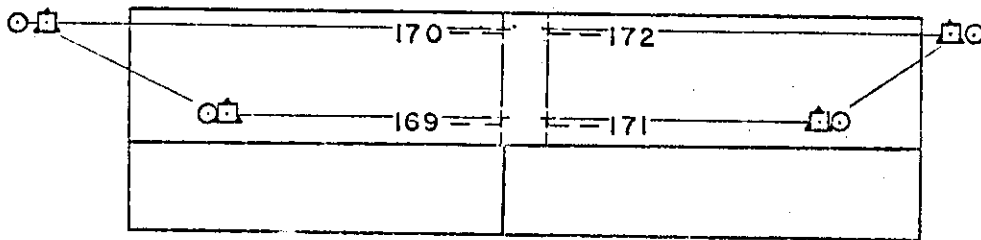
GAGES 169, 170,
171, & 172 ARE
NOT SHOWN IN
THIS VIEW.
THEY ARE LOCATED
ON THE OUTBOARD
SIDE OF THE SHELL PLATE.

DATE OF EXPERIMENT
1972

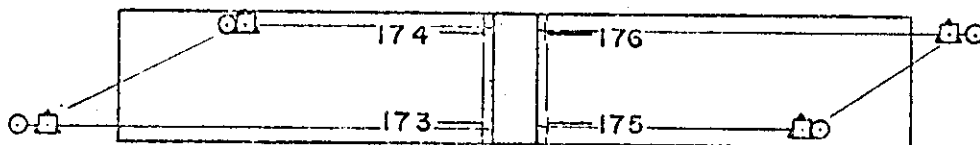
SCALE OF STRESS



- △ (-) LARGE B.M.
- (-) 1/2 (LARGE B.M.)
- (+) 1/2 (LARGE B.M.)



LOOKING OUTBOARD SHELL PLATE → FWD



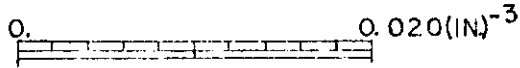
BHD 178
LOOKING OUTBOARD TORSION BOX → FWD

SECTION BETWEEN FRAMES 178 & 194

LONGITUDINAL STRESSES DUE TO
 SINGLE GAGES - 2(250 BG)
 NO. OF ROSETTES - 4(125 RA)
 - 12(250 RA)

DATE OF EXPERIMENT 1972

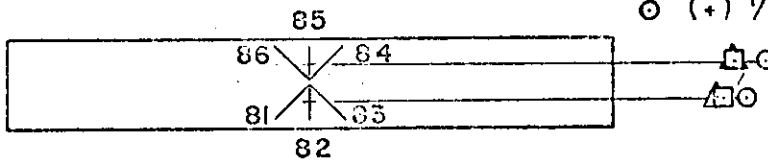
SCALE OF STRESS



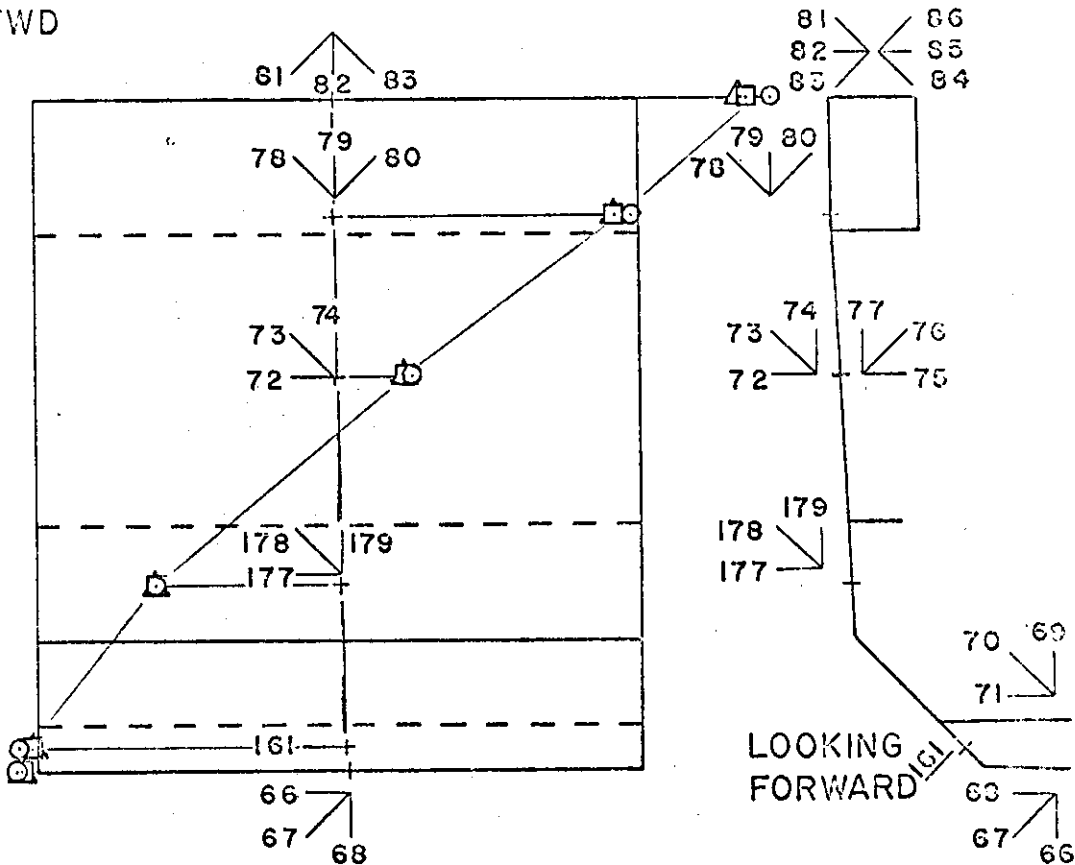
△ (-) LARGE B.M.

□ (-) 1/2 (LARGE B.M.)

○ (+) 1/2 (LARGE B.M.)



← FWD



SECTION BETWEEN FRAMES 178 & 194

LONGITUDINAL STRESSES DUE TO
 SINGLE GAGES - 2(250 BG)
 NO. OF ROSETTES - 4(125 RA)
 -12(250 RA)

DATE OF EXPERIMENT

1972

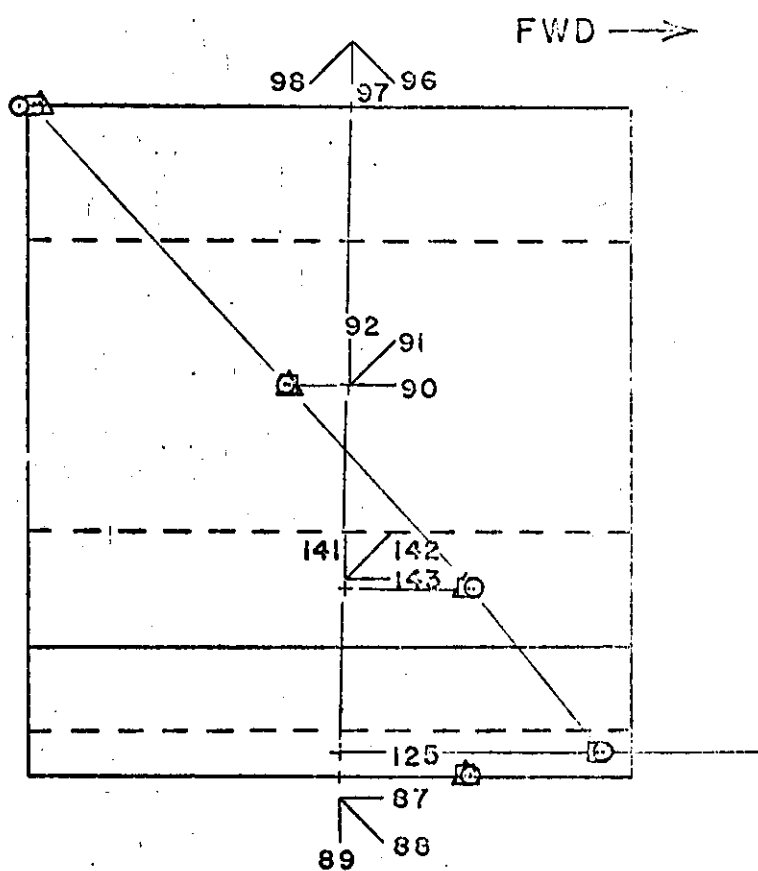
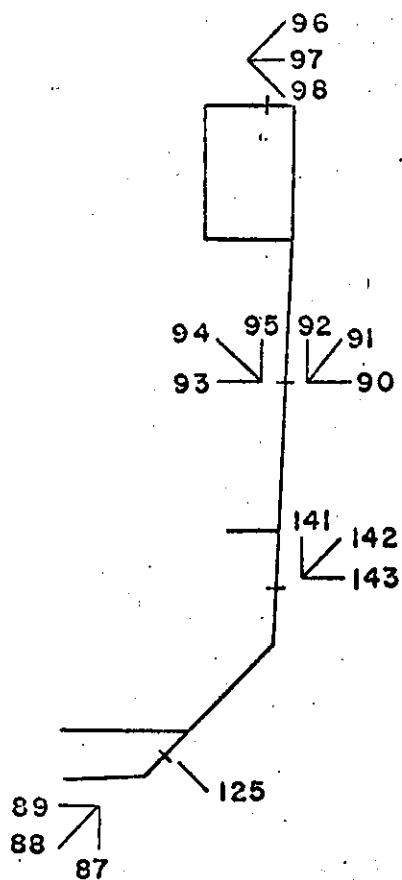
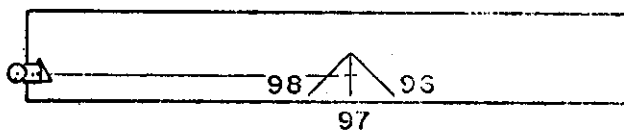
SCALE OF STRESS

△ (-) LARGE B.M.



□ (-) 1/2 (LARGE B.M.)

○ (+) 1/2 (LARGE B.M.)

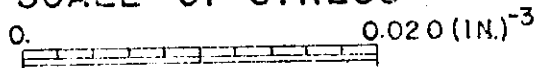


SECTION BETWEEN FRAMES 178 & 194

LONGITUDINAL STRESSES DUE TO
SINGLE GAGES - 2(250 BG)
NO. OF ROSETTES - 4(125 RA)
- 12(250 RA)

DATE OF EXPERIMENT 1972

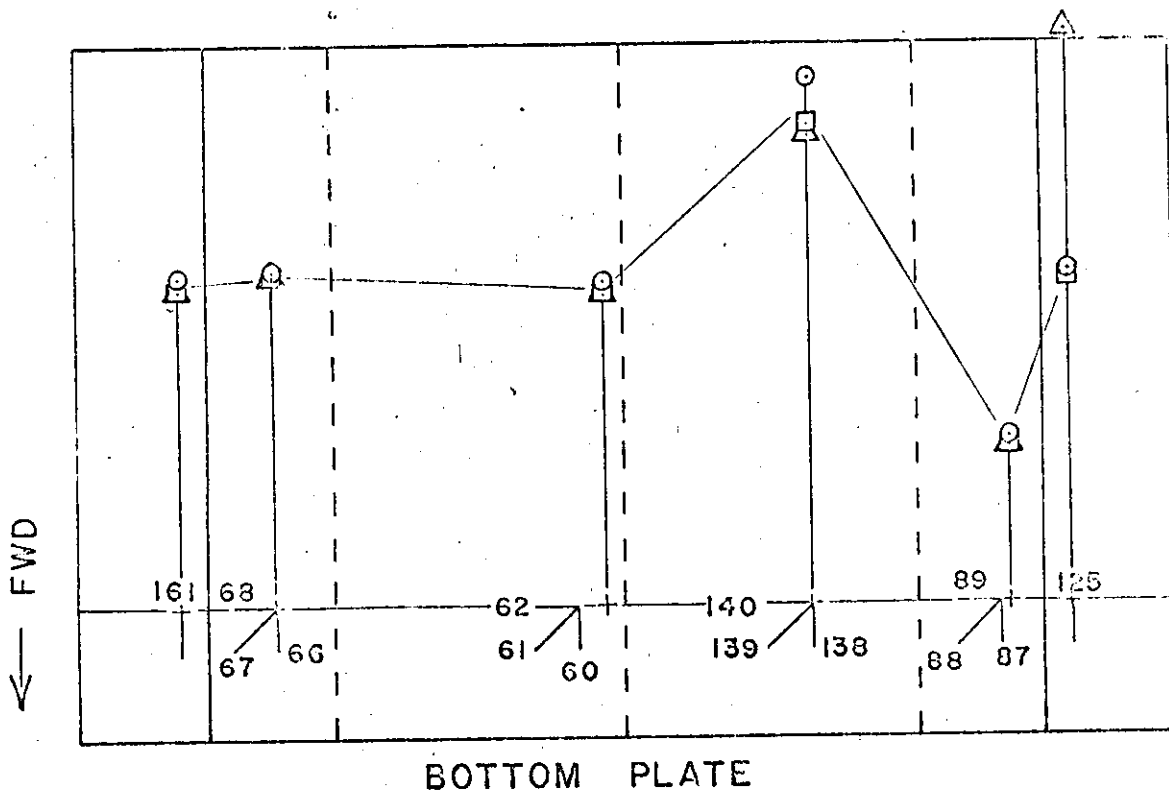
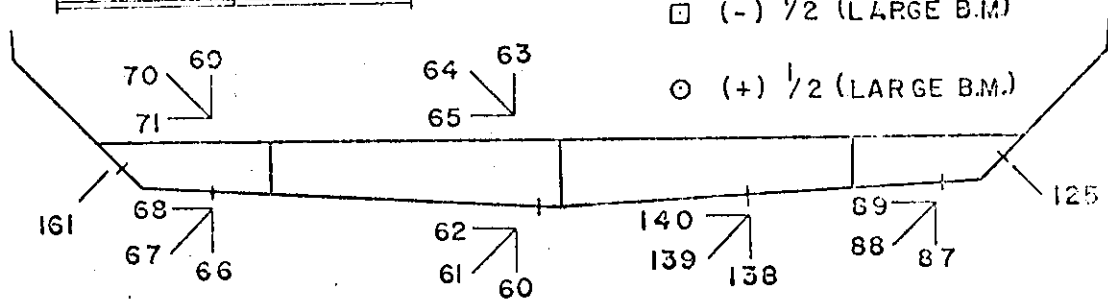
SCALE OF STRESS



△ (-) LARGE B.M.

□ (-) 1/2 (LARGE B.M.)

○ (+) 1/2 (LARGE B.M.)

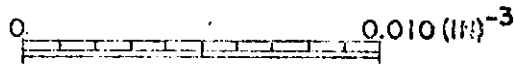


SECTION BETWEEN FRAMES 178 & 194

LONGITUDINAL STRESSES DUE TO
SINGLE GAGES - 2(250 BG)
NO. OF ROSETTES - 4(125 RA)
-12(250 RA)

DATE OF EXPERIMENT 1972

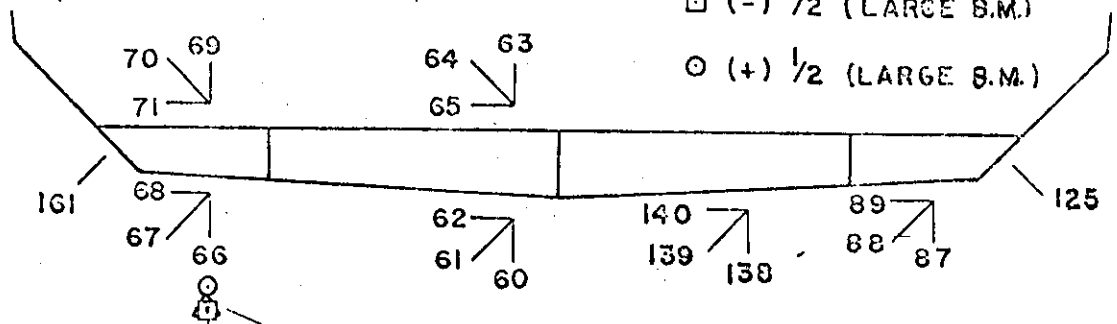
SCALE OF STRESS



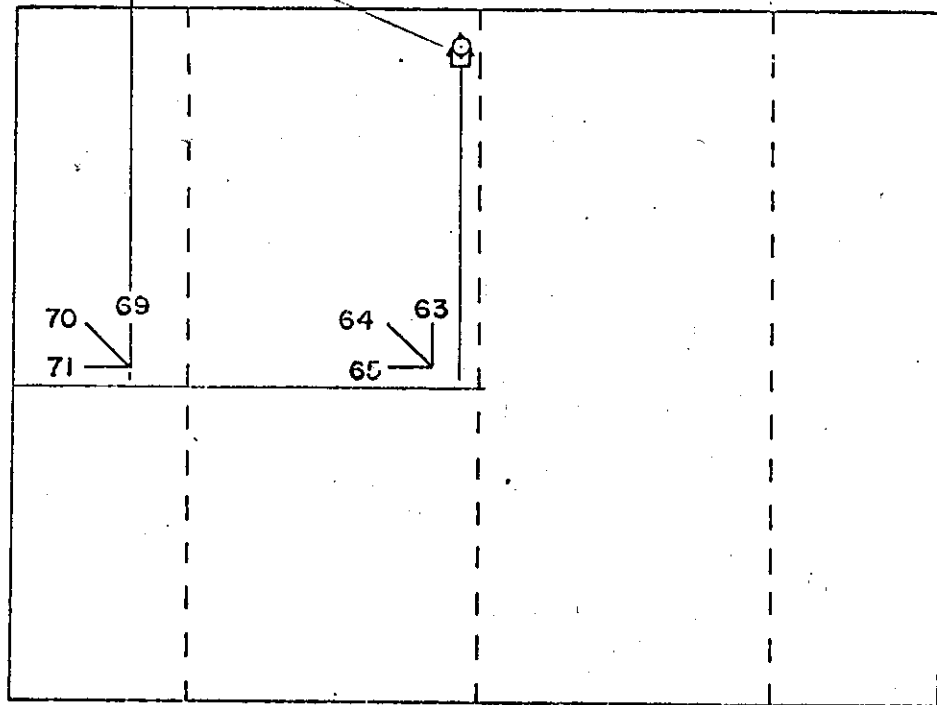
△ (-) LARGE B.M.

□ (-) 1/2 (LARGE B.M.)

○ (+) 1/2 (LARGE B.M.)



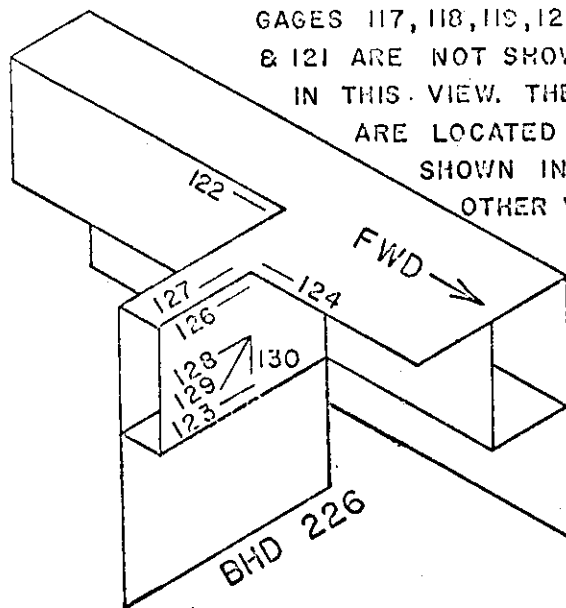
FWD ↑



TANK TOP

SECTION AT HATCH CORNER PORT SIDE FRAME 226

LONGITUDINAL STRESSES DUE TO



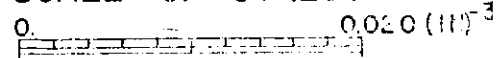
GAGES 117, 118, 119, 120,
& 121 ARE NOT SHOWN
IN THIS VIEW. THEY
ARE LOCATED AS
SHOWN IN
OTHER VIEWS.

NO. OF ROSETTES
- 1(250 RA)
SINGLE GAGES
- 10(250 BG)

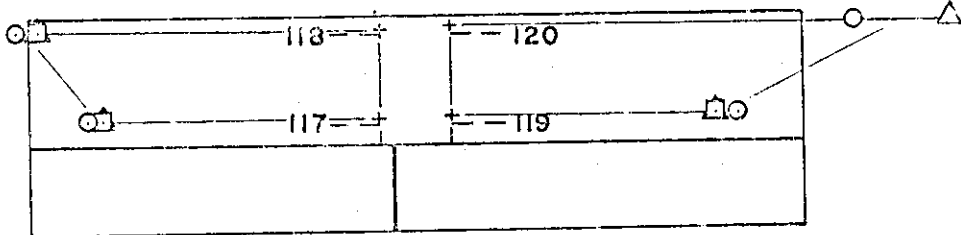
DATE OF EXPERIMENT

1972

SCALE OF STRESS

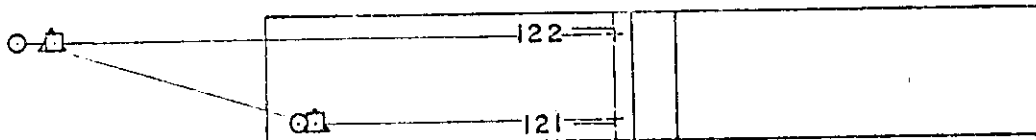


- △ (-) LARGE B.M.
- (-) 1/2 (LARGE B.M.)
- (+) 1/2 (LARGE B.M.)



LOOKING OUTBOARD
SHELL PLATE

→ FWD



BHD
226

LOOKING OUTBOARD
TORSION BOX

SECTION 1" AFT OF FRAME 290

LONGITUDINAL STRESSES DUE TO

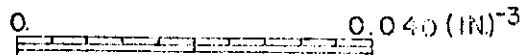
NO. OF ROSETTES - 2(250 RA)

- 1(125 RA)

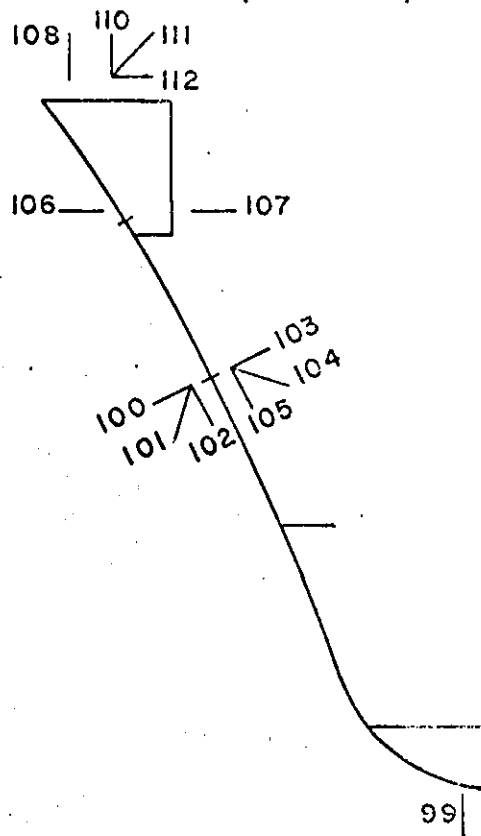
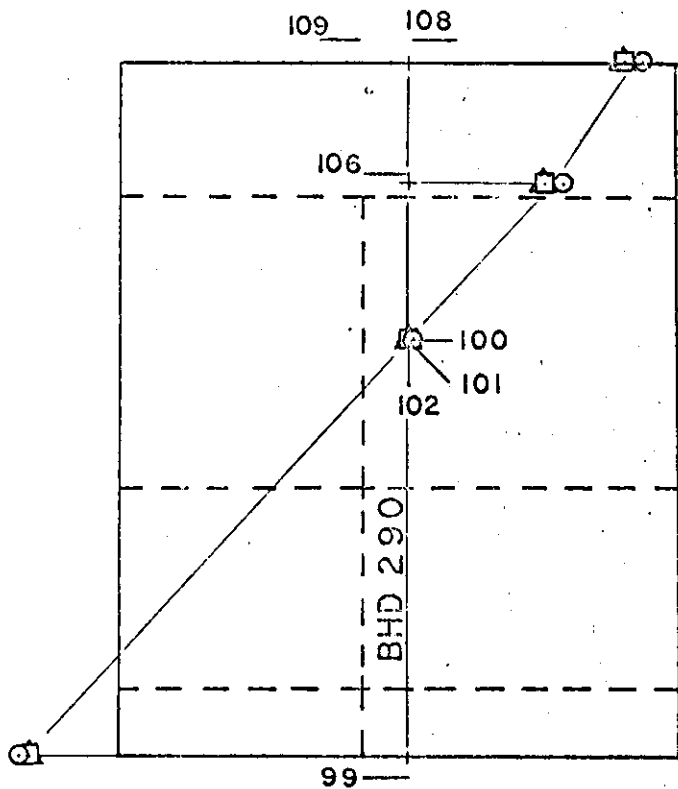
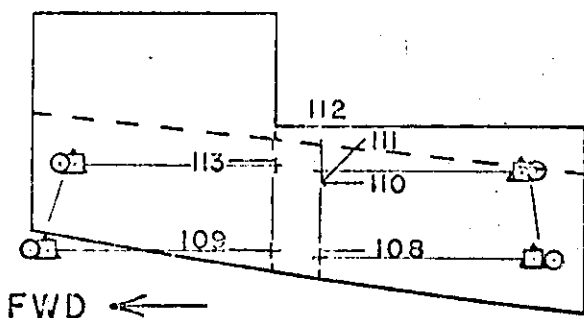
SINGLE GAGES - 6(250 BG)

DATE OF EXPERIMENT
1972

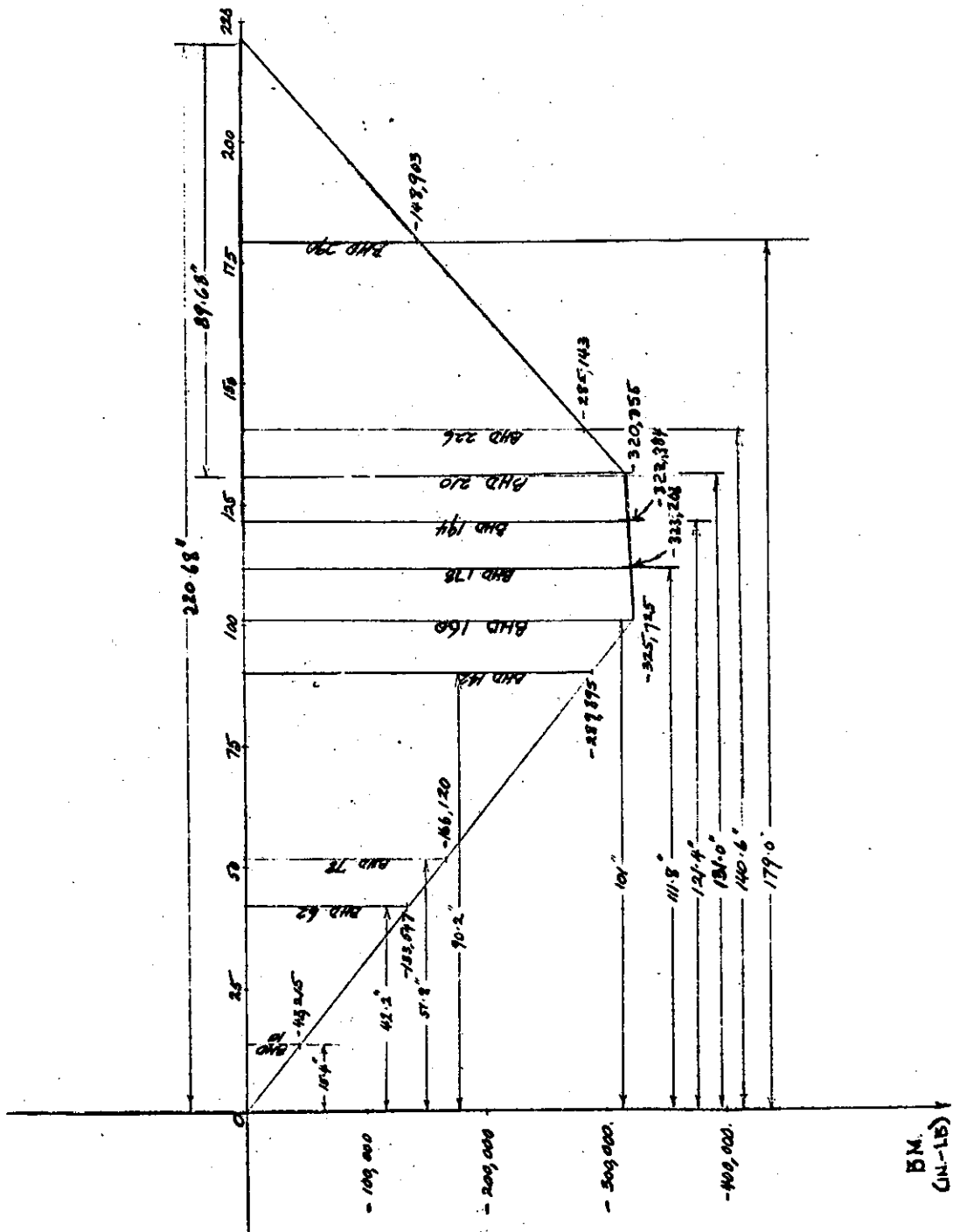
SCALE OF STRESS

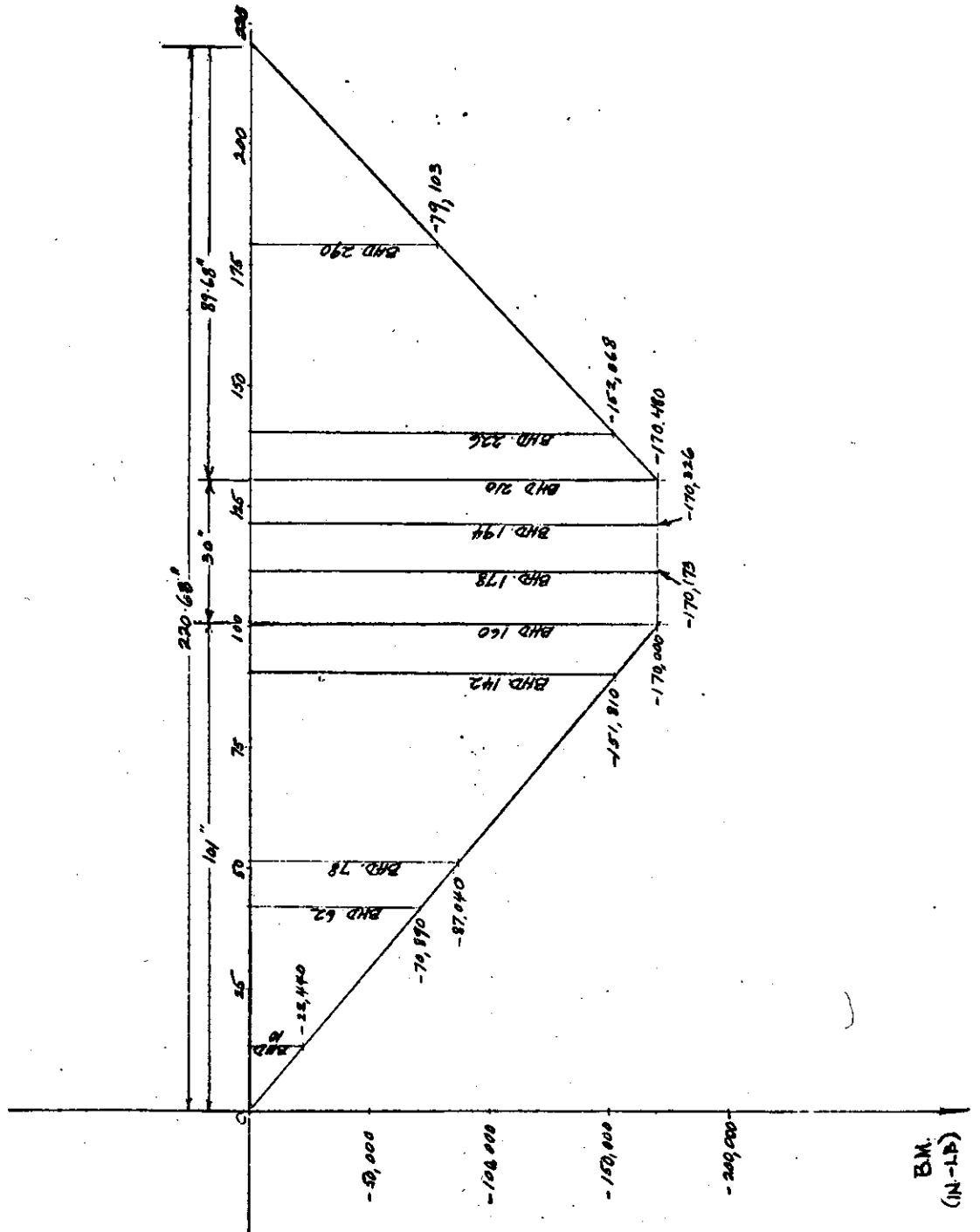


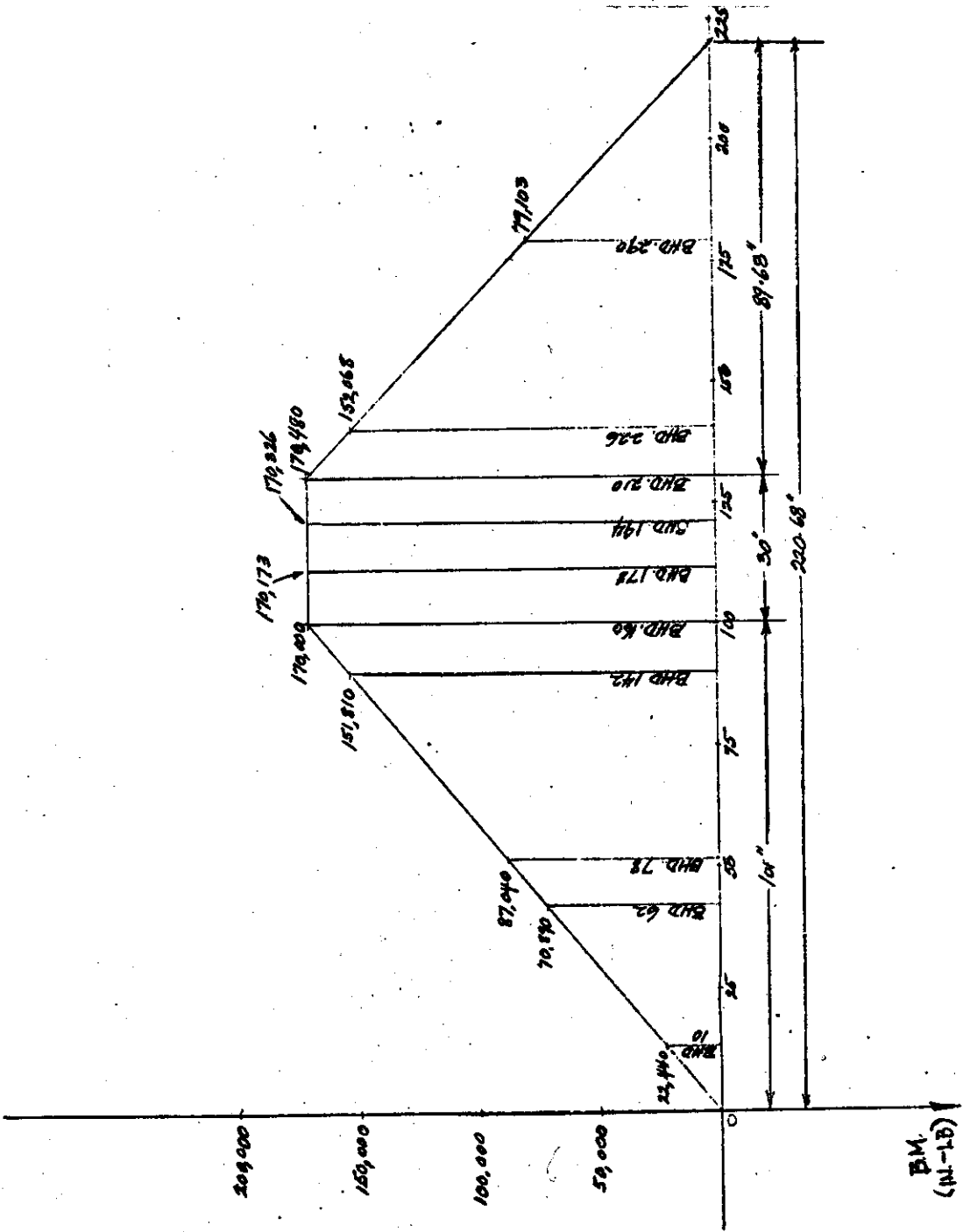
- △ (-) LARGE B.M.
- ◻ (-) 1/2 (LARGE B.M)
- (+) 1/2 (LARGE B.M)



LOOKING FORWARD







LONGITUDINAL BENDING MOMENT

BHD 10 (PORT SIDE)

GAGE LOCATION			(-) LARGE			(-) 1/2 (LARGE)			(+) 1/2 (LARGE)		
GAGE NO.	FWD OF BHD (IN)	AFT OF BHD (IN)	B.M. (LBS-IN)	LONGL STRESS (psi)	NORMALIZED (1/IN ³) x10 ⁻¹	B.M. (LBS-IN)	LONGL STRESS (psi)	NORMALIZED (1/IN ³) x10 ⁻¹	B.M. (LBS-IN)	LONGL STRESS (psi)	NORMALIZED (1/IN ³) x10 ⁻¹
0	1.97		49,568	3,606	0.727	25,739	1965	0.763	25,739	2037	0.791
1	2.09		49,955	315.5 *	0.0632	25,940	203.5 *	0.785	25,940	68.5	0.0264
8	2.25		50,471	-1848	-0.366	26,208	-937	-0.358	26,208	-1119	-0.427
9	2.06		49,858	-3507	-0.703	25,890	-1797	-0.694	25,890	-2019	-0.780
10	2.00		49,665	-3352	-0.675	25,789	-1702	-0.660	25,789	-1999	-0.775
13		0.38	41,990	-5376	-1.280	21,804	-2781	-1.275	21,804	-3096	-1.420
14		0.24	42,119	-7335	-1.741	21,871	-3786	-1.731	21,871	-4272	-1.953

B-19

LONGITUDINAL BENDING MOMENT

BHD 62 (PORT SIDE)

GAGE LOCATION			(-) LARGE			(-) 1/2 (LARGE)			(+1) 1/2 (LARGE)		
GAGE NO.	FWD OF BHD (IN)	AFT OF BHD (IN)	B.M. (LBS-IN)	LONGL STRESS (psi)	NORMALIZED (1/IN ³) x10 ⁻¹	B.M. (LBS-IN)	LONGL STRESS (psi)	NORMALIZED (1/IN ³) x10 ⁻¹	B.M. (LBS-IN)	LONGL STRESS (psi)	NORMALIZED (1/IN ³) x10 ⁻¹
15		0.94	130,572	-2313	-0.177	69,311	-1170	-0.169	69,311	-1341	-0.193
16		0.94	130,572	-3294	-0.252	69,311	-1689	-0.244	69,311	-1866	-0.269
17	2.50		141,459	-2334	-0.165	75,090	-1194	-0.159	75,090	-1317	-0.175
18	2.47		141,364	-3498	-0.247	75,039	-1791	-0.239	75,039	-2001	-0.267
26			141,364	-4284	-0.303	75,039	-2226	-0.297	75,039	-2442	-0.325
27			141,459	-2418	-0.171	75,090	-1257	-0.167	75,090	-1398	-0.186

B-20

BHD 142 (PORT SIDE)

GAGE LOCATION			(-) LARGE			(-)1/2 (LARGE)			(+)1/2 (LARGE)		
GAGE NO.	FWD OF BHD (IN.)	AFT OF BHD (IN.)	B.M. (LBS-IN.)	LONGL STRESS (psi)	NORMALIZED (1/IN ³) x10 ⁻¹	B.M. (LBS-IN.)	LONGL STRESS (psi)	NORMALIZED (1/IN ³) x10 ⁻¹	B.M. (LBS-IN.)	LONGL STRESS (psi)	NORMALIZED (1/IN ³) x10 ⁻¹
30	2.53		298,506	-2136	-0.072	156,068	-1107	-0.071	156,068	-1271	-0.081
36	2.25		297,126	-4086	-0.138	155,597	-2097	-0.135	155,597	-2319	-0.149
38	2.25		297,126	-6507	-0.219	155,597	-3342	-0.215	155,597	-3585	-0.230
39	2.16		296,837	-5100	-0.172	155,445	-2620	-0.169	155,445	-2871	-0.185
42		0.94	286,874	-5604	-0.195	150,228	-2901	-0.193	150,228	-3108	-0.207
43		0.84	287,195	-4788	-0.167	150,386	-2481	-0.165	150,386	-2667	-0.177

LONGITUDINAL BENDING MOMENT

BHD 142 (STARBOARD)

GAGE LOCATION			(-) LARGE			(-) 1/2 (LARGE)			(+) 1/2 (LARGE)		
GAGE NO.	FWD OF BHD (IN)	AFT OF BHD (IN)	B.M. (LBS-IN)	LONGL STRESS (psi)	NORMALIZED (1/IN ³) x10 ⁻¹	B.M. (LBS-IN)	LONGL STRESS (psi)	NORMALIZED (1/IN ³) x10 ⁻¹	B.M. (LBS-IN)	LONGL STRESS (psi)	NORMALIZED (1/IN ³) x10 ⁻¹
48	2.06		296,516	-2071	-0.070	155,277	-1665	-0.069	155,277	-1144	-0.074
54	2.00		296,323	-4173	-0.141	155,176	-2166	-0.140	155,176	-2289	-0.148
56	2.09		296,612	-6315	-0.213	155,328	-3285	-0.211	155,328	-3489	-0.225
57	2.00		296,323	-4639	-0.157	155,176	-2413	-0.156	155,176	-2617	-0.169

B-23

BHD 142 (Bottom)

LONGITUDINAL BENDING MOMENT

GAGE LOCATION			(-) LARGE			(-) 1/2 (LARGE)			(+) 1/2 (LARGE)		
GAGE NO.	FWD OF BHD (IN.)	AFT OF BHD (IN.)	B.M. (LBS-IN.)	LONGL STRESS (psi)	NORMALIZED (1/IN ³) x10 ⁻¹	B.M. (LBS-IN.)	LONGL STRESS (psi)	NORMALIZED (1/IN ³) x10 ⁻¹	B.M. (LBS-IN.)	LONGL STRESS (psi)	NORMALIZED (1/IN ³) x10 ⁻¹
28	2.19		296,933	4113	0.139	155,496	2181	0.140	155,496	2310	0.149
29	2.34		297,416	5283	0.178	155,748	2775	0.178	155,748	2832	0.182
47	2.22		297,030	5319	0.179	155,546	2766	0.178	155,546	2853	0.183

B-24

LONGITUDINAL BENDING MOMENT

BHD 186 (PORT SIDE)

GAGE LOCATION			(-) LARGE			(-) 1/2 (LARGE)			(+) 1/2 (LARGE)		
GAGE NO.	FWD OF BHD (IN.)	AFT OF BHD (IN.)	B.M. (LBS-IN)	LONGL STRESS (psi)	NORMALIZED (1/IN ³) x 10 ⁻¹	B.M. (LBS-IN)	LONGL STRESS (psi)	NORMALIZED (1/IN ³) x 10 ⁻¹	B.M. (LBS-IN)	LONGL STRESS (psi)	NORMALIZED (1/IN ³) x 10 ⁻¹
72		4.94	322,973	-1274	-0.039	170,247	-689.9	-0.039	170,247	-707.8	-0.042
78		4.88	322,963	-5143	-0.159	170,248	-2682	-0.158	170,248	-2868	-0.168
81		4.53	322,900	-7386	-0.229	170,254	-3949	-0.232	170,254	-4183	-0.246
84		4.59	322,911	-7713	-0.239	170,253	-4068	-0.239	170,253	-4376	-0.257
161		4.53	322,900	5709	0.177	170,254	3012	0.177	170,254	3126	0.184
177		5.00	322,984	3302	0.102	170,246	1746	0.103	170,246	1768	0.104

B-26

LONGITUDINAL BENDING MOMENT

BHD 194 (STBD SIDE)

GAGE LOCATION			(-) LARGE			(-) 1/2 (LARGE)			(-) 1/2 (LARGE)		
GAGE NO.	FWD OF BHD (IN)	AFT OF BHD (IN)	B.M. (LBS-IN)	LONGL STRESS (psi)	NORMALIZED (1/IN ³) x10 ⁻¹	B.M. (LBS-IN)	LONGL STRESS (psi)	NORMALIZED (1/IN ³) x10 ⁻¹	B.M. (LBS-IN)	LONGL STRESS (psi)	NORMALIZED (1/IN ³) x10 ⁻¹
90		5.19	323,218	-1333	-0.038	170,243	-737.5	-0.042	170,243	-789.1	-0.046
96		4.81	322,950	-7082	-0.219	170,249	-3790	-0.223	170,249	-3980	-0.234
125		4.56	322,906	10341	0.320	170,253	3078	0.181	170,253	3162	0.186
141		5.16	323,012	2730	0.085	170,244	1457	0.086	170,244	1537	0.090

B-27

LONGITUDINAL BENDING MOMENT

BHD 194 (BOTTOM SHELL)

GAGE LOCATION			(-) LARGE			(-) 1/2 (LARGE)			(+) 1/2 (LARGE)		
GAGE NO.	FWD OF BHD (IN.)	AFT OF BHD (IN.)	B.M. (LBS-IN)	LONGL STRESS (psi)	NORMALIZED (1/IN ³) x10 ⁻¹	B.M. (LBS-IN)	LONGL STRESS (psi)	NORMALIZED (1/IN ³) x10 ⁻¹	B.M. (LBS-IN)	LONGL STRESS (psi)	NORMALIZED (1/IN ³) x10 ⁻¹
60		4.84	322,955	5616	0.174	170,249	2962	0.174	170,249	3085	0.181
66		4.78	322,945	5974	0.185	170,250	3132	0.184	170,250	3186	0.187
87		4.81	322,950	2842	0.088	170,249	1477	0.087	170,249	1567	0.092
138		4.81	322,950	8458	0.262	170,249	4568	0.268	170,249	5029	0.295

B-28

LONGITUDINAL BENDING MOMENT

BHD 226 (PORT SIDE)

GAGE LOCATION			(-) LARGE			(-) 1/2 (LARGE)			(+) 1/2 (LARGE)		
GAGE NO.	FWD OF BHD (IN.)	AFT OF BHD (IN.)	B.M. (LBS-IN)	LONGL STRESS (psi)	NORMALIZED (1/IN ³) x 10 ⁻¹	B.M. (LBS-IN)	LONGL STRESS (psi)	NORMALIZED (1/IN ³) x 10 ⁻¹	B.M. (LBS-IN)	LONGL STRESS (psi)	NORMALIZED (1/IN ³) x 10 ⁻¹
117		1.09	289,024	-4635	-0.160	154,138	-2484	-0.161	154,138	-2619	-0.170
118		1.13	289,167	-5757	-0.199	154,214	-3072	-0.199	154,214	-3273	-0.212
119	1.66		279,232	-4338	-0.155	148,916	-2289	-0.154	148,916	-2481	-0.167
120	1.59		279,481	-8169	-0.292	149,049	BAD READING	-	149,049	-3519	-0.236
121		1.07	289,024	-5031	-0.174	154,138	-2676	-0.174	154,138	-2859	-0.185
122		1.13	289,167	-9456	-0.327	154,214	-5025	-0.326	154,214	-5373	-0.348

B-30

LONGITUDINAL BENDING MOMENT

BHD 290 (PORT SIDE)

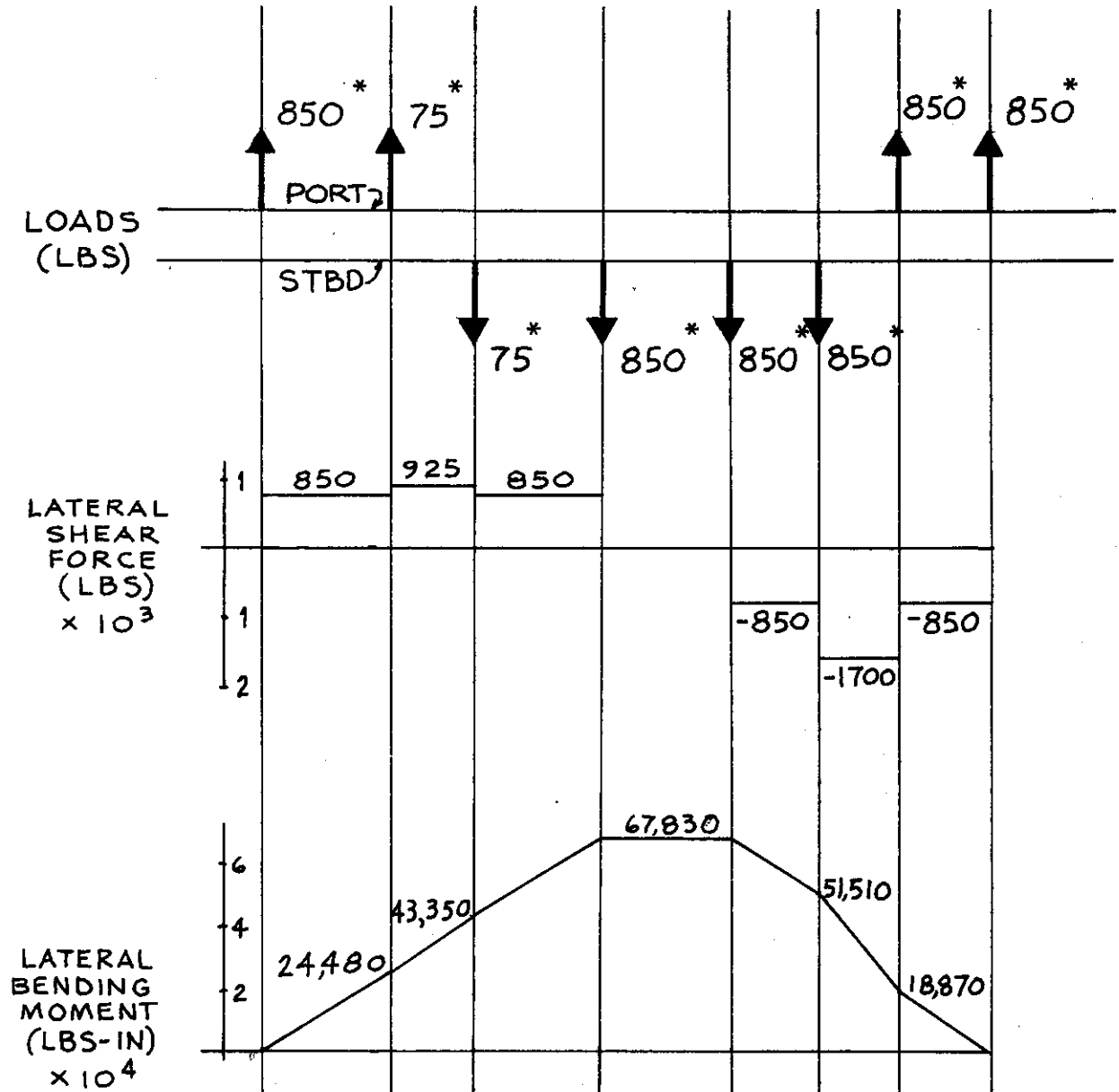
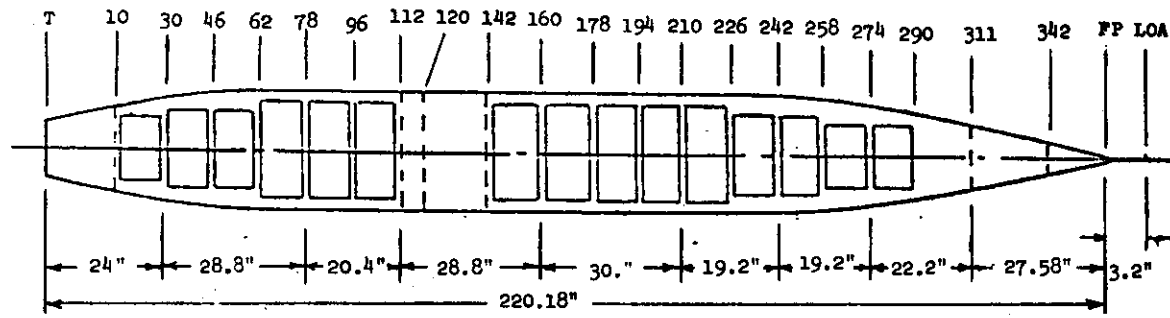
GAGE LOCATION			(-) LARGE			(-) 1/2 (LARGE)			(+1) 1/2 (LARGE)		
GAGE NO.	FWD OF BHD (IN)	AFT OF BHD (IN)	B.M. (LBS-IN)	LONGL STRESS (psi)	NORMALIZED (1/IN ³) x10 ⁻¹	B.M. (LBS-IN)	LONGL STRESS (psi)	NORMALIZED (1/IN ³) x10 ⁻¹	B.M. (LBS-IN)	LONGL STRESS (psi)	NORMALIZED (1/IN ³) x10 ⁻¹
99		1.13	155,940	6492	0.424	81,248	3456	0.425	81,248	3543	0.436
100		0.63	151,154	1:0	0.	80,299	18.5 *	0.002	80,299	-109.6 *	-0.014
106		0.91	152,154	-2370	-0.156	80,830	-1257	-0.156	80,830	-1395	-0.173
108		0.91	152,154	-3711	-0.244	80,830	-1947	-0.241	80,830	-2118	-0.262
109	0.88		145,759	-3699	-0.254	77,433	-1953	-0.252	77,433	-2091	-0.270
110		0.84	151,904	-3469	-0.228	80,697	-1823	-0.226	80,697	-1947	-0.241
113	0.94		145,545	-3306	-0.227	77,319	-1743	-0.225	77,319	-1872	-0.242

B-31

LATERAL BENDING MOMENT

+ LATERAL BENDING AUGUST 21, 1972
- (-LATERAL BENDING) AUGUST 22, 1972

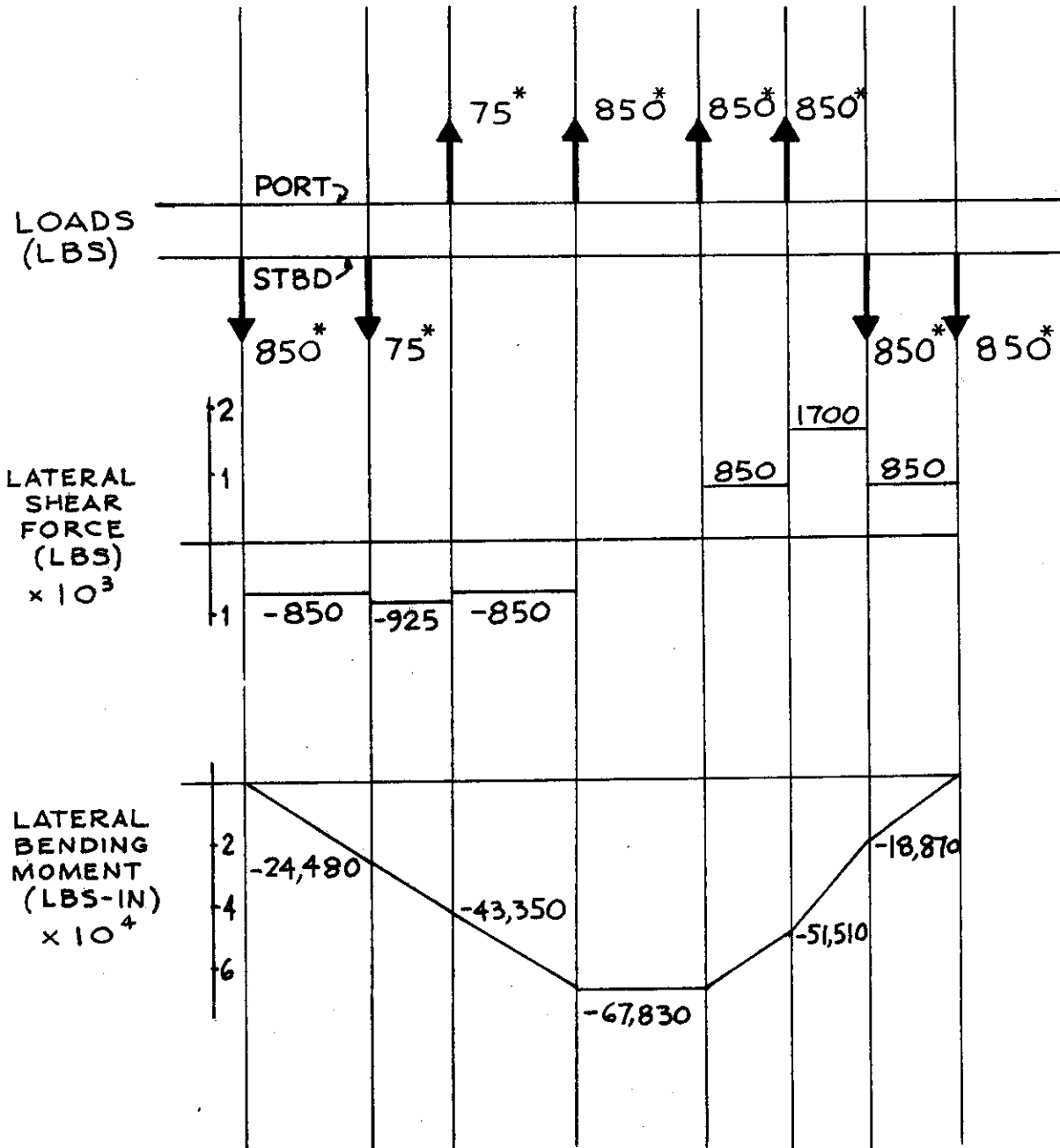
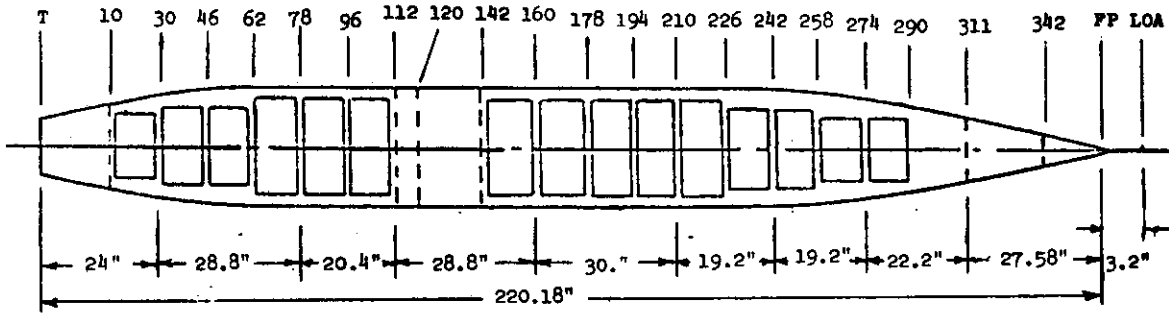
B-33



* Includes a mechanical advantage of 2, by the pulleys.

Date of Experiment 21 August 1972

B-34



*Includes a mechanical advantage of 2, by the pulleys.

Date of Experiment 22 August 1972

SECTION 2" FORWARD OF FRAME 10

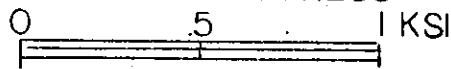
LONGITUDINAL STRESSES DUE TO LATERAL BENDING

NO. OF ROSETTES - 3 (125 RA)

SINGLE GAGES - 6 (250 BG)

DATE OF EXPERIMENT AUG. 21 & 22, 1972

SCALE OF STRESS



○ + B.M.
▽ - (-B.M)

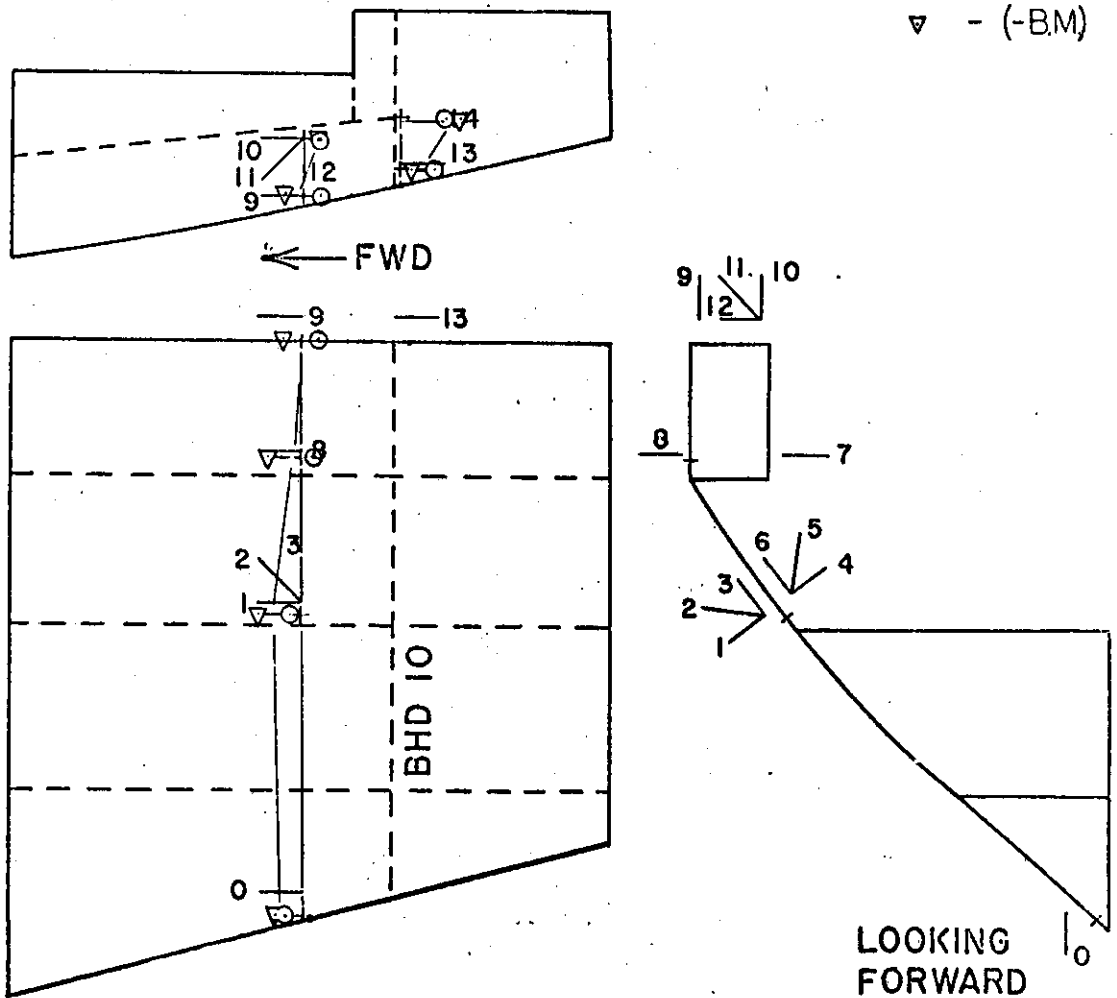
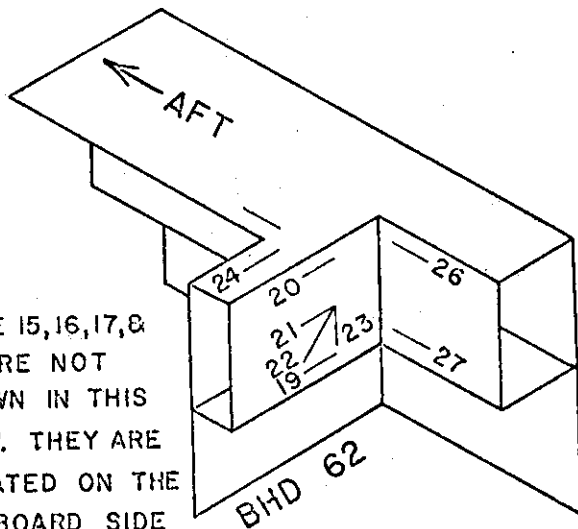


FIG. 1

SECTION AT HATCH CORNER PORT SIDE FRAME 62

LONGITUDINAL STRESSES DUE TO LATERAL BENDING



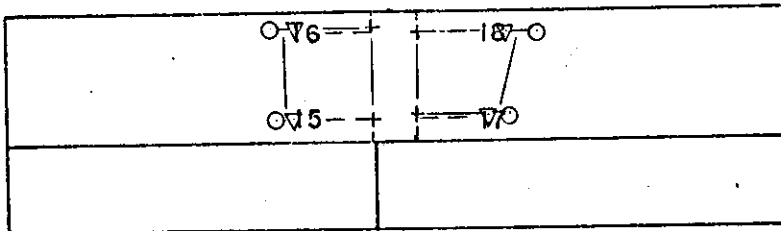
GAGE 15, 16, 17, & 18 ARE NOT SHOWN IN THIS VIEW. THEY ARE LOCATED ON THE OUTBOARD SIDE OF THE SHELL PLATE.

NO. OF ROSETTES
-1(250 RA)
SINGLE GAGES
-10(250 BG)

DATE OF EXPERIMENT
AUG. 21 & 22, 1972

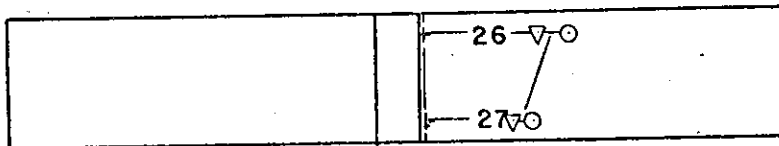
SCALE OF STRESS
0 5 1 KSI

○ + B.M.
▽ - (-B.M.)



LOOKING OUTBOARD
SHELL PLATE

FWD →



BHD
62

LOOKING OUTBOARD
TORSION BOX

FIG. 2

SECTION 5.4" FORWARD OF FRAME 78

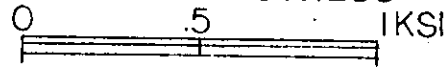
SHEAR STRESS DUE TO LATERAL BENDING

NO. OF ROSETTES - 2(125 RA)
 - 4(250 RA)

SINGLE GAGES - 1(250 BG)

DATE OF EXPERIMENT AUG 21 & 22, 1972

SCALE OF STRESS



⊙ +B.M.
▽ - (-B.M.)

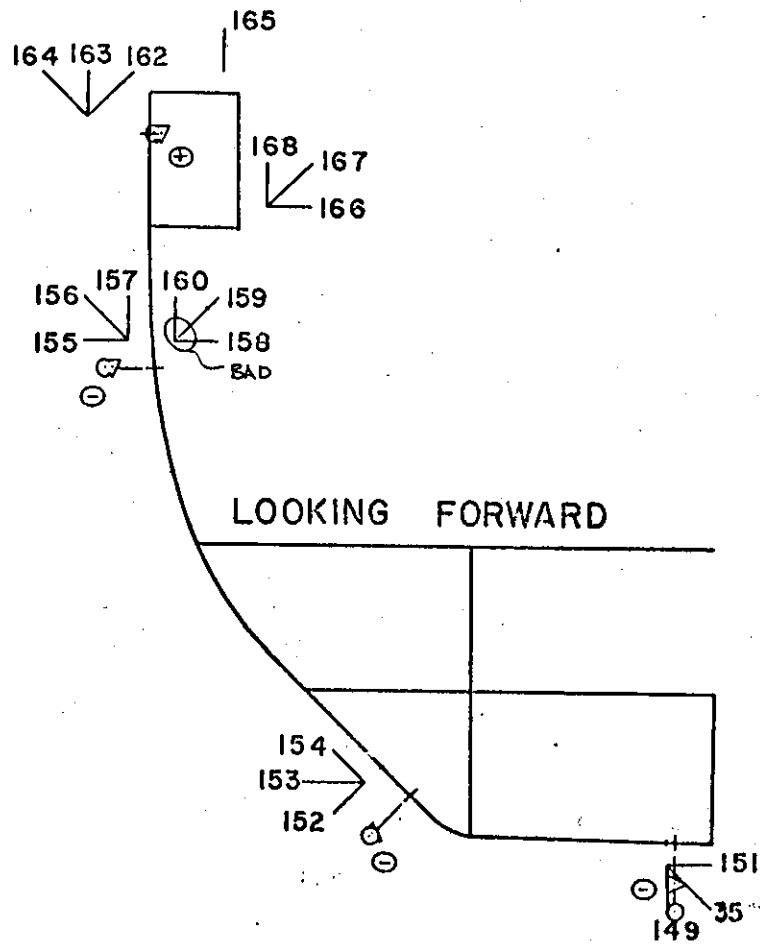


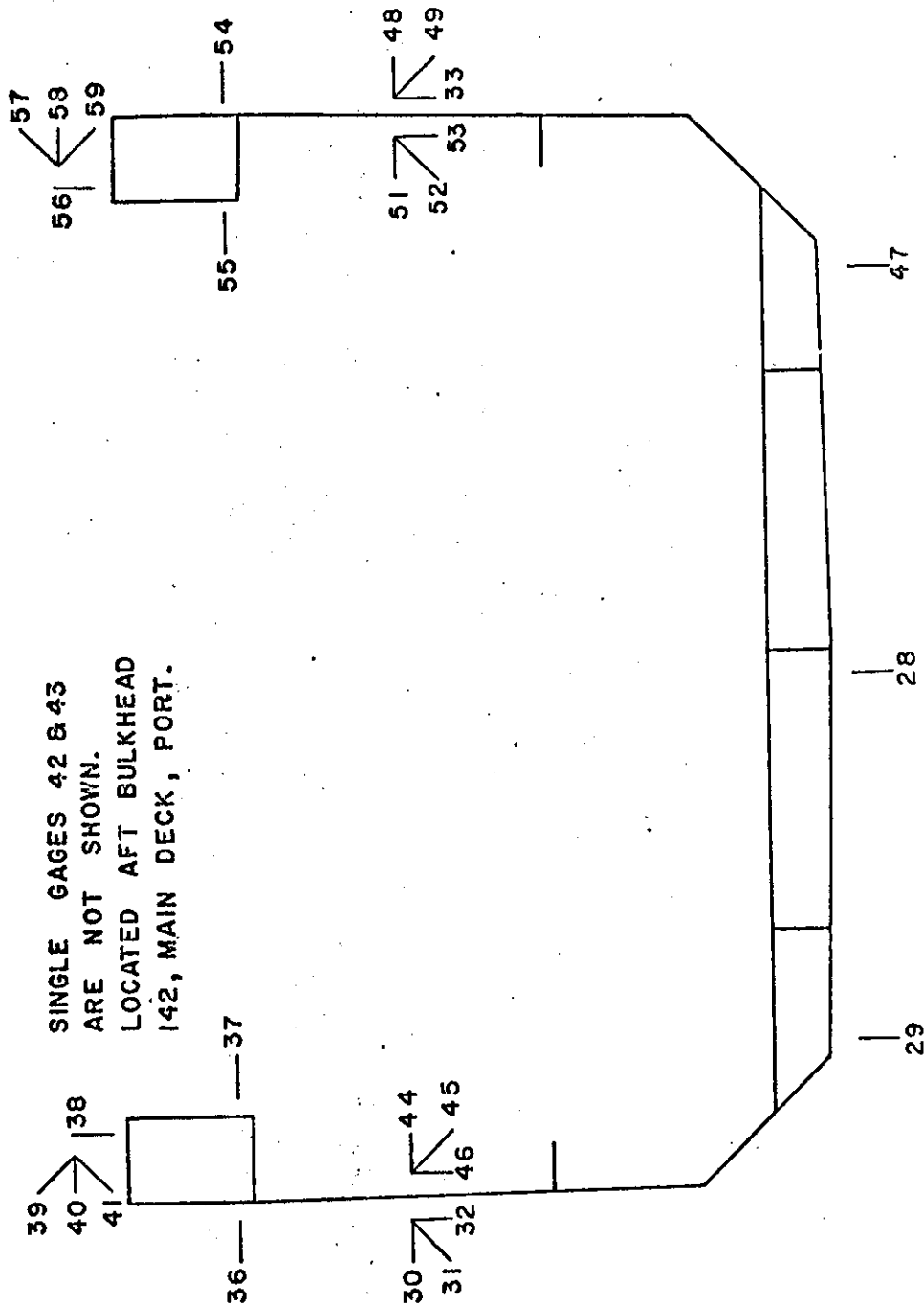
FIG. 3

SECTION 2" FORWARD OF FRAME 142

LOCATION OF GAGES

NO. OF ROSETTES - 4 (250 RA)
- 2 (125 RA)
SINGLE GAGES - 9 (250 BG)

SINGLE GAGES 42 & 43
ARE NOT SHOWN.
LOCATED AFT BULKHEAD
142, MAIN DECK, PORT.



LOOKING FORWARD

B-39

SECTION 2" FORWARD OF FRAME 142

LONGITUDINAL STRESSES DUE TO LATERAL BENDING

NO. OF ROSETTES - 4 (125 RA)

- 2 (250 RA)

SINGLE GAGES - 9 (250 BG)

DATE OF EXPERIMENT - AUG. 21, 22, 1972

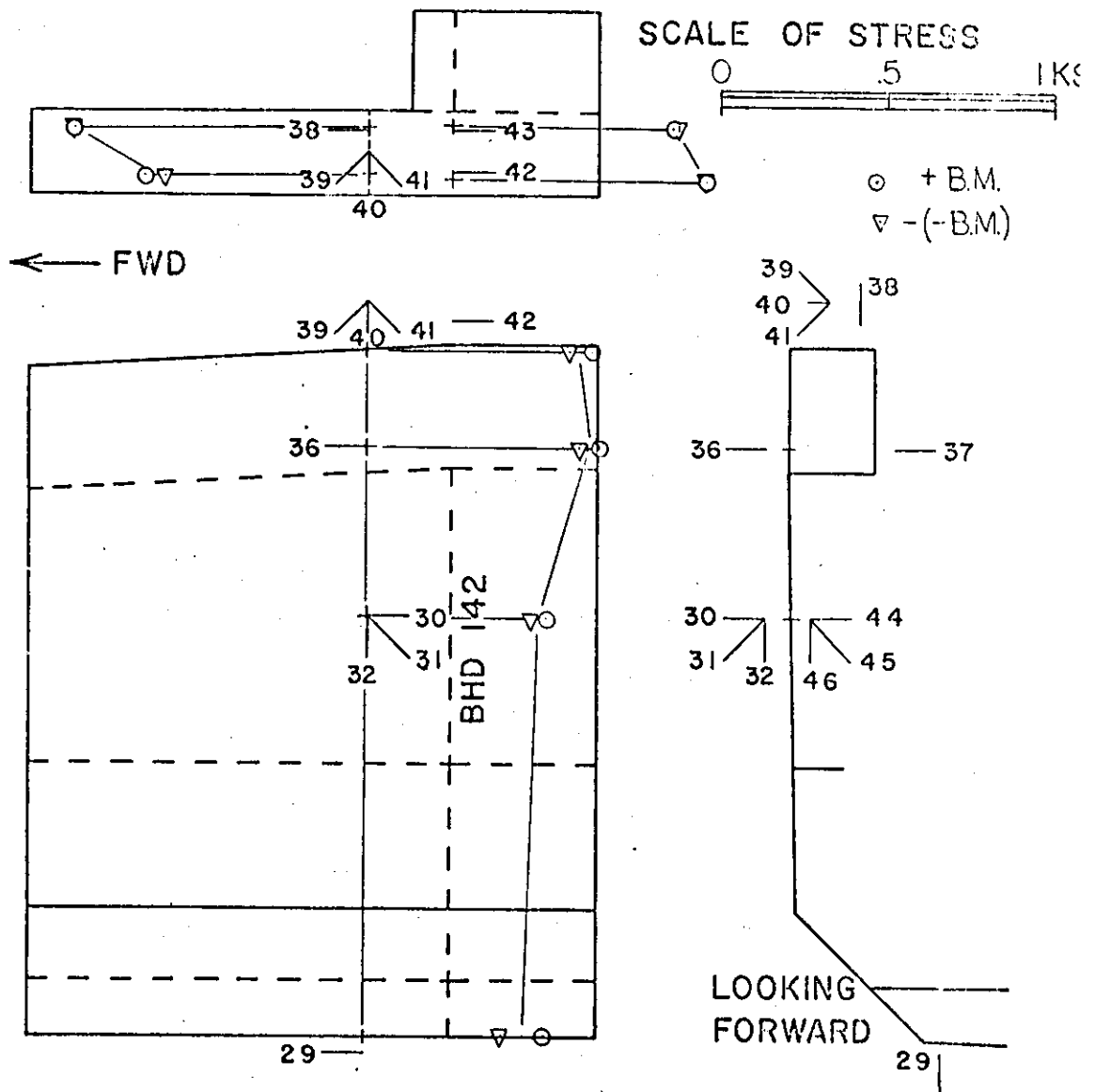


FIG. 4a

SECTION 2" FORWARD OF FRAME 142

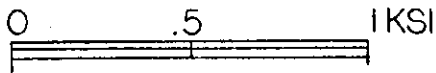
LONGITUDINAL STRESSES DUE TO LATERAL BENDING

NO. OF ROSETTES - 4 (125 RA)
 - 2 (250 RA)

SINGLE GAGES - 9 (250 BG)

DATE OF EXPERIMENT AUG. 21/22, 1972

SCALE OF STRESS



○ + B.M.
▽ - (-B.M.)

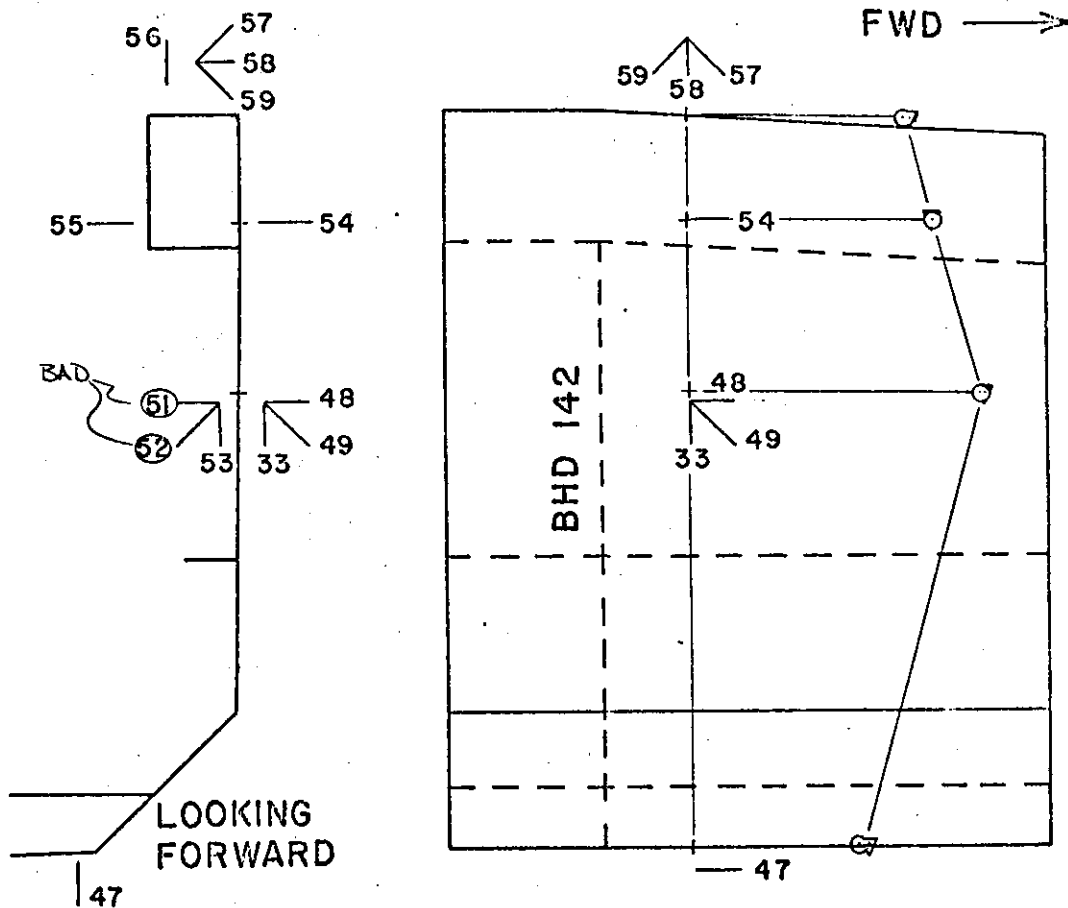
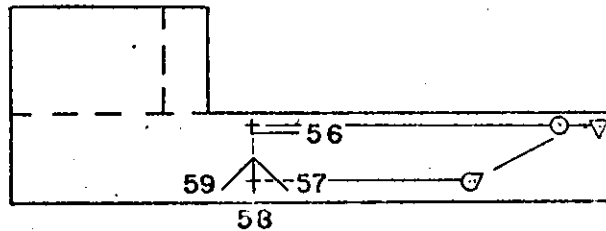


FIG. 4b

SECTION 2" FORWARD OF FRAME 142

LONGITUDINAL STRESSES DUE TO LATERAL BENDING

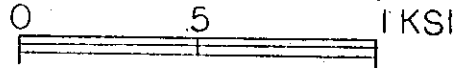
NO. OF ROSETTES - 4 (125 RA)

- 2 (250 RA)

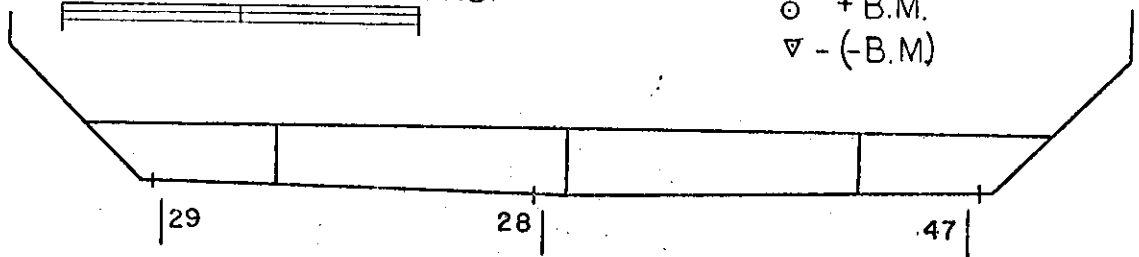
SINGLE GAGES - 9 (250 BG)

DATE OF EXPERIMENT AUG. 21 & 22, 1972

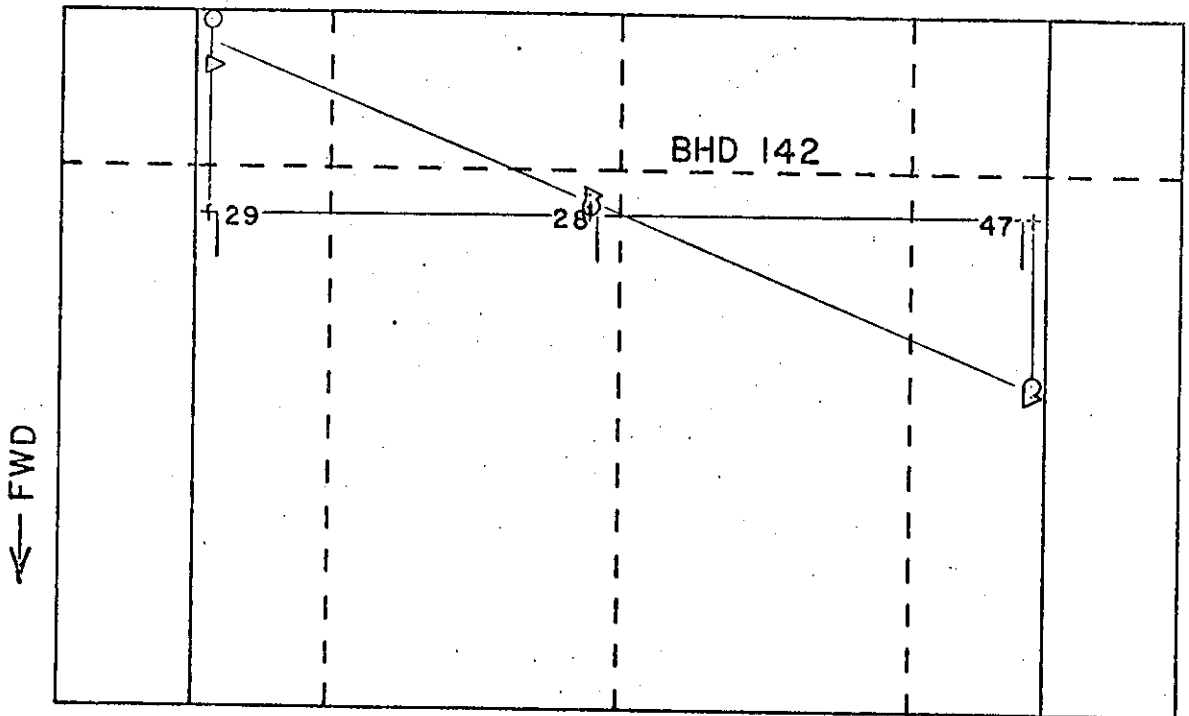
SCALE OF STRESS



○ + B.M.
▽ - (-B.M)



LOOKING FORWARD



BOTTOM PLATE

FIG. 4c

B-42
SECTION AT HATCH CORNER
PORT SIDE FRAME 178

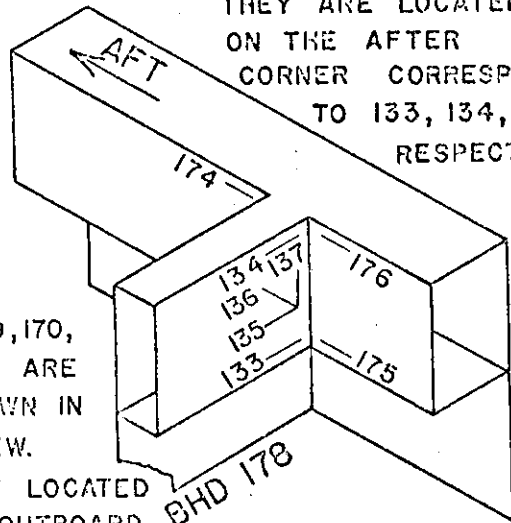
LONGITUDINAL STRESSES DUE TO LATERAL BENDING

GAGES 131, 132, & 173

ARE NOT SHOWN.

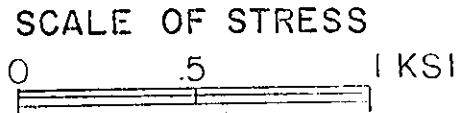
THEY ARE LOCATED ON THE AFTER CORNER CORRESPONDING TO 133, 134, & 175 RESPECTIVELY.

NO. OF ROSETTES
 -1(250 RA)
 SINGLE GAGES
 -12(250 BG)

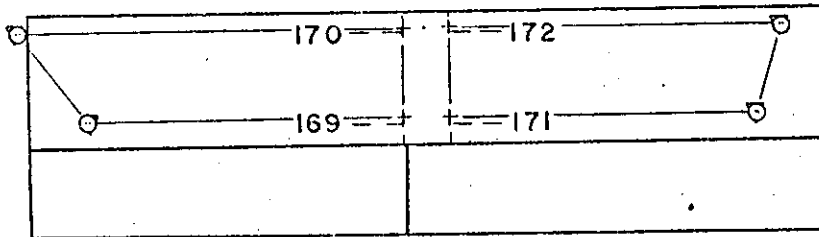


GAGES 169, 170, 171, & 172 ARE NOT SHOWN IN THIS VIEW. THEY ARE LOCATED ON THE OUTBOARD SIDE OF THE SHELL PLATE.

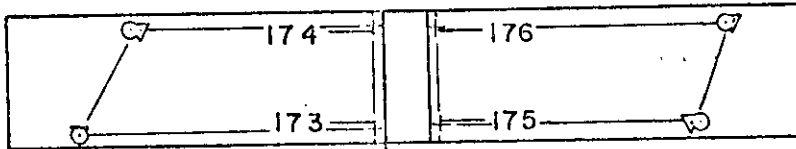
DATE OF EXPERIMENT
 AUG. 21 & 22, 1972



○ + B.M.
 ▼ - (-B.M)



LOOKING OUTBOARD SHELL PLATE → FWD



BHD 178
 LOOKING OUTBOARD TORSION BOX → FWD

SECTION BETWEEN FRAMES 178 & 194

LOCATION OF GAGES

NO. OF SINGLE GAGE- 2 (250 BG)
NO. OF ROSETTES - 4 (125 RA)
- 12 (250 RA)

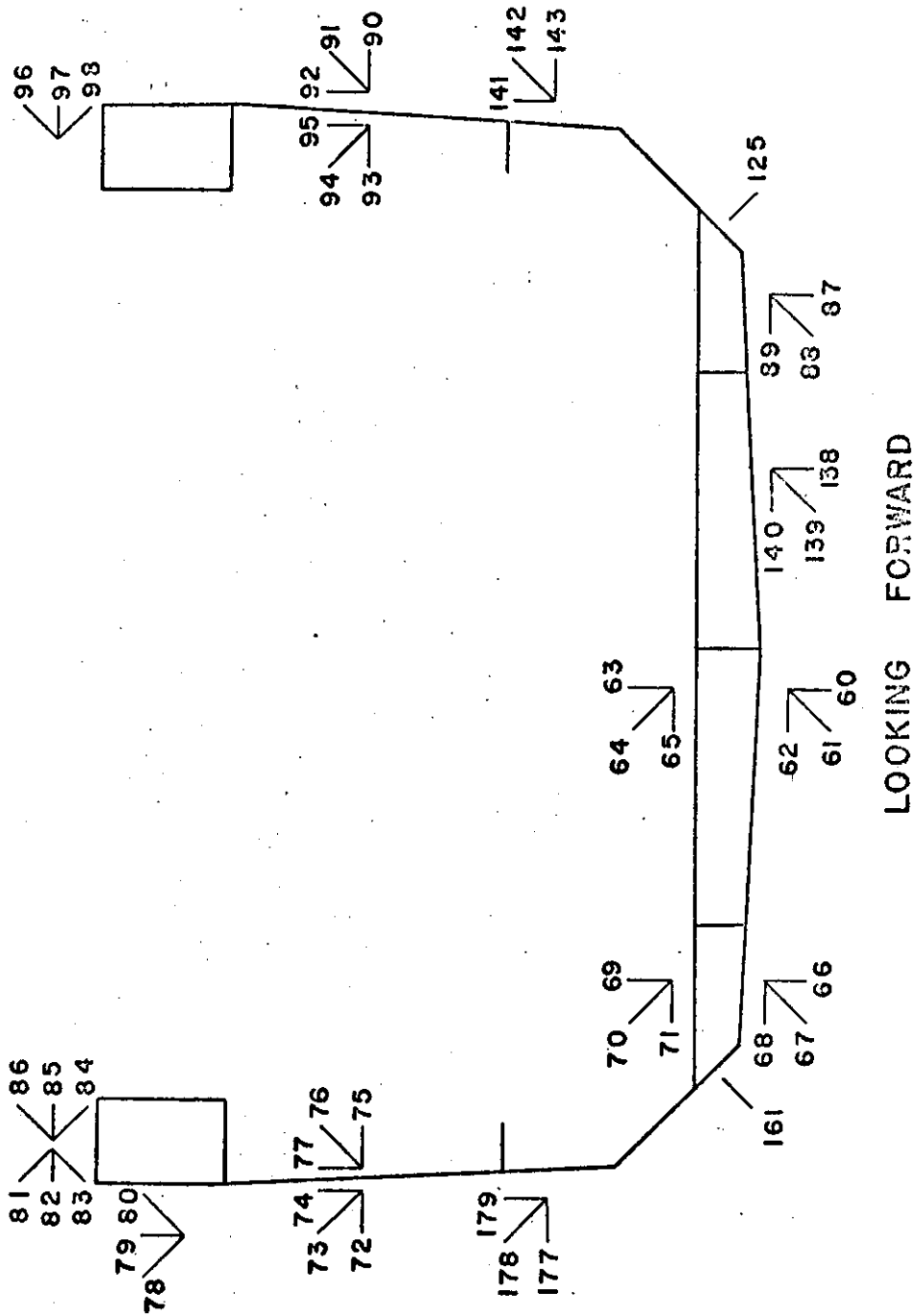


FIG. 6

SECTION BETWEEN FRAMES 178 & 194

LONGITUDINAL STRESSES DUE TO LATERAL BENDING

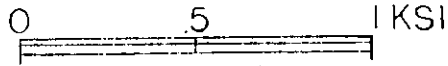
SINGLE GAGES - 2(250 BG)

NO. OF ROSETTES - 4(125 RA)

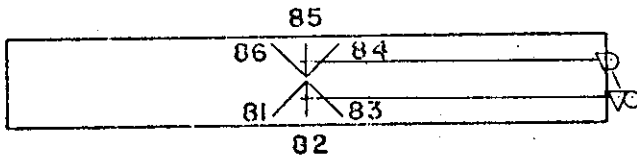
- 12(250 RA)

DATE OF EXPERIMENT AUG 21st 22, 1972

SCALE OF STRESS



○ + B.M.
 ▼ - (-B.M.)



← FWD

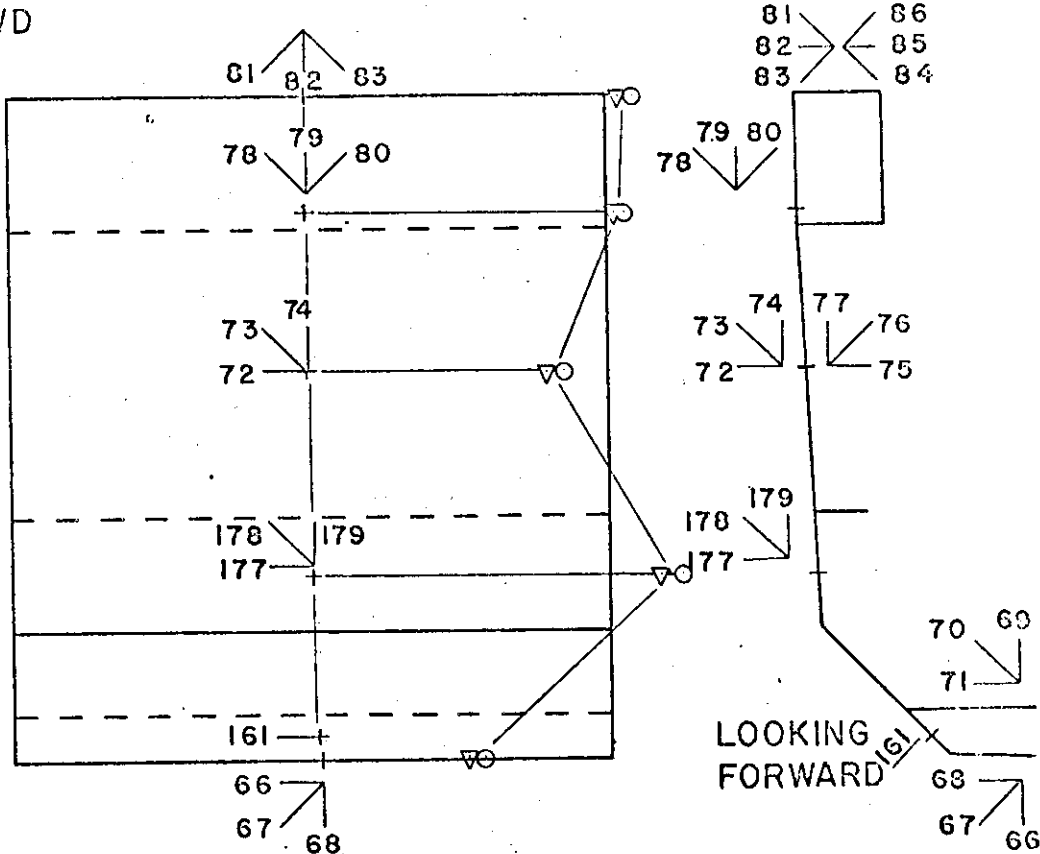


FIG 6.2

SECTION BETWEEN FRAMES 178 & 194

LONGITUDINAL STRESSES DUE TO LATERAL BENDING

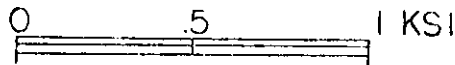
SINGLE GAGES - 2(250 BG)

NO. OF ROSETTES - 4(125 RA)

-12(250 RA)

DATE OF EXPERIMENT AUG. 21/22, 1972

SCALE OF STRESS



○ + BM
▽ - (-BM)

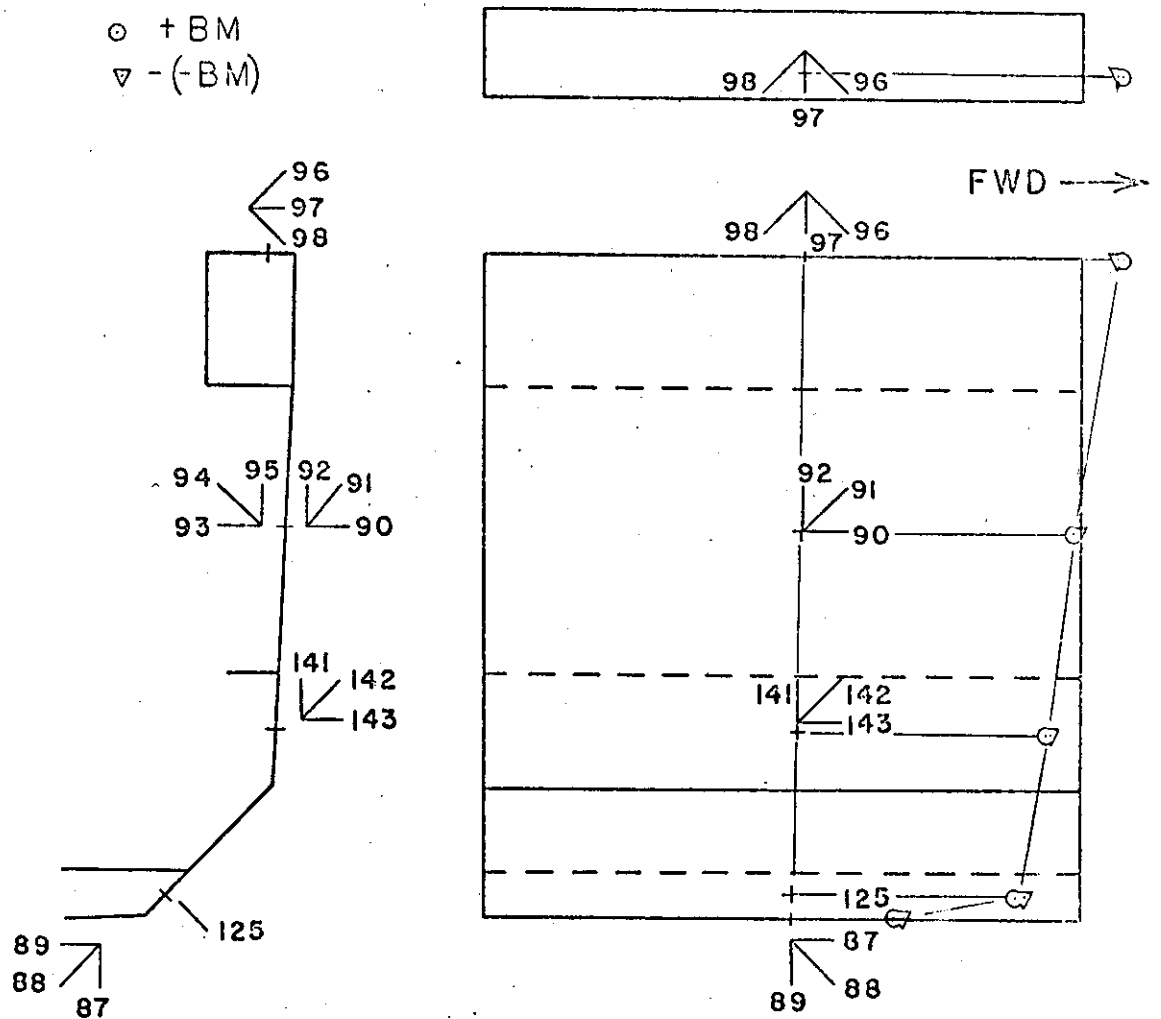


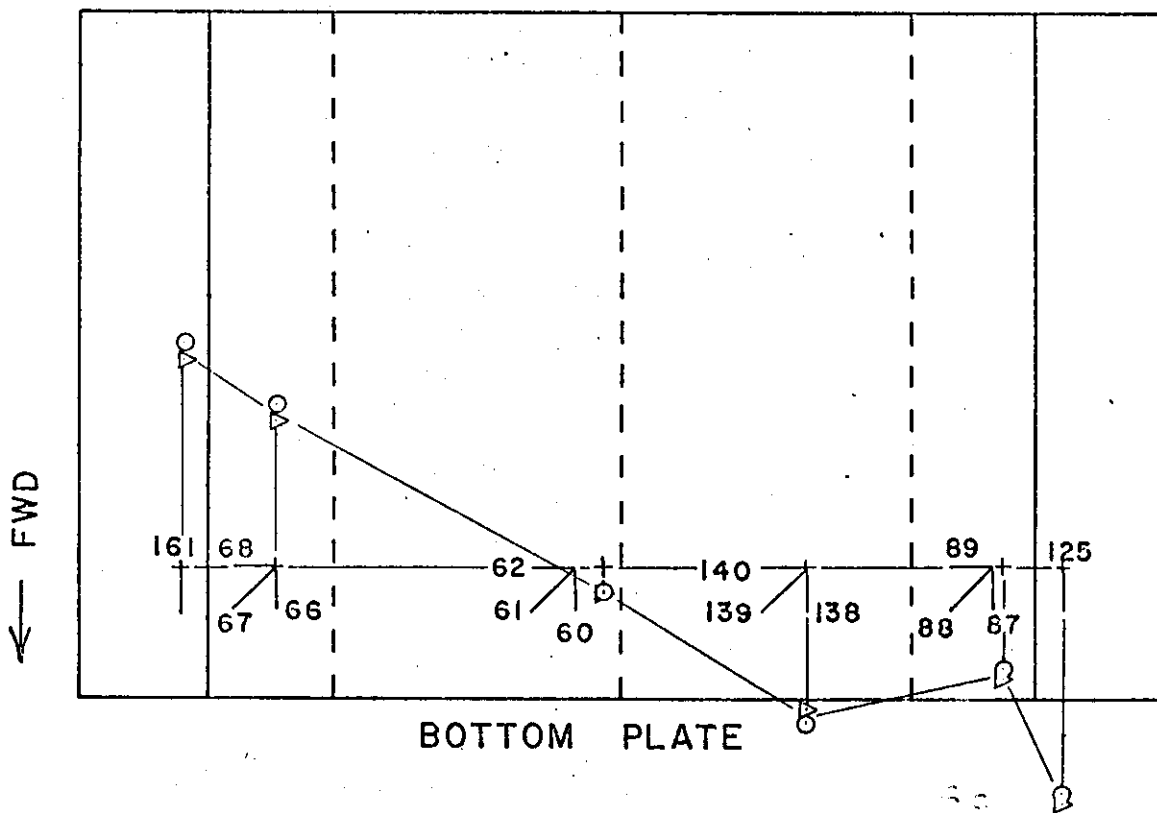
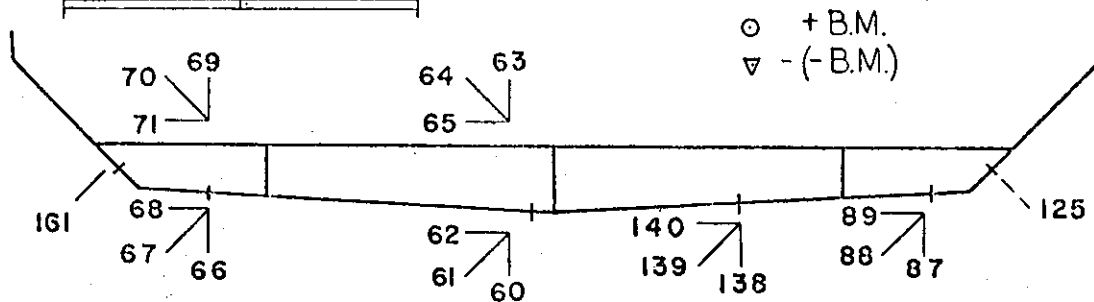
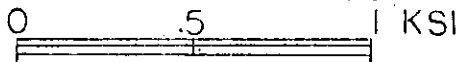
FIG. 6b

SECTION BETWEEN FRAMES 178 & 194

LONGITUDINAL STRESSES DUE TO LATERAL BENDING
SINGLE GAGES - 2(250 BG)
NO. OF ROSETTES - 4(125 RA)
 - 12(250 RA)

DATE OF EXPERIMENT AUG 24th 1972

SCALE OF STRESS



SECTION BETWEEN FRAMES 178 & 194

SHEAR STRESSES DUE TO LATERAL BENDING

SINGLE GAGES - 2 (250 BG)

NO. OF ROSETTES - 4 (125 RA)

- 12 (250 RA)

DATE OF EXPERIMENT AUG 21/22, 1972

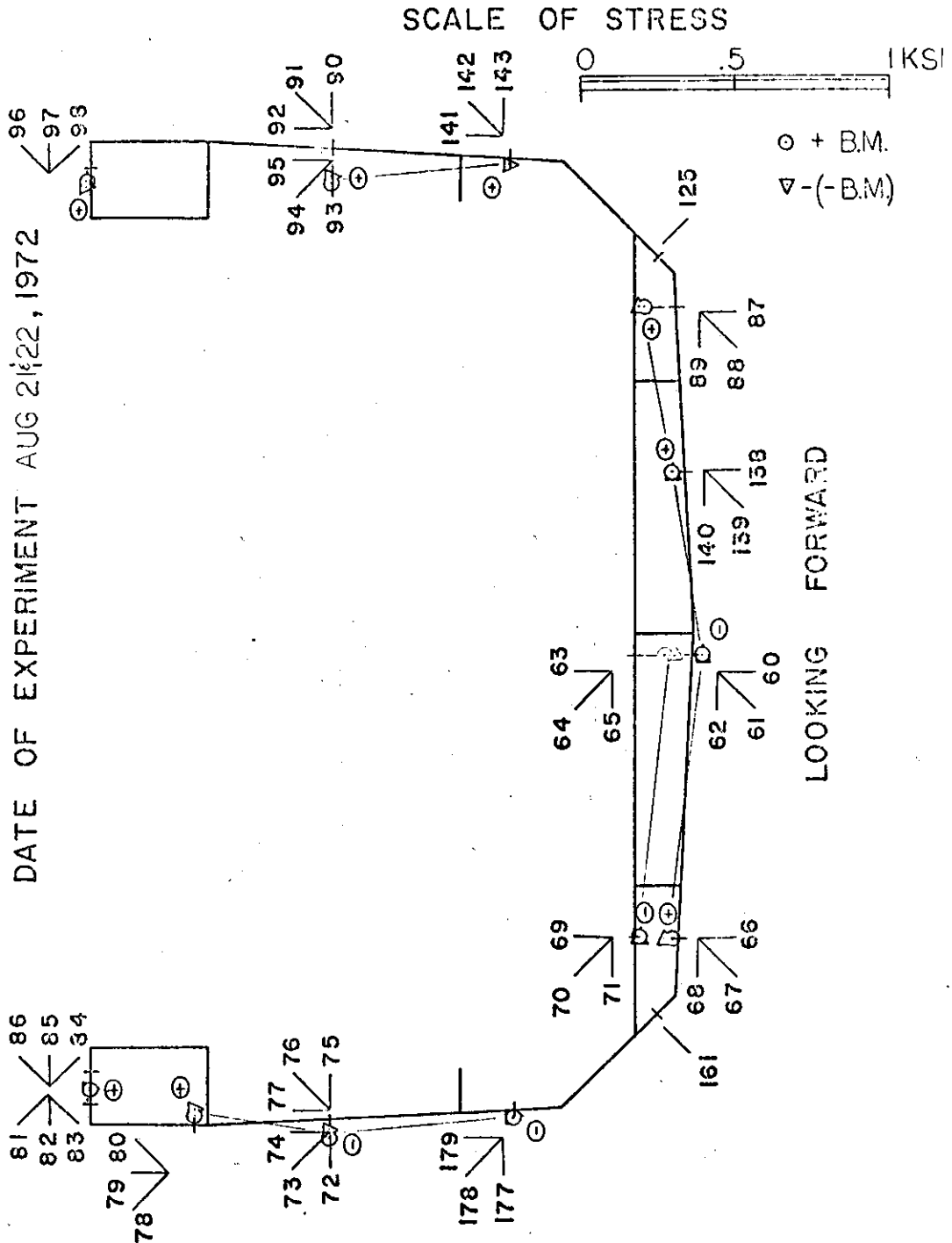
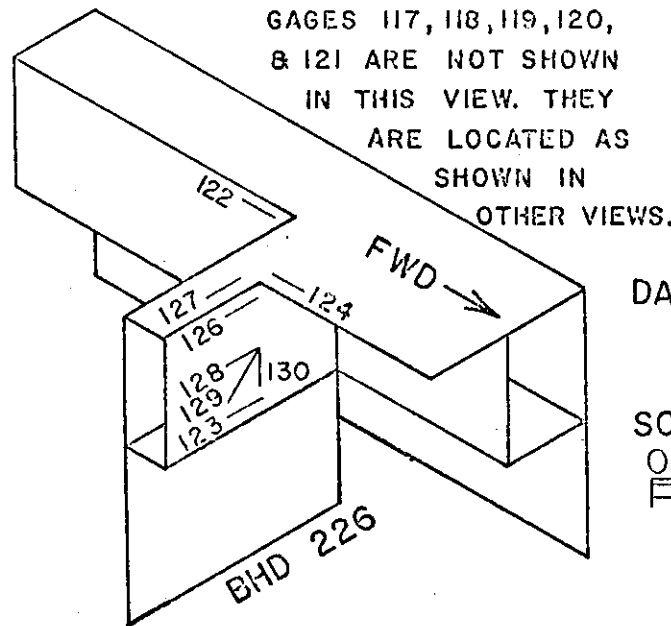


FIG. 7

SECTION AT ^{B-49} HATCH CORNER PORT SIDE FRAME 226

LONGITUDINAL STRESSES DUE TO LATERAL BENDING



NO. OF ROSETTES
- 1(250 RA)
SINGLE GAGES
- 10(250 BG)

DATE OF EXPERIMENT

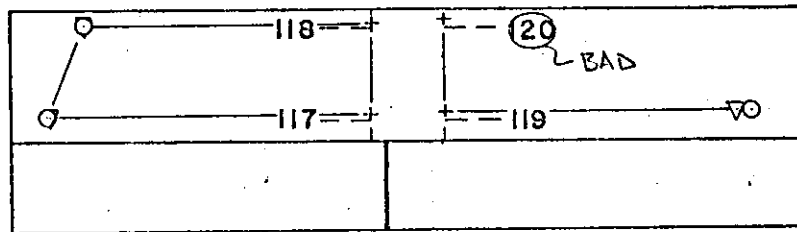
AUG 21 & 22, 1972

SCALE OF STRESS



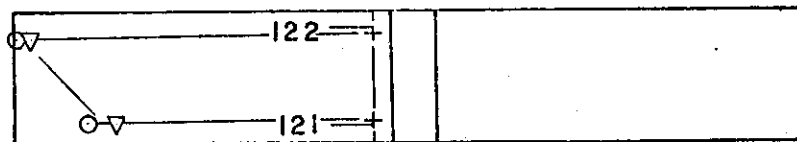
○ + B.M.

▽ - (- B.M.)



LOOKING OUTBOARD
SHELL PLATE

→ FWD



BHD
226

LOOKING OUTBOARD
TORSION BOX

FIG. 3

SECTION 1" AFT OF FRAME 290

LONGITUDINAL STRESSES DUE TO LATERAL BENDING

NO. OF ROSETTES - 2(250 RA)

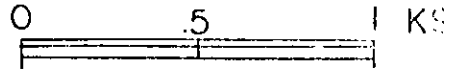
- 1(125 RA)

SINGLE GAGES - 6(250 BG)

DATE OF EXPERIMENT

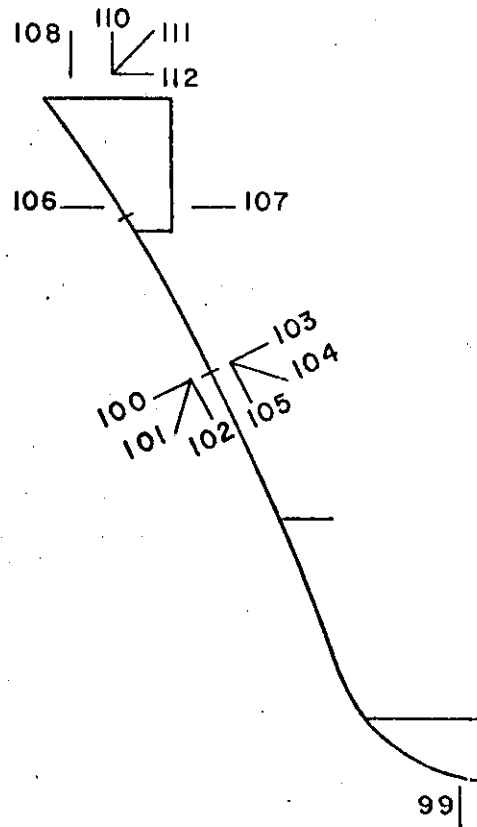
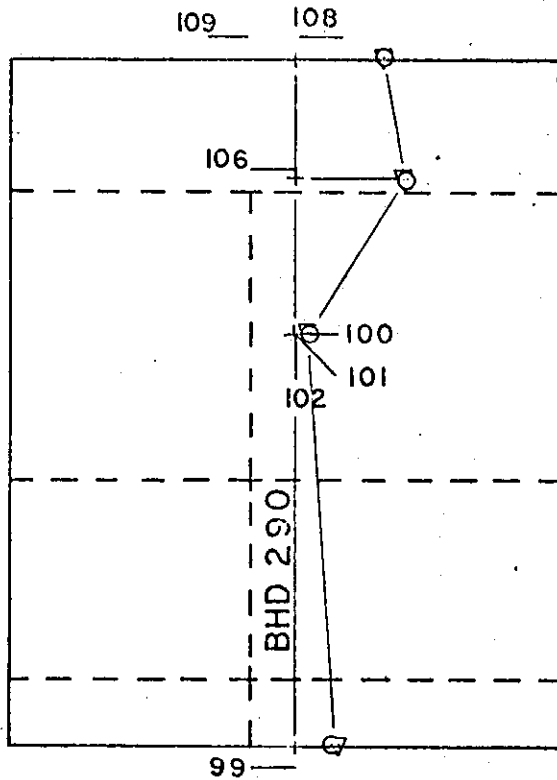
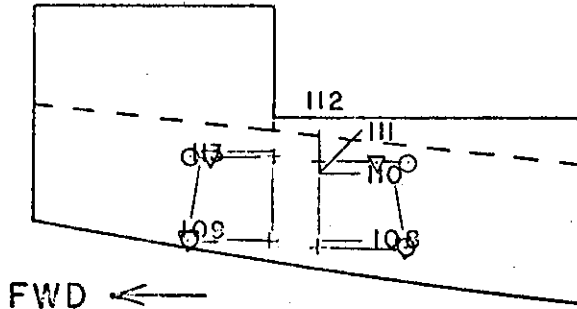
AUG 21 & 22, 1972

SCALE OF STRESS



⊙ + B.M.

▽ (- B.M.)



LOOKING FORWARD

FIG. 9

STRESSES (KSI)

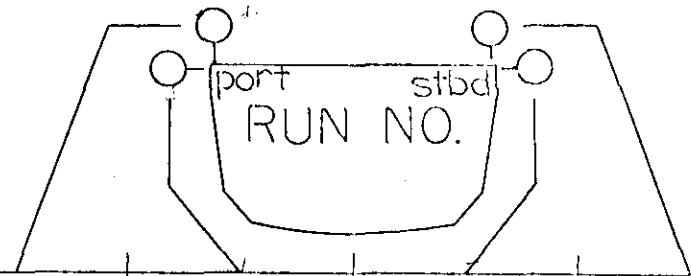
FIG.	GAGE NUMBER	0	∇	FIG.	GAGE NUMBER	0	∇
		1	2			1	2
1	0	.048	.075	4b	47	.465	.495
	1	.027	.123		48	.819	.827
	8	-.033	.013		54	.690	.690
	9	-.045	-.048		57	.603	.621
	10	-.048	-.042		56	.864	.975
	13	-.046	-.033	4c	29	-.537	-.411
	14	-.126	-.168		28	-.027	.054
2	15	-.216	-.234		47	.465	.495
	16	-.288	-.216	5	169	-.897	-.888
	17	-.273	-.213		170	-1.092	-1.104
	18	-.245	-.258		171	-.882	-.876
	26	-.417	-.327		172	-.945	-.939
	27	-.312	-.249		173	-.843	-.840
3 (SHEAR)	149	-.193			174	-.687	-.657
	152	-.166			175	-.735	-.714
	155	-.140			176	-.828	-.852
	162	.012		6a	66	-.457	-.415
4a	29	-.537	-.411		161	-.639	-.585
	30	-.876	-.756		177	-1.053	-.987
	36	-.693	-.630		72	-.386	-.348
	38	-.882	-.882		78	-.912	-.879
	39	-.671	-.608		81	-.929	-.886
	42	-.765	-.765		84	-.867	-.850
	43	-.660	-.678				

FIG.	GAGE NUMBER	0	▽
		1	2
6b			
	87	.289	.319
	125	.639	.666
	141	.711	.726
	90	1.245	1.313
	96	.909	.891
6c			
	161	-.639	-.585
	66	-.457	-.415
	60	.072	.075
	138	.438	.400
	87	.289	.319
	125	.639	.666
6d			
	69	-.508	-.496
	63	.012	-.038
7 (SILAR)			
	81	.059	.053
	78	.032	.046
	72	-.048	-.029
	177	-.029	.016
	66	.016	.046
	69	-.013	-.017
	60	-.032	-.030
	63	-.092	-.132
	138	.037	.036
	87	.102	.120

FIG	GAGE NUMBER	0	▽
		1	2
7(Cont'd)			
	141		-.020
	90	.062	.036
	96	.044	.058
8			
	117	-.918	-.709
	118	-.816	-.822
	119	-.873	-.828
	120		
	121	-.810	-.729
	122	-1.020	-.969
9			
	99	-.105	-.123
	100	-.056	-.040
	106	-.318	-.309
	108	-.246	-.249
	109	-.234	-.234
	110	-.252	-.161
	113	-.240	-.177

B-53

± LATERAL BM.
AUG. 21, 22



BHD.

MODEL DEFLECTION FROM THE
NO-LOAD CONDITION, IN INCHES.

+ LAT. BM. ⇨
- (-LAT. B.M.) ⇨

342	0.00 0.002	-0.001 -0.002	0.001 0.001	0.00 -0.001
290	0.00 0.003	-0.006 -0.008	0.006 0.008	0.00 -0.004
226	-0.002 +0.002	-0.011 -0.011	0.011 0.011	+0.002 -0.003
142	-0.002 +0.001	-0.010 -0.010	0.010 0.010	+0.005 -0.002
96	-0.001 +0.001	-0.007 -0.008	0.007 0.008	+0.008 -0.002
10	0.00 0.00	-0.002 -0.001	0.002 0.002	+0.005 -0.002

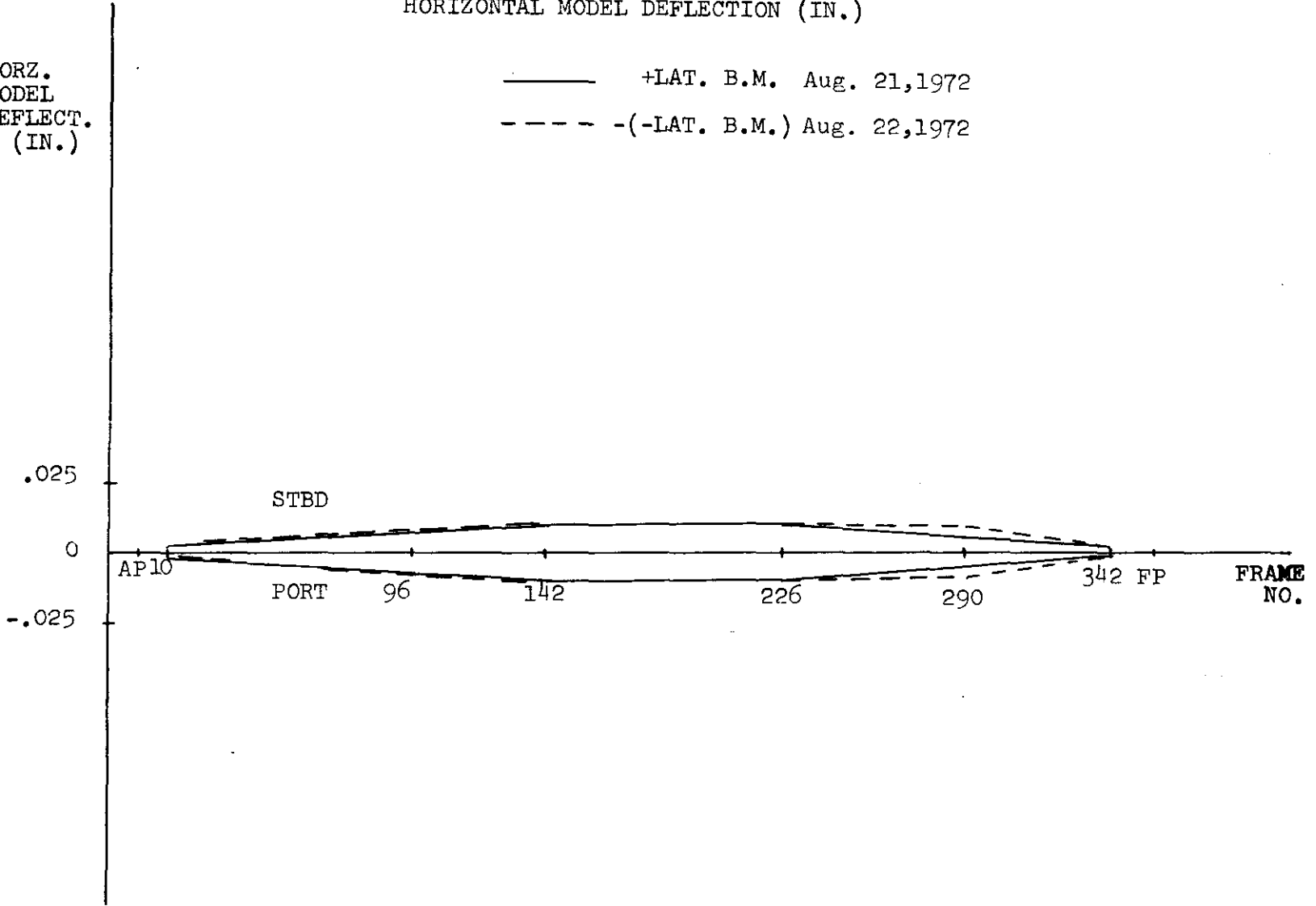
EQUIVALENT DEFLECTIONS OF
FULL SCALE SHIP, IN INCHES.

342	0.00 0.10	-0.05 -0.10	0.05 0.05	0.00 -0.05
290	0.00 0.15	-0.30 -0.40	0.30 0.40	0.00 -0.20
226	-0.10 +0.10	-0.55 -0.55	0.55 0.55	+0.10 -0.15
142	-0.10 +0.05	-0.50 -0.50	0.50 0.50	+0.25 -0.10
96	-0.05 +0.05	-0.35 -0.40	0.35 0.40	+0.40 -0.10
10	0.00 0.00	-0.10 -0.05	0.10 0.10	+0.25 -0.10

HORIZONTAL MODEL DEFLECTION (IN.)

HORZ.
MODEL
DEFLECT.
(IN.)

———— +LAT. B.M. Aug. 21, 1972
----- -(-LAT. B.M.) Aug. 22, 1972

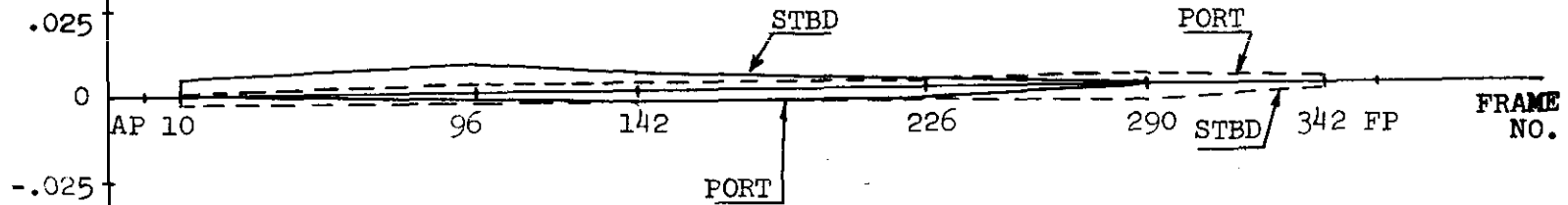


VERTICAL MODEL DEFLECTIONS (IN.)

VERT
MODEL
DEFLECT.
(IN.)

———— + LAT. B.M. Aug. 21, 1972

----- (- LAT. B.M.) Aug. 22, 1972

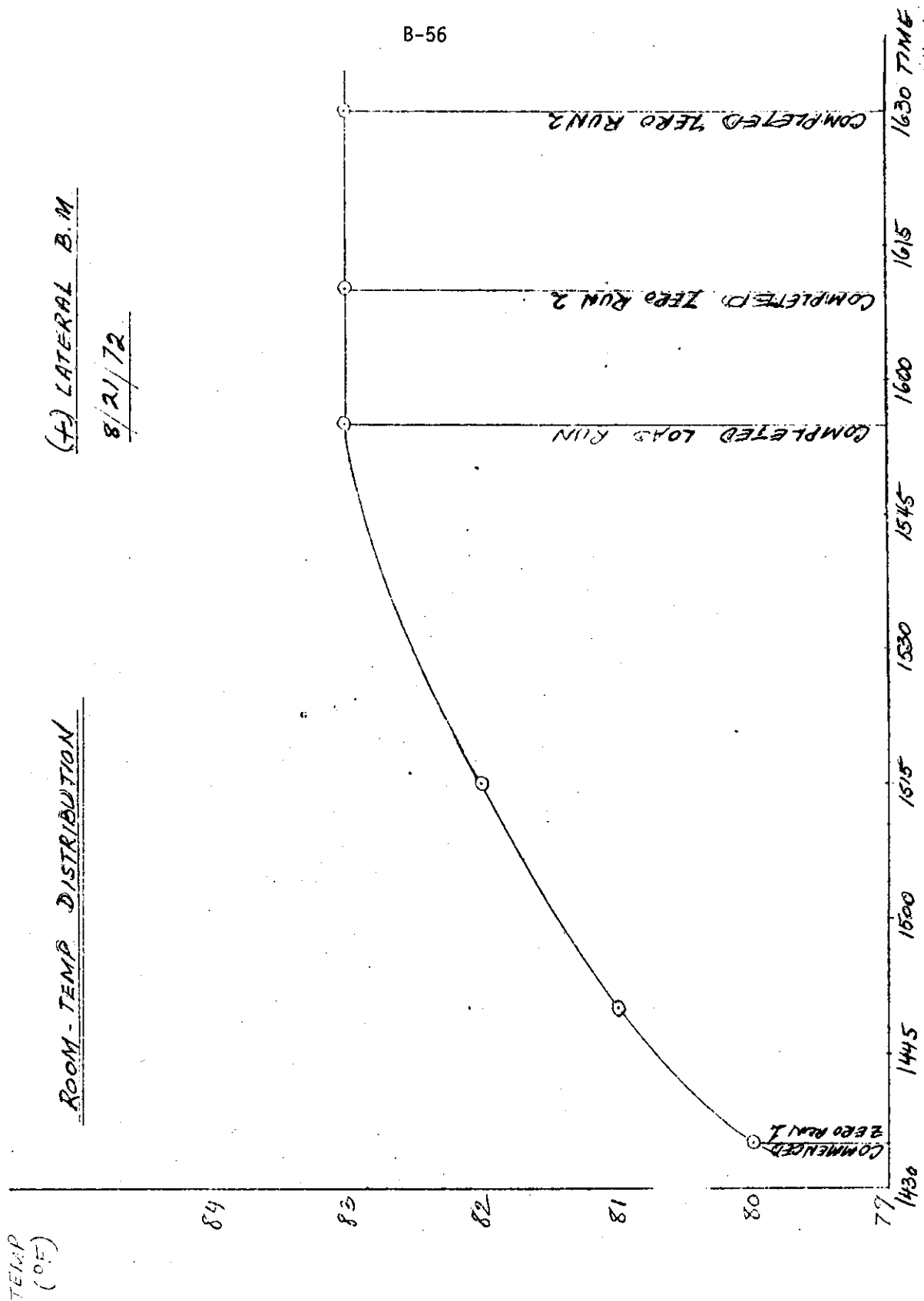


B-56

(+) LATERAL B.M

8/21/72

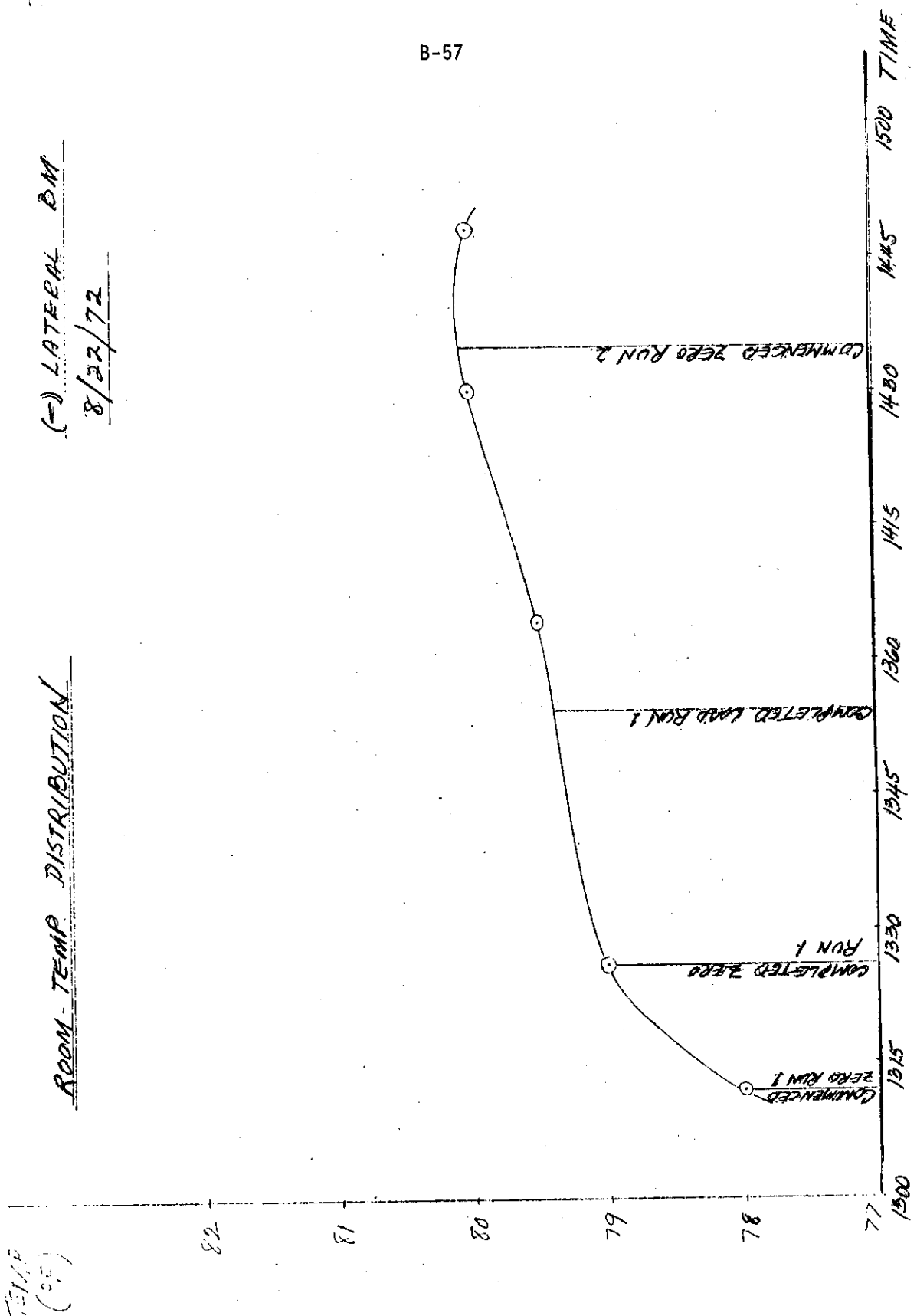
ROOM-TEMP DISTRIBUTION



(-) LATERAL DM

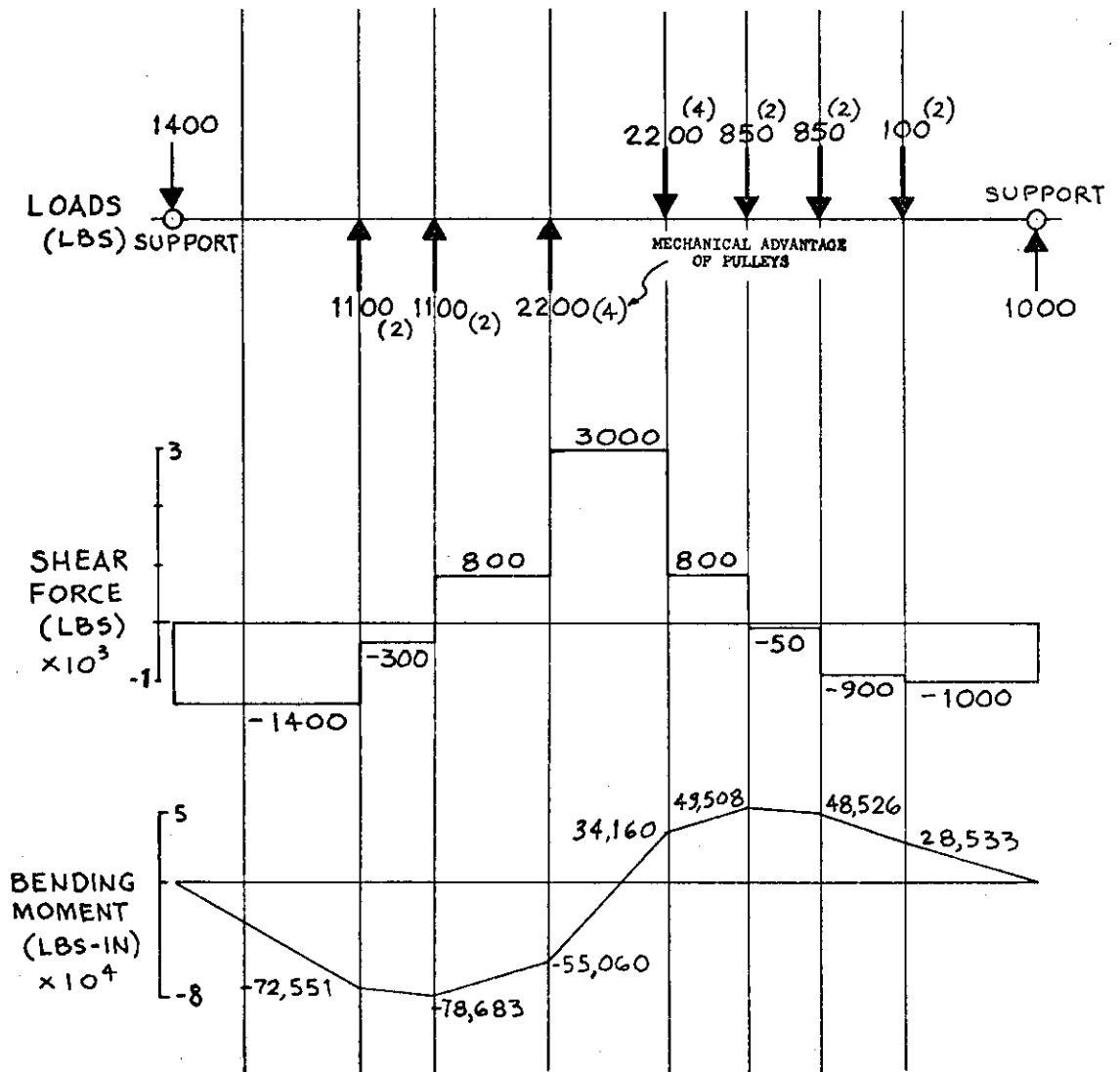
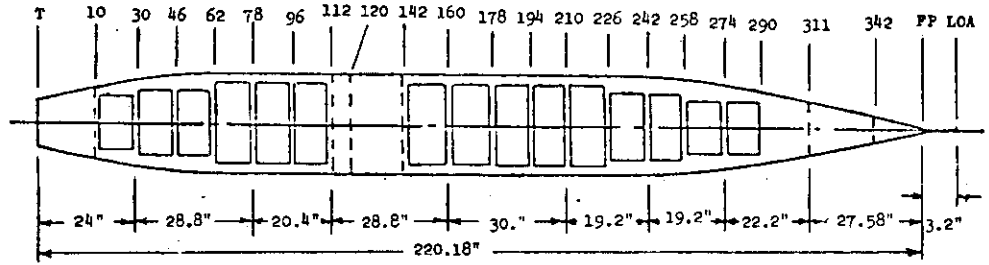
8/22/72

ROOM-TEMP DISTRIBUTION

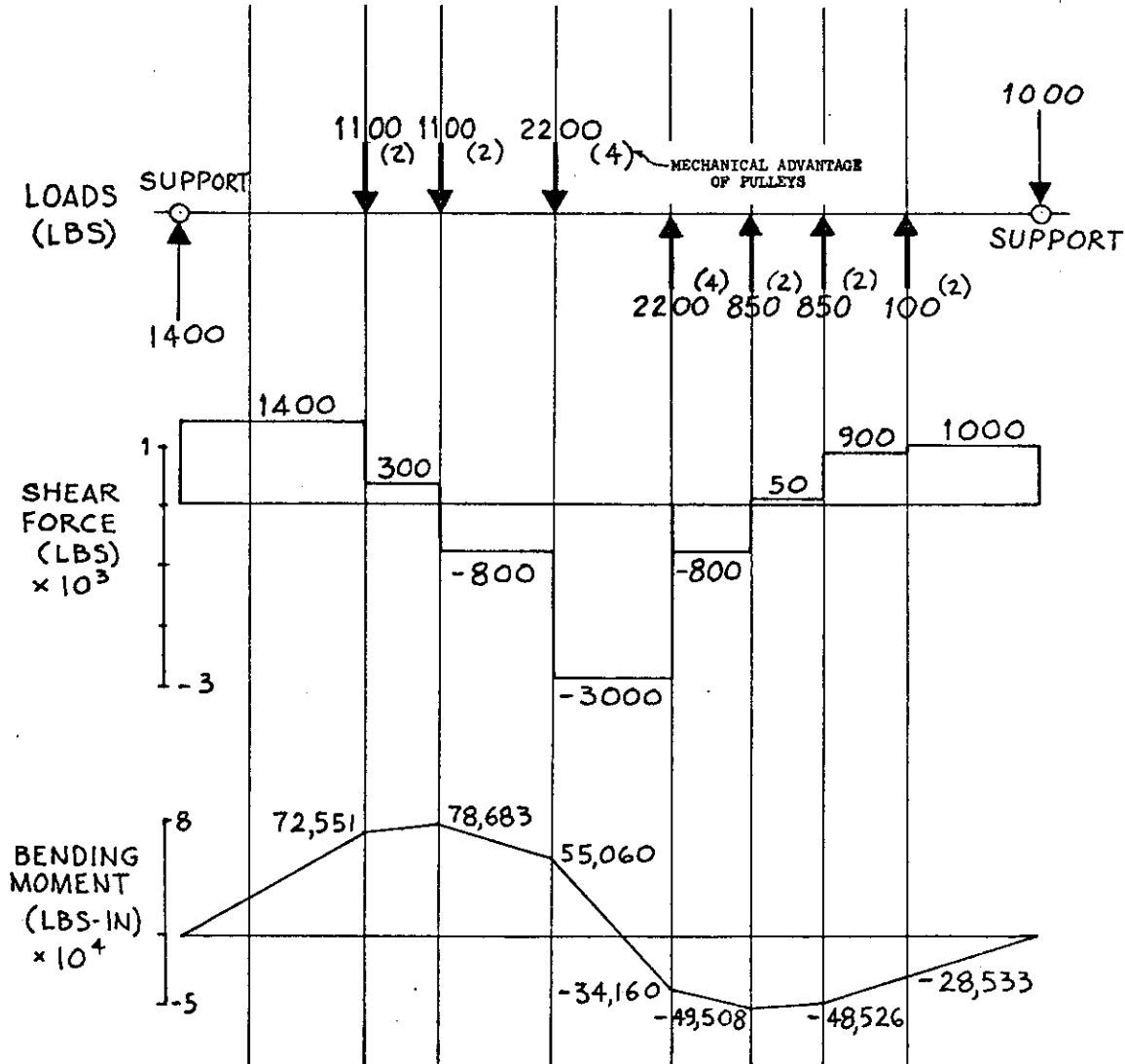
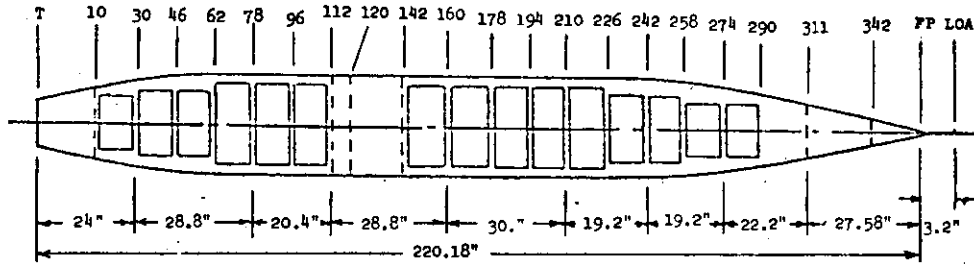


LARGE MIDSHIP SHEAR

+ LARGE SHEAR	JULY 6, 1972
- (-LARGE SHEAR)	JULY 11, 1972



Date of Experiment 6 July 1972



Date of Experiment 11 July 1972

SECTION 5.4" FORWARD OF FRAME 78

SHEAR STRESS DUE TO MIDSHIP SHEAR

NO. OF ROSETTES - 2(125 RA)
- 4(250 RA)

SINGLE GAGES - 1(250 BG)

DATE OF EXPERIMENT JULY 6th, 1972

SCALE OF STRESS

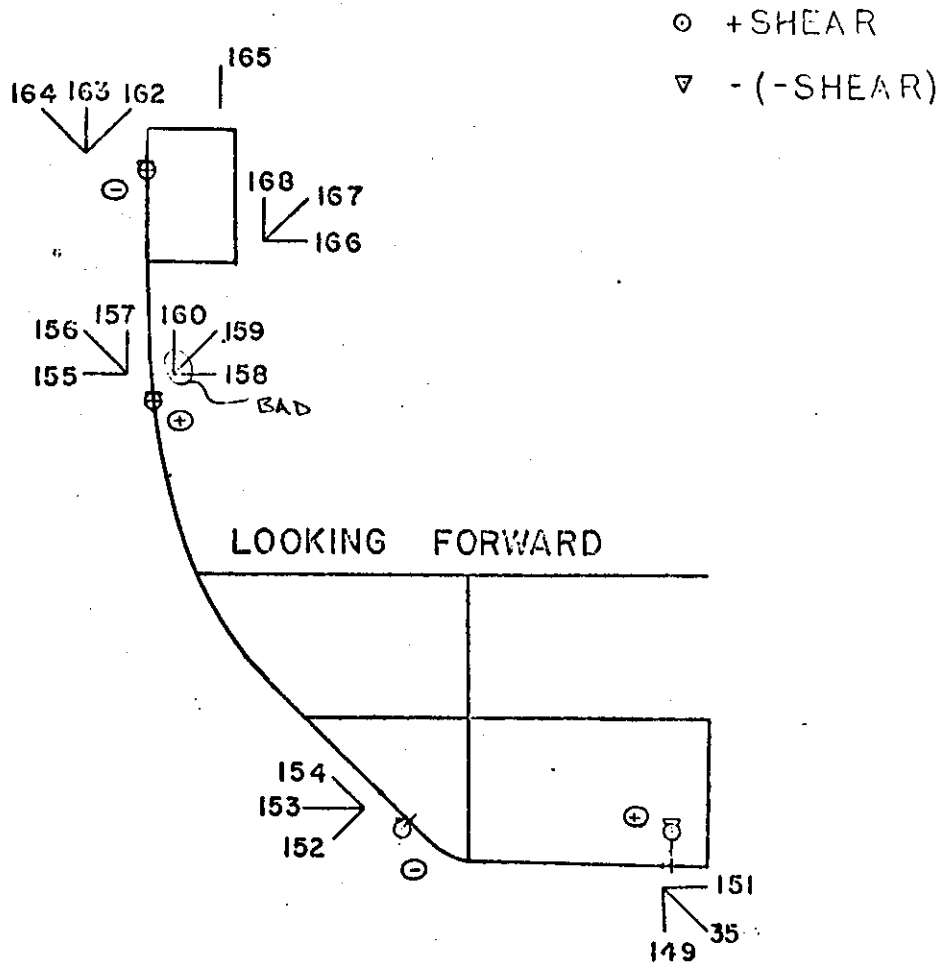
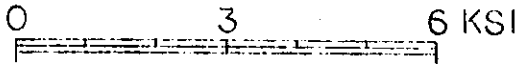


FIGURE 3

SECTION 2" FORWARD OF FRAME 142

B-63

LOCATION OF GAGES

NO. OF ROSETTES - 4 (250 RA)
 - 2 (125 RA)
SINGLE GAGES - 9 (250 BG)

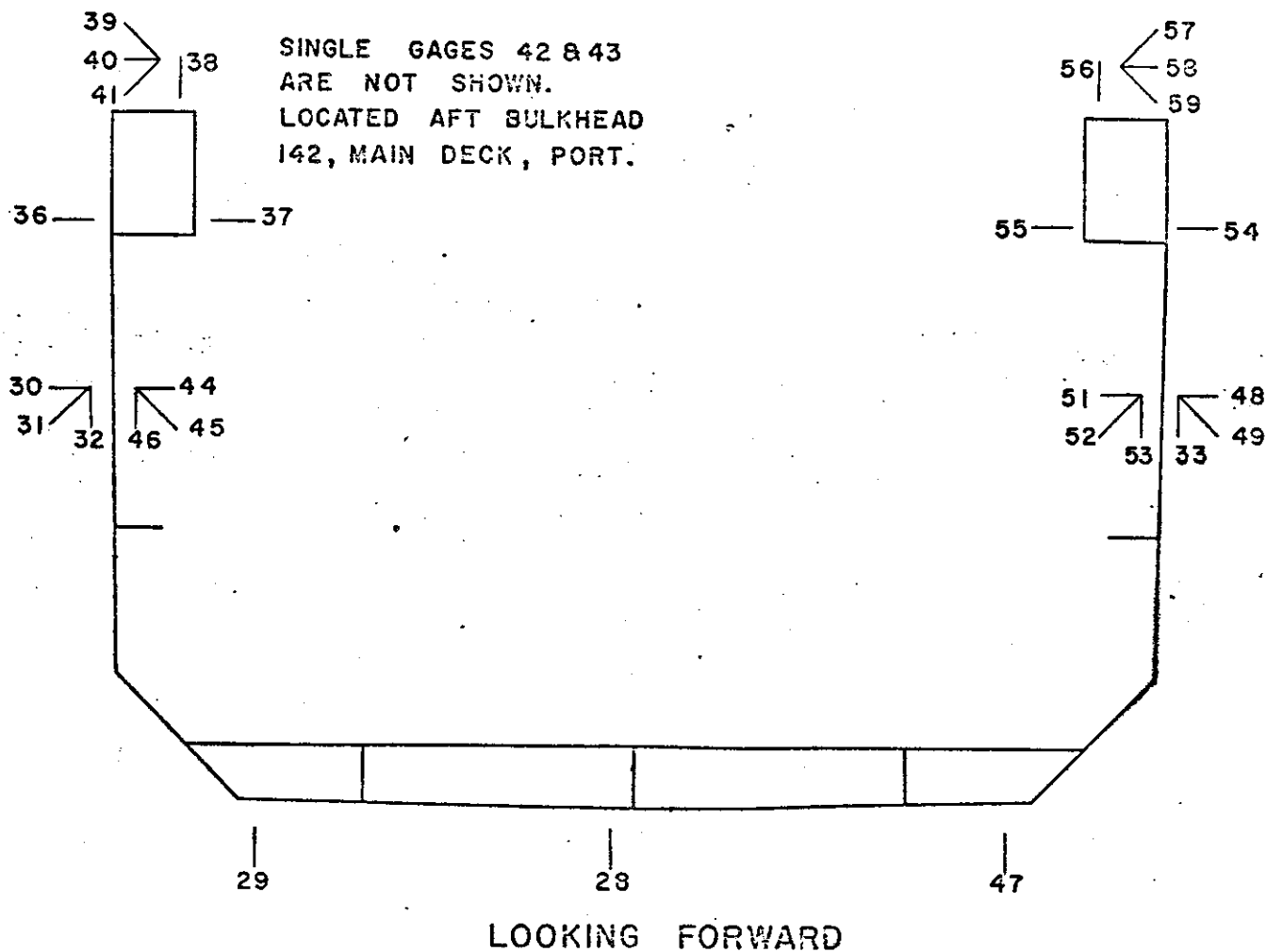


FIGURE 4

SECTION 2" FORWARD OF FRAME 142

LONGITUDINAL STRESSES DUE TO MIDSHIP SHEAR

NO. OF ROSETTES - 4 (125 RA)

- 2 (250 RA)

SINGLE GAGES - 9 (250 BG)

DATE OF EXPERIMENT JULY 6th, 1972

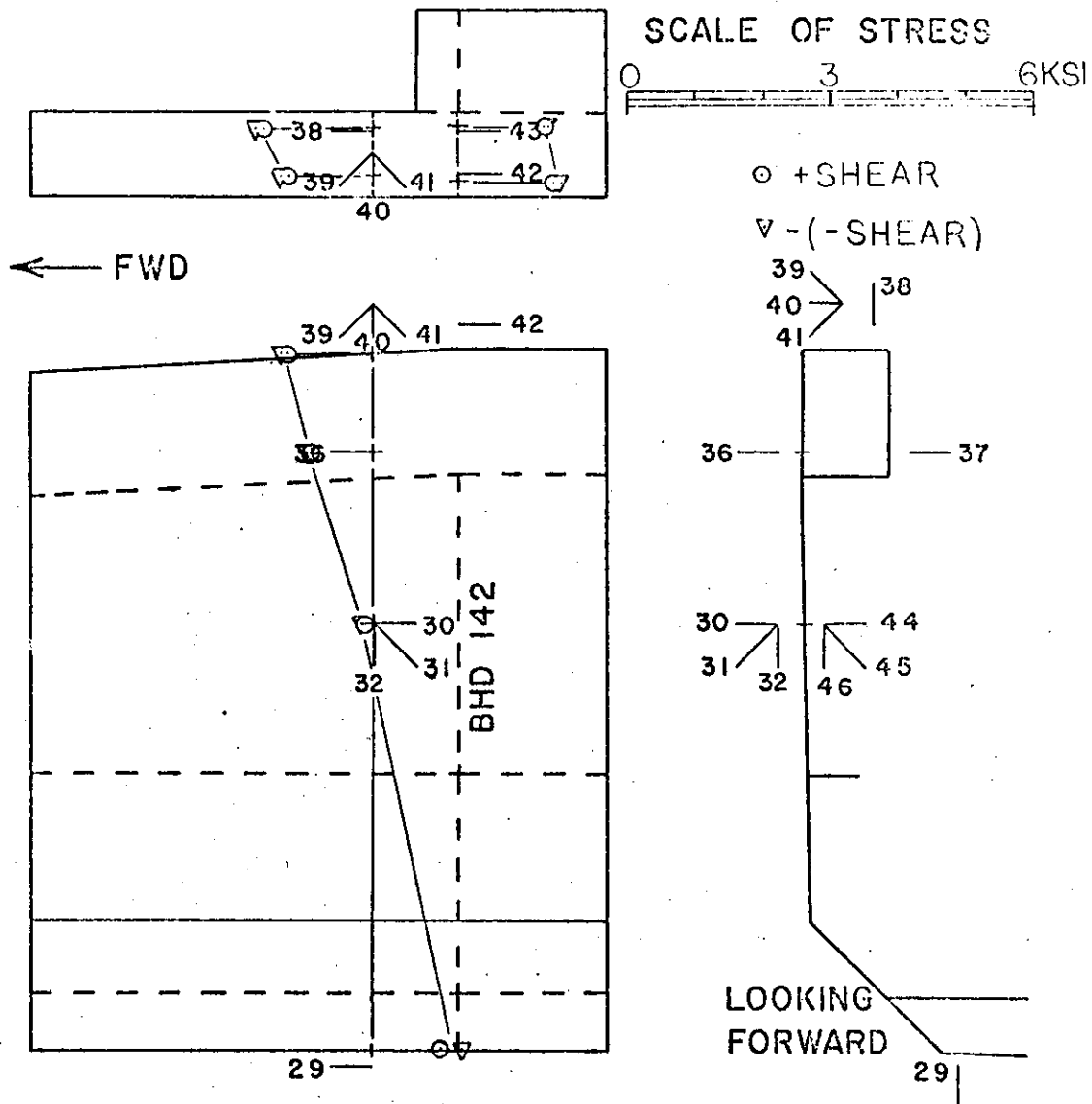


FIGURE 4a

B-65
SECTION 2" FORWARD OF FRAME 142

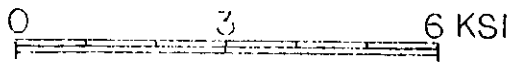
LONGITUDINAL STRESSES DUE TO MIDSHIP SHEAR

NO. OF ROSETTES - 4 (125 RA)
 - 2 (250 RA)

SINGLE GAGES - 9 (250 BG)

DATE OF EXPERIMENT JULY 6th, 1972

SCALE OF STRESS



○ +SHEAR
▽ - (-SHEAR)

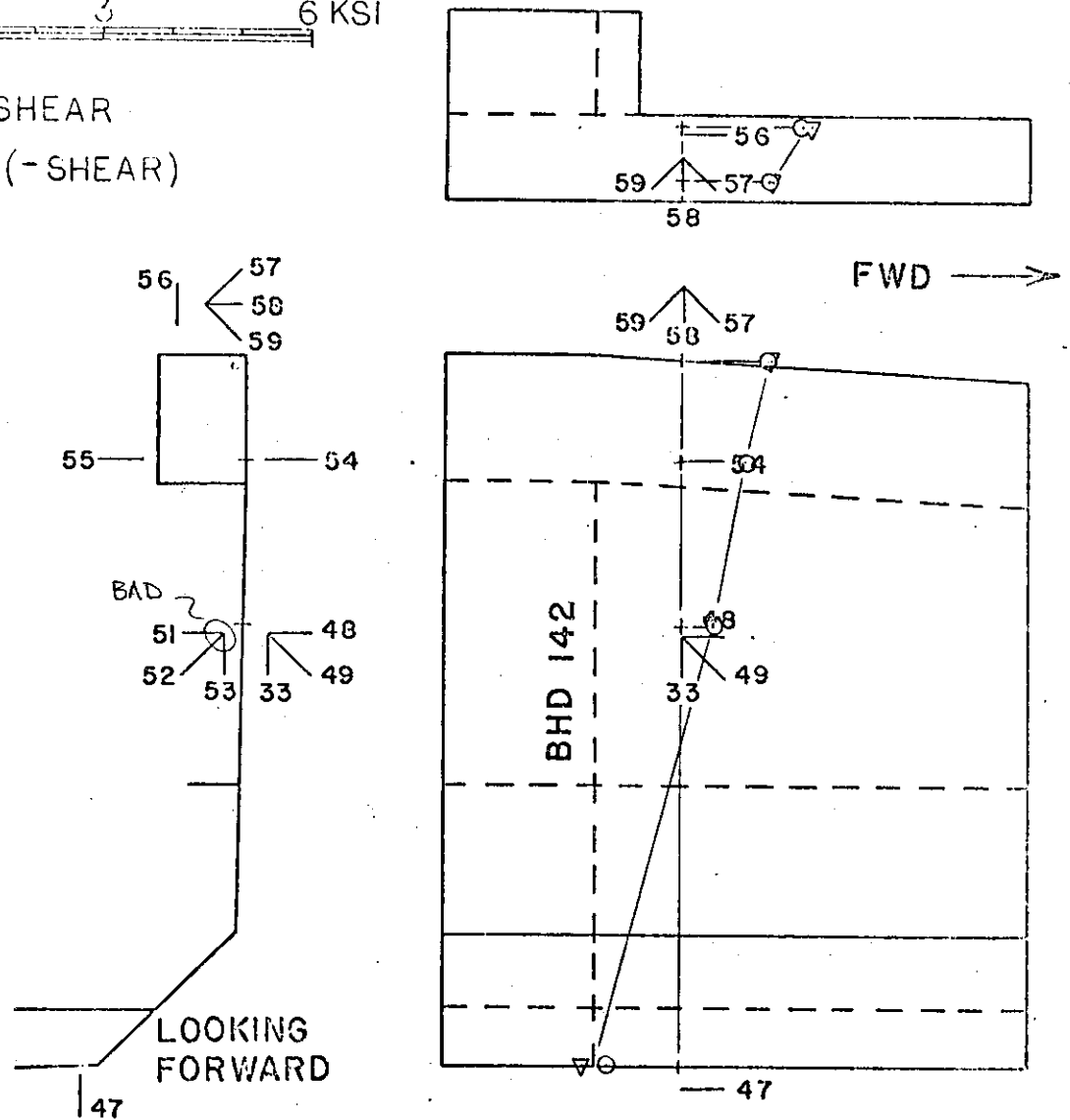


FIGURE 4 b

SECTION 2" FORWARD OF FRAME 142

LONGITUDINAL STRESSES DUE TO MIDSHIP SHEAR

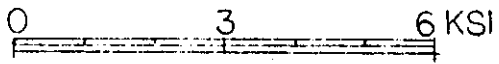
NO. OF ROSETTES - 4 (I25 RA)

- 2 (250 RA)

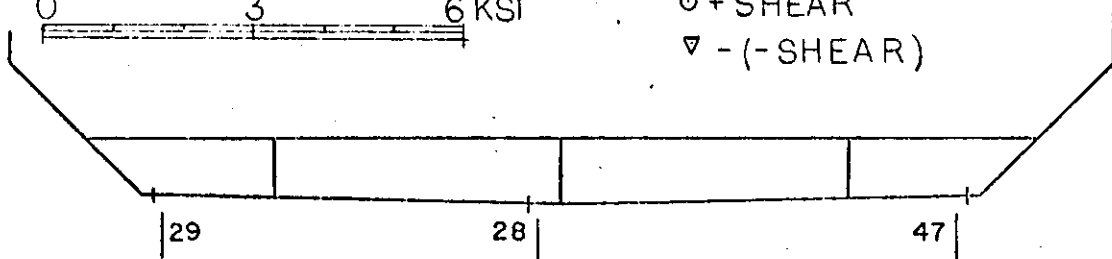
SINGLE GAGES - 9 (250 BG)

DATE OF EXPERIMENT JULY 6-11, 1972

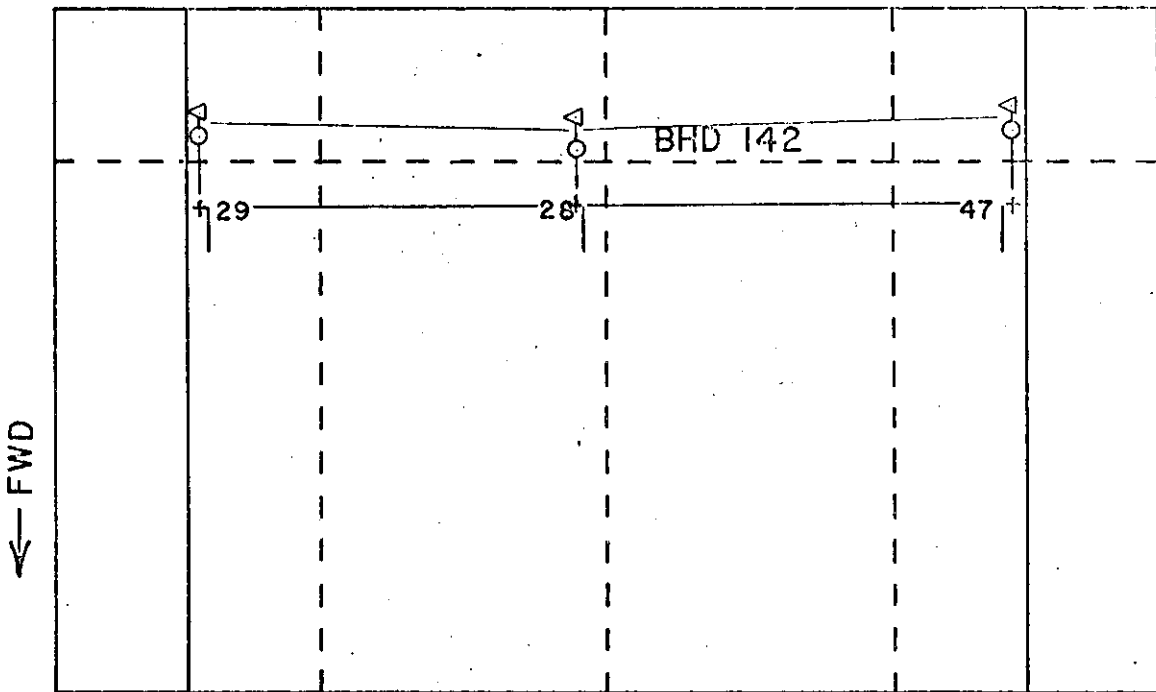
SCALE OF STRESS



○ + SHEAR
▽ - (-SHEAR)



LOOKING FORWARD



BOTTOM PLATE

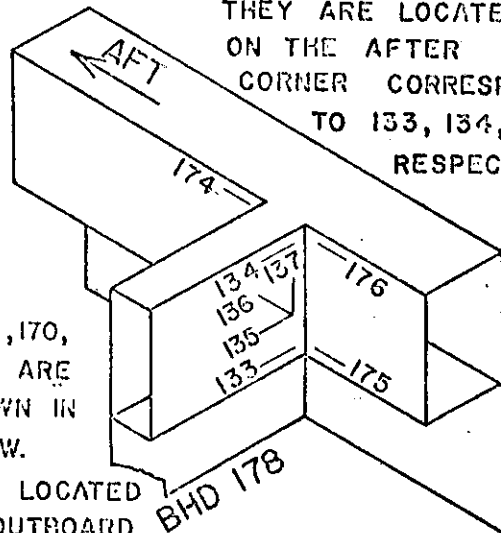
FIGURE 4c

SECTION AT HATCH CORNER ^{B-67} PORT SIDE FRAME 178

LONGITUDINAL STRESSES DUE TO MIDSHIP SHEAR
GAGES 131, 132, & 173
ARE NOT SHOWN.

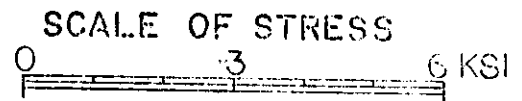
THEY ARE LOCATED NO. OF ROSETTES
ON THE AFTER CORNER CORRESPONDING
TO 133, 134, & 175
RESPECTIVELY.

-1(250 RA)
SINGLE GAGES
-12(250 BG)

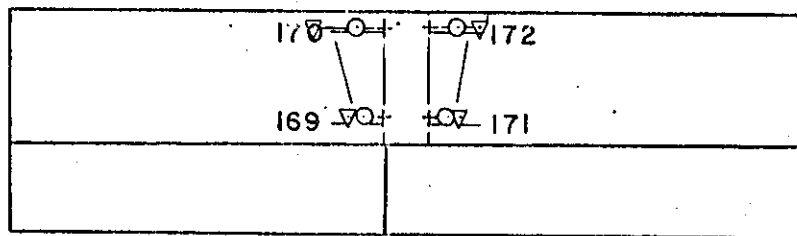


GAGES 169, 170, 171, & 172 ARE NOT SHOWN IN THIS VIEW. THEY ARE LOCATED ON THE OUTBOARD SIDE OF THE SHELL PLATE.

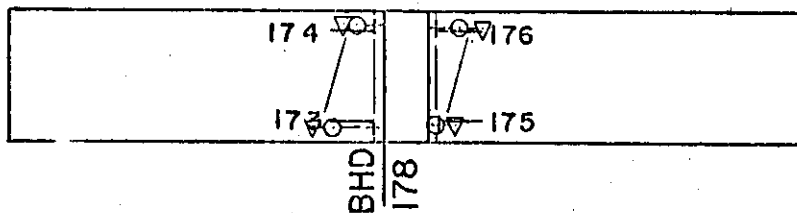
DATE OF EXPERIMENT
JULY 6 & 11, 1972



⊙ + SHEAR
▽ (-) SHEAR



LOOKING OUTBOARD SHELL PLATE → FWD



LOOKING OUTBOARD TORSION BOX → FWD

FIGURE 5

SECTION BETWEEN FRAMES 178 & 194

LOCATION OF GAGES

NO. OF SINGLE GAGE- 2 (250 BG)
NO. OF ROSETTES - 4 (125 RA)
- 12 (250 RA)

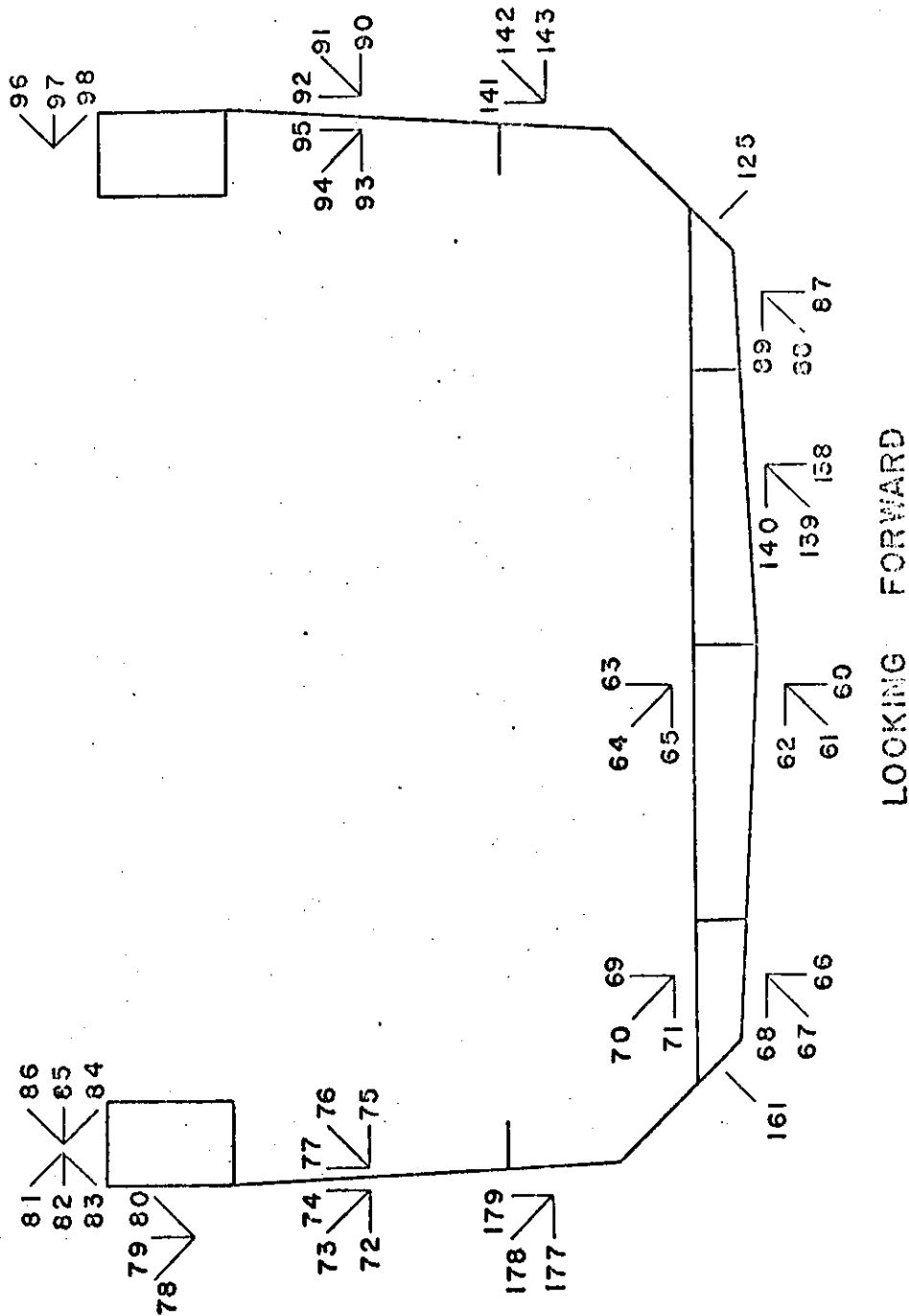


FIGURE 6

SECTION BETWEEN FRAMES 178 & 194

LONGITUDINAL STRESSES DUE TO MIDSHIP SHEAR

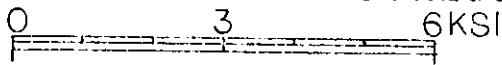
SINGLE GAGES - 2(250 BG)

NO. OF ROSETTES - 4(125 RA)

- 12(250 RA)

DATE OF EXPERIMENT JULY 6th 11, 1972

SCALE OF STRESS



○ + SHEAR
 ▽ - (-SHEAR)

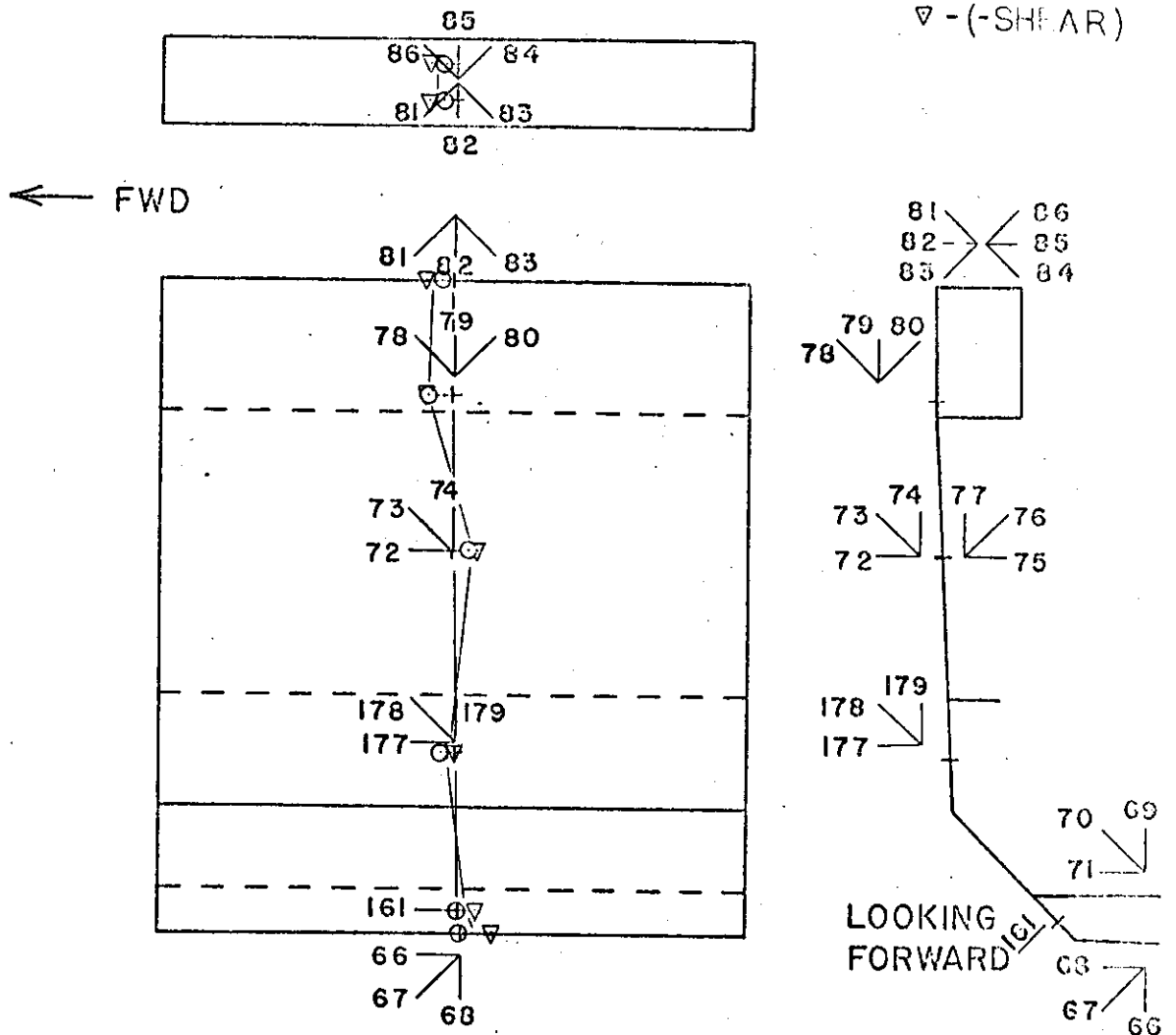


FIGURE 6 a

SECTION BETWEEN FRAMES 178 & 194

LONGITUDINAL STRESSES DUE TO MIDSHIP SHEAR

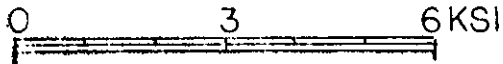
SINGLE GAGES - 2(250 BG)

NO. OF ROSETTES - 4(125 RA)

-12(250 RA)

DATE OF EXPERIMENT JULY 6th 11, 1972

SCALE OF STRESS



○ + SHEAR

▽ -(SHEAR)

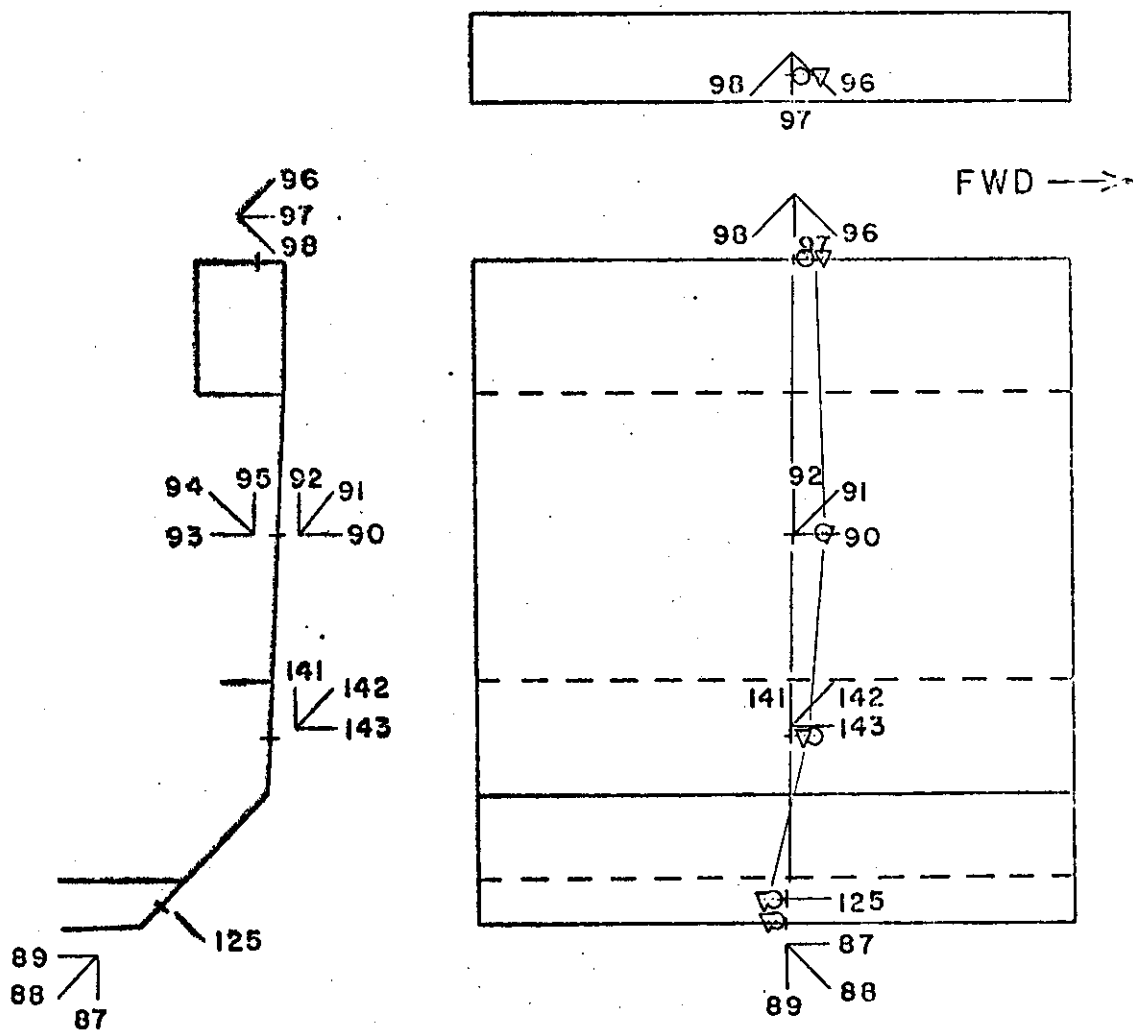


FIGURE 6b

SECTION BETWEEN FRAMES 178 & 194

LONGITUDINAL STRESSES DUE TO MIDSHIP SHEAR
SINGLE GAGES - 2(250 BG)
NO. OF ROSETTES - 4(125 RA)
- 12(250 RA)

DATE OF EXPERIMENT JULY 6th, 1972

SCALE OF STRESS

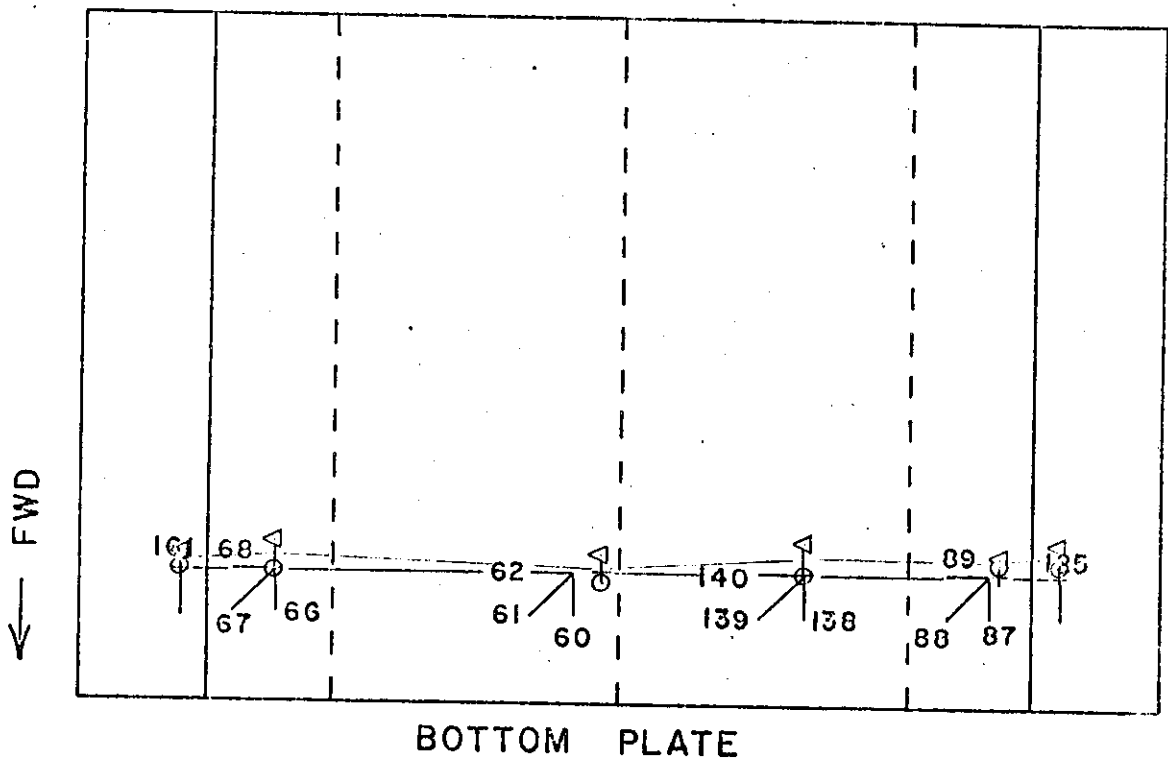
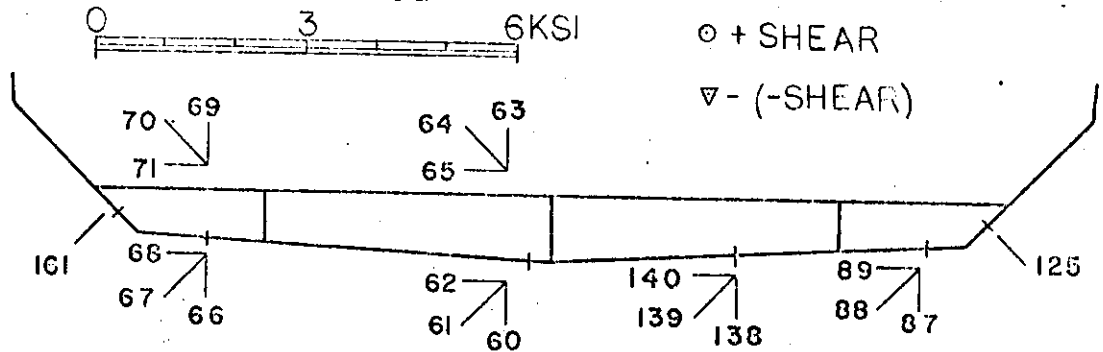


FIGURE 6c

SECTION BETWEEN FRAMES 178 & 194

LONGITUDINAL STRESSES DUE TO MIDSHIP SHEAR

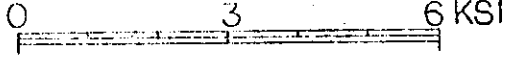
SINGLE GAGES - 2(250 BG)

NO. OF ROSETTES - 4(125 RA)

-12(250 RA)

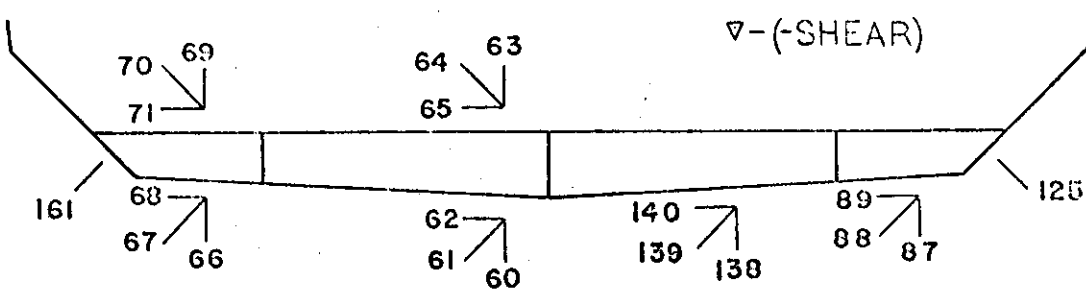
DATE OF EXPERIMENT JULY 6-11, 1972

SCALE OF STRESS

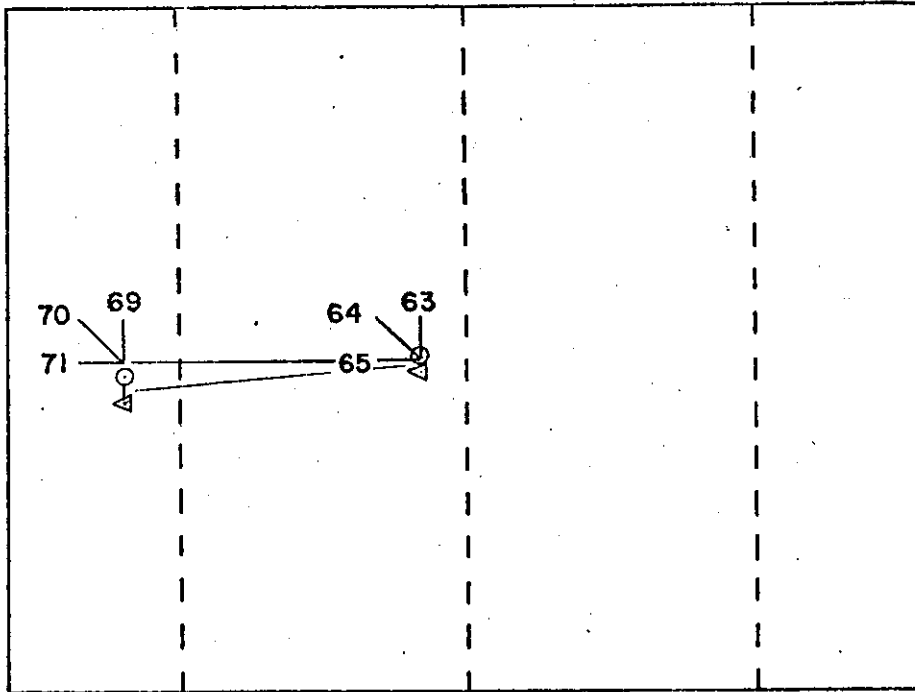


○ +SHEAR

▽ (-SHEAR)



FWD ↑



TANK TOP

FIGURE 6 d

SECTION BETWEEN FRAMES 178 & 194

B-73

SHEAR STRESSES DUE TO MIDSHIP SHEAR

SINGLE GAGES - 2 (250 BG)
 NO. OF ROSETTES - 4 (125 RA)
 - 12 (250 RA)

DATE OF EXPERIMENT JULY 6th 11, 1972

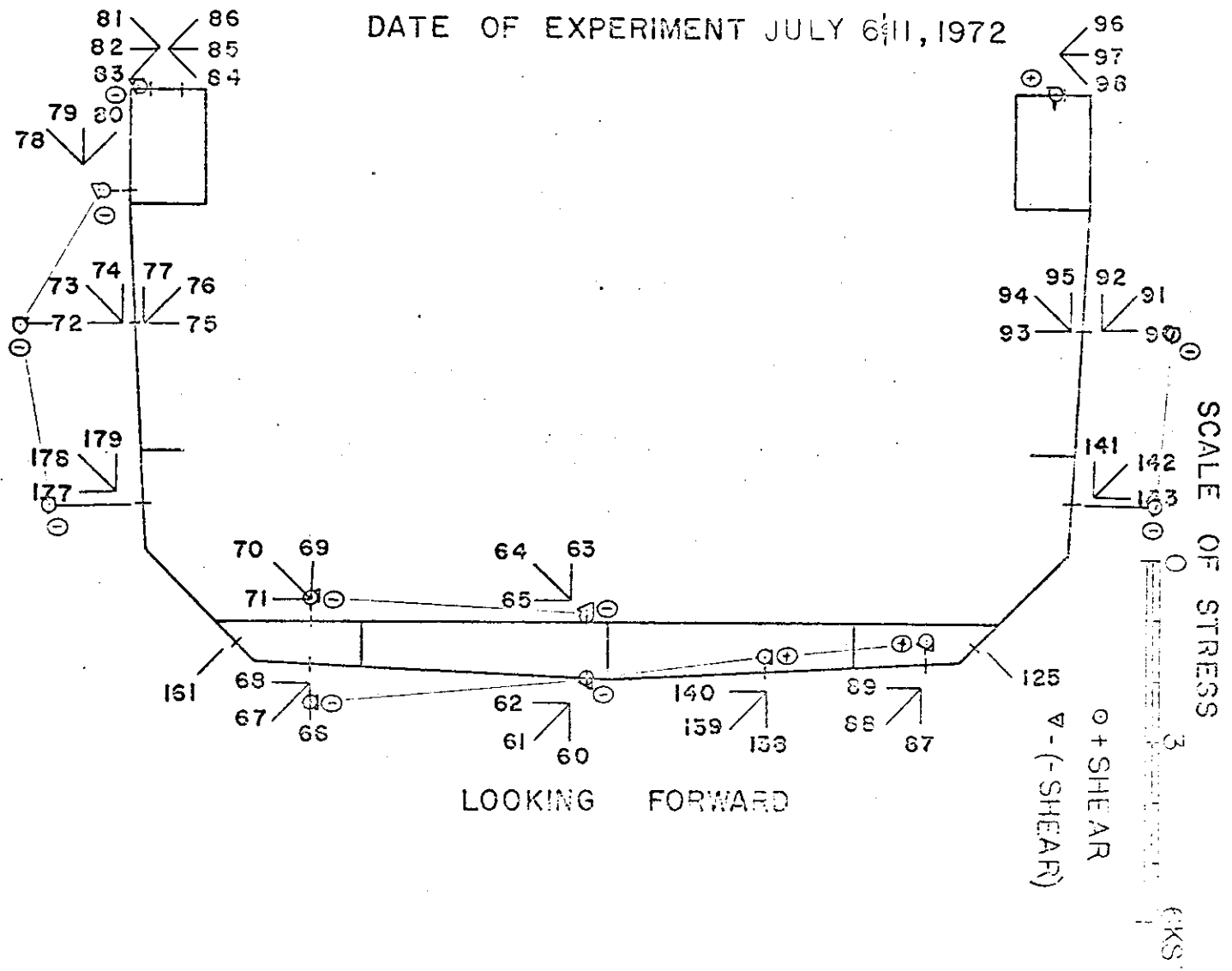
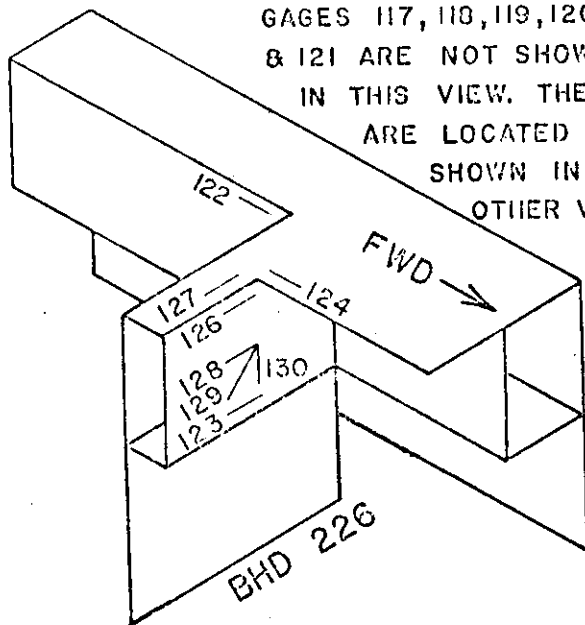


FIGURE 7

B-74
SECTION AT HATCH CORNER
PORT SIDE FRAME 226

LONGITUDINAL STRESSES DUE TO MIDSHIP SHEAR



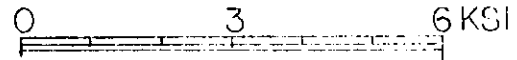
GAGES 117, 118, 119, 120,
 & 121 ARE NOT SHOWN
 IN THIS VIEW. THEY
 ARE LOCATED AS
 SHOWN IN
 OTHER VIEWS.

NO. OF ROSETTES
 - 1 (250 RA)
 SINGLE GAGES
 - 10 (250 BG)

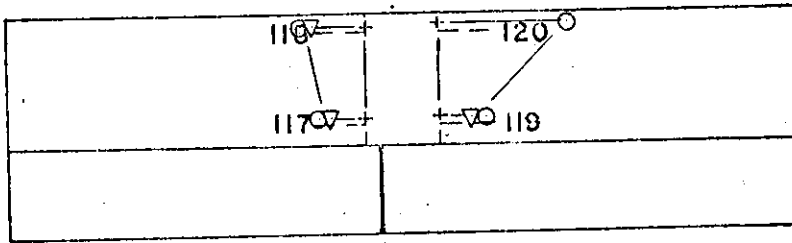
DATE OF EXPERIMENT

JULY 6 & 11, 1972

SCALE OF STRESS

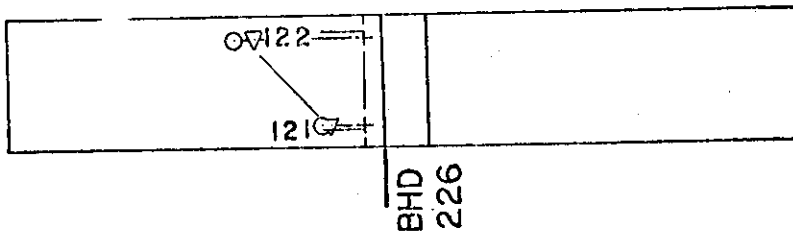


○ + SHEAR
 ▽ - (-SHEAR)



LOOKING OUTBOARD
 SHELL PLATE

→ FWD



LOOKING OUTBOARD
 TORSION BOX

FIGURE 8

B-75
SECTION 1" AFT OF FRAME 290

LONGITUDINAL STRESSES DUE TO MIDSHIP SHEAR

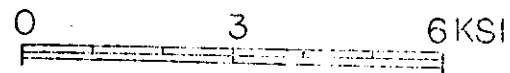
NO. OF ROSETTES - 2(250 RA)

- 1(125 RA)

SINGLE GAGES - 6(250 BG)

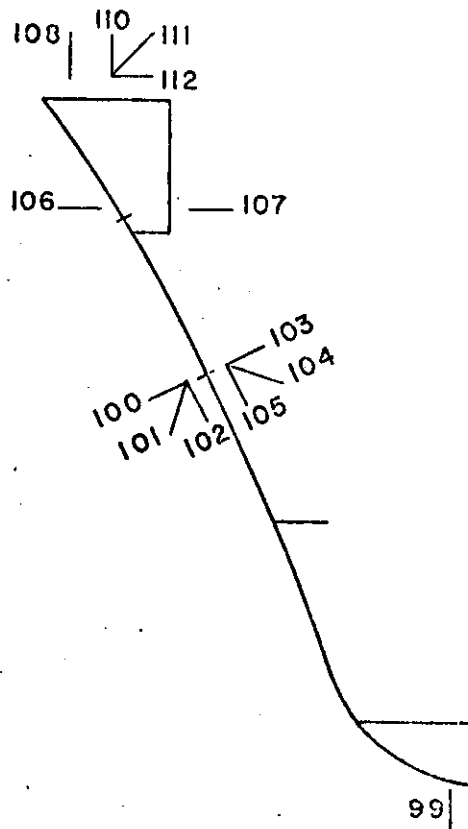
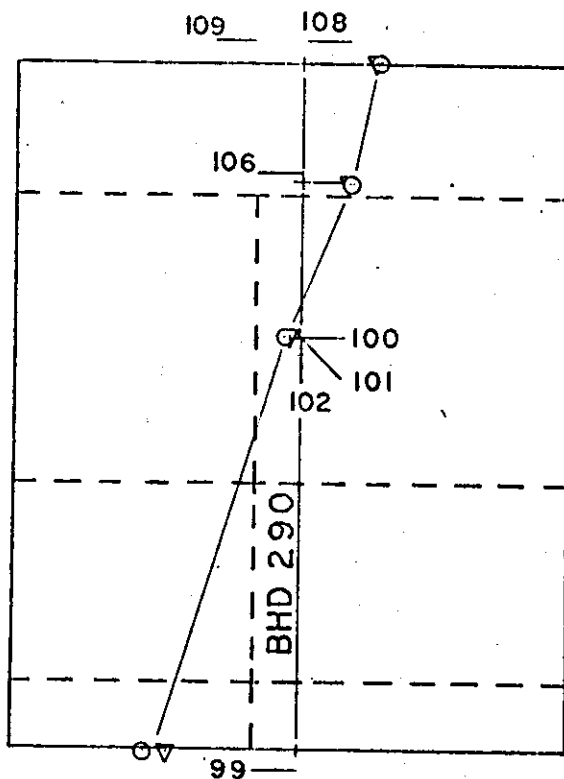
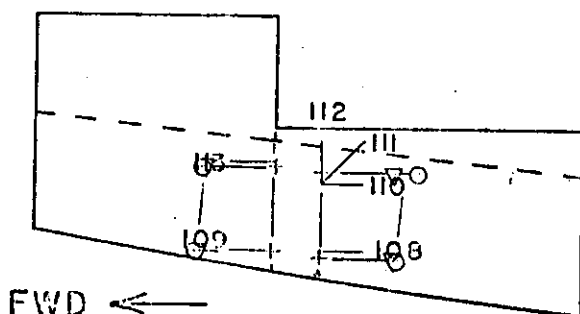
DATE OF EXPERIMENT
 JULY 6th 11, 1972

SCALE OF STRESS



⊙ + SHEAR

▽ (-SHEAR)



LOOKING FORWARD

FIGURE 9

STRESSES (KSI)

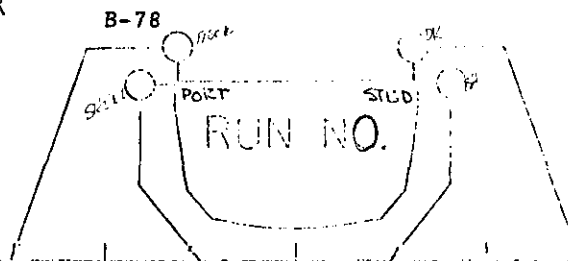
FIG.	<u>GAGE</u> <u>NUMBER</u>	○ 1	▽ 2	FIG.	<u>GAGE</u> <u>NUMBER</u>	○ 1	▽ 2
1	0	-1.587	-1.971	4b	47	-1.056	1.404
	1	-.428	-.598		48	.488	.457
	8	.948	1.014		54	.900	
	9	1.632	1.761		57	1.231	1.256
	10	1.484	1.554		56	1.758	1.878
	13	2.403	2.661	4c	29	-1.014	-1.341
	14	3.237	3.594		28	-.804	-1.272
2	15	1.074	1.056		47	-1.056	-1.404
	16	1.542	1.608	5	169	.291	.507
	17	1.011	1.032		170	.666	.987
	18	1.764	1.761		171	.285	.465
	26	2.139	2.154		172	.399	.708
	27	1.170	1.047		173	.576	.882
3 (SHFAR)	149	.499	.545		174	.261	.438
	152	-.145	-.117		175	.045	.237
	155	.012	.009		176	.297	.663
	162	-.069	-.085	6a	66	.054	-.440
4a	29	-1.014	-1.341		161	.030	-.258
	30	.177	.205		177	.193	-.029
	36	.915	.978		72	-.663	-.092
	38	1.602	1.761		78	.302	.332
	39	1.251	1.321		81	.184	.408
	42	1.401	1.533		84	.172	.407
	43	1.257	1.308				

FIG.	GAGE NUMBER	○ 1	▽ 2
6b	87	-.144	-.265
	125	-.185	-.411
	141	.341	-.189
	90	-.587	-.524
	96	.169	.410
6c	161	.030	-.258
	66	.054	-.440
	60	.150	-.242
	138	.064	-.444
	87	-.144	-.265
	125	-.180	-.471
6d	69	-.213	-.599
	63	.026	-.134
7 (SHEAR)	81	-.157	-.181
	78	-.473	-.534
	72	-1.662	-1.629
	177	-1.563	-1.576
	66	-.380	-.403
	69	-.389	-.403
	68	-.012	-.084
	63	-.124	-.215
	138	.274	.238
	87	.414	.349

FIG.	GAGE NUMBER	○ 1	▽ 2
7 (CONT'D)	141	-1.420	-1.375
	90	-1.802	-1.711
	96	.142	.150
8	117	-.669	-.477
	118	-.969	-.756
	119	-.660	-.457
	120	-1.845	
	121	-.618	-.456
	122	-1.872	-1.569
9	99	2.187	1.851
	100	.218	.174
	106	-.714	-.657
	68	-1.110	-1.053
	109	-1.104	-1.008
	110	-1.406	-1.056
	113	-1.071	-.993

LARGE MIDSHIPS SHEAR

JULY 6/11



BHD.

MODEL DEFLECTION FROM THE NO-LOAD CONDITION, IN INCHES.

+ SHEAR ⇨
- (-SHEAR) ⇦

342	- 0.002 - 0.001	0.000 0.000	+ 0.002 + 0.002	- 0.002 + 0.001
290	- 0.005 - 0.002	+ 0.003 + 0.002	+ 0.003 + 0.002	- 0.004 0.000
226	+ 0.004 + 0.006	- 0.001 0.000	0.000 - 0.001	+ 0.007 + 0.010
142	+ 0.031 + 0.030	0.000 + 0.001	- 0.001 - 0.002	+ 0.025 + 0.035
96	+ 0.039 + 0.038	0.000 + 0.001	0.000 - 0.001	+ 0.045 + 0.041
10	+ 0.037 + 0.029	- 0.001 + 0.001	- 0.003 - 0.002	+ 0.041 + 0.033

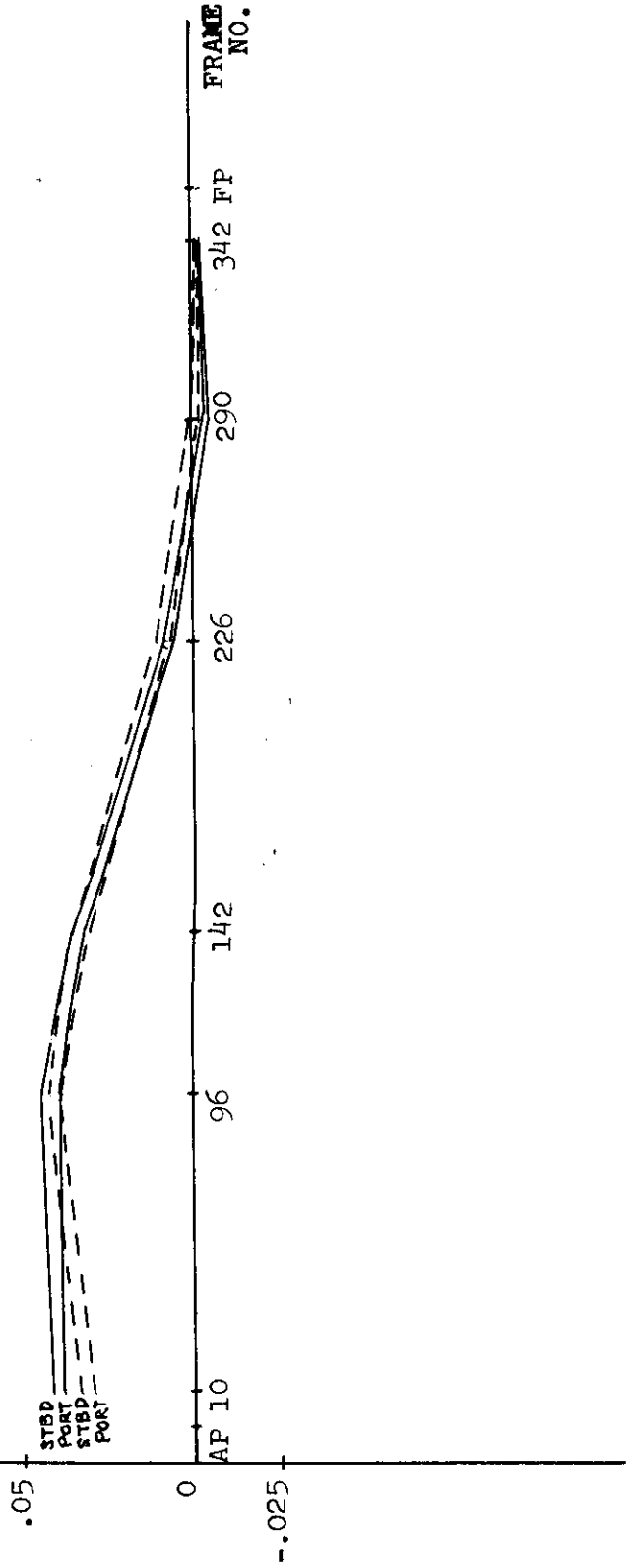
EQUIVALENT DEFLECTIONS OF FULL SCALE SHIP, IN INCHES.

342	- 0.10 - 0.05	0.00 0.00	+ 0.10 + 0.10	- 0.10 + 0.05
290	- 0.25 - 0.10	+ 0.15 + 0.10	+ 0.15 + 0.10	- 0.20 0.00
226	+ 0.20 + 0.30	- 0.05 0.00	0.00 - 0.05	+ 0.35 + 0.50
142	+ 1.55 + 1.50	0.00 + 0.05	- 0.05 - 0.10	+ 1.75 + 1.75
96	+ 1.95 + 1.90	0.00 + 0.05	0.00 - 0.05	+ 2.15 + 2.05
10	+ 1.85 + 1.45	- 0.05 + 0.05	- 0.15 - 0.10	+ 2.05 + 1.65

VERTICAL MODEL DEFLECTIONS (IN.)

VERT
MODEL
DEFLECT.
(IN.)

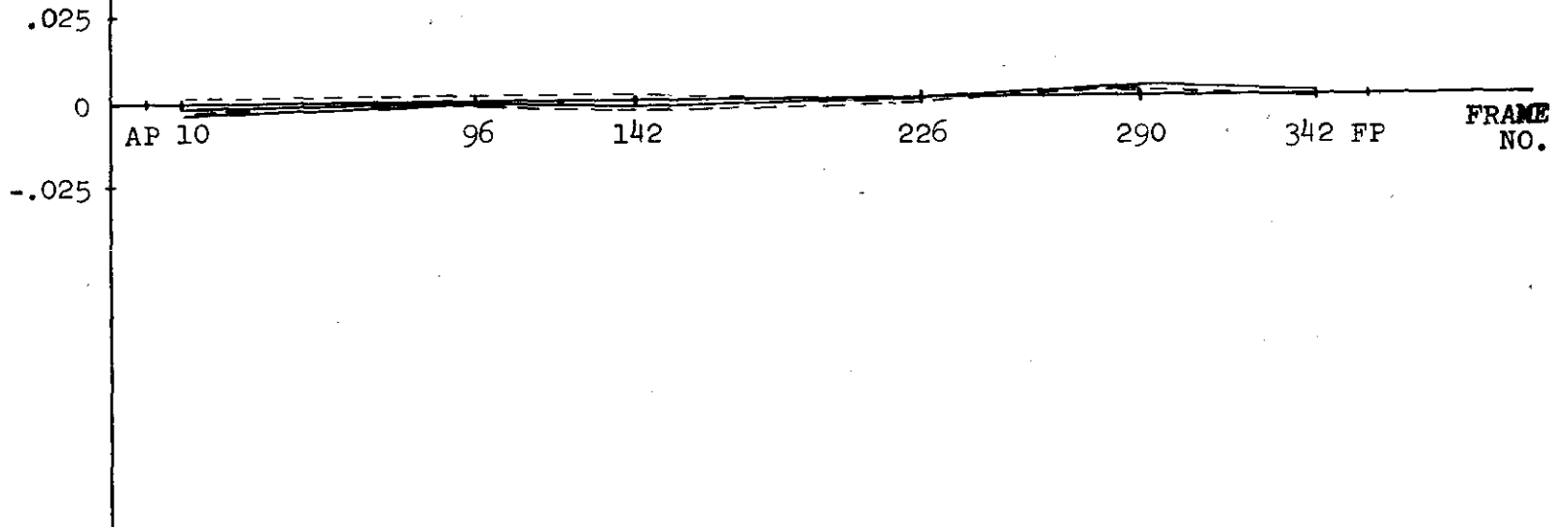
— + SHEAR July 6, 1972
- - - - (- SHEAR) July 11, 1972



HORIZONTAL MODEL DEFLECTIONS (IN.)

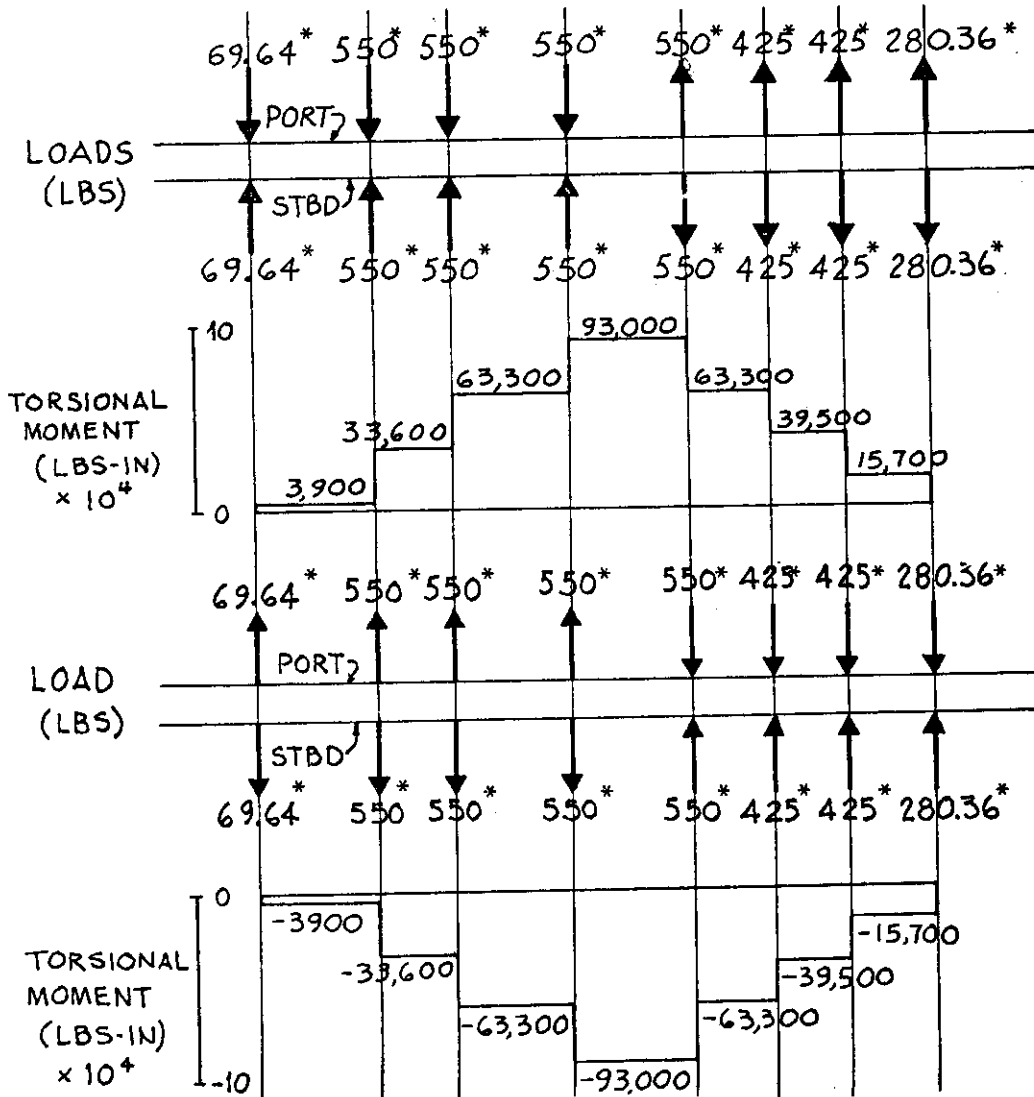
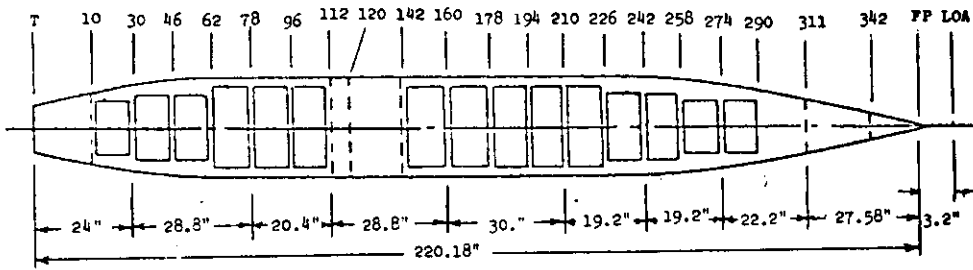
HORZ.
MODEL
DEFLECT.
(IN.)

—— + SHEAR July 6, 1972
--- (- SHEAR) July 11, 1972



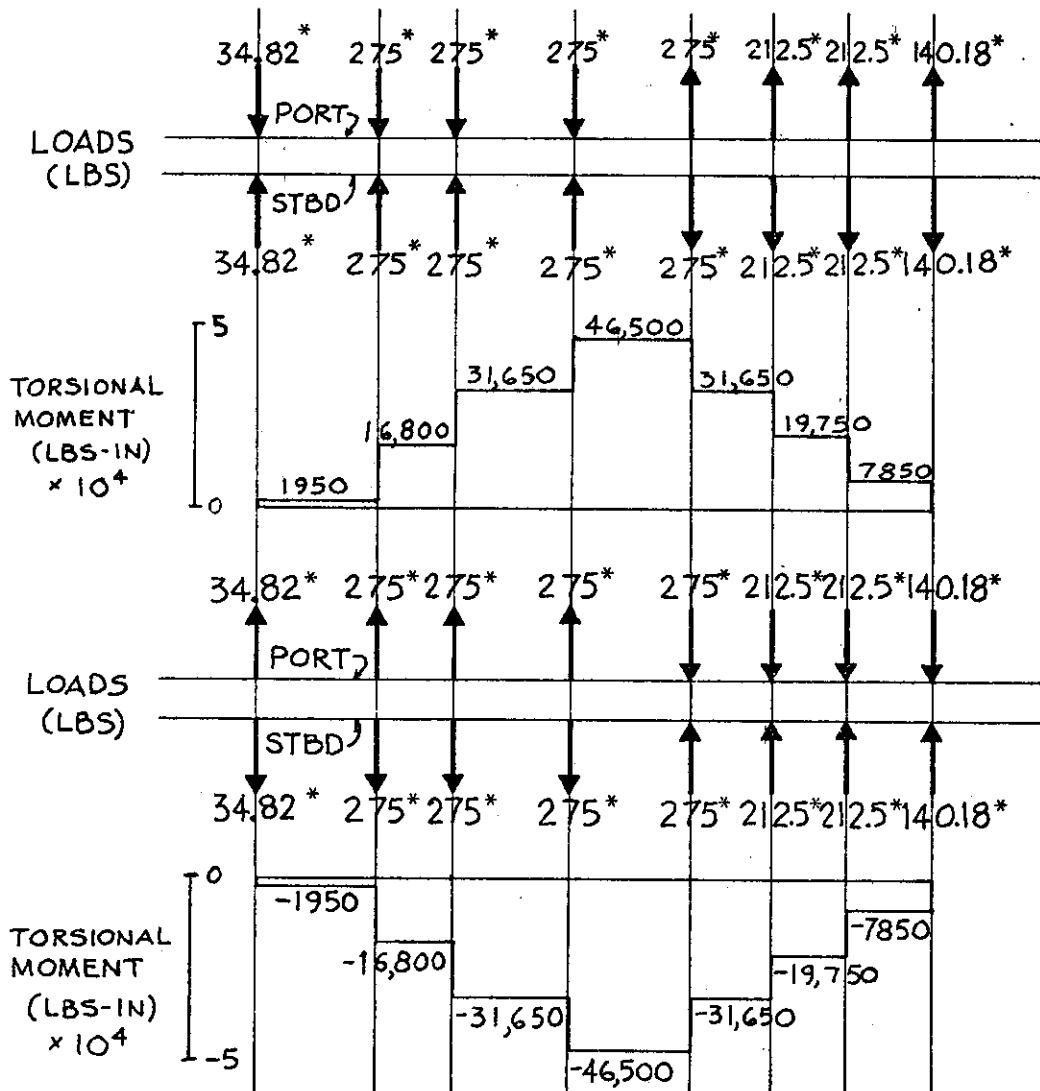
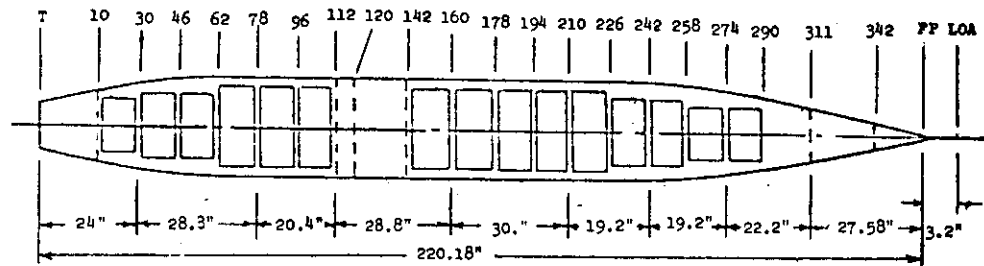
TORSION

- 1 +LARGE TORQUE JULY 18
- 2 -(-LARGE TORQUE) JULY 24
- 3 2(+ $\frac{1}{2}$ LARGE TORQUE) AUG 1
- 4 -2(- $\frac{1}{2}$ LARGE TORQUE) JULY 31



* Includes a mechanical advantage of 2, by the pulleys.

Date of Experiment 18 & 24 July 1972



* Includes a mechanical advantage of 2, by the pulleys.

Date of Experiment 1 August & 31 July 1972

SECTION 2" FORWARD OF FRAME 10

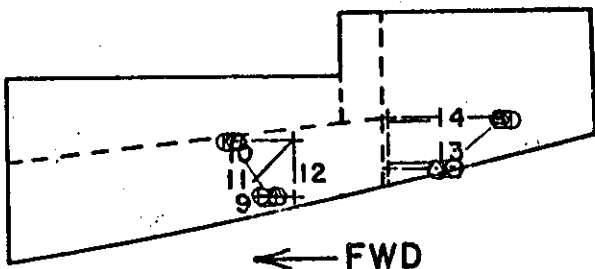
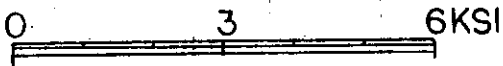
LONGITUDINAL STRESSES DUE TO TORSION

NO. OF ROSETTES - 3(125 RA)

SINGLE GAGES - 6(250 BG)

DATE OF EXPERIMENT JULY & AUG, 1972

SCALE OF STRESS



- +LARGE
- ▽ -(-LARGE)
- 2(+1/2 LARGE)
- -2(-1/2 LARGE)

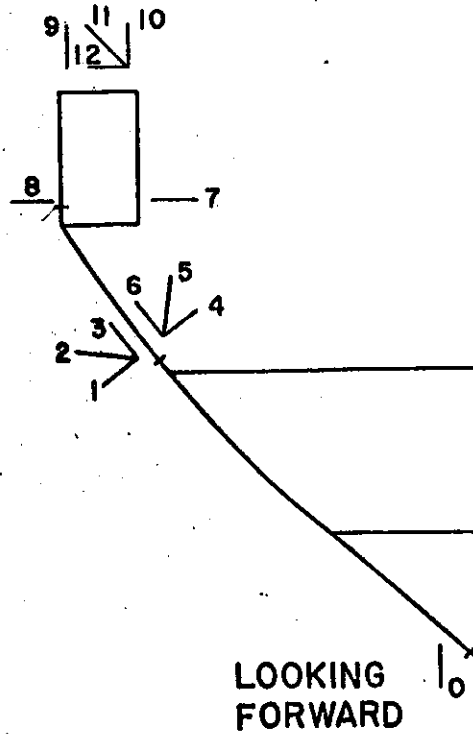
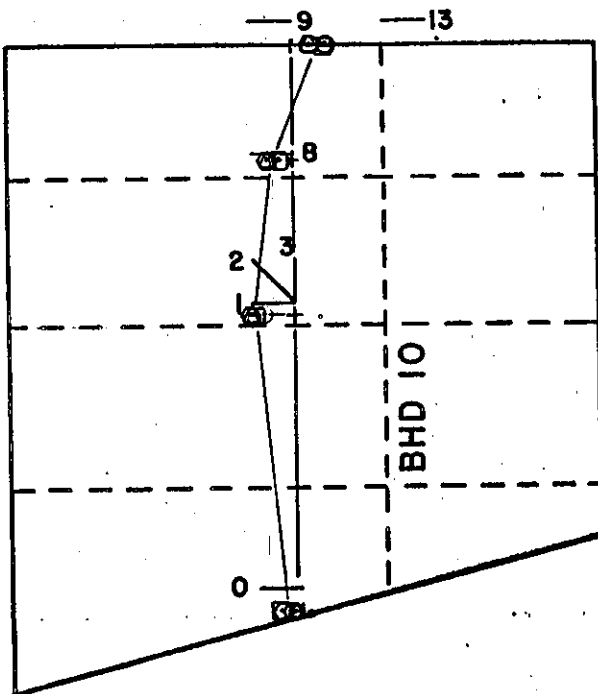
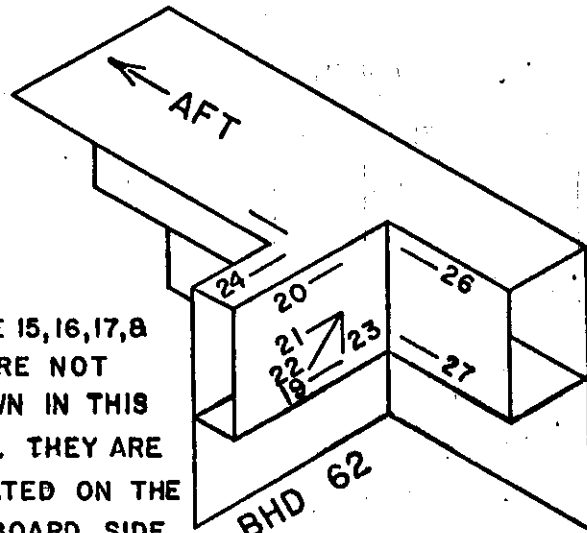


FIGURE 1

B-85
SECTION AT HATCH CORNER
PORT SIDE FRAME 62

LONGITUDINAL STRESSES DUE TO TORSION

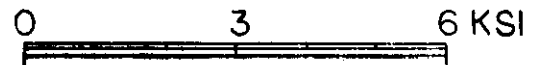


GAGE 15, 16, 17, & 18 ARE NOT SHOWN IN THIS VIEW. THEY ARE LOCATED ON THE OUTBOARD SIDE OF THE SHELL PLATE.

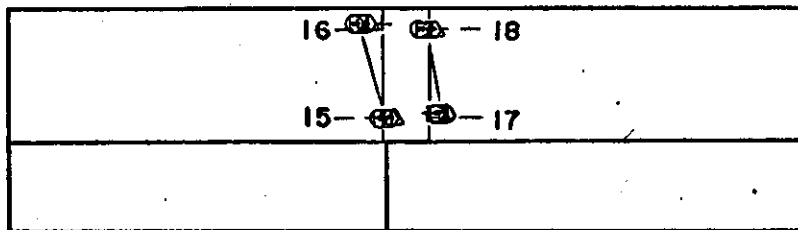
NO. OF ROSETTES
-1(250 RA)
SINGLE GAGES
-10(250 BG)

DATE OF EXPERIMENT
JULY/AUG, 1972

SCALE OF STRESS

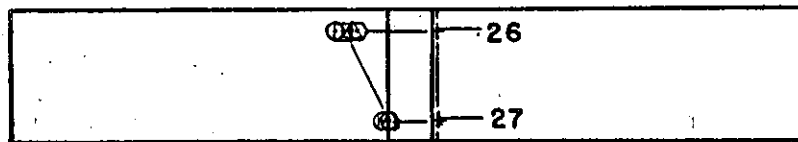


- + LARGE
- ▽ -(- LARGE)
- ◻ 2(+1/2 LARGE)
- -2(-1/2 LARGE)



LOOKING OUTBOARD
SHELL PLATE

FWD →



BHD
62
LOOKING OUTBOARD
TORSION BOX

FIGURE 2

SECTION 5.4" FORWARD OF FRAME 78

SHEAR STRESS DUE TO TORSION

NO. OF ROSETTES - 2(125 RA)
 - 4(250 RA)

SINGLE GAGES - 1(250 BG)

DATE OF EXPERIMENT JULY & AUG, 1972

SCALE OF STRESS

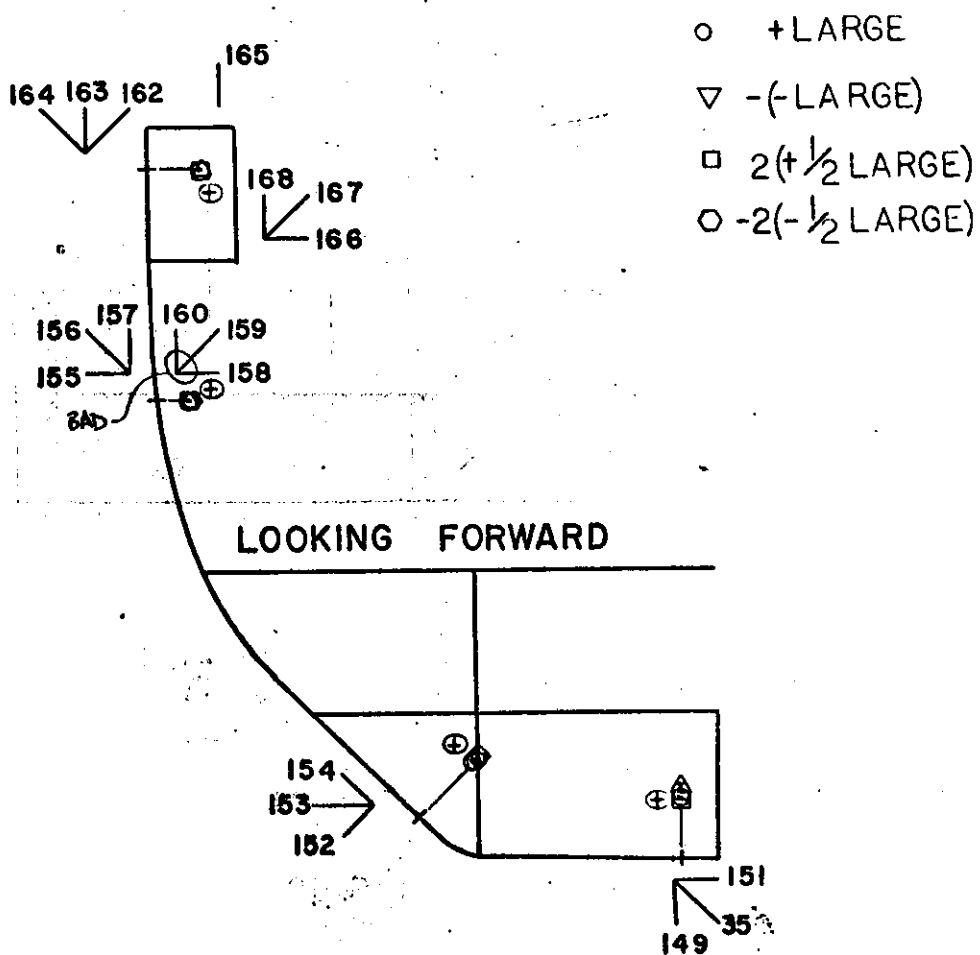


FIGURE 3

SECTION 2" FORWARD OF FRAME 142

LOCATION OF GAGES

NO. OF ROSETTES - 4 (250 RA)
- 2 (125 RA)
SINGLE GAGES - 9 (250 BG)

SINGLE GAGES 42 & 43
ARE NOT SHOWN.
LOCATED AFT BULKHEAD
142, MAIN DECK, PORT.

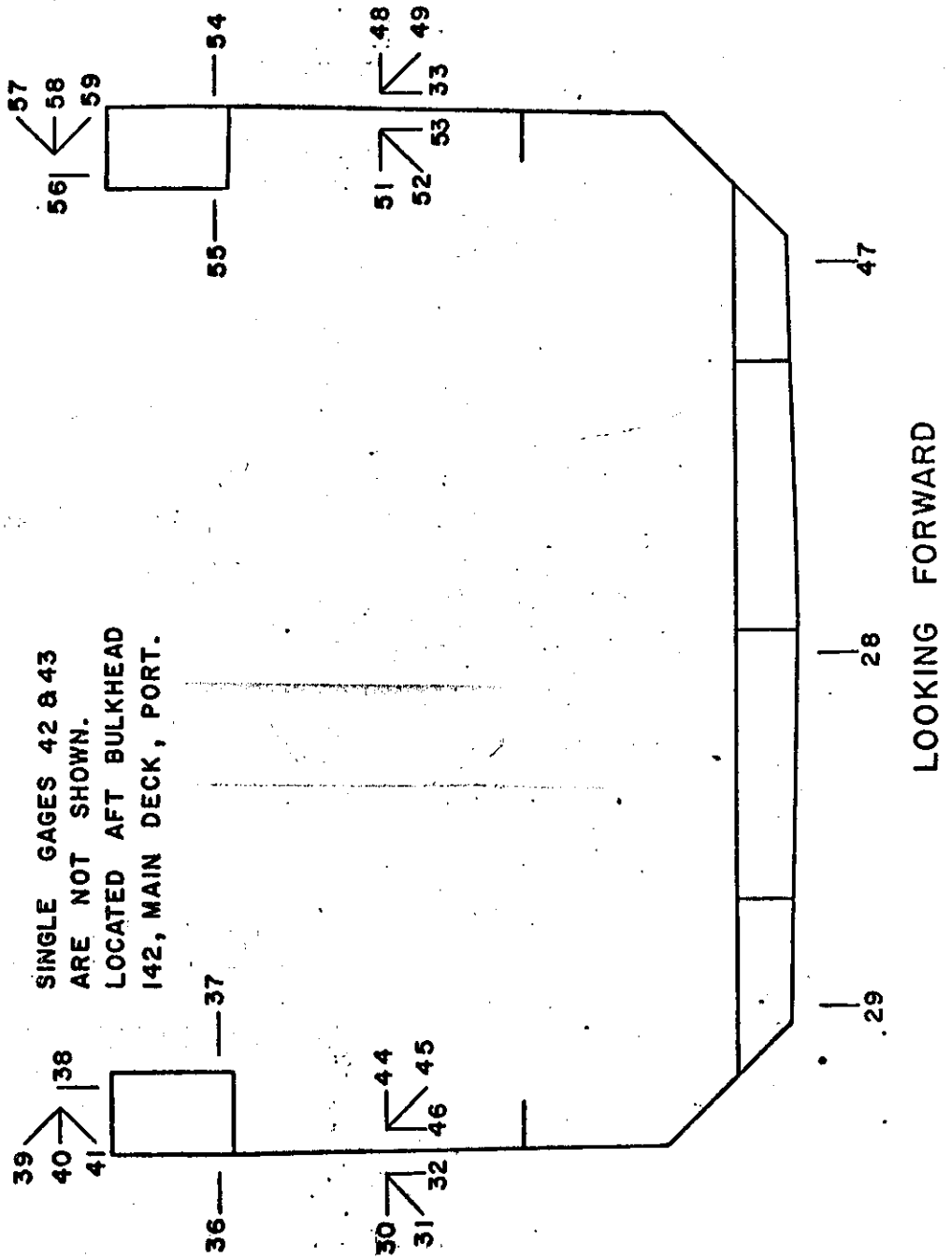


FIGURE 4

SECTION 2" FORWARD OF FRAME 142

LONGITUDINAL STRESSES DUE TO TORSION

NO. OF ROSETTES - 4 (I25 RA)
 - 2 (250 RA)

SINGLE GAGES - 9 (250 BG)

DATE OF EXPERIMENT JULY/AUG, 1972

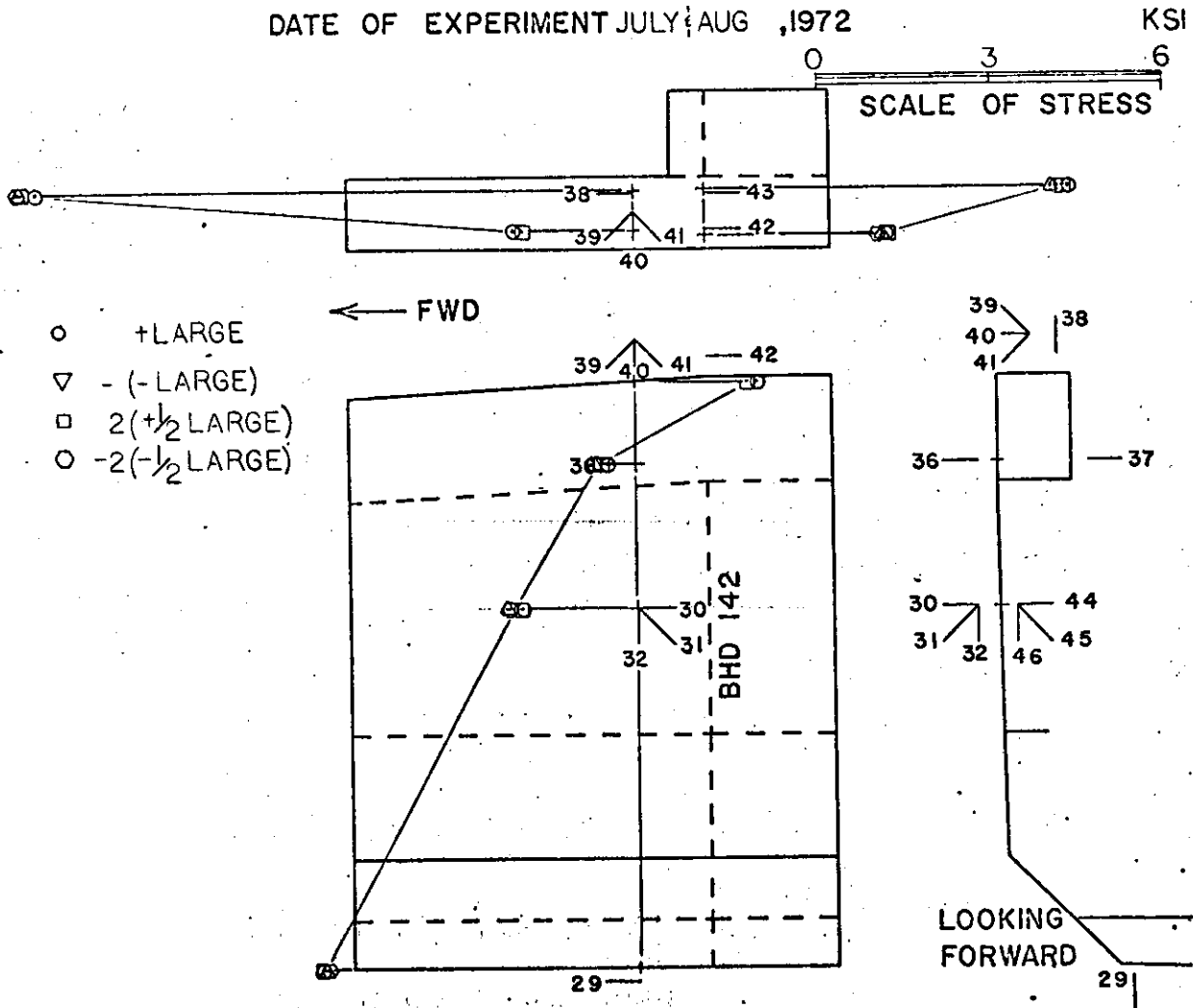


FIGURE 4a

SECTION 2" FORWARD OF FRAME 142

LONGITUDINAL STRESSES DUE TO TORSION

NO. OF ROSETTES - 4 (I25 RA)
 - 2 (250 RA)

SINGLE GAGES - 9 (250 BG)

DATE OF EXPERIMENT JULY $\frac{1}{2}$ AUG, 1972

SCALE OF STRESS

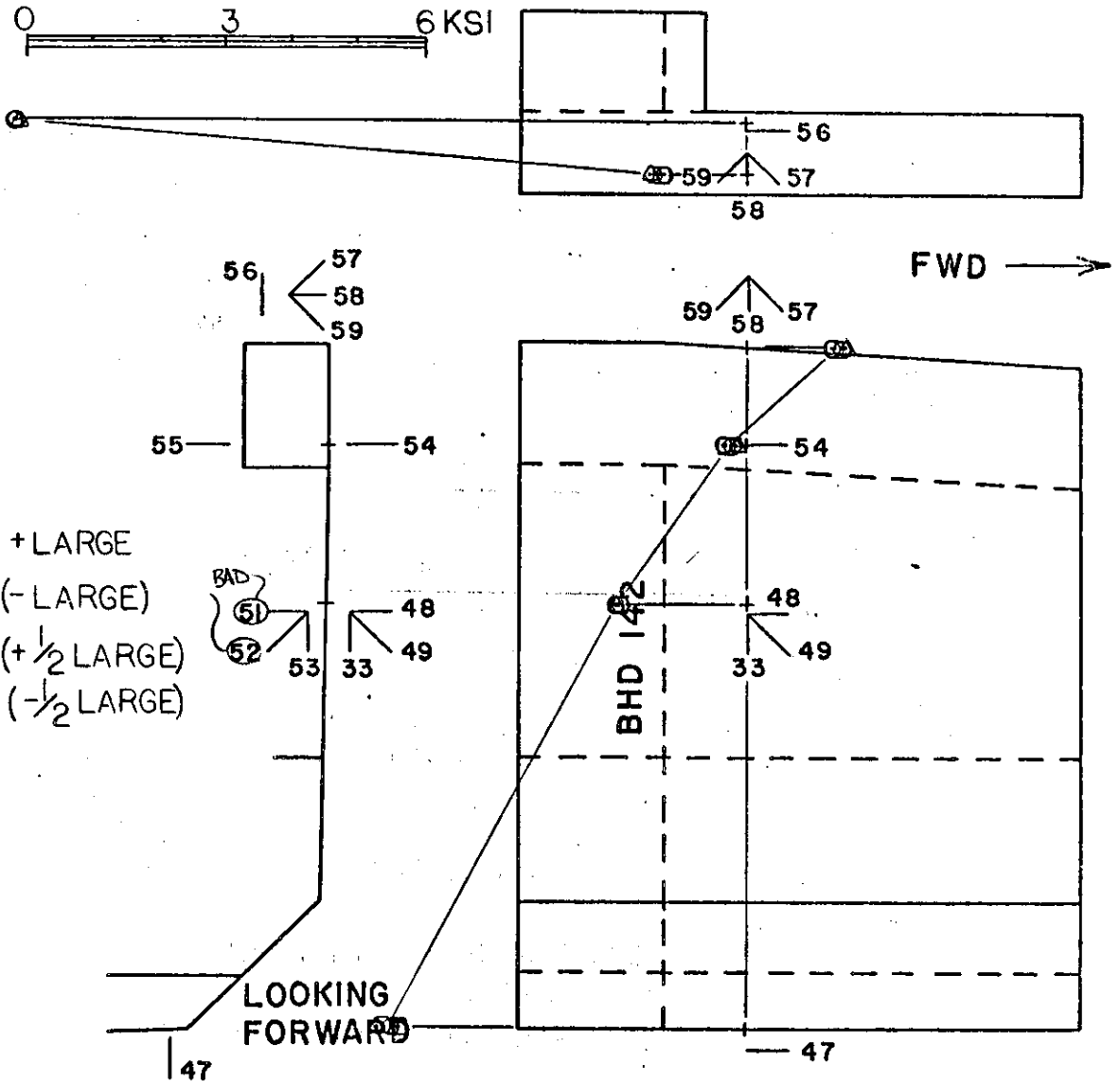


FIGURE 4b

SECTION 2" FORWARD OF FRAME 142

LONGITUDINAL STRESSES DUE TO TORSION

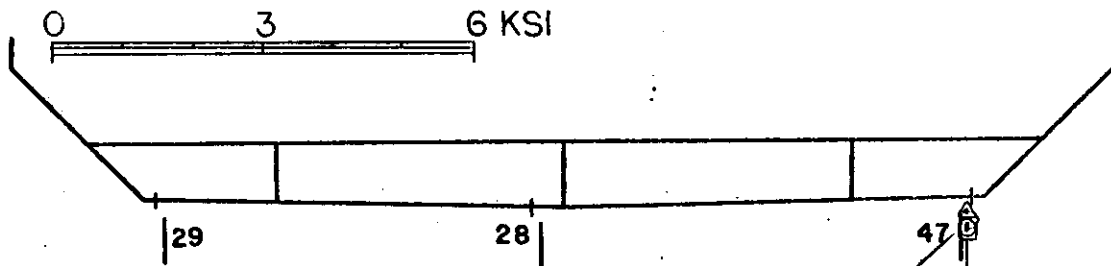
NO. OF ROSETTES - 4 (125 RA)
 - 2 (250 RA)

SINGLE GAGES - 9 (250 BG)

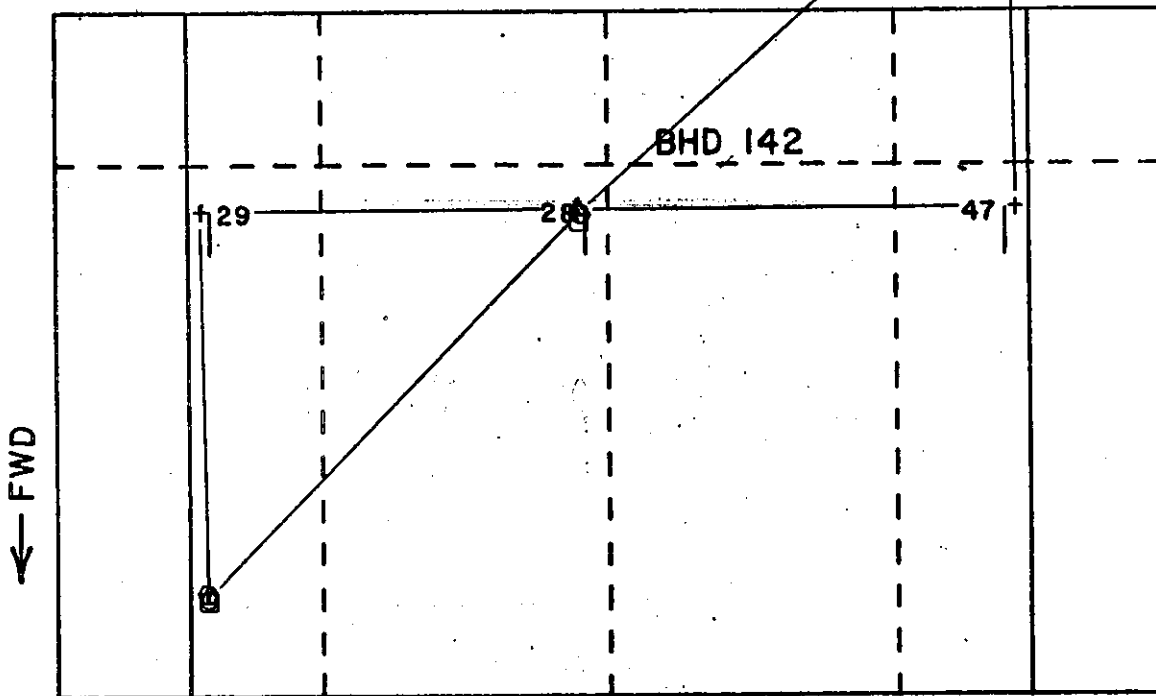
DATE OF EXPERIMENT JULY & AUG, 1972

SCALE OF STRESS

- +LARGE
- ▽ - (-LARGE)
- 2(+1/2 LARGE)
- -2(-1/2 LARGE)



LOOKING FORWARD



BOTTOM PLATE

FIGURE 4c

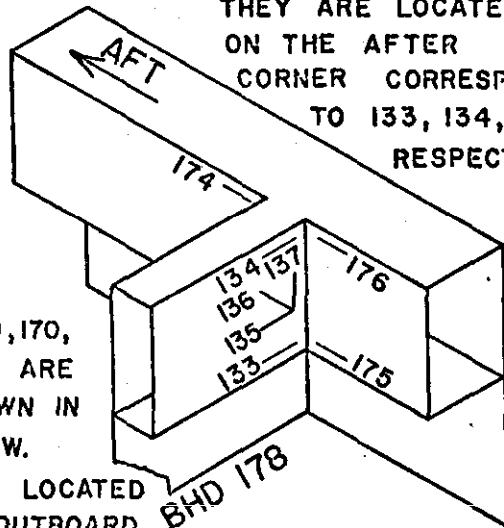
B-91
SECTION AT HATCH CORNER
PORT SIDE FRAME 178

LONGITUDINAL STRESSES DUE TO TORSION

GAGES 131, 132, & 173
ARE NOT SHOWN.

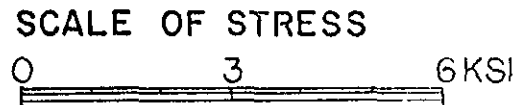
THEY ARE LOCATED ON THE AFT CORNER CORRESPONDING TO 133, 134, & 175 RESPECTIVELY.

NO. OF ROSETTES
-1(250 RA)
SINGLE GAGES
-12(250 BG)

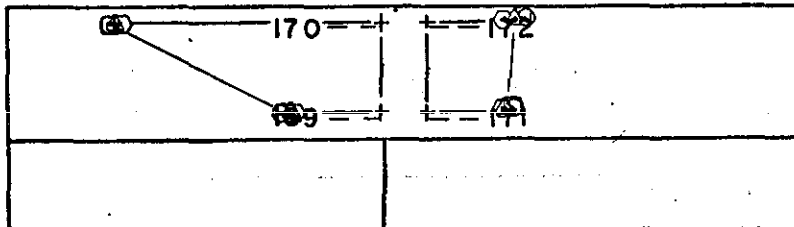


GAGES 169, 170, 171, & 172 ARE NOT SHOWN IN THIS VIEW. THEY ARE LOCATED ON THE OUTBOARD SIDE OF THE SHELL PLATE.

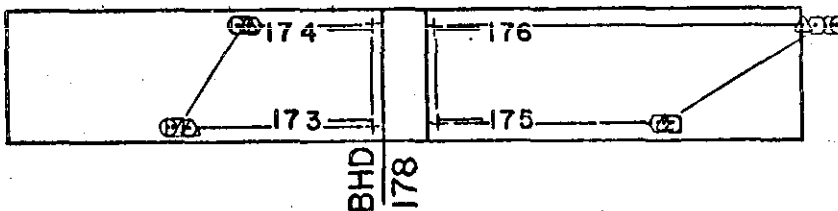
DATE OF EXPERIMENT
JULY & AUG, 1972



- +LARGE
- ▽ -(-LARGE)
- ◻ 2(+1/2 LARGE)
- ⊙ -2(-1/2 LARGE)



LOOKING OUTBOARD SHELL PLATE → FWD



LOOKING OUTBOARD TORSION BOX → FWD

FIGURE 5

SECTION BETWEEN FRAMES 178 & 194

LOCATION OF GAGES

NO. OF SINGLE GAGE- 2 (250 BG)
NO. OF ROSETTES - 4 (125 RA)
- 12 (250 RA)

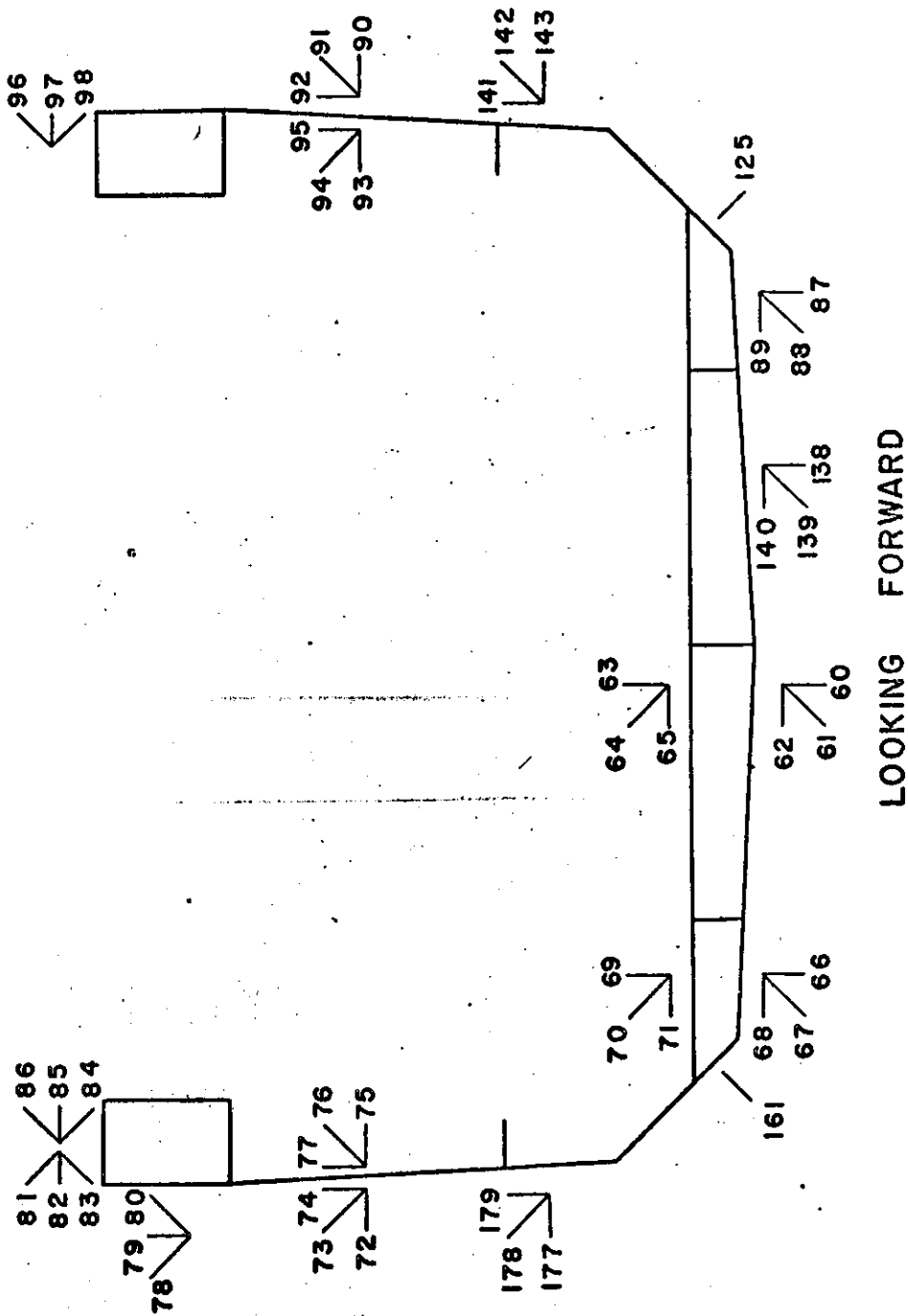


FIGURE 6

SECTION BETWEEN FRAMES 178 & 194

LONGITUDINAL STRESSES DUE TO TORSION

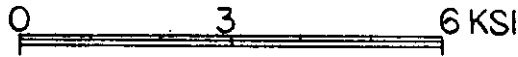
SINGLE GAGES - 2(250 BG)

NO. OF ROSETTES - 4(125 RA)

- 12(250 RA)

DATE OF EXPERIMENT JULY & AUG, 1972

SCALE OF STRESS



- +LARGE
- ▽ (-) -LARGE
- 2(+ $\frac{1}{2}$ LARGE)
- -2(- $\frac{1}{2}$ LARGE)

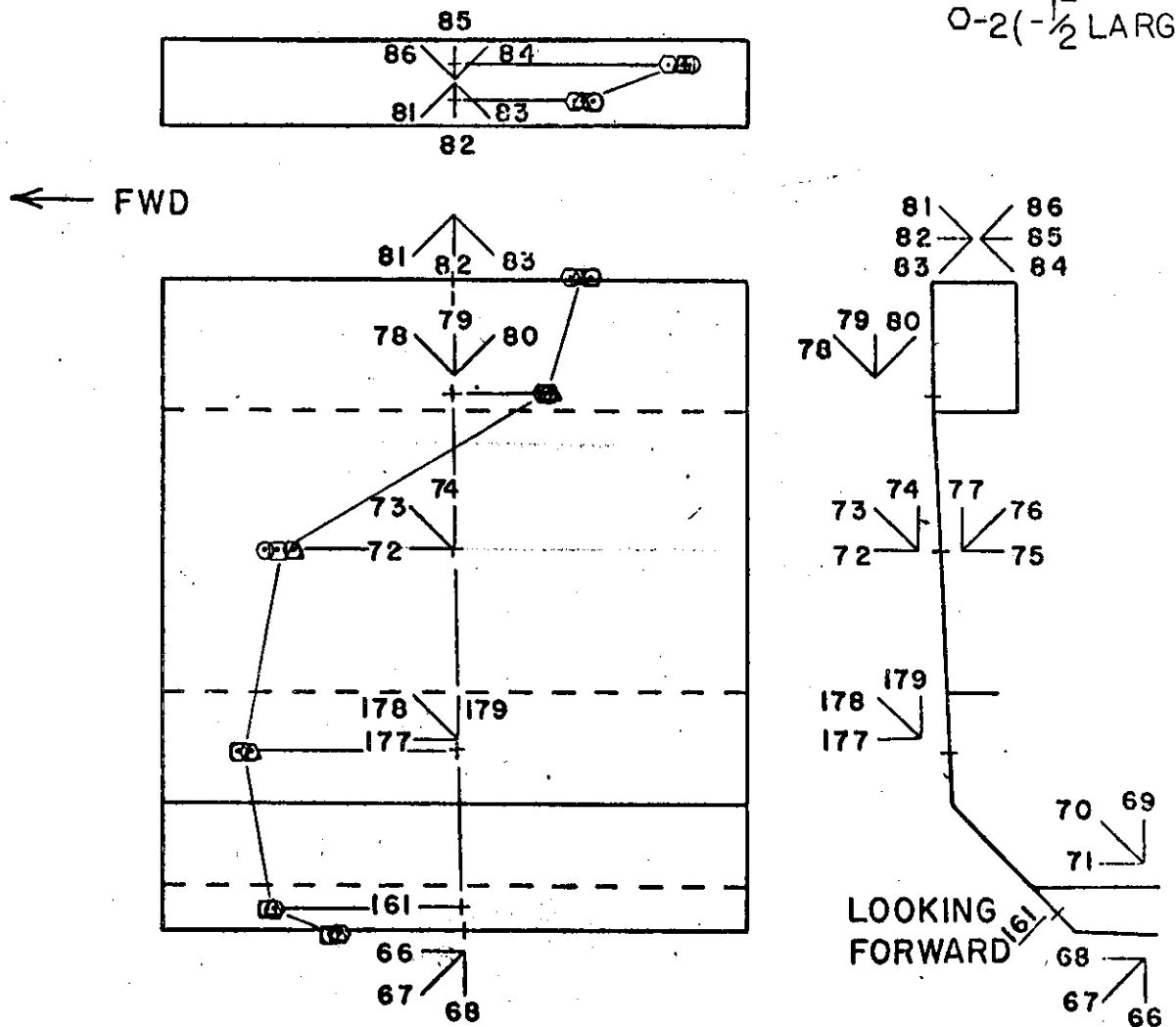


FIGURE 6a

SECTION BETWEEN FRAMES 178 & 194

LONGITUDINAL STRESSES DUE TO TORSION

SINGLE GAGES - 2(250 BG)

NO. OF ROSETTES - 4(125 RA)

-12(250 RA)

DATE OF EXPERIMENT JULY & AUG, 1972

SCALE OF STRESS



- +LARGE
- △ - (-LARGE)
- ◻ 2(+ $\frac{1}{2}$ LARGE)
- 2(- $\frac{1}{2}$ LARGE)

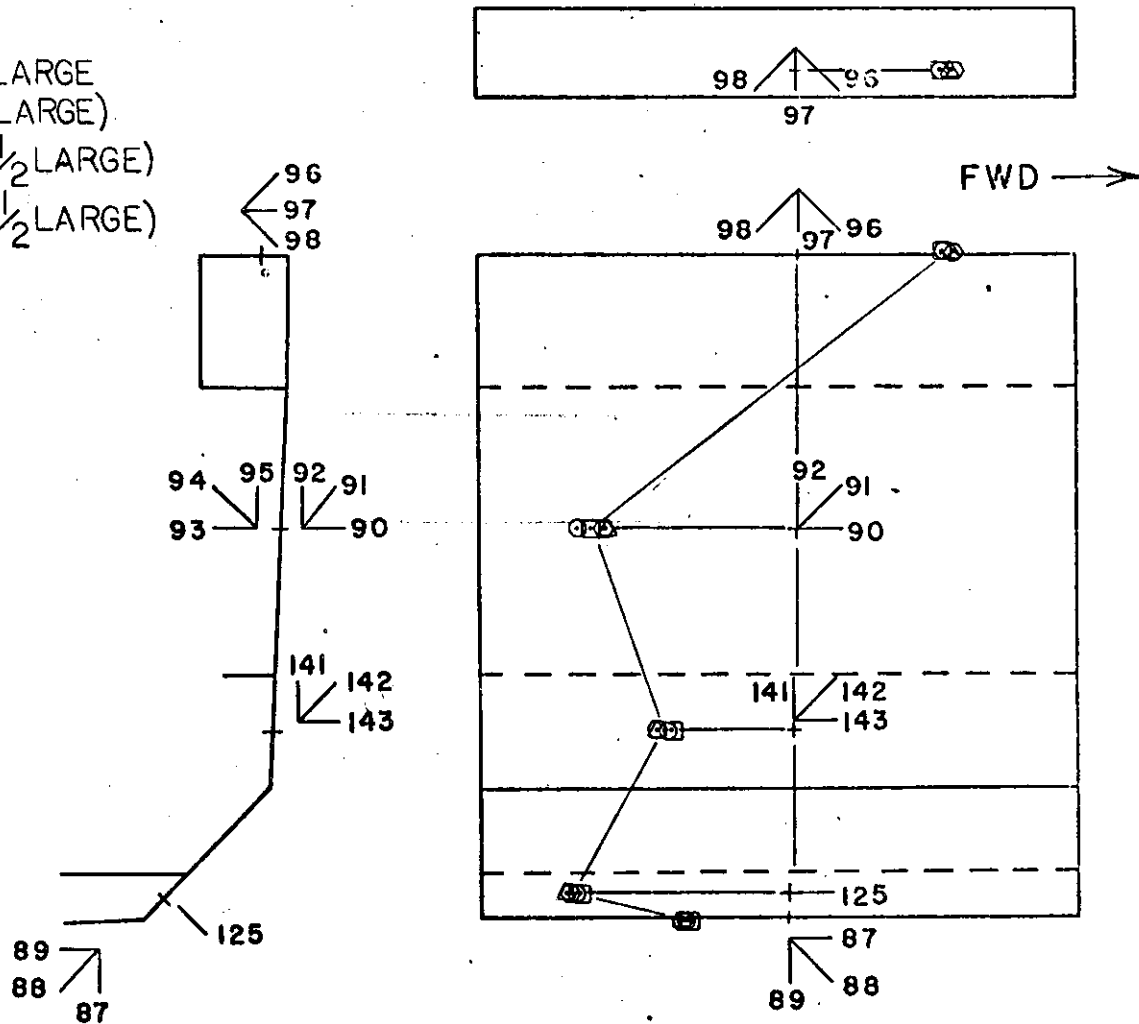


FIGURE 6b

SECTION BETWEEN FRAMES 178 & 194

LONGITUDINAL STRESSES DUE TO TORSION

SINGLE GAGES - 2(250 BG)

NO. OF ROSETTES - 4(125 RA)

- 12(250 RA)

DATE OF EXPERIMENT JULY & AUG, 1972

SCALE OF STRESS

- +LARGE
- △ -(-LARGE)
- $2(+\frac{1}{2}$ LARGE)
- $-2(-\frac{1}{2}$ LARGE)

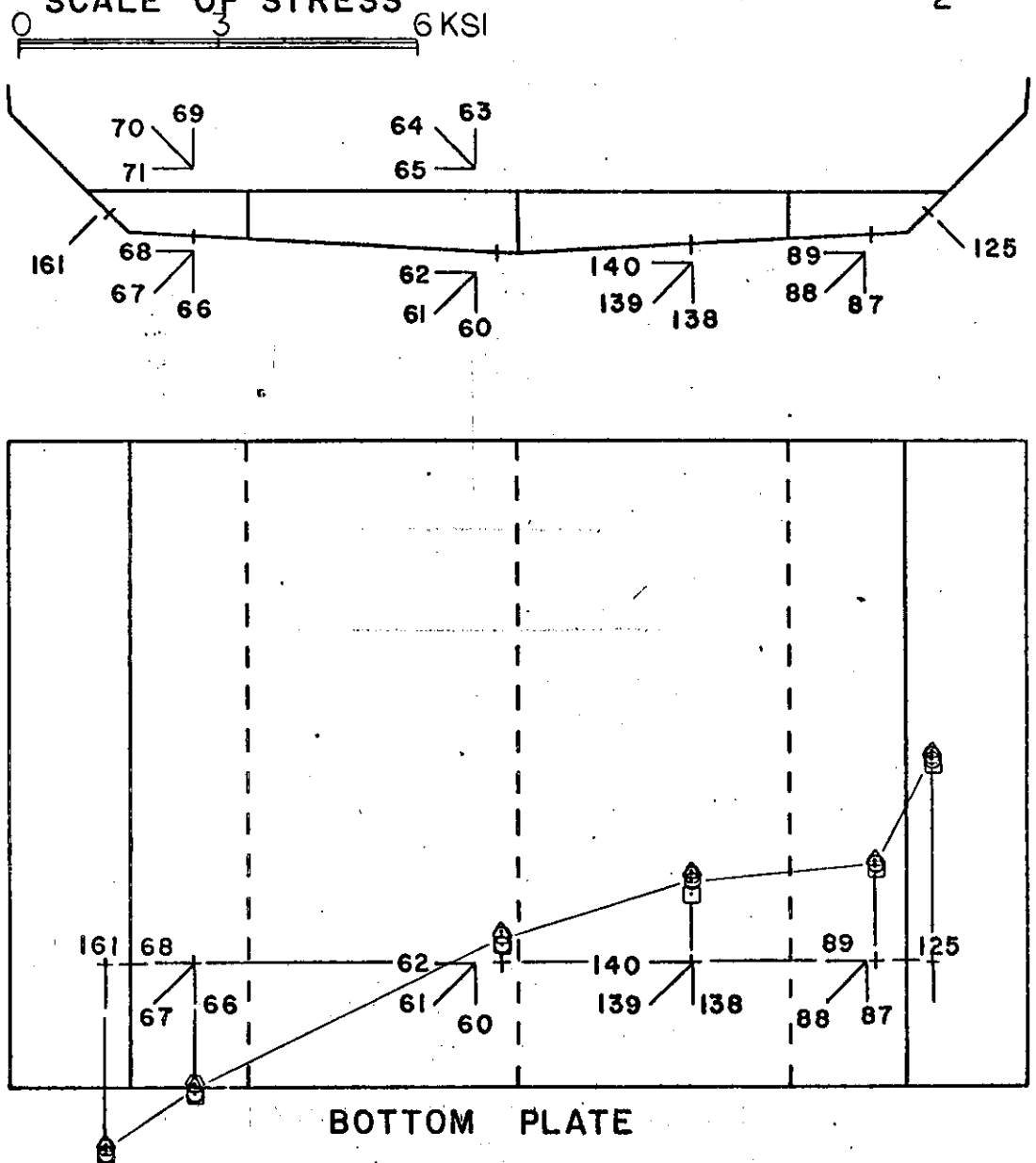


FIGURE 6c

SECTION BETWEEN FRAMES 178 & 194

LONGITUDINAL STRESSES DUE TO TORSION

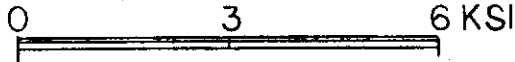
SINGLE GAGES - 2(250 BG)

NO. OF ROSETTES - 4(125 RA)

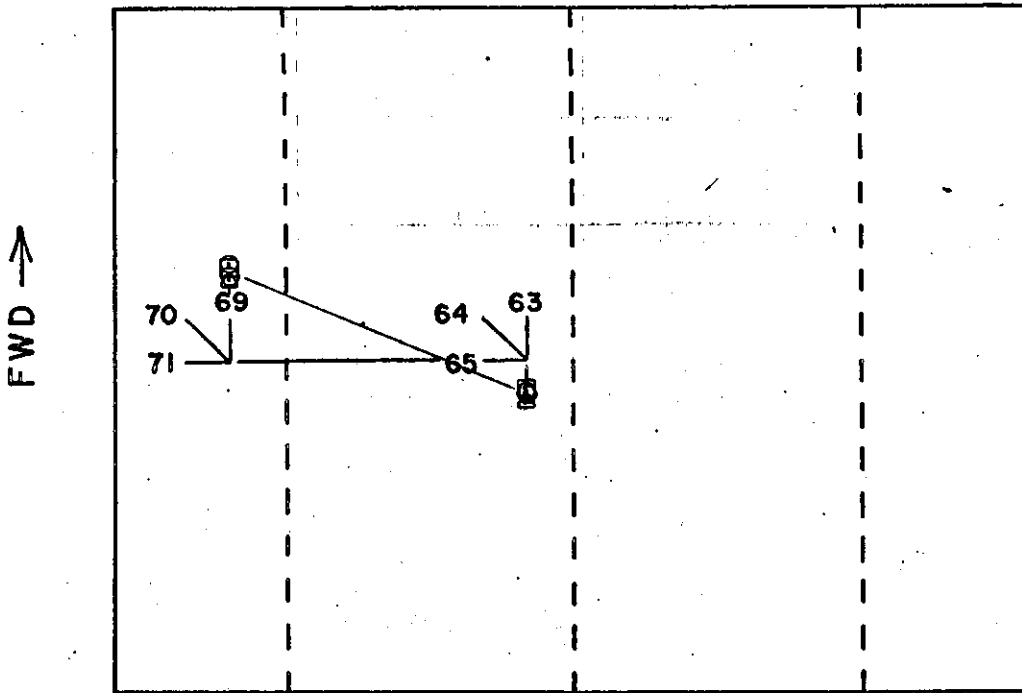
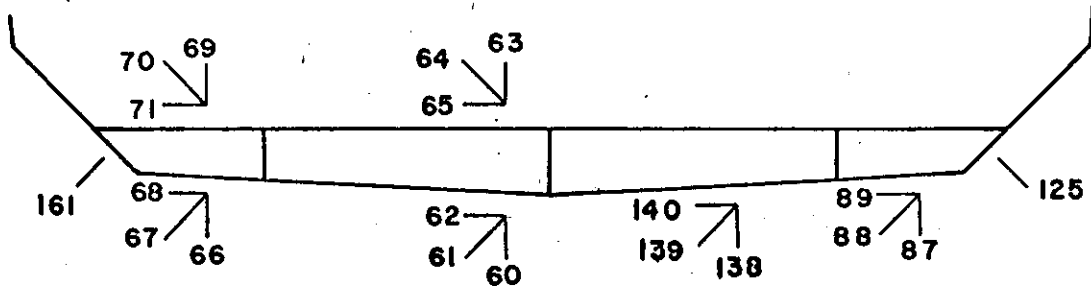
-12(250 RA)

DATE OF EXPERIMENT JULY & AUG, 1972

SCALE OF STRESS



- +LARGE
- △ -(-LARGE)
- 2(+1/2 LARGE)
- -2(-1/2 LARGE)



TANK TOP

FIGURE 6d

SECTION BETWEEN FRAMES 178 & 194

B-97

SHEAR STRESSES DUE TO TORSION

SINGLE GAGES - 2 (250 BG)
 NO. OF ROSETTES - 4 (125 RA)
 - 12 (250 RA)

DATE OF EXPERIMENT JULY/AUG, 1972

- +LARGE
- △ -(-LARGE)
- 2(+1/2 LARGE)
- -2(-1/2 LARGE)

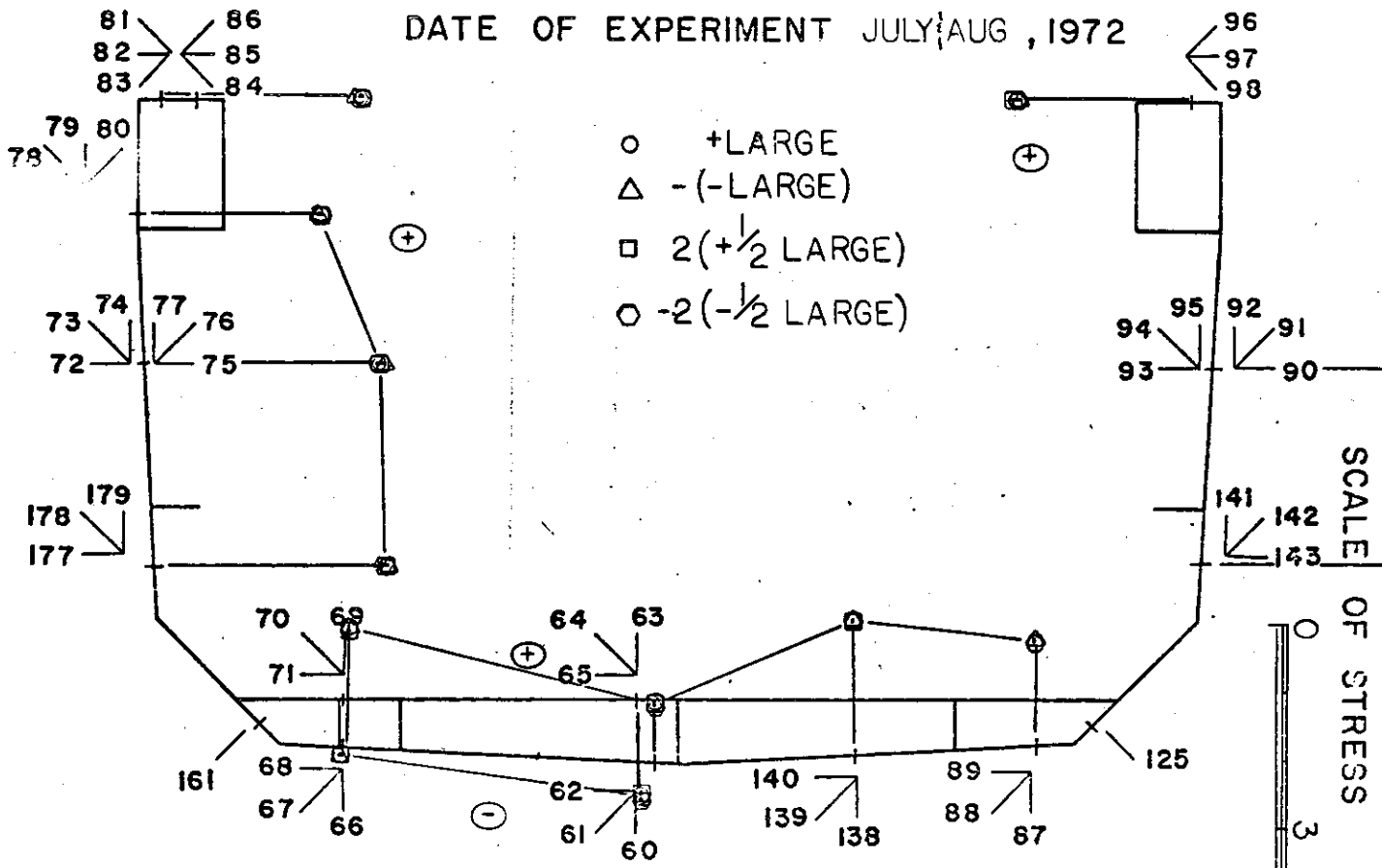
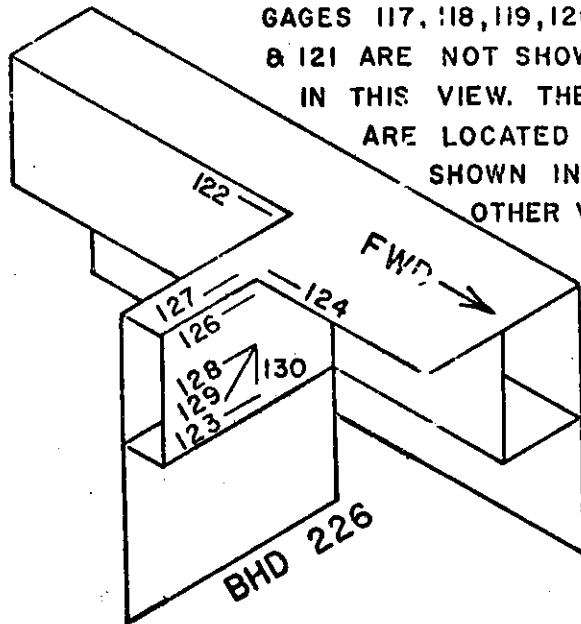


FIGURE 7

B-98
SECTION AT HATCH CORNER
PORT SIDE FRAME 226

LONGITUDINAL STRESSES DUE TO TORSION



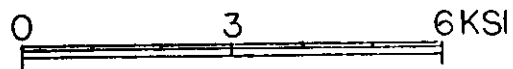
GAGES 117, 118, 119, 120, & 121 ARE NOT SHOWN IN THIS VIEW. THEY ARE LOCATED AS SHOWN IN OTHER VIEWS.

NO. OF ROSETTES
 - 1(250 RA)
 SINGLE GAGES
 - 10(250 BG)

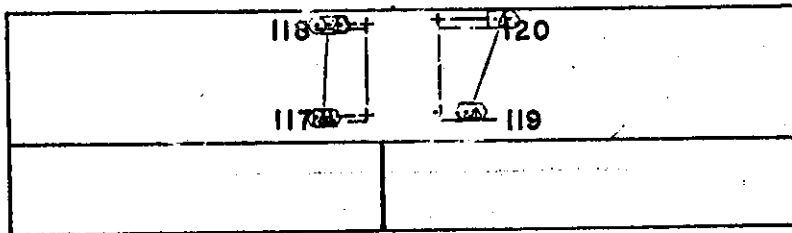
DATE OF EXPERIMENT

JULY & AUG, 1972

SCALE OF STRESS



- +LARGE
- △ -(-LARGE)
- 2(+1/2 LARGE)
- -2(-1/2 LARGE)



LOOKING OUTBOARD
 SHELL PLATE

→ FWD



BHD 226

LOOKING OUTBOARD
 TORSION BOX

FIGURE 8

SECTION 1" AFT OF FRAME 290

LONGITUDINAL STRESSES DUE TO TORSION

NO. OF ROSETTES - 2 (250 RA)

- 1 (125 RA)

SINGLE GAGES - 6 (250 BG)

DATE OF EXPERIMENT
JULY & AUG, 1972

SCALE OF STRESS

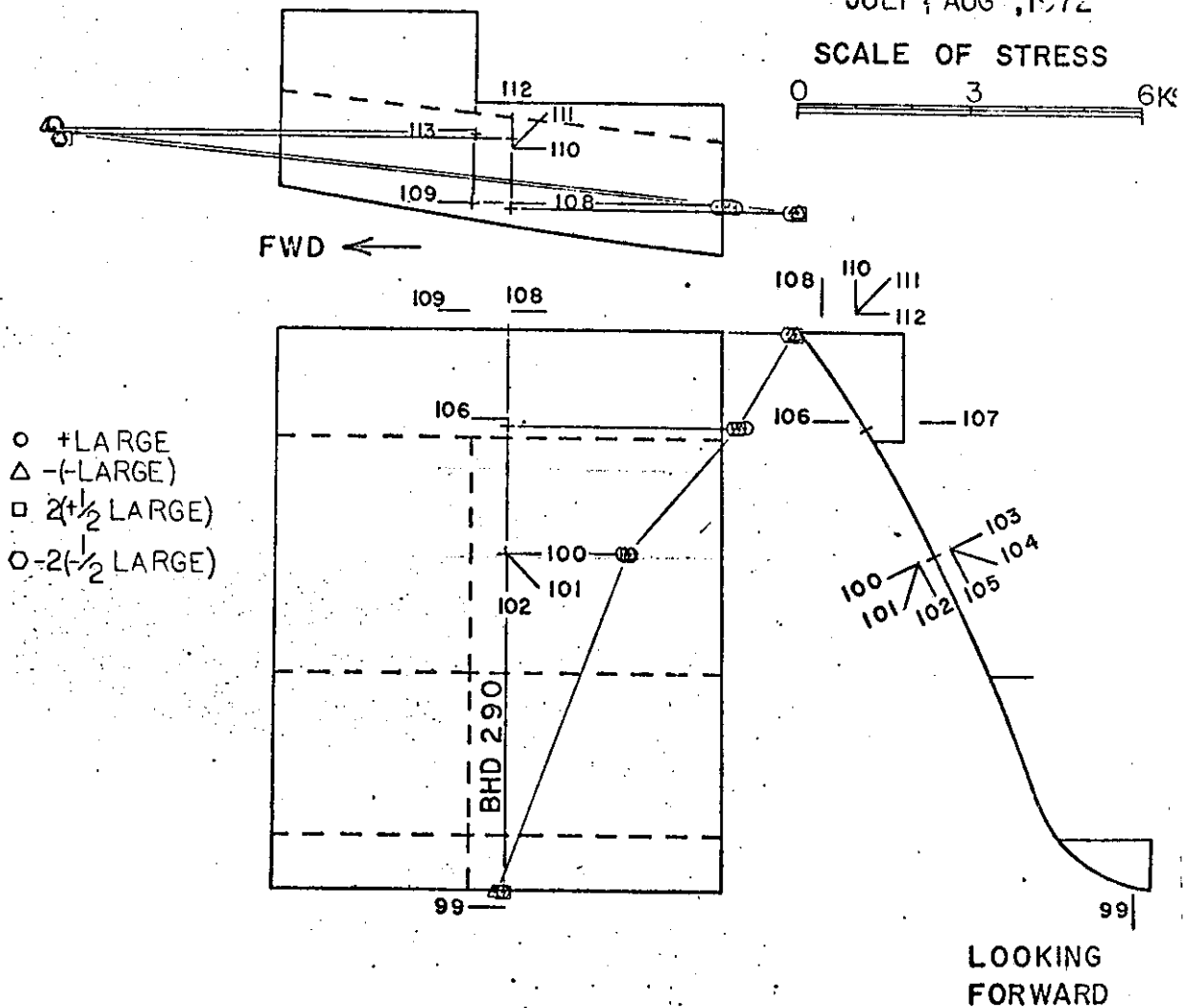


FIGURE 9

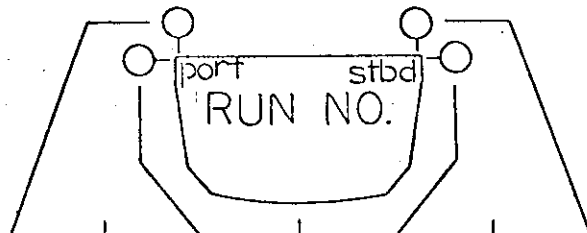
STRESSES (KSI)

FIG.	SAGE NUMBER	○ +LARGE	△ -LARGE	□ $2(+\frac{1}{2}LG)$	○ $-2(-\frac{1}{2}LG)$	
1	0	.14	.11	.28	.27	
	1	.46	.58	.56	.63	
	8	.17	.36	.18	.41	
	9	-.46	-.25	-.41	-.25	
	10	-.97	-.81	-.89	-.83	
	13	-.93	-.70	-.91	-.70	
	14	-1.75	-1.55	-1.67	-1.59	
	2	15	-.06	+.09	0.0	+.05
		16	-.41	-.21	-.35	-.22
		17	.10	.26	.16	.25
18		-.16	+.04	-.10	+.01	
26		-1.43	-1.22	-1.34	-1.15	
27		-.82	-.73	-.74	-.73	
3 (SHEAR)		149	.89	1.04	.86	.99
		152	1.11	1.14	1.17	1.13
	155	.43	.44	.44	.47	
	162	.74	.75	.74		
4a	29	5.52	5.47	5.54	5.42	
	30	2.00	2.30	2.06	2.25	
	36	.50	.72	.53	.72	
	38	-10.46	-10.74	-10.69	-10.76	
	39	-2.12		-1.94		
	42	-3.10	-3.08	-3.16	-2.98	
	43	-6.51	-6.02	-6.23	-6.13	

FIG.	SAGE NUMBER	○ +LARGE	△ -LARGE	□ $2(+\frac{1}{2}LG)$	○ $-2(-\frac{1}{2}LG)$	
4b	47	-5.32	-5.56	-5.26	-5.45	
	48	-1.99	-1.98	-1.97	-1.95	
	54	-.34	-.14	-.31	-.22	
	57	1.26	1.48	1.33	1.42	
	56	+11.06	+10.96	-12.11	+11.02	
	4c	29	5.52	5.47	5.54	5.42
28			.02	.15	.04	
47		-5.32	-5.56	-5.26	-5.45	
5	169	-1.44	-1.31	-1.37	-1.27	
	170	-3.90	-3.80	-3.87	-3.72	
	171	-1.23	-1.11	-1.19	-1.09	
	172	-1.33	-1.25	-1.29	-1.12	
	173	-2.95	-2.66	-2.88	-2.68	
	174	-1.97	-1.82	-1.95	-1.77	
	175	-3.34	-3.20	-3.30	-3.13	
	176	-5.64	-5.28	-5.62	-5.36	
	6a	66	1.98	1.85	1.96	1.84
		161	2.85	2.74	2.85	2.73
177		3.22	3.00	3.21	3.03	
72		2.75	2.32	2.56	2.38	
78		-1.35	-1.44	-1.32	-1.29	
81		-2.00	-1.84	-1.92	-1.71	
84		-3.36	-3.28	-3.23	-3.10	

FIG.	GAGE NUMBER	○ +LARGE	△ -LARGE	□ 2(+½ LG.)	○ -2(-½ LG.)
6b	87	-1.44	-1.51	-1.40	-1.46
	125	-3.06	-3.19	-2.97	-3.13
	141	-1.82	-1.95	-1.74	-1.93
	90	-3.16	-2.69	-2.93	-2.71
	96	2.06	2.20	2.04	2.21
6c	161	2.85	2.74	2.85	2.76
	66	1.98	1.85	1.98	1.84
	60	-.29	-.49	-.29	-.42
	138	-1.22	-1.37	-1.06	-1.34
	87	-1.44	-1.51	-1.40	-1.46
	125	-3.06	-3.19	-2.97	-3.13
6d	69	1.39	1.17	1.36	1.21
	63	-.43	-.56	-.42	-.51
7 (SHEAR)	81	2.95	2.84	2.95	2.91
	78	2.67	2.63	2.66	2.66
	72	3.41	3.53	3.42	3.46
	177	3.37	3.41	3.36	3.34
	66	1.81	1.79	1.77	1.75
	69	-.79	-.80	-.79	-.79
	60	.81	.82	.87	.82
	63	-1.41	-1.46	-1.39	-1.47
	138	2.00	2.01	1.97	1.98
	87	1.52	1.56	1.52	1.52
7 (cont'd)	141	-2.83	-2.88	-2.83	-2.84
	90	-3.81	-3.60	-3.76	-3.63
	96	2.55	2.64	2.54	2.58
8	117	-.72	-.59	-.66	-.52
	118	-.72	-.38	-.57	-.40
	119	.34	.45	.36	.50
	120		.96	.80	1.00
	121	1.27	1.36	1.30	1.42
	122	2.21	2.29	2.20	2.48
9	99	-.02	-.19	0.0	-.08
	100	-2.17	-2.17	-2.13	-2.02
	106	-4.16	-4.04	-4.01	-3.93
	108	-5.01	-5.05	-5.02	-4.88
	109	-4.59	-4.44	-4.48	-4.30
	110	9.95	7.93	7.89	7.94
	113	7.40	7.52	7.40	7.39

TORSION
JULY & AUG, 1972



BHD.

MODEL DEFLECTION FROM THE
NO-LOAD CONDITION, IN INCHES.

- 1 +LARGE →
- 2 - (-LARGE) →
- 3 2 (+1/2 LARGE) →
- 4 -2 (-1/2 LARGE) →

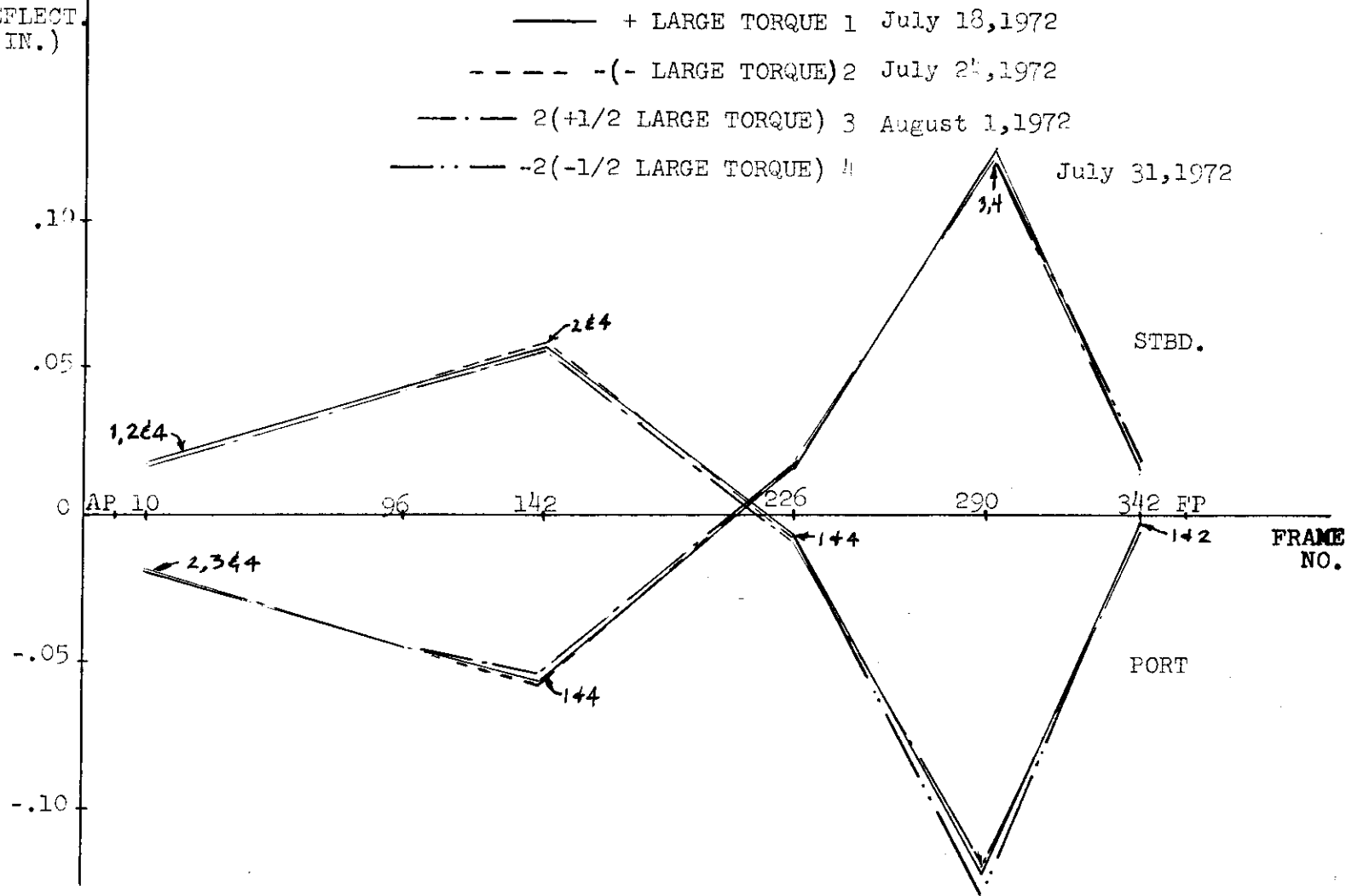
342	+0.042 +0.046 +0.040 +0.046	-0.003 -0.003 -0.006 -0.002	+0.016 +0.014 +0.016 +0.018	-0.042 -0.042 -0.044 -0.044
290	+0.094 +0.113 +0.100 +0.100	-0.122 <u>+0.031</u> 240 -0.120 -0.130	+0.125 <u>+0.020</u> 240 +0.122 +0.122	-0.112 -0.110 -0.112 -0.114
226	+0.078 +0.093 +0.074 +0.092	-0.012 -0.013 -0.014 -0.012	+0.016 +0.017 +0.018 +0.018	-0.092 -0.086 -0.092 -0.092
142	+0.016 +0.032 +0.014 +0.034	+0.057 +0.058 +0.056 +0.058	-0.056 -0.057 -0.054 -0.056	-0.032 -0.025 -0.032 -0.032
96	+0.005 +0.022 +0.002 +0.026	+0.044 +0.044 +0.042 +0.044	<u>+0.057</u> 240 -0.044 -0.044 -0.044	-0.021 -0.012 -0.012 -0.016
10	-0.003 +0.011 -0.004 +0.014	+0.012 +0.018 +0.016 +0.018	-0.019 -0.018 -0.018 -0.018	-0.007 +0.001 -0.008 -0.002

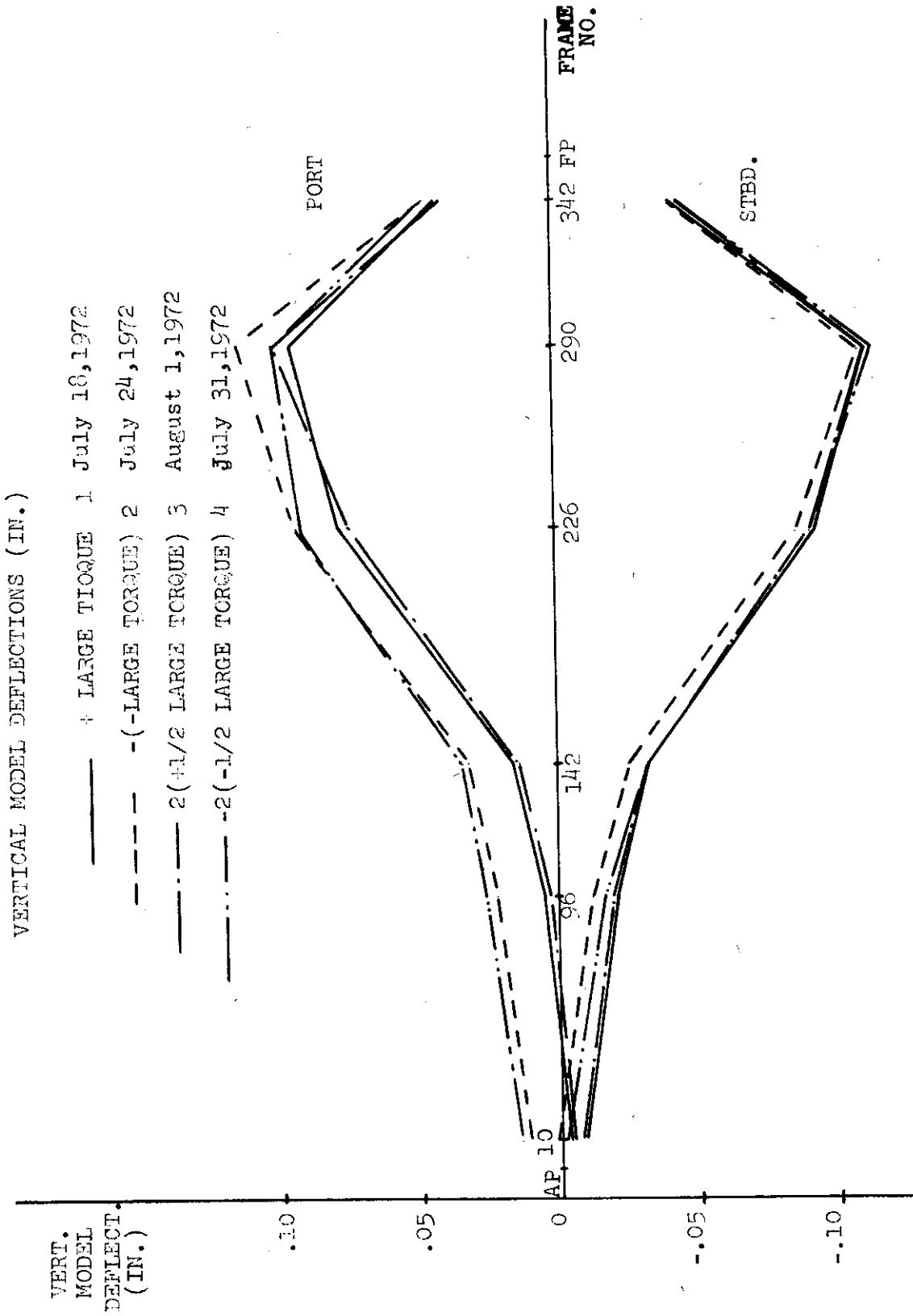
EQUIVALENT DEFLECTIONS OF
FULL SCALE SHIP, IN INCHES.

342	+2.10 +2.30 +2.00 +2.30	-0.15 -0.15 -0.30 -0.10	+0.80 +0.70 +0.80 +0.90	-2.10 -2.10 -2.20 -2.20
290	+4.70 +5.65 +5.00 +5.00	-6.10 +1.55 -6.00 -6.50	+6.25 +1.00 +6.10 +6.10	-5.60 -5.50 -5.60 -5.70
226	+3.90 +4.65 +3.70 +4.60	-0.60 -0.65 -0.70 -0.60	+0.80 +0.85 +0.90 +0.90	-4.65 -4.30 -4.60 -4.60
142	+0.80 +1.60 +0.70 +1.70	+2.85 +2.90 +2.80 +2.90	-2.80 -2.85 -2.70 -2.80	-1.60 -1.25 -1.60 -1.60
96	+0.25 +1.10 +0.10 +1.30	+2.20 +2.20 +2.10 +2.20	+2.85 -2.20 -2.20 -2.20	-1.05 -0.60 -1.00 -0.60
10	-0.15 +0.55 -0.20 +0.70	+0.90 +0.90 +0.80 +0.90	-0.95 -0.90 -0.90 -0.90	-0.45 +0.55 -0.40 -0.10

HORZ.
MODEL
DEFLECT.
(IN.)

HORIZONTAL MODEL DEFLECTIONS (IN.)

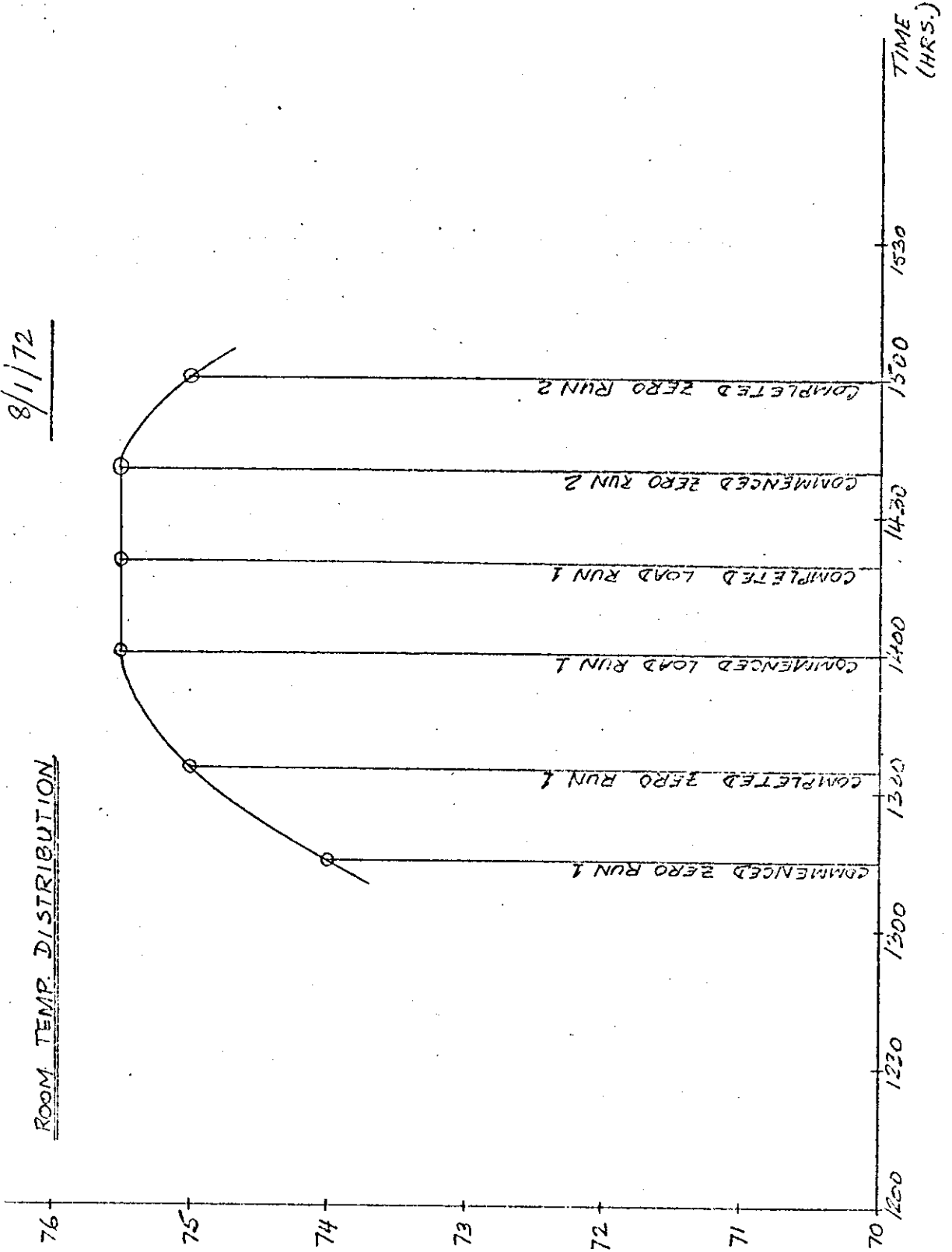




(+) 1/2 (LARGE TORQUE)

8/1/72

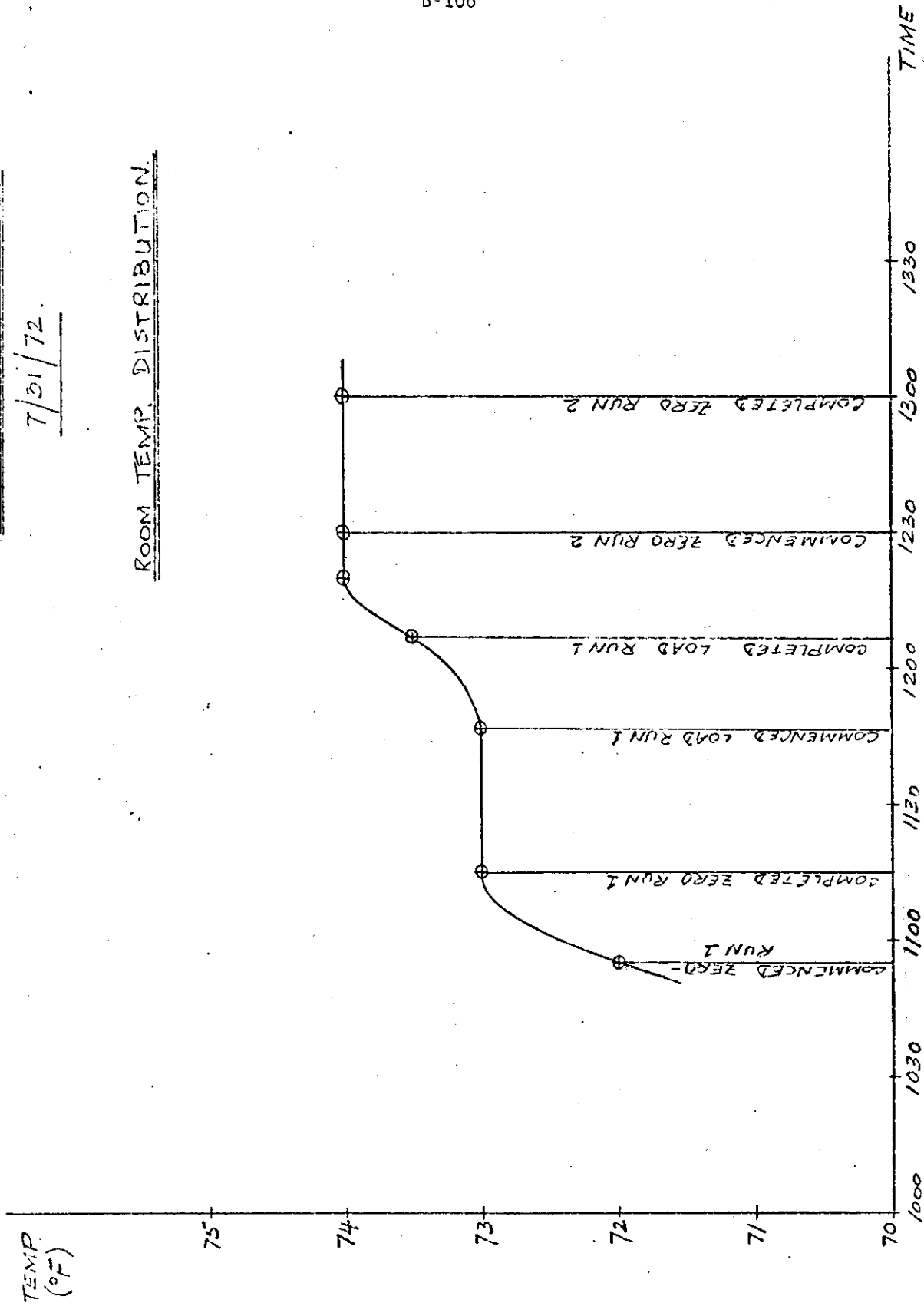
ROOM TEMP DISTRIBUTION



(-) 1/2 (LARGE TORQUE)

7/31/72.

ROOM TEMP. DISTRIBUTION.



LATERAL BENDING + TORSION

1 $[(+LONG.,+LAT.,+TOR.) - (+LONG.,-LAT.,-TOR.)] / 2$

OCTOBER 30 † NOVEMBER 17, 1972

2 +LATERAL BENDING, +TORSION

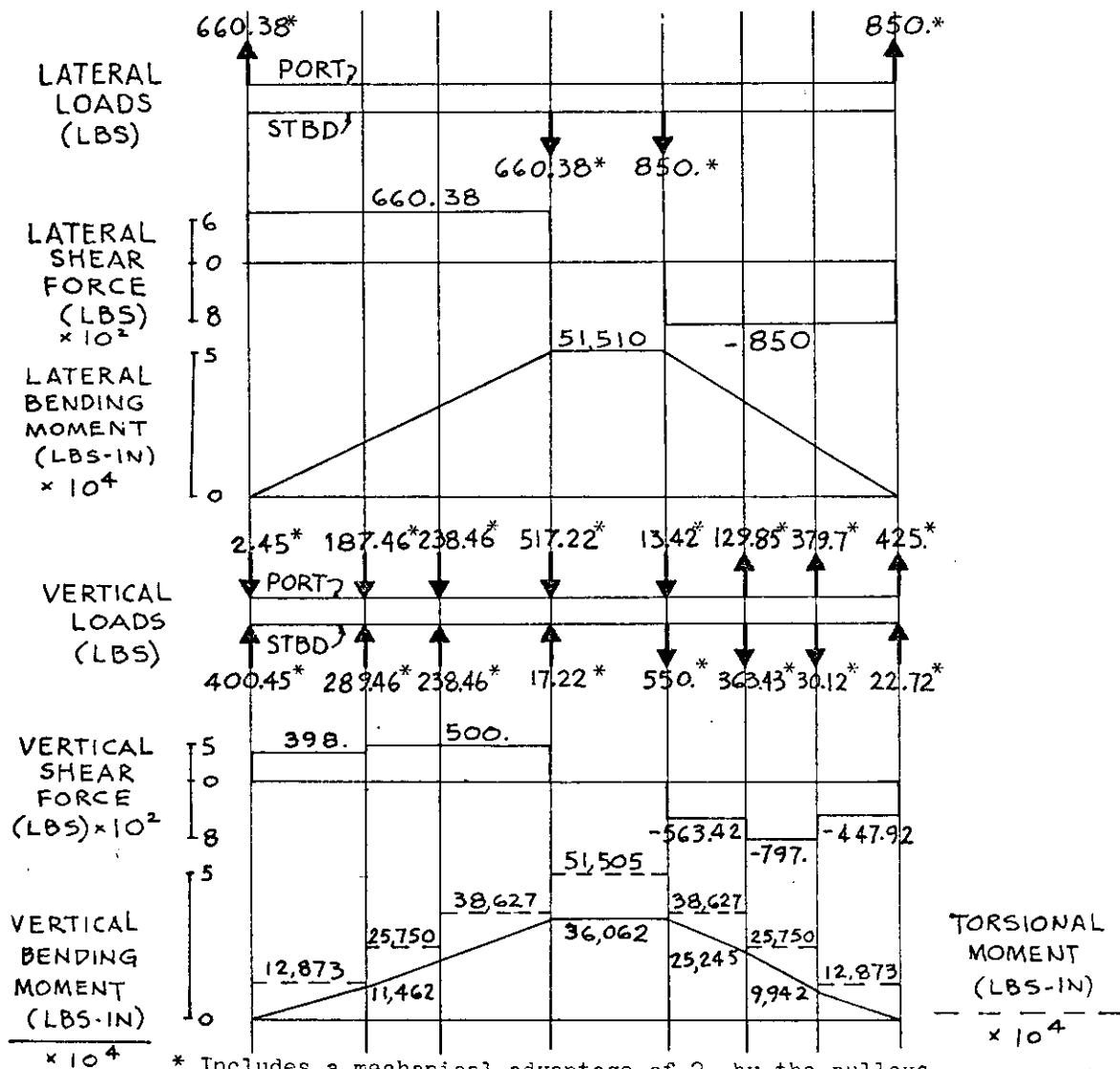
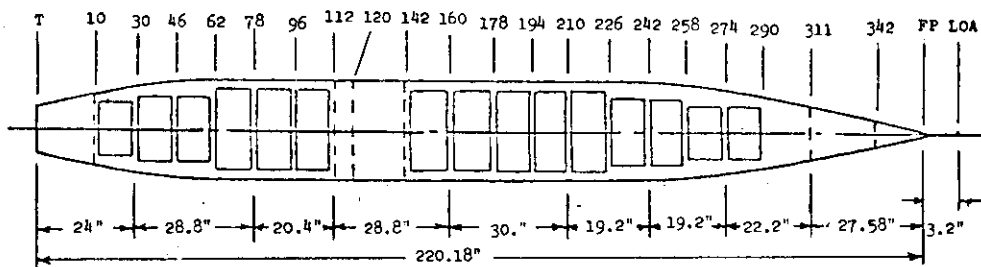
OCTOBER 5, 1972

3 +LATERAL BENDING, +TORSION

OCTOBER 11, 1972

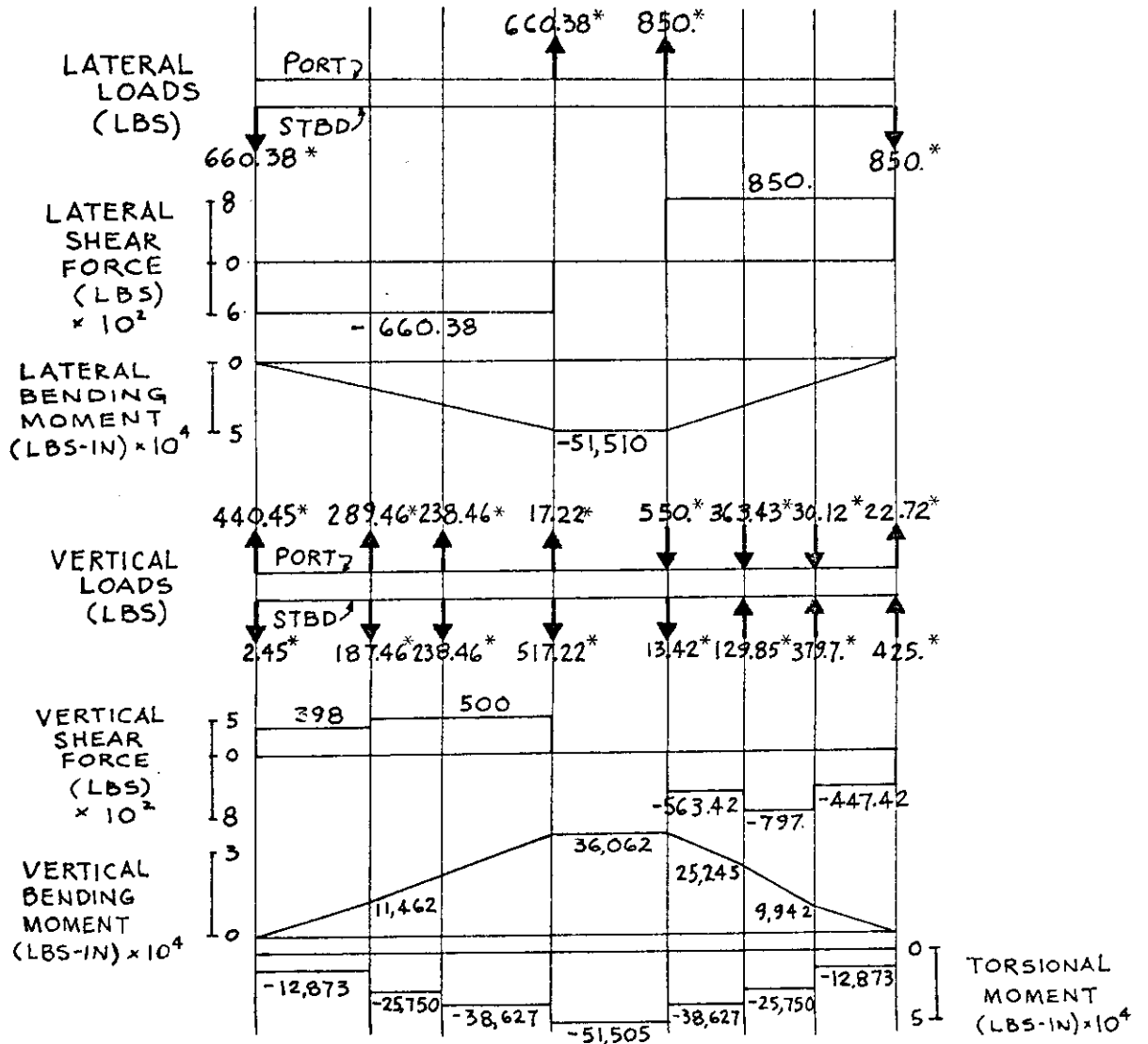
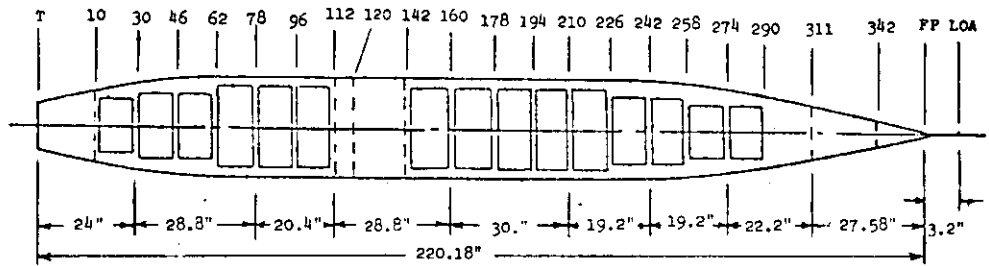
4 -(-LATERAL BENDING, -TORSION)

SEPTEMBER 25, 1972



* Includes a mechanical advantage of 2, by the pulleys.

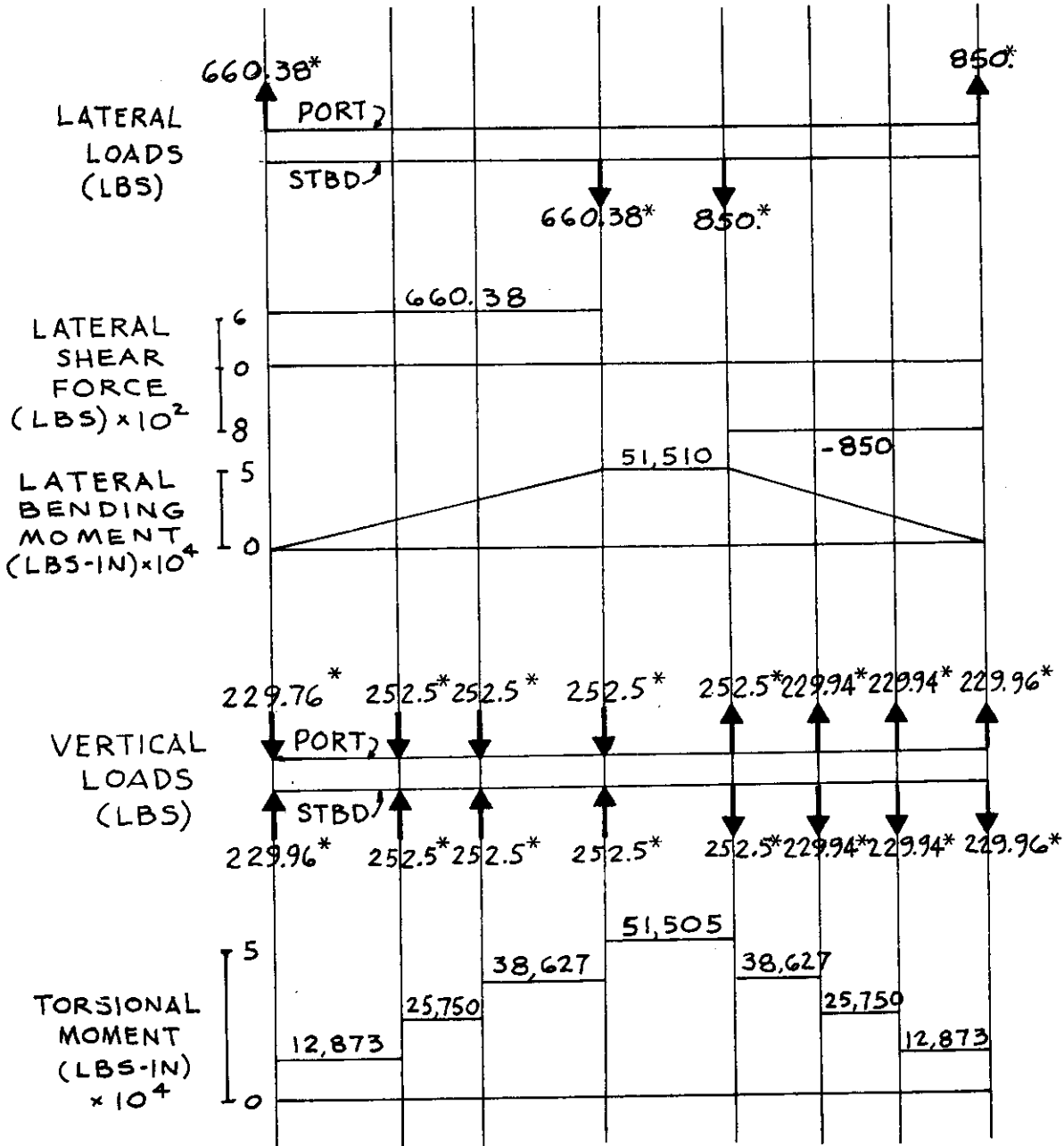
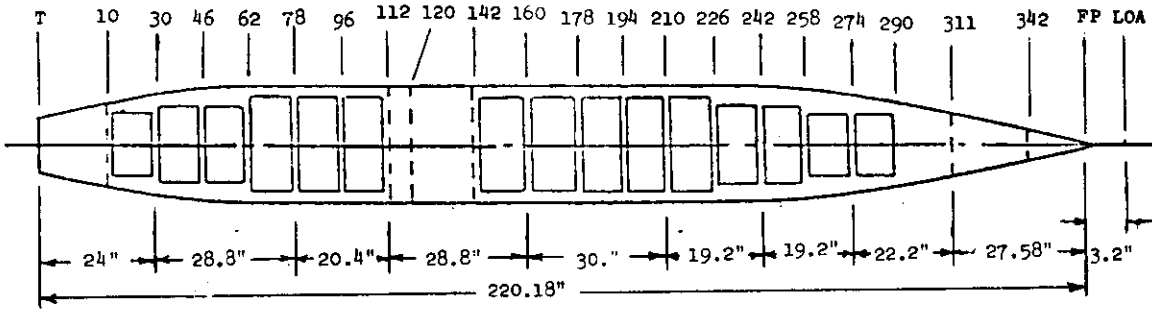
Date of Experiment 30 October 1972



* Includes a mechanical advantage of 2, by the pulleys.

Date of Experiment 17 November 1972

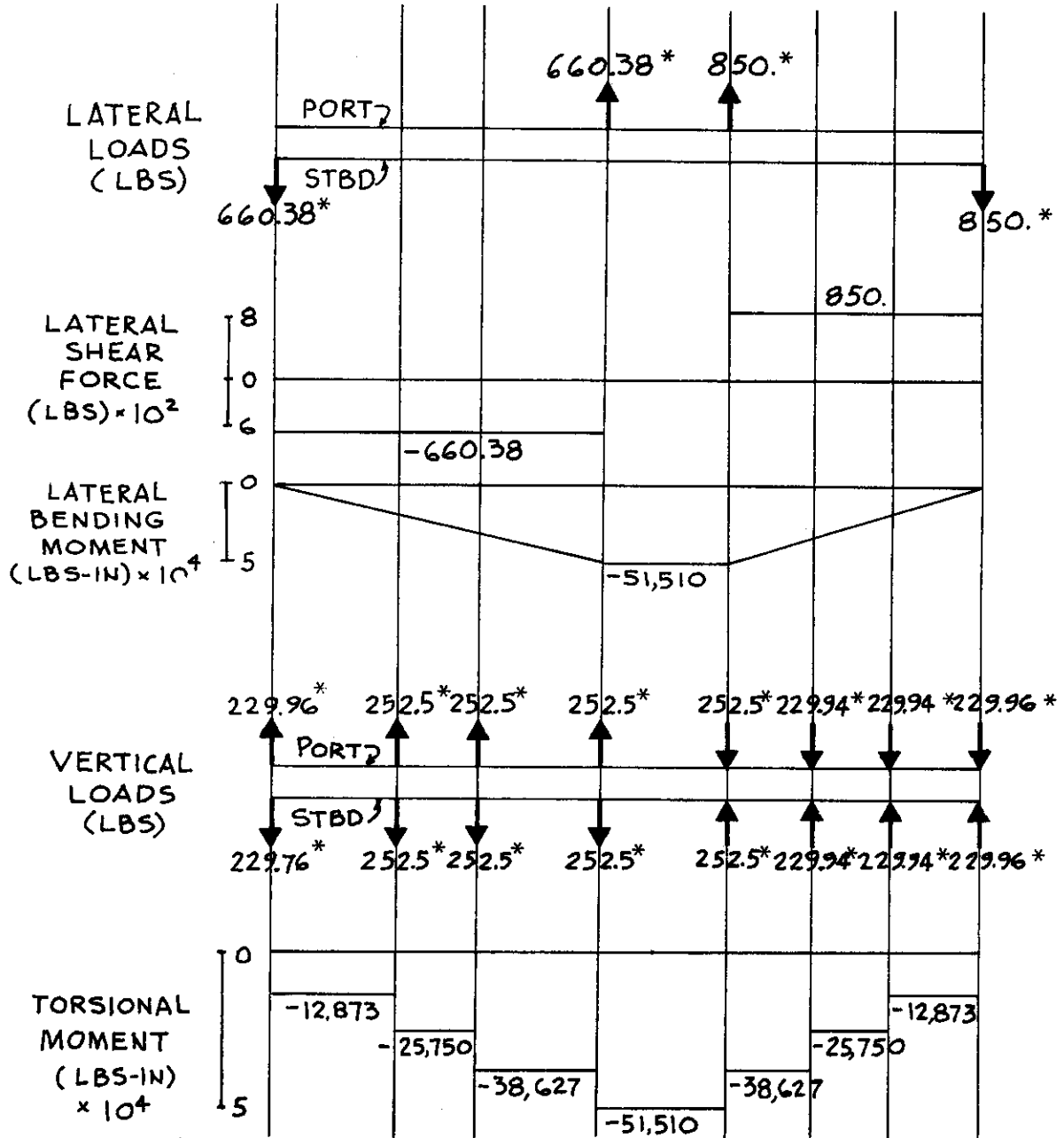
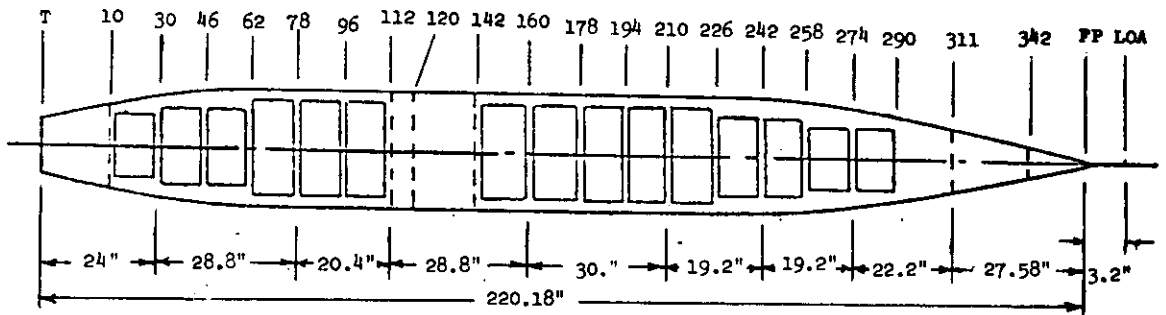
B-110



* Includes a mechanical advantage of 2, by the pulleys.

Date of Experiment 5 & 11 October 1972

B-111



* Includes a mechanical advantage of 2, by the pulleys.

Date of Experiment 25 September 1972

SECTION 2" FORWARD OF FRAME 10

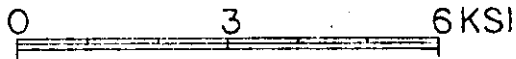
LONGITUDINAL STRESSES DUE TO LAT. B.M. + TORSION

NO. OF ROSETTES - 3 (125 RA)

SINGLE GAGES - 6 (250 BG)

DATE OF EXPERIMENT , 1972

SCALE OF STRESS



- 1
- 2
- 3
- △ 4

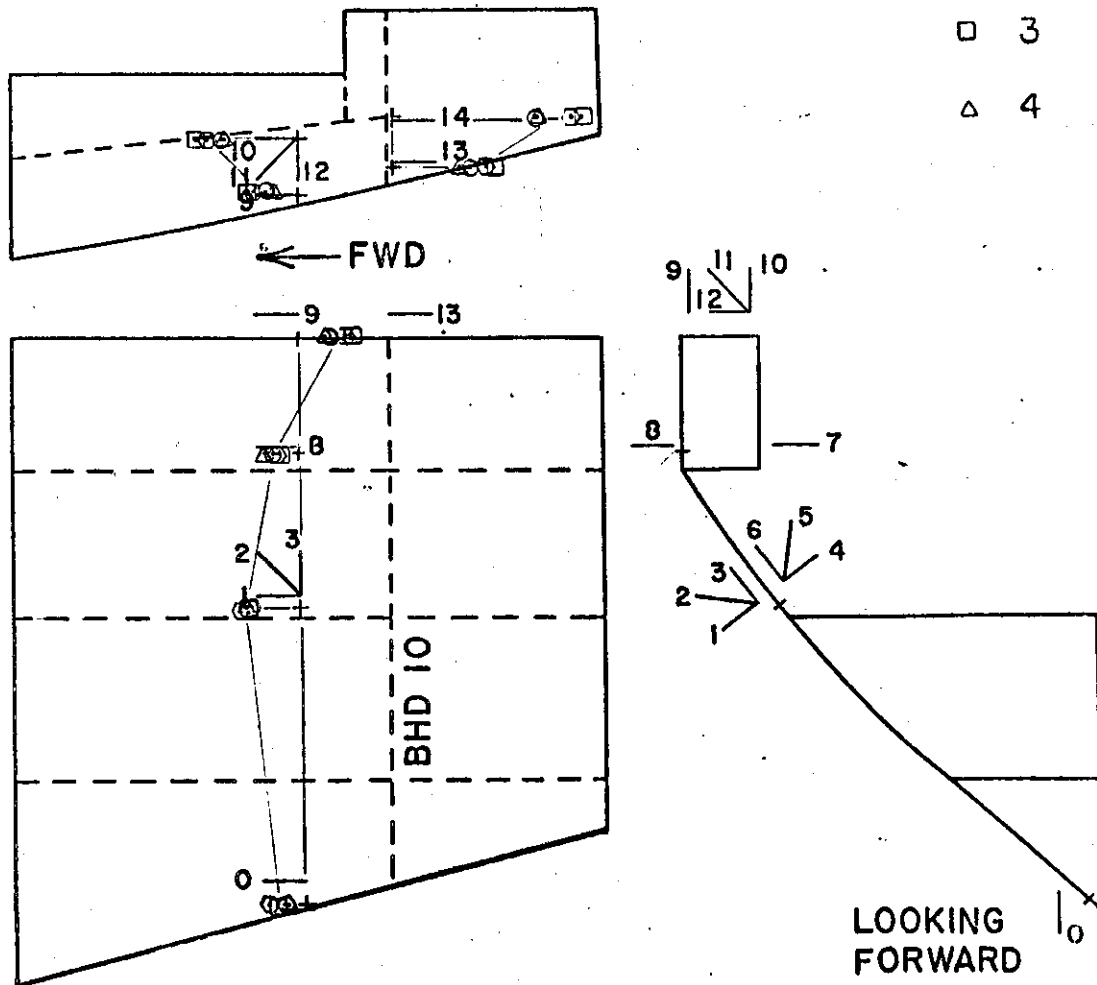


FIGURE 1

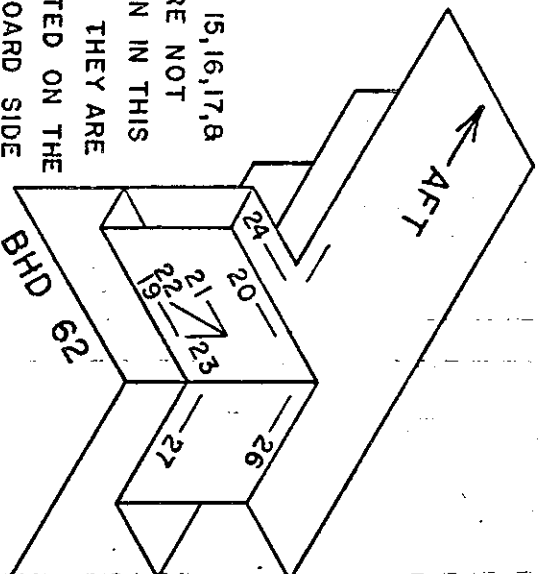
SECTION AT HATCH CORNER

B-113

PORT SIDE FRAME 62

LONGITUDINAL STRESSES DUE TO LAT. B.M. + TORSION

GAGE 15,16,17,8
18 ARE NOT
SHOWN IN THIS
VIEW, THEY ARE
LOCATED ON THE
OUTBOARD SIDE
OF THE SHELL PLATE.



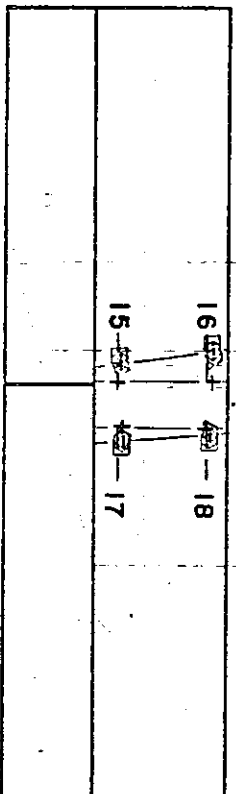
NO. OF ROSETTES
-1(250 RA)
SINGLE GAGES
-10(250 BG)

DATE OF EXPERIMENT
.1972

SCALE OF STRESS

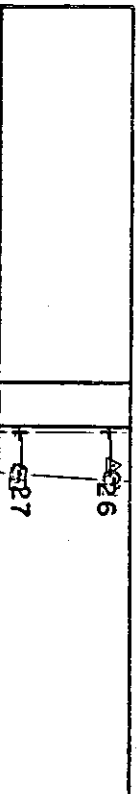


- 1
- 2
- 3
- △ 4



LOOKING OUTBOARD
SHELL PLATE

FWD →



LOOKING OUTBOARD
TORSION BOX

FIGURE 2

SECTION 5.4" FORWARD OF FRAME 78

SHEAR STRESS DUE TO LAT. B.M. + TORSION

NO. OF ROSETTES - 2(125 RA)

- 4(250 RA)

SINGLE GAGES - 1(250 BG)

DATE OF EXPERIMENT , 1972

SCALE OF STRESS

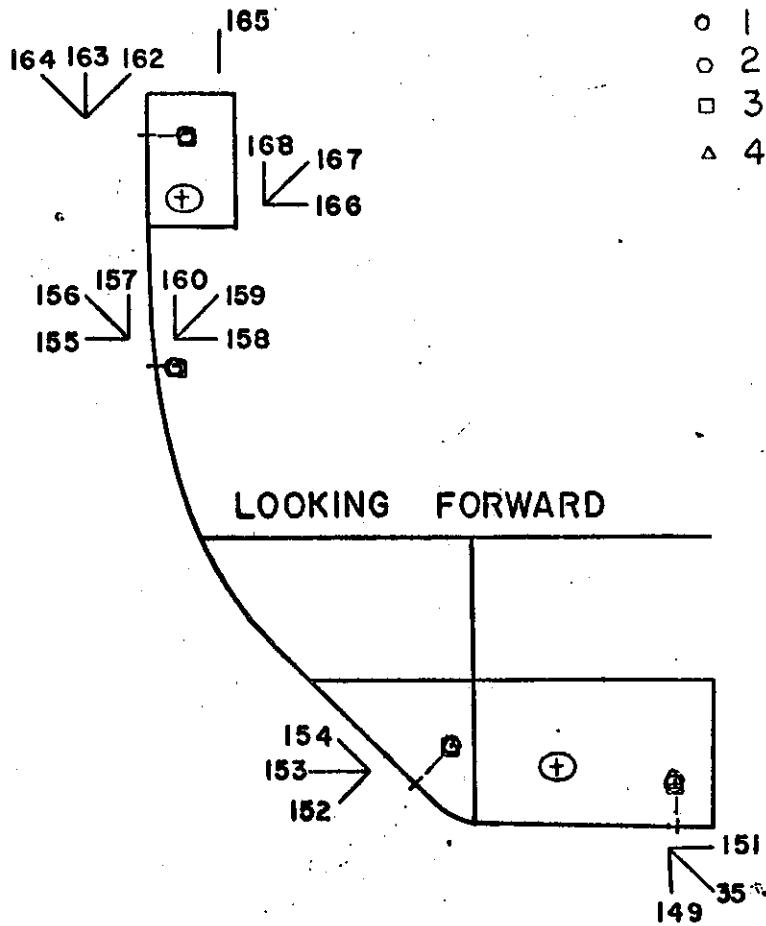
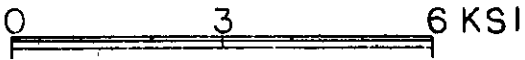


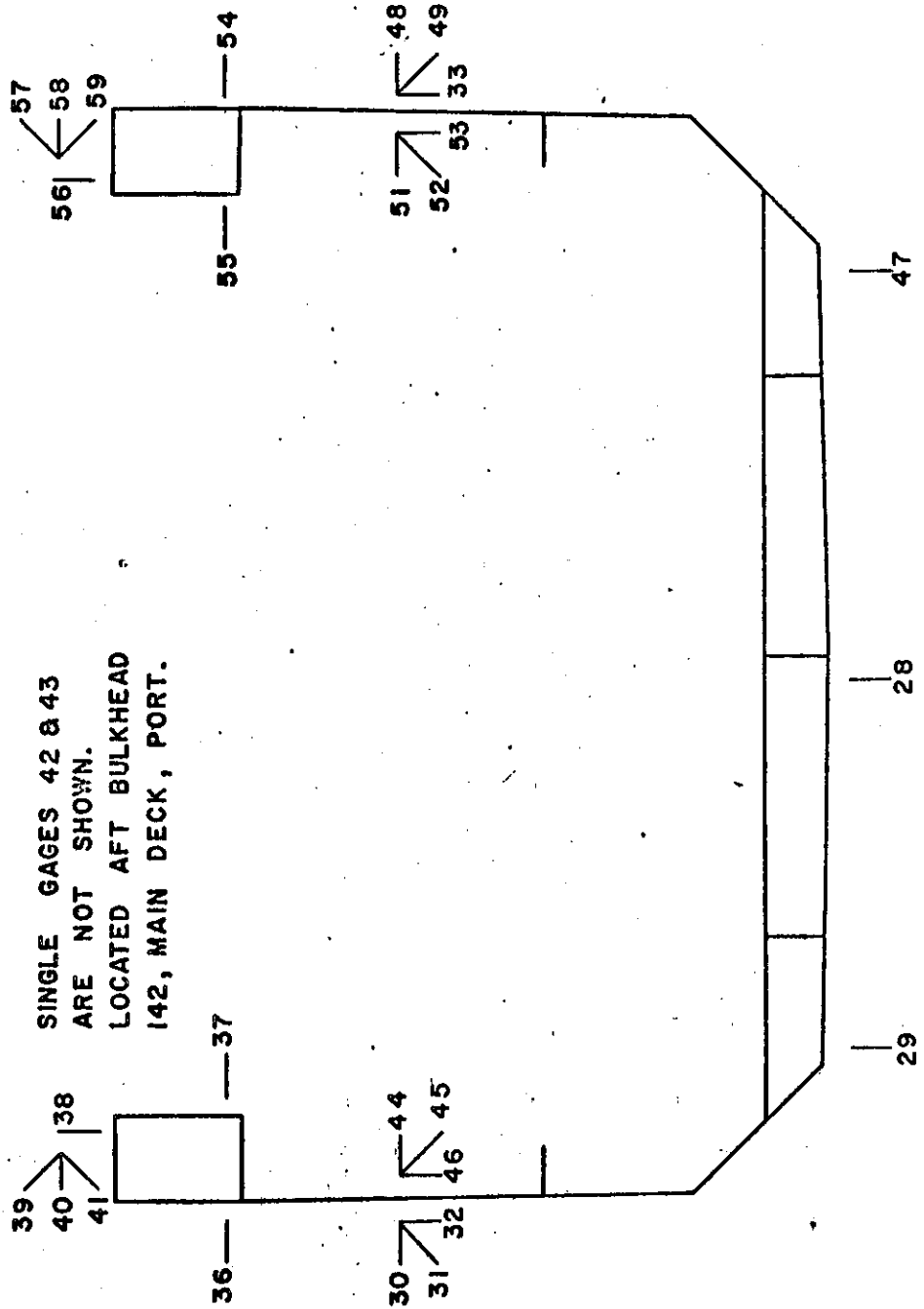
FIGURE 3

SECTION 2" FORWARD OF FRAME 142

LOCATION OF GAGES

NO. OF ROSETTES - 4 (250 RA)
- 2 (125 RA)
SINGLE GAGES - 9 (250 BG)

SINGLE GAGES 42 & 43
ARE NOT SHOWN.
LOCATED AFT BULKHEAD
142, MAIN DECK, PORT.



LOOKING FORWARD

FIGURE 4

SECTION 2" FORWARD OF FRAME 142

LONGITUDINAL STRESSES DUE TO

NO. OF ROSETTES - 4 (125 RA)
 - 2 (250 RA)

SINGLE GAGES - 9 (250 BG)

DATE OF EXPERIMENT , 1972

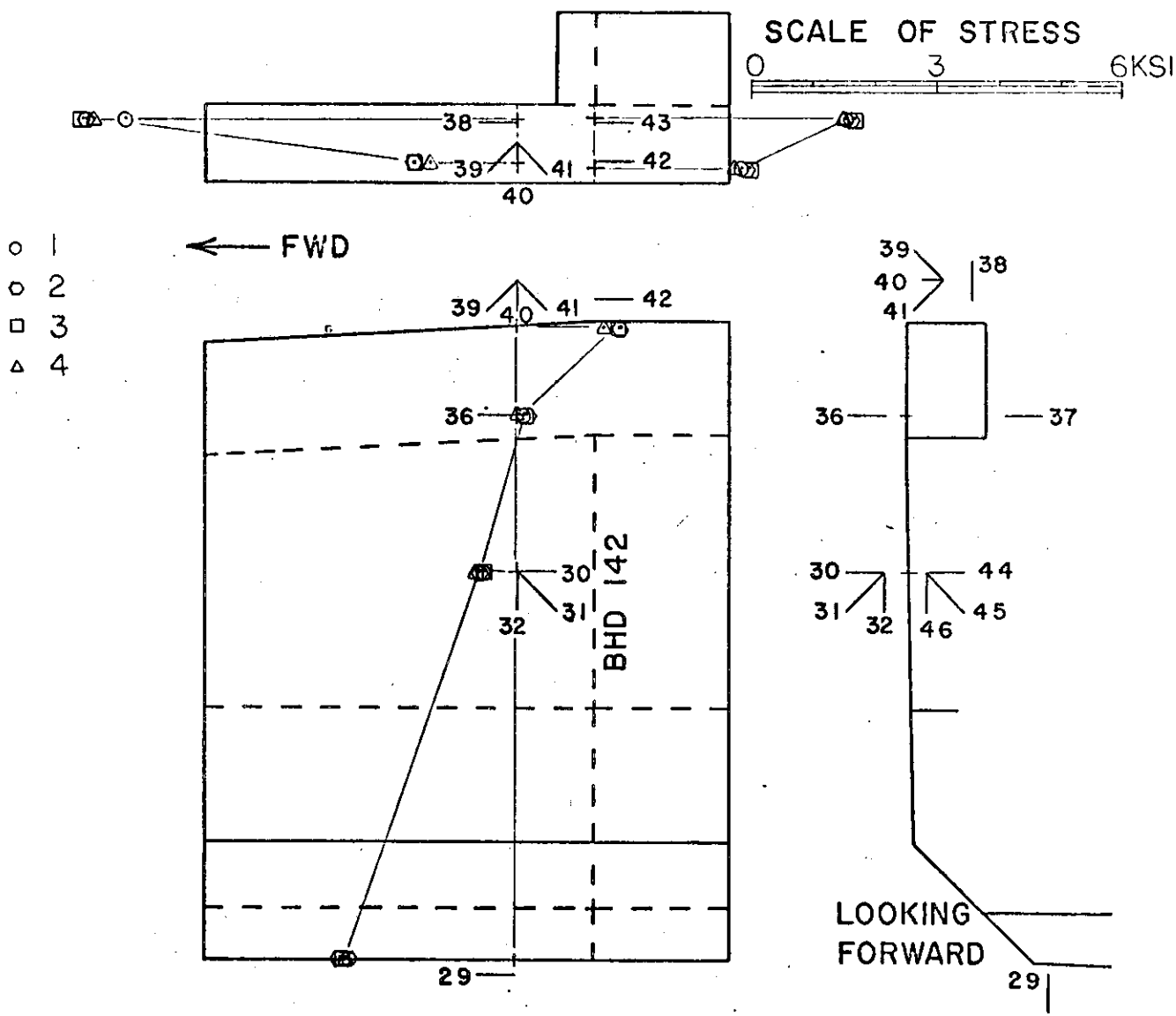


FIGURE 4a

SECTION 2" FORWARD OF FRAME 142

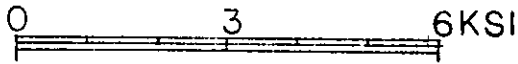
LONGITUDINAL STRESSES DUE TO LAT. B.M. + TORSION

NO. OF ROSETTES - 4 (I25 RA)
 - 2 (250 RA)

SINGLE GAGES - 9 (250 BG)

DATE OF EXPERIMENT , 1972

SCALE OF STRESS



- 1
- 2
- 3
- △ 4

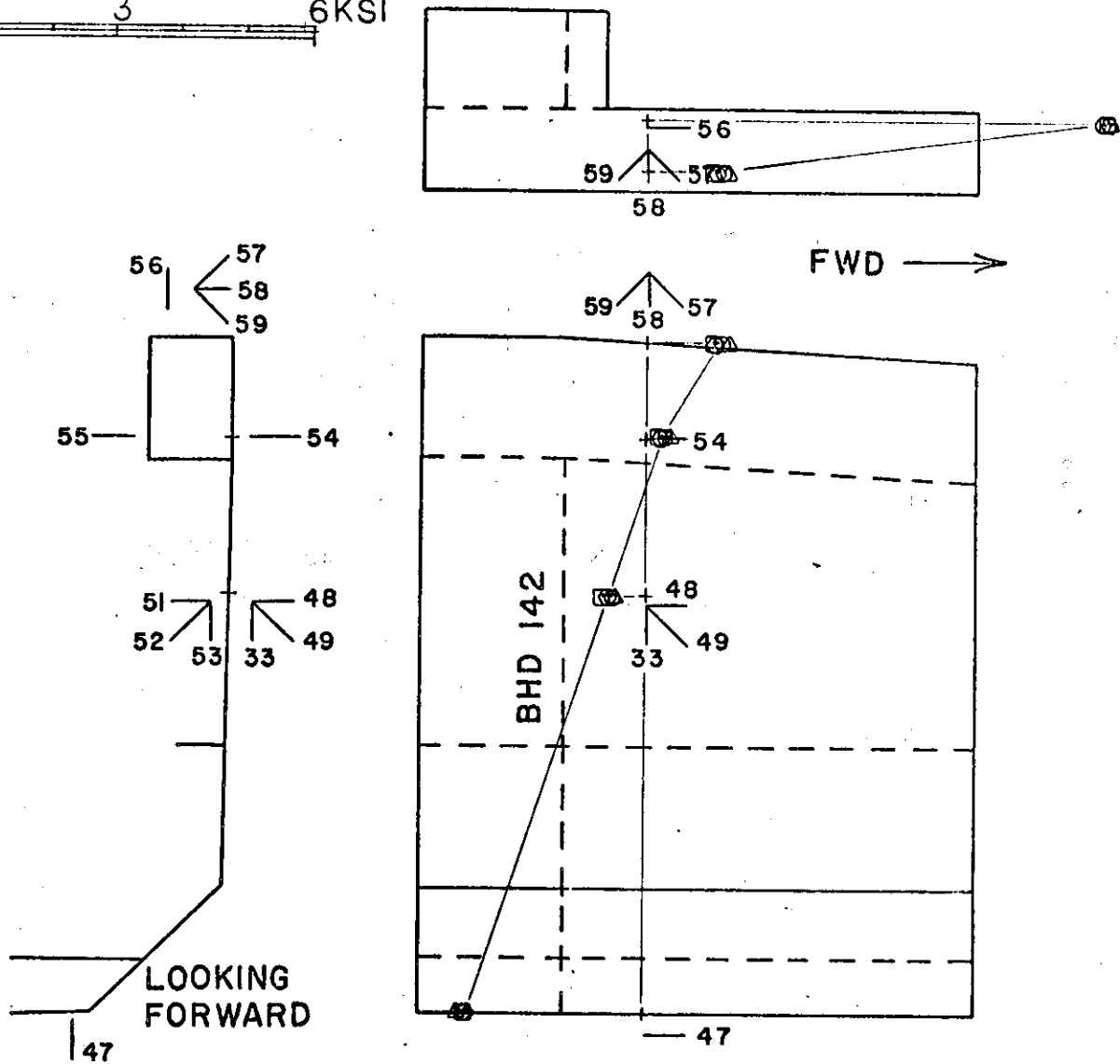


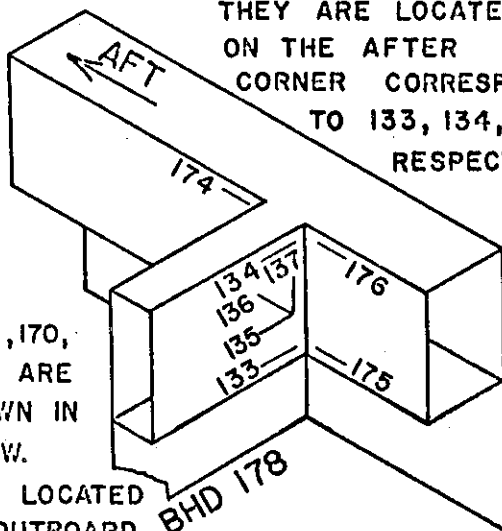
FIGURE 4b

SECTION AT HATCH CORNER PORT SIDE FRAME 178

LONGITUDINAL STRESSES DUE TO
GAGES 131, 132, & 173
ARE NOT SHOWN.

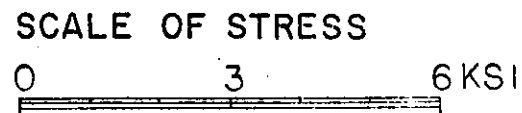
THEY ARE LOCATED ON THE AFT CORNER CORRESPONDING TO 133, 134, & 175 RESPECTIVELY.

NO. OF ROSETTES
-1(250 RA)
SINGLE GAGES
-12(250 BG)

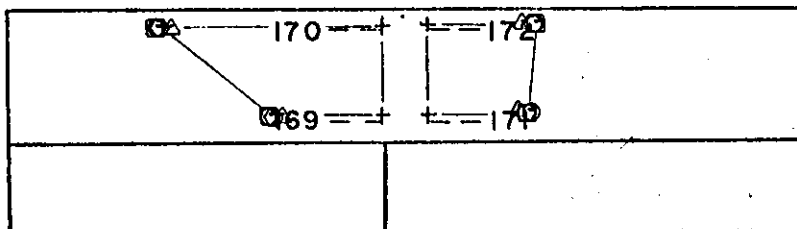


GAGES 169, 170, 171, & 172 ARE NOT SHOWN IN THIS VIEW. THEY ARE LOCATED ON THE OUTBOARD SIDE OF THE SHELL PLATE.

DATE OF EXPERIMENT
,1972

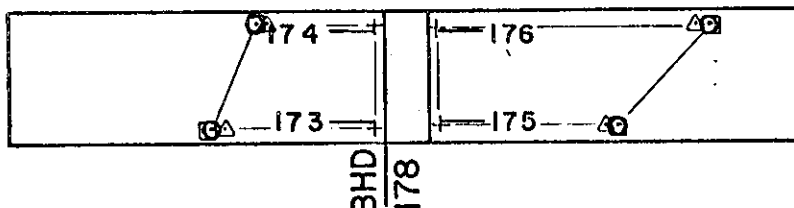


- 1
- 2
- 3
- △ 4



LOOKING OUTBOARD
SHELL PLATE

→ FWD



LOOKING OUTBOARD
TORSION BOX

→ FWD

FIGURE 5

SECTION BETWEEN FRAMES 178 & 194

LOCATION OF GAGES

NO. OF SINGLE GAGE- 2 (250 BG)
NO. OF ROSETTES - 4 (125 RA)
- 12 (250 RA)

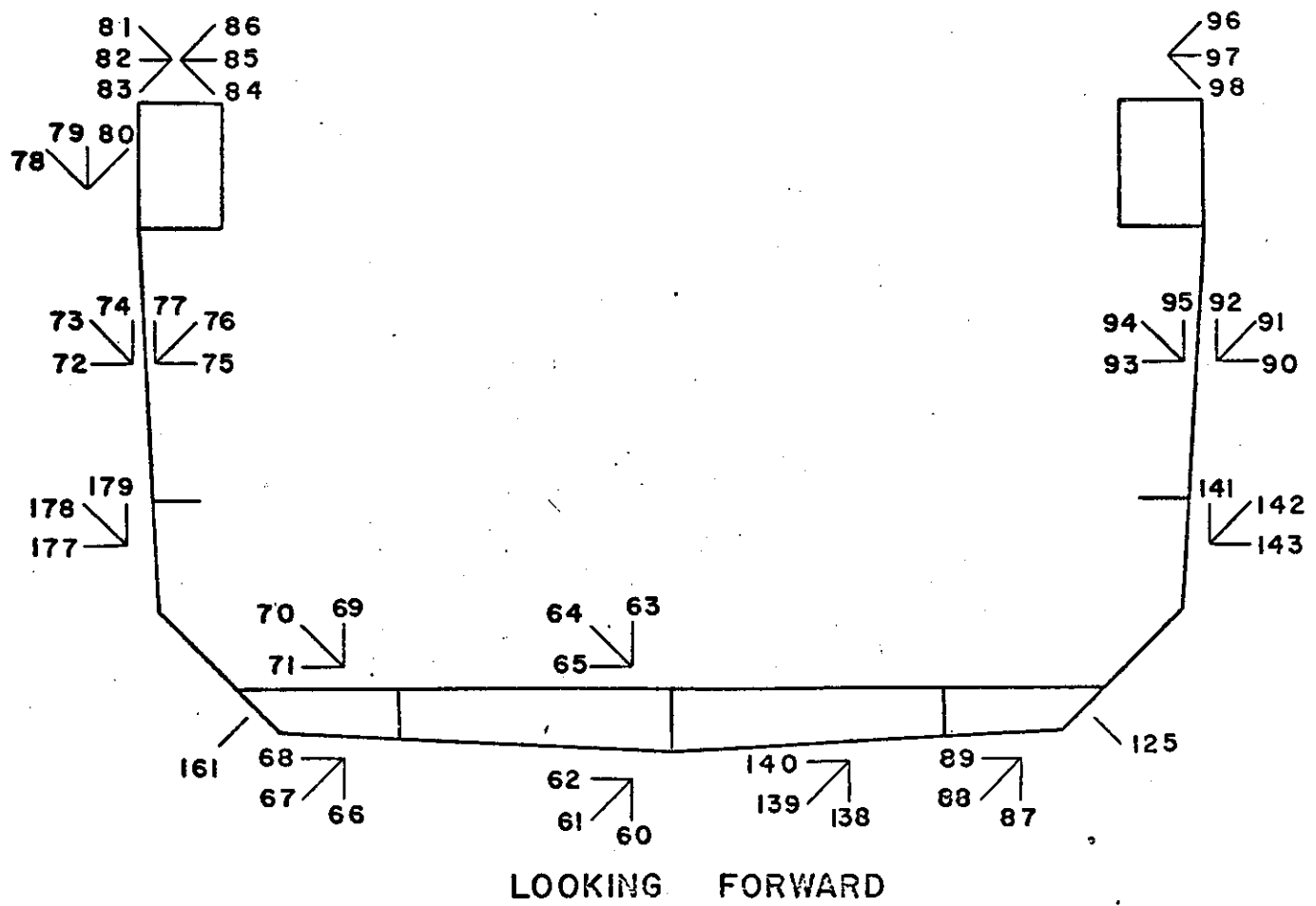


FIGURE 6

SECTION BETWEEN FRAMES 178 & 194

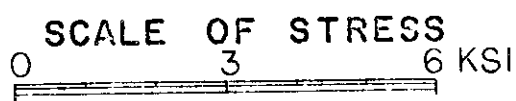
LONGITUDINAL STRESSES DUE TO LAT. BM. + TORSION

SINGLE GAGES - 2(250 BG)

NO. OF ROSETTES - 4(125 RA)

- 12(250 RA)

DATE OF EXPERIMENT , 1972



- 1
- 2
- 3
- △ 4

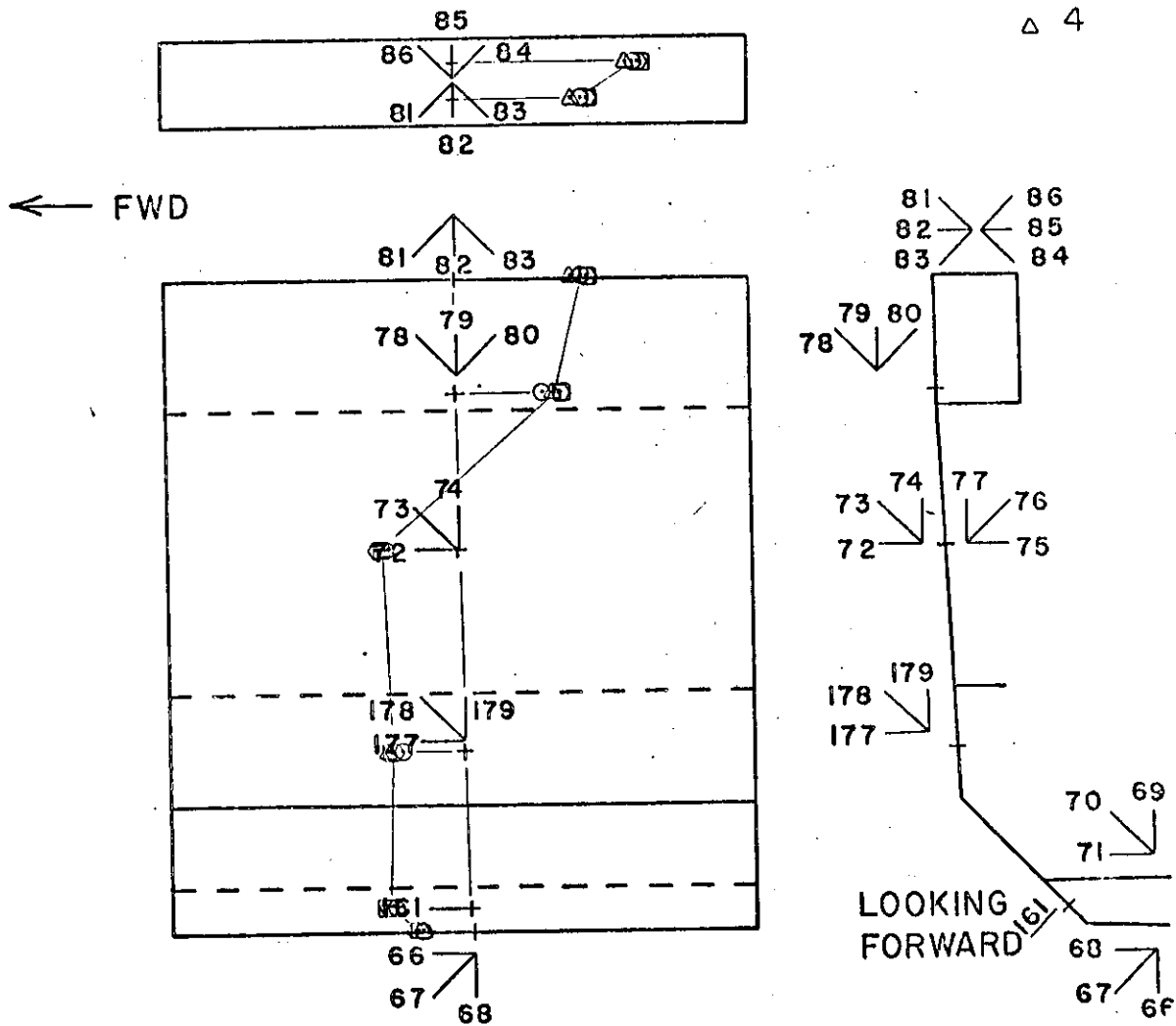


FIGURE 6a

SECTION BETWEEN FRAMES 178 & 194

LONGITUDINAL STRESSES DUE TO LAT. B.M. + TORSION

SINGLE GAGES - 2(250 BG)

NO. OF ROSETTES - 4(125 RA)

-12(250 RA)

- 1
- 2
- 3
- △ 4

DATE OF EXPERIMENT , 1972

SCALE OF STRESS

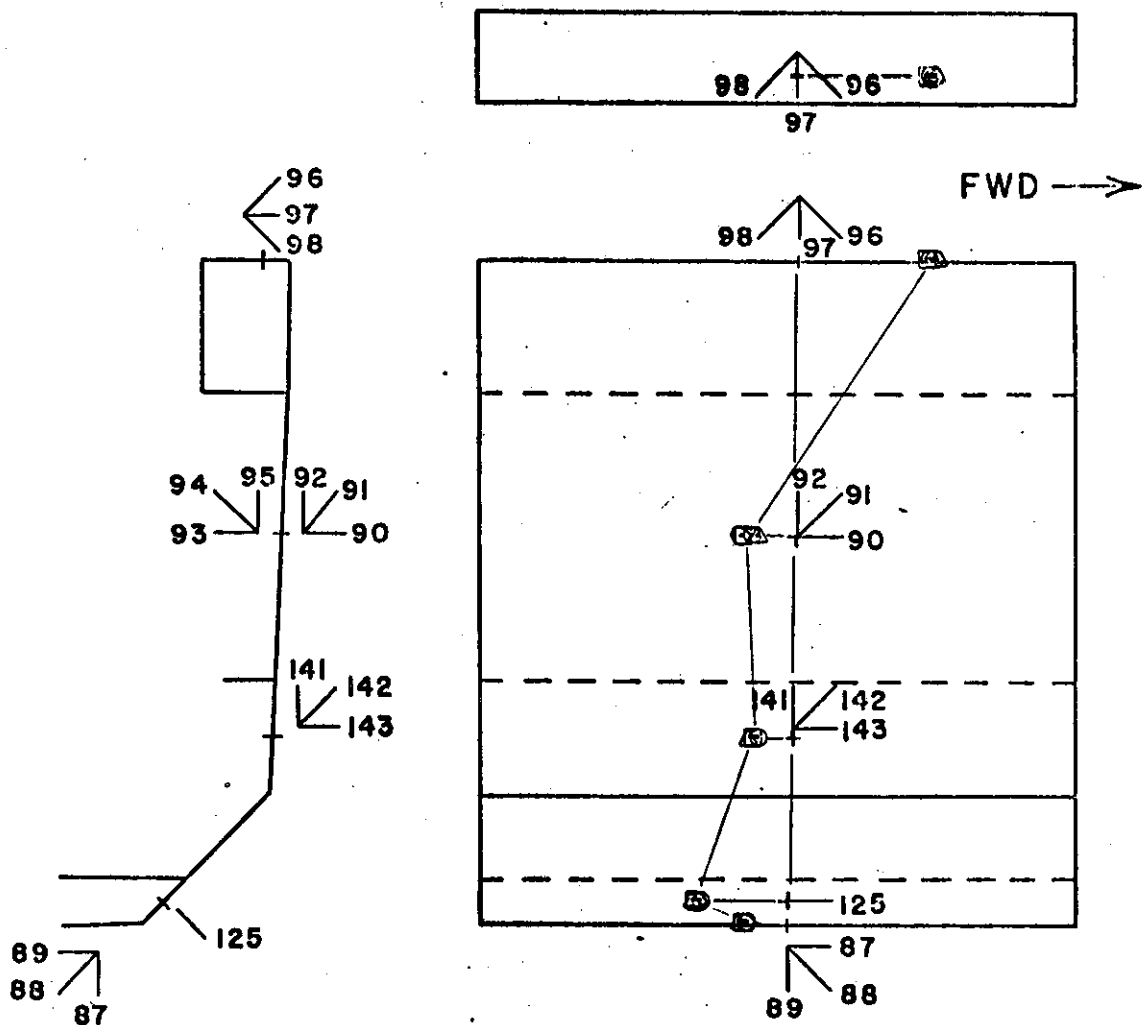
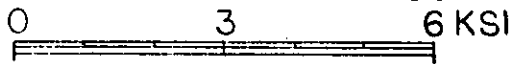


FIGURE 6b

B-124
SECTION BETWEEN FRAMES 178 & 194

LONGITUDINAL STRESSES DUE TO LAT. B.M. + TORSION

SINGLE GAGES - 2(250 BG)

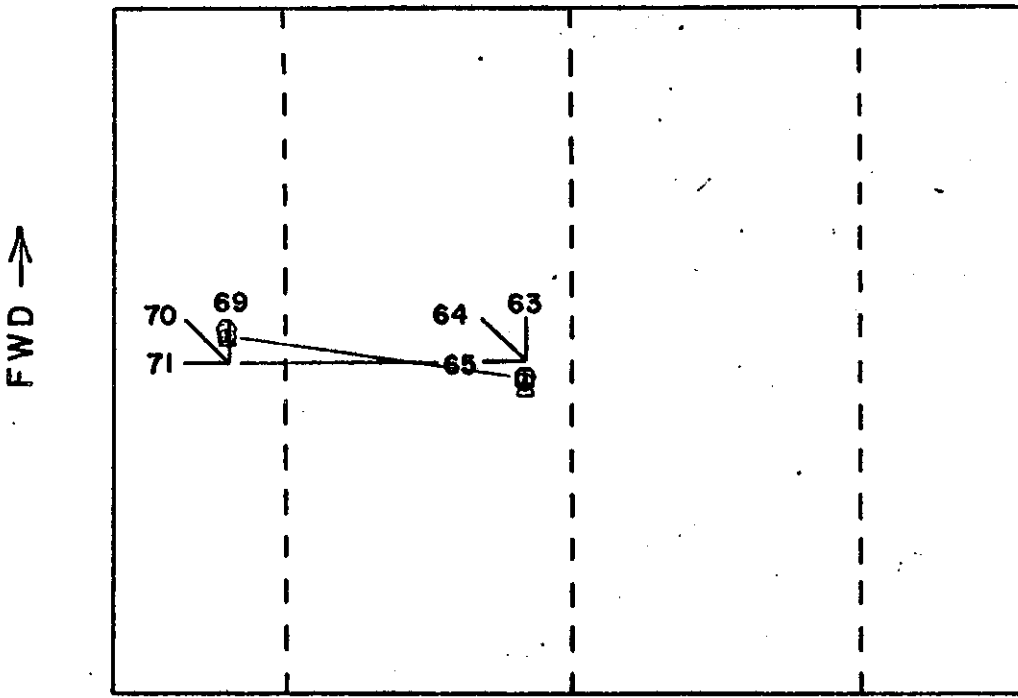
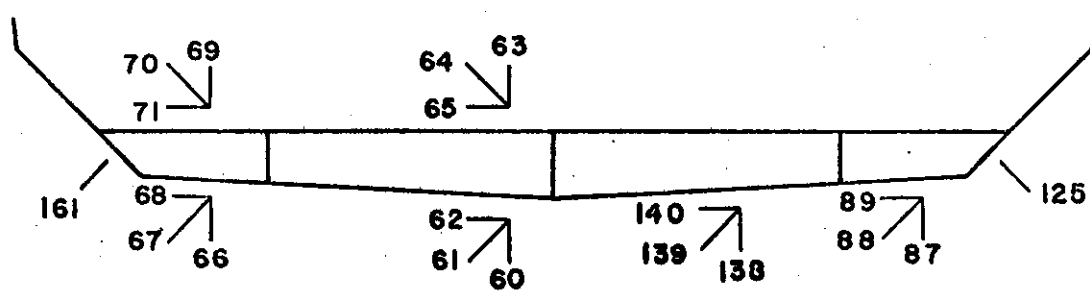
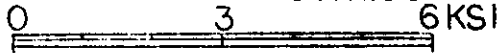
NO. OF ROSETTES - 4(125 RA)

- 12(250 RA)

DATE OF EXPERIMENT ,1972

- 1
- 2
- 3
- △ 4

SCALE OF STRESS



TANK TOP

FIGURE 6d

SECTION BETWEEN FRAMES 178 & 184

SHEAR STRESSES DUE TO LAT. B.M. + TORSION

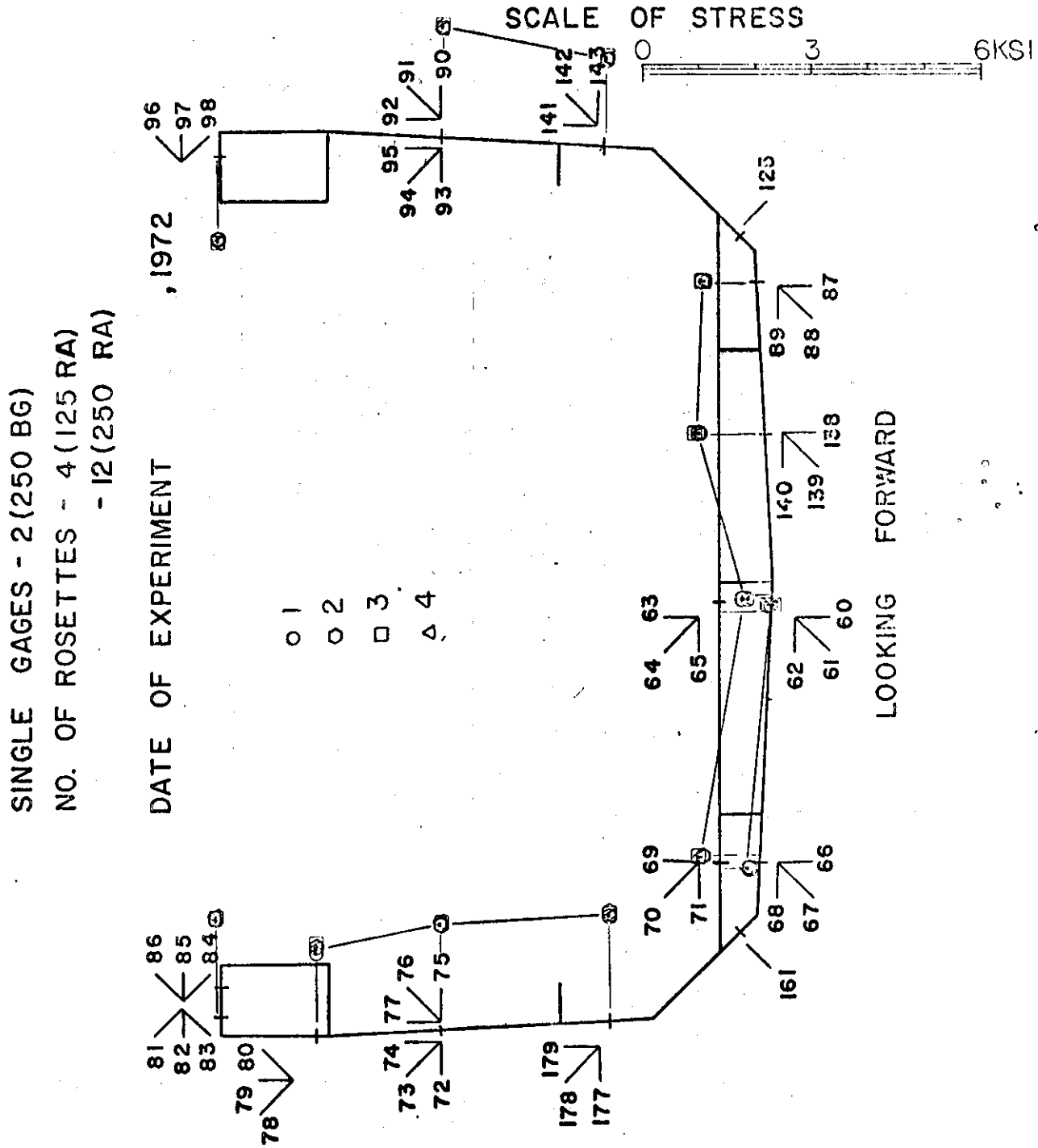
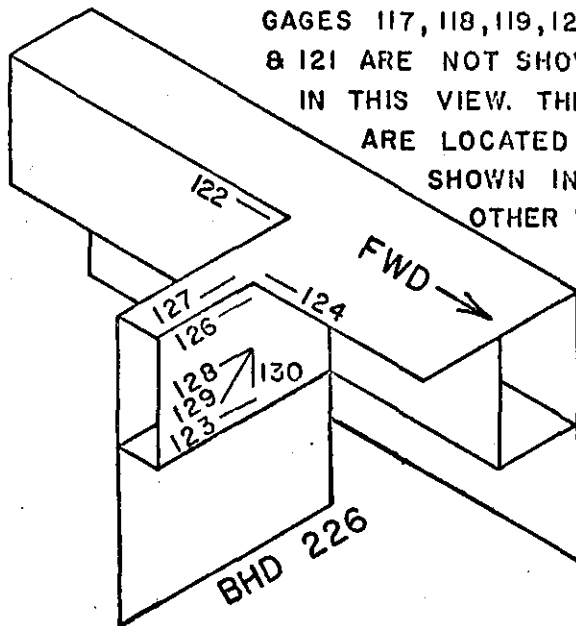


FIGURE 7

SECTION AT HATCH CORNER PORT SIDE FRAME 226

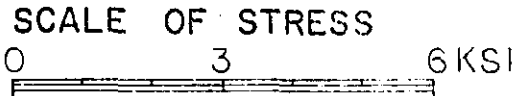
LONGITUDINAL STRESSES DUE TO LAT. BM. + TORSION



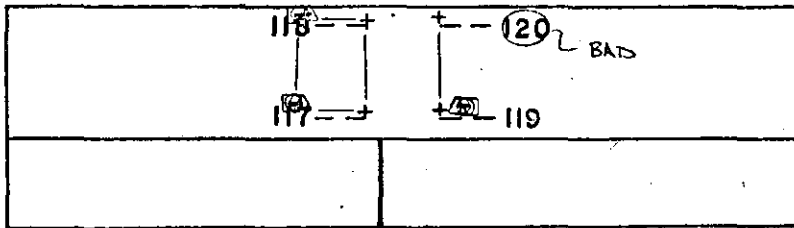
GAGES 117, 118, 119, 120,
& 121 ARE NOT SHOWN
IN THIS VIEW. THEY
ARE LOCATED AS
SHOWN IN
OTHER VIEWS.

NO. OF ROSETTES
- 1(250 RA)
SINGLE GAGES
- 10(250 BG)

DATE OF EXPERIMENT
,1972

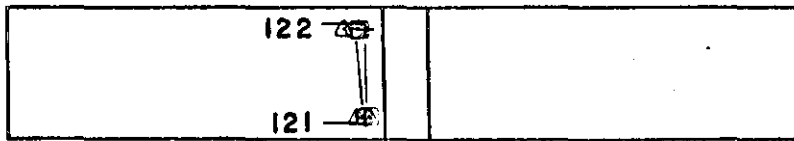


- 1
- 2
- 3
- △ 4



LOOKING OUTBOARD
SHELL PLATE

→ FWD



LOOKING OUTBOARD
TORSION BOX

BHD
226

FIGURE 8

SECTION 1" AFT OF FRAME 290

LONGITUDINAL STRESSES DUE TO LAT. B.M. + TORSION

NO. OF ROSETTES - 2 (250 RA)

- 1 (125 RA)

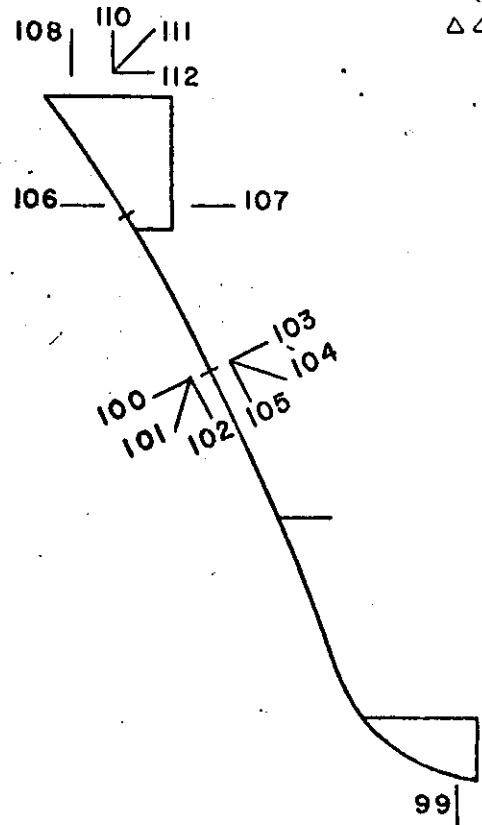
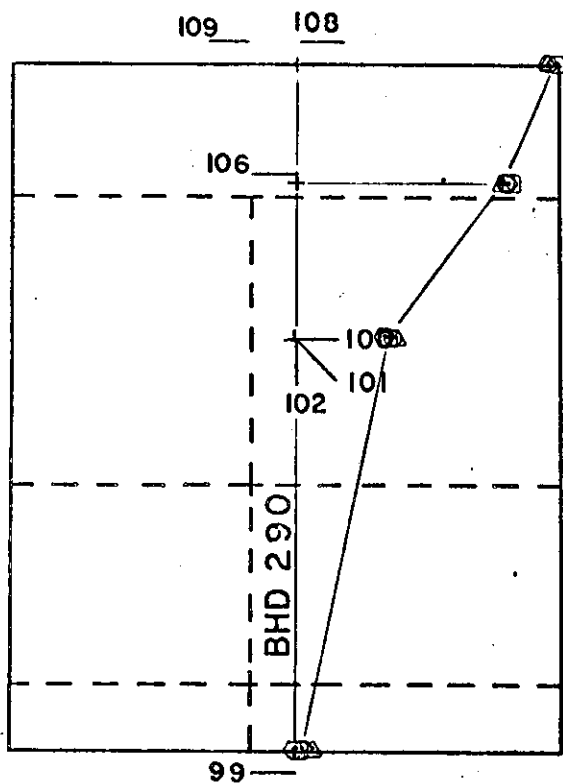
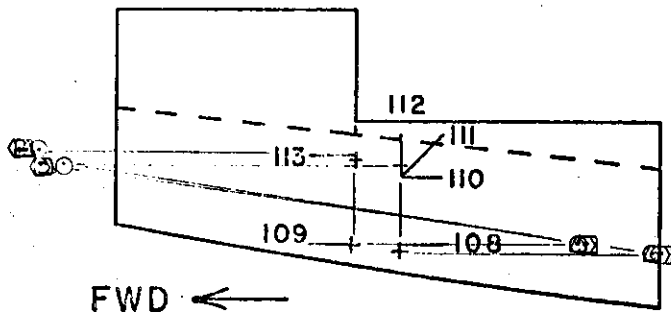
SINGLE GAGES - 6 (250 BG)

DATE OF EXPERIMENT
1972

SCALE OF STRESS



- 1
- 2
- 3
- △ 4



LOOKING FORWARD

FIGURE 9

STRESSES (KSI)

FIG.	GAGE NUMBER	○ 1	○ 2	□ 3	△ 4
1	0	.30	.54	.42	.25
	1	.71	.86	.77	.79
	8	.35	.32	.25	.47
	9	-.47	-.66	-.74	-.37
	10	-1.08	-1.30	-1.46	-1.06
	13	-1.07	-1.31	-1.43	-.95
	14	-2.03	-2.55	-2.71	-2.05
2	15	-.26	-.30	-.38	-.18
	16	-.39	-.44	-.52	-.31
	17	-.19	-.22	-.29	-.14
	18	-.09	-.13	-.18	-.01
	26	-.66	-.71	-.73	-.47
	27	-.58	-.56	-.67	-.55
3 (SHEAR)	149	.62	.65	.60	.65
	152		.75	.74	.75
	155	.25	.29	.31	.28
	162	.55	.56	.57	.56
4a	29	2.71	2.83	2.78	2.74
	30	.55	.59	.49	.65
	36	-.13	-.20	-.18	.01
	38	-6.35	-6.98	-7.01	-6.85
	39		-1.68	-1.66	-1.42
	42	-2.37	-2.46	-2.48	-2.26
	43	-4.09	-4.22	-4.23	-4.04

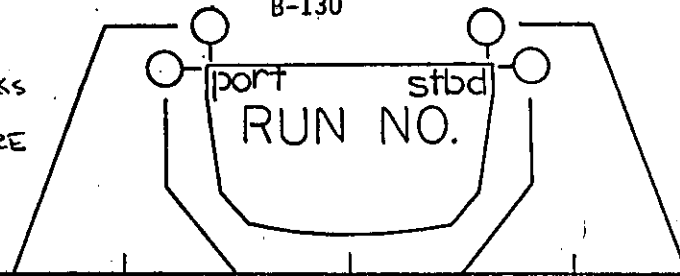
FIG.	GAGE NUMBER	○ 1	○ 2	□ 3	△ 4
4b	47	-2.70	-2.68	-2.71	-2.79
	48	-.53	-.59	-.65	-.46
	54	.32	.25	.19	.37
	57	1.17	1.07	1.04	1.26
	56	6.97	7.09	7.08	7.10
4c	29	2.71	2.83	2.78	2.74
	28	.02	1.28	.03	.92
	47	-2.70	-2.68	-2.71	-2.79
5	169	-1.60	-1.58	-1.59	-1.42
	170	-3.19	-3.18	-3.20	-2.98
	171	-1.48	-1.44	-1.44	-1.29
	172	-1.56	-1.54	-1.55	-1.35
	173	-2.34	-2.34	-2.35	-2.15
	174	-1.70	-1.68	-1.67	-1.53
	175	-2.56	-2.52	-2.55	-2.36
	176	-3.92	-3.93	-3.94	-3.72
6a	66	.75	.85	.82	.75
	161	1.14	1.22	1.23	1.13
	177	.90	1.08	1.09	1.11
	72	1.07	1.21	1.17	1.02
	78	-1.27	-1.53	-1.54	-1.44
	81	-1.84	-1.93	-1.93	-1.69
	84	-2.59	-2.69	-2.71	-2.49

FIG.	GAGE NUMBER	○	○	□	△	FIG.	GAGE NUMBER	○	○	□	△
		1	2	3	4			1	2	3	4
6b	87	-.61	-.58	-.65	-.67	7 (CONT'D)	141	-1.56	-1.54	-1.59	-1.57
	125	-1.29	-1.30	-1.31	-1.36		90	-1.95	-1.96	-2.00	-1.95
	141	-.53		-.56	-.61		96	1.49	1.50	1.51	1.51
	90	-.64	-.80	-.78	-.57	8					
	96	1.88	1.93	1.82	1.96		117	-1.00	-.98	-1.04	-.90
6c	161	1.14	1.22	1.23	1.13		118	-.94	-.97	-1.02	-.84
	66	.75	.85	.82	.75		119	-.35	-.31	-.39	-.25
	60	-.18	-.10	-.13	-.24		120			.33	-5.47
	138	-.39	-.31	-.35	-.51		121	.02	.01	-.05	.12
	87	-.61	-.58	-.65	-.67	9	122	.19	.11	.09	.30
	125	-1.29	-1.30	-1.31	-1.36		99	-.12	.01	-.04	-.26
6d	69	.36	.45	.43	.33		100	-1.38	-1.29	-1.33	-1.41
	63	-.29	-.21	-.26	-.36		106	-2.92	-2.96	-3.00	-2.91
7 (SHARP)	81	1.68	1.70	1.73	1.70		108	-3.59	-3.70	-3.72	-3.59
	78	1.42	1.52	1.54	1.51		109	-3.20	-3.31	-3.34	-3.22
	72	1.83	1.83	1.85	1.86		110	4.88	5.16	5.14	5.08
	177	1.85	1.87	1.86	1.85		113	4.53	4.82	4.76	4.72
	66	1.03	1.03	1.06	1.04						
	69	-.48	-.49	-.50	-.47						
	60	.47	.50	.49	.44						
	63	-.89	-.88	-.87	-.96						
	138	1.15	1.17	1.19	1.16						
	87	.94	.96	.96	.94						

LAT. B.M. + TORSION

B-130

NOTE: DEFLECTION READINGS FOR CASE 1 WERE UNRELIABLE AND THEREFORE EXCLUDED



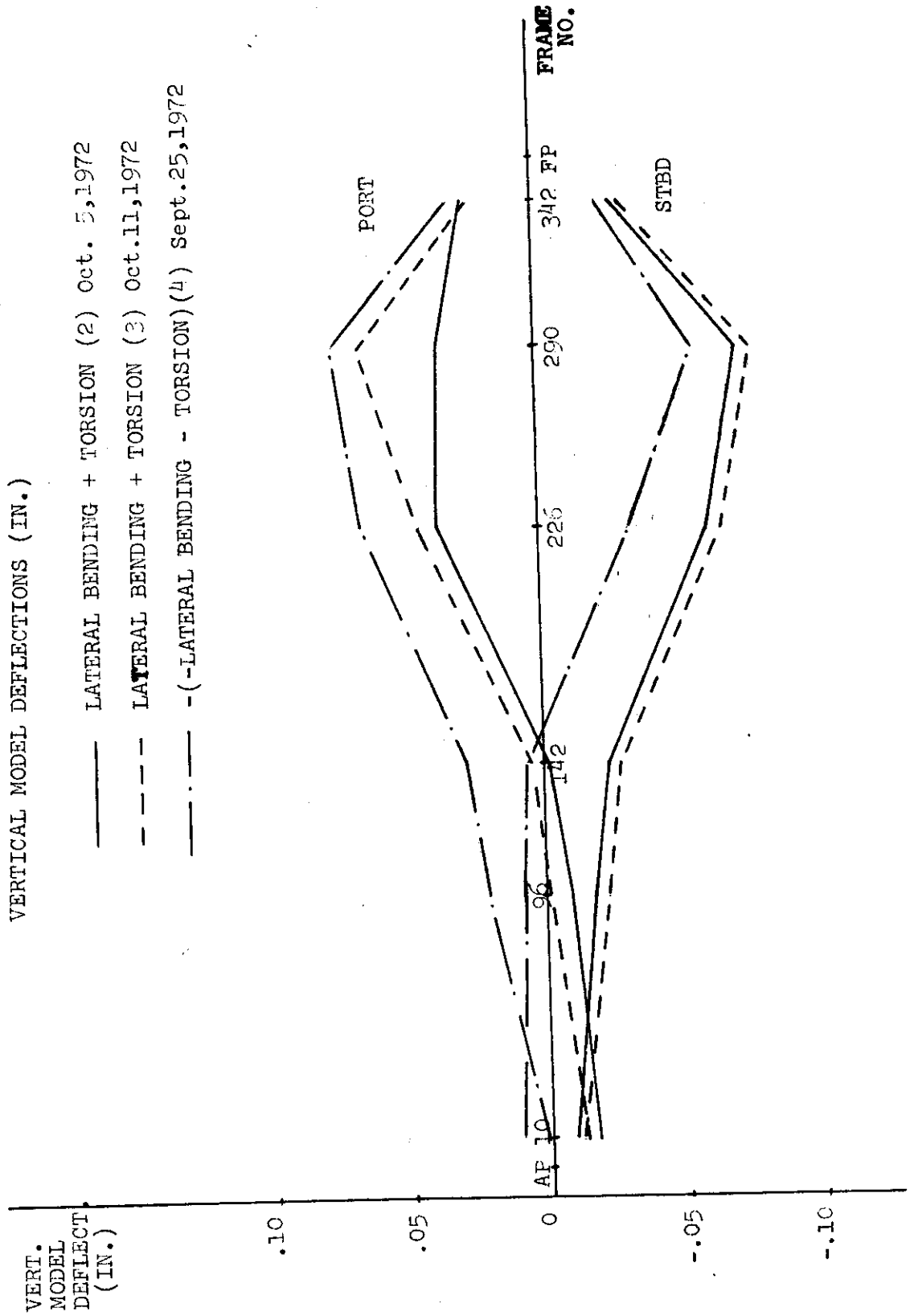
BHD.

MODEL DEFLECTION FROM THE NO-LOAD CONDITION, IN INCHES.

2 3 4	342	.025	-.003	.011	-.028
		.023	-.001	.013	-.031
		.030	-.008	.009	-.023
	290	.035	-.078	.082	-.072
		.063	-.080	.085	-.077
		.073	-.091	.072	-.056
	226	.036	-.015	.019	-.060
		.043	-.015	.018	-.065
		.064	-.015	.018	-.032
	142	-.002	.024	-.023	-.024
		+.004	.024	-.023	-.028
		+.028	.023	-.024	+.005
	96	-.009	.017	-.017	-.018
		-.002	.018	-.018	-.023
		+.025	.018	-.019	+.008
	10	-.017	.011	-.011	-.008
		-.013	.012	-.001	-.012
		+.003	.012	-.011	+.010

EQUIVALENT DEFLECTIONS OF FULL SCALE SHIP, IN INCHES.

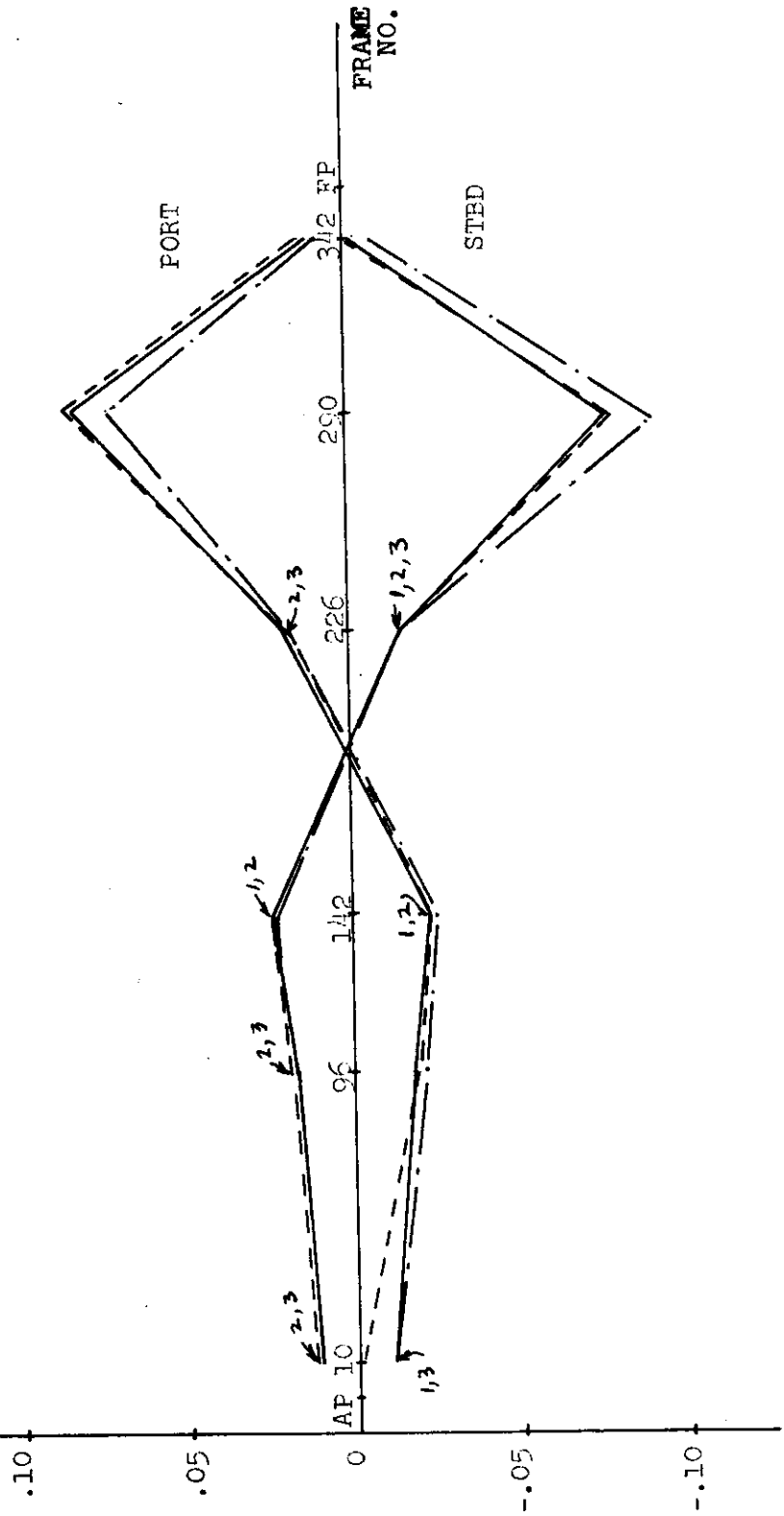
	342	1.25 1.15 1.5	-.15 -.05 -.40	.55 .65 .45	-1.40 -1.55 -1.15
	290	1.15 3.15 3.65	-3.90 -4.00 -4.55	4.10 4.25 3.6	-3.60 -3.85 -2.80
	226	1.80 2.15 3.2	-.75 -.75 -.75	.95 .90 .90	-3.00 -3.25 -1.6
	142	-.10 +.20 +1.4	1.20 1.20 1.15	-1.15 -1.15 -1.2	-1.10 -1.40 +.25
	96	-.45 -.10 +.10	.85 .90 .90	-.85 -.90 -.95	-.90 -1.15 +.40
	10	-.85 -.65 +.15	.55 .60 .60	-.55 -.05 -.95	-.40 -.60 +.50



HORIZONTAL MODEL DEFLECTIONS (IN.)

HORZ.
MODEL
DEFLECT.
(IN.)

- LATERAL BENDING + TORSION (2) Oct. 5, 1972
- - - LATERAL BENDING + TORSION (3) Oct. 11, 1972
- . - (-LATERAL BENDING - TORSION) (4) Sept. 25, 1972



ROOM-TEMP. DISTRIBUTION
COMBINED (+) LATERAL E.M. &
(+) TORSION.

OCT 11, 1972.

TE. (°F)

72

71

70

0930

0945

1000

1015

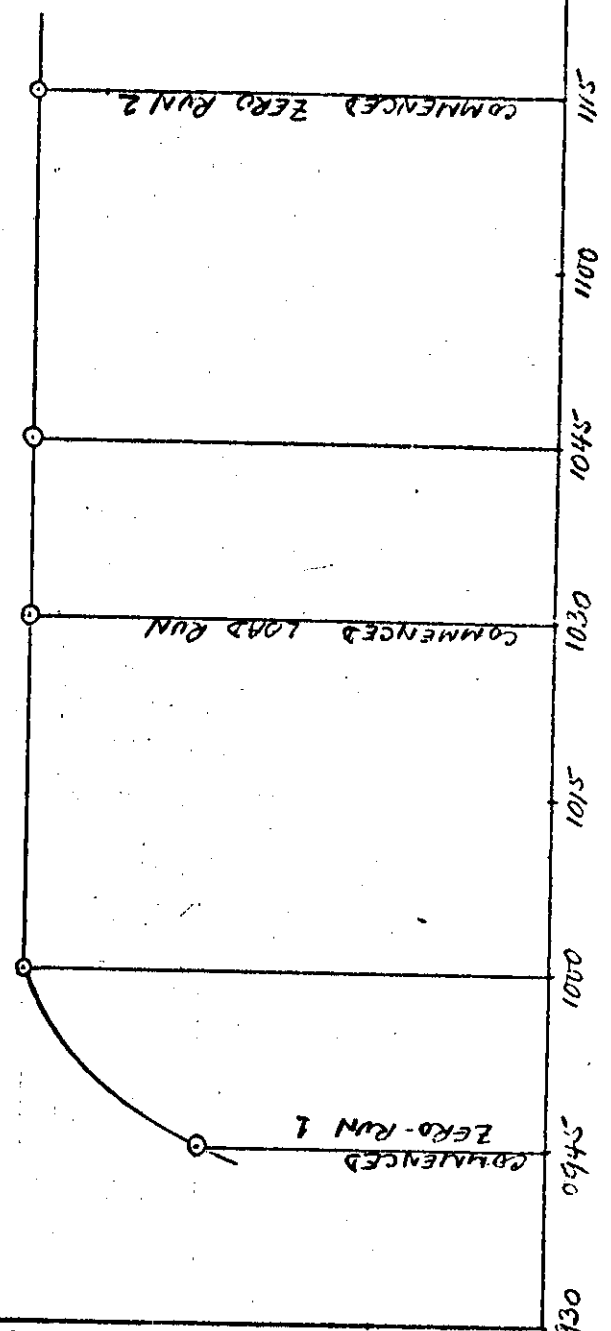
1030

1045

1100

1115

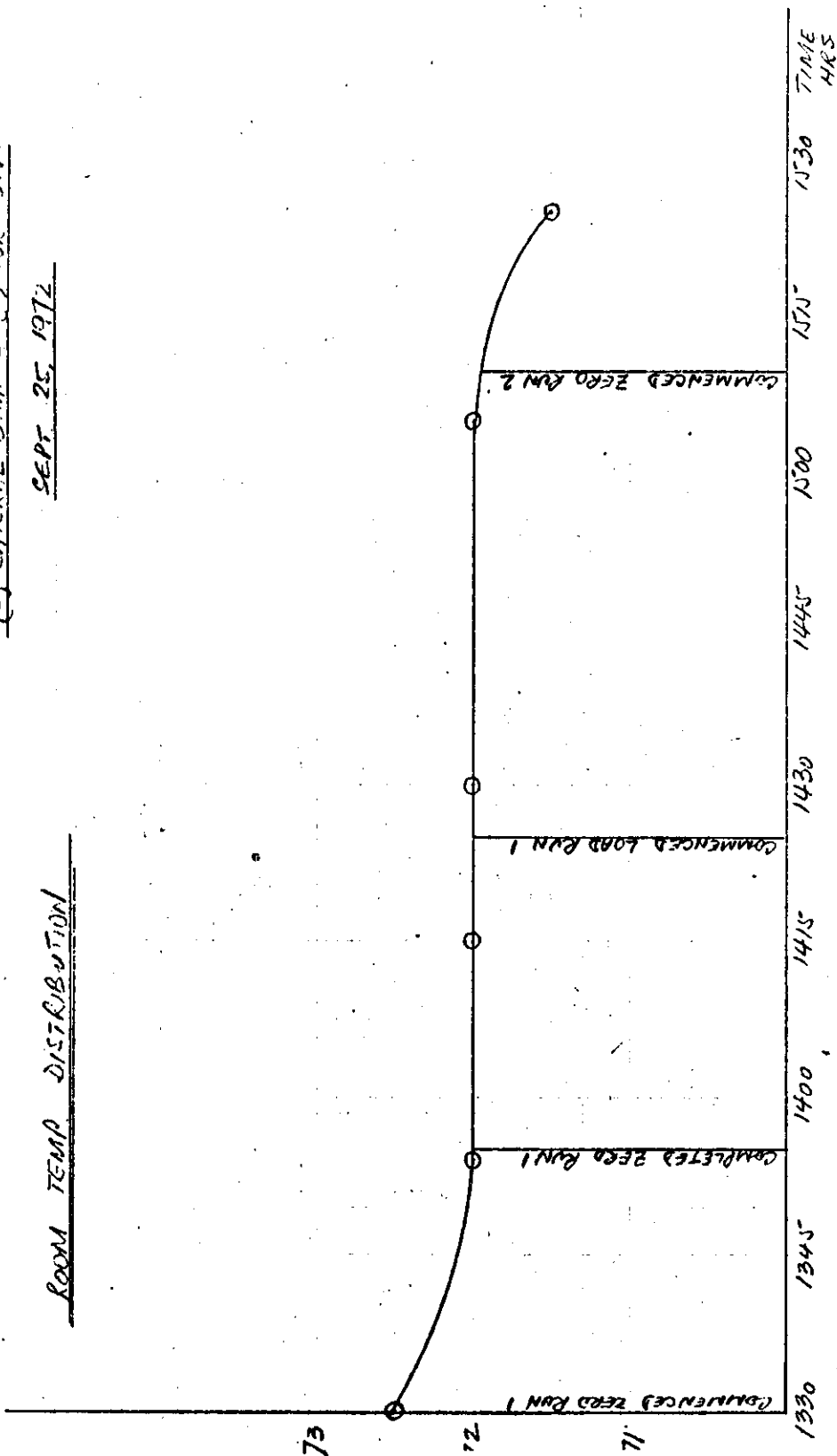
1130 TIME (MSE)



(-) LATERAL B.M. & (-) TORSION.

SEPT. 25, 1972

ROOM TEMP DISTRIBUTION

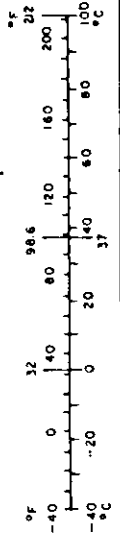
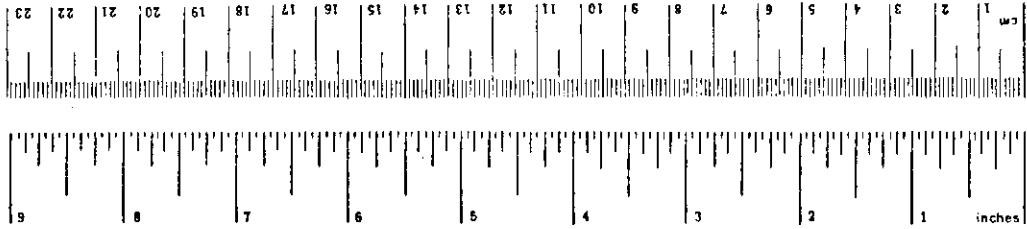


METRIC CONVERSION FACTORS

Approximate Conversions to Metric Measures

Symbol	When You Know	Multiply by	To Find	Symbol
LENGTH				
in	inches	2.5	centimeters	cm
ft	feet	30	centimeters	cm
yd	yards	0.9	meters	m
mi	miles	1.6	kilometers	km
AREA				
m ²	square inches	6.5	square centimeters	cm ²
ft ²	square feet	0.09	square meters	m ²
yd ²	square yards	0.8	square meters	m ²
mi ²	square miles	2.6	square kilometers	km ²
	acres	0.4	hectares	ha
MASS (weight)				
oz	ounces	28	grams	g
lb	pounds	0.45	kilograms	kg
	short tons (2000 lb)	0.9	tonnes	t
VOLUME				
tsp	teaspoons	5	milliliters	ml
Tbsp	tablespoons	15	milliliters	ml
fl oz	fluid ounces	30	milliliters	ml
c	cups	0.24	liters	l
pt	pints	0.47	liters	l
qt	quarts	0.95	liters	l
gal	gallons	3.8	liters	l
ft ³	cubic feet	0.03	cubic meters	m ³
yd ³	cubic yards	0.76	cubic meters	m ³
TEMPERATURE (exact)				
°F	Fahrenheit temperature	5/9 (after subtracting 32)	Celsius temperature	°C

Symbol	When You Know	Multiply by	To Find	Symbol
LENGTH				
mm	millimeters	0.04	inches	in
cm	centimeters	0.4	inches	in
m	meters	3.3	feet	ft
m	meters	1.1	yards	yd
km	kilometers	0.6	miles	mi
AREA				
cm ²	square centimeters	0.16	square inches	in ²
m ²	square meters	1.2	square yards	yd ²
km ²	square kilometers	0.4	square miles	mi ²
ha	hectares (10,000 m ²)	2.5	acres	ac
MASS (weight)				
g	grams	0.035	ounces	oz
kg	kilograms	2.2	pounds	lb
t	tonnes (1000 kg)	1.1	short tons	st
VOLUME				
ml	milliliters	0.03	fluid ounces	fl oz
l	liters	2.1	pints	pt
l	liters	1.06	quarts	qt
l	liters	0.26	gallons	gal
m ³	cubic meters	35	cubic feet	ft ³
m ³	cubic meters	1.3	cubic yards	yd ³
TEMPERATURE (exact)				
°C	Celsius temperature	9/5 (then add 32)	Fahrenheit temperature	°F



* U.S. Standard Weights and Measures, Price \$2.25, SD Catalog No. C13, 10-286.

DOCUMENT CONTROL DATA - R & D

(Security classification of title, body of abstract and indexing annotation must be entered when the overall report is classified)

1. ORIGINATING ACTIVITY (Corporate author) University of California - Berkeley		2a. REPORT SECURITY CLASSIFICATION Unclassified	
		2b. GROUP	
3. REPORT TITLE STRUCTURAL TESTS OF SL-7 SHIP MODEL			
4. DESCRIPTIVE NOTES (Type of report and inclusive dates)			
5. AUTHOR(S) (First name, middle initial, last name) W. C. Webster and H. G. Payer			
6. REPORT DATE 1977		7a. TOTAL NO. OF PAGES 248	7b. NO. OF REFS -
8a. CONTRACT OR GRANT NO.		9a. ORIGINATOR'S REPORT NUMBER(S) SSC-269	
b. PROJECT NO.		9b. OTHER REPORT NO(S) (Any other numbers that may be assigned this report) SL-7-11	
c.			
d.			
10. DISTRIBUTION STATEMENT Distribution of this document is unlimited			
11. SUPPLEMENTARY NOTES		12. SPONSORING MILITARY ACTIVITY Naval Ship Systems Command	
13. ABSTRACT			

DD FORM 1473 (PAGE 1)
1 NOV 65

S/N 0101-807-6801

Security Classification

SHIP RESEARCH COMMITTEE
Maritime Transportation Research Board
National Academy of Sciences-National Research Council

The Ship Research Committee has technical cognizance of the interagency Ship Structure Committee's research program:

PROF. J. E. GOLDBERG, Chairman, *Professor Emeritus, Purdue University*
MR. D. P. COURTSAL, *General Manager, Engrg. Works Division, DRAVO Corp.*
MR. E. S. DILLON, *Consultant, Silver Spring, Md.*
DEAN D. C. DRUCKER, *College of Engineering, University of Illinois*
MR. G. E. KAMPSCHAEFER, Jr., *Manager, Technical Services, ARMCO Steel Corp.*
PROF. L. LANDWEBER, *Inst. of Hydraulic Research, The University of Iowa*
MR. O. H. OAKLEY, *Consultant, McLean, Virginia*
MR. D. P. ROSEMAN, *Chief Naval Architect, Hydronautics, Inc.*
DEAN R. D. STOUT, *Graduate School, Lehigh University*
MR. R. W. RUMKE, *Executive Secretary, Ship Research Committee*

The Ship Design, Response, and Load Criteria Advisory Group prepared the project prospectus and evaluated the proposals for this project:

MR. D. P. ROSEMAN, Chairman, *Chief Naval Architect, Hydronautics, Inc.*
MR. M. D. BURKHART, *Head, Marine Science Affairs, Dept. of Navy*
DR. D. D. KANA, *Manager, Structural Dynamics & Acoustics, S. W. Res. Inst.*
MR. W. J. LANE, *Structural Engineer, Bethlehem Steel Corp.*
DR. M. K. OCHI, *Research Scientist, Naval Ship Research & Dev. Center*
PROF. W. D. PILKEY, *Department of Mechanics, University of Virginia*
PROF. J. C. SAMUELS, *Dept. of Electrical Engineering, Howard University*
PROF. M. SHINOZUKA, *Dept. of Civil Engineering, Columbia University*
MR. H. S. TOWNSEND, *Consultant, Westport, Conn.*
PROF. G. A. WEMPNER, *School of Engrg. Science & Mechanics, Georgia Inst. of Technology*

The SL-7 Program Advisory Committee provided the liaison technical guidance, and reviewed the project reports with the investigator:

MR. R. C. STRASSER, Chairman, *Consultant, Newport News, Va.*
MR. E. R. ASHEY, *Asst. for Advanced Technology, Naval Ship Engrg. Center*
PROF. J. E. GOLDBERG, *Professor Emeritus, Purdue University*
PROF. E. V. LEWIS, *Director of Research, Webb Inst. of Naval Architecture*
MR. J. H. ROBINSON, *Staff Naval Architect, Naval Ship Res. & Dev. Center*
MR. D. P. ROSEMAN, *Chief Naval Architect, Hydronautics, Inc.*
PROF. R. A. YAGLE, *Dept. of Naval Architecture, University of Michigan*

SHIP STRUCTURE COMMITTEE PUBLICATIONS

These documents are distributed by the National Technical Information Service, Springfield, Va. 22151. These documents have been announced in the Clearinghouse journal U.S. Government Research & Development Reports (USGRDR) under the indicated AD numbers.

SL-7 PUBLICATIONS TO DATE

- SL-7-1, (SSC-238) - *Design and Installation of a Ship Response Instrumentation System Aboard the SL-7 Class Containership S.S. SEA-LAND McLEAN* by R. A. Fain. 1974. AD 780090.
- SL-7-2, (SSC-239) - *Wave Loads in a Model of the SL-7 Containership Running at Oblique Headings in Regular Waves* by J. F. Dalzell and M. J. Chiocco. 1974. AD 780065.
- SL-7-3, (SSC-243) - *Structural Analysis of SL-7 Containership Under Combined Loading of Vertical, Lateral and Torsional Moments Using Finite Element Techniques* by A. M. Elbatouti, D. Liu, and H. Y. Jan. 1974. AD-A002620
- SL-7-4, (SSC-246) - *Theoretical Estimates of Wave Loads on the SL-7 Containership in Regular and Irregular Seas* by P. Kaplan, T. P. Sargent, and J. Cilmi. 1974. AD-A004554.
- SL-7-5, (SSC-257) - *SL-7 Instrumentation Program Background and Research Plan* by W. J. Siekierka, R. A. Johnson, and CDR C. S. Loosmore, USCG. 1976. AD-A021337.
- SL-7-6, (SSC-259) - *Verification of the Rigid Vinyl Modeling Techniques: The SL-7 Structure* by J. L. Rodd. 1976. AD-A025717.
- SL-7-7, (SSC-263) - *Static Structural Calibration of Ship Response Instrumentation System Aboard the SEA-LAND McLEAN* by R. R. Boentgen and J. W. Wheaton. 1976. AD-A031527.
- SL-7-8, (SSC-264) - *First Season Results from Ship Response Instrumentation Aboard the SL-7 Class Containership S.S. SEA-LAND McLEAN in North Atlantic Service* by R. R. Boentgen, R. A. Fain, and J. W. Wheaton. 1976. AD-A039752
- SL-7-9, *Second Season Results from Ship Response Instrumentation Aboard the SL-7 Class Containership S.S. Sea-Land McLean in North Atlantic Service* by J. W. Wheaton and R. R. Boentgen. 1976.
- SL-7-10, *Third Season Results from Ship Response Instrumentation Aboard the SL-7 Class Containership S.S. Sea-Land McLean in North Atlantic Service* by R. R. Boentgen. 1976.
- SL-7-11, *Structural Tests of SL-7 Ship Model* by W. C. Webster and H. G. Payer. 1977.